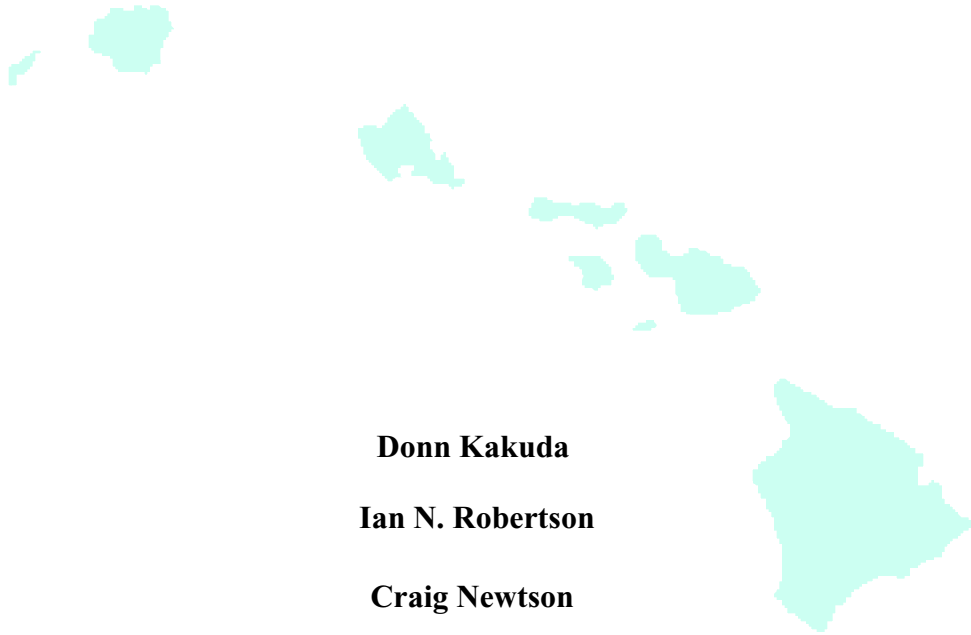


**EVALUATION OF NON-DESTRUCTIVE TECHNIQUES FOR
CORROSION DETECTION IN CONCRETE EXPOSED
TO A MARINE ENVIRONMENT**



Donn Kakuda

Ian N. Robertson

Craig Newton



**Prepared in cooperation with the State of Hawaii Department of Transportation,
Highways Division and U.S. Department of Transportation, Federal Highway
Administration**

**UNIVERSITY OF HAWAII
COLLEGE OF ENGINEERING**

DEPARTMENT OF CIVIL AND ENVIRONMENTAL ENGINEERING

Research Report UHM/CEE/05-04

May 2005

**EVALUATION OF NON-DESTRUCTIVE TECHNIQUES FOR CORROSION
DETECTION IN CONCRETE EXPOSED TO A MARINE ENVIRONMENT**

Donn Kakuda
Ian N. Robertson
Craig Newton

Prepared in cooperation with the:

State of Hawaii
Department of Transportation
Highways Division
and
U.S. Department of Transportation
Federal Highway Administration

Research Report UHM/CEE/05-04
May 2005

Acknowledgements

This report is based on a Master of Science thesis prepared by Donn Kakuda under the direction of Dr. Ian Robertson of the Department of Civil and Environmental Engineering at the University of Hawaii at Manoa, and Dr. Craig Newton of the Department of Civil and Environmental Engineering at New Mexico State University.

The authors wish to acknowledge the considerable contributions made by the State of Hawaii Department of Transportation (HDOT), Ameron Hawaii, and Hawaiian Cement during this project. Funding for this project was provided by the HDOT. Aggregates and other constituents for the concrete mixtures were donated by Ameron Hawaii and Hawaiian Cement.

The authors also acknowledge Drs. H. Ronald Riggs and Panos Prevedouros for their contribution in reviewing this report and providing valuable suggestions. Special thanks are also extended to laboratory technicians Andrew Oshita and Miles Wagner for their technical assistance. Special thanks to Drs. Pavel Zinin and Murli Manghnani for assistance with the acoustic microscopy. Appreciation is also extended to Grant Okunaga, John Uno, and Gaur Johnson for their assistance in the Structures Laboratory.

Abstract

A study was conducted to evaluate electrical tests and chemical tests of reinforced concrete specimens subjected to a cyclic laboratory simulated marine environment. The tests compared the electrical tests to visual inspections involving acoustic and optical microscopy. The specimens were proportioned using corrosion-inhibiting admixtures intended to slow the corrosion process. The corrosion-inhibiting admixtures included Darex Corrosion Inhibitor (DCI), Rheocrete CNI, Rheocrete 222+, FerroGard 901, Xypex Admix C-2000, latex, fly ash, and silica fume. Relevant tests such as pH level, air permeability, chloride content, macrocell current, and half-cell potential were performed. Both electrical test of macrocell current and half-cell potential proved effective in predicting moderate to substantial corrosion. When macrocell currents measured over $10 \mu A$, substantial corrosion was found 94% of the time. Similarly when the half-cell readings indicated 90% probability of corrosion, substantial corrosion was found 100% of the time. However, when the half-cell readings indicated less than 10% probability of corrosion, 65% of the specimens had signs of corrosion. Overall, the air permeability and pH values do not indicate any correlations to the various levels of corrosion. Using chlorides and half-cell values certain limits could be related to certain levels of corrosion. In all cases chloride values (mass of cement) above 3% and half-cell values over 90% probability of corrosion (-350mV) were all substantially corroded.

TABLE OF CONTENTS

Acknowledgements.....	iii
Abstract.....	v
CHAPTER 1 - INTRODUCTION.....	1
1.1 Introduction.....	1
1.2 Objective.....	2
CHAPTER 2 - LITERATURE REVIEW.....	3
2.1 Introduction.....	3
2.2 Admixtures.....	3
2.2.1 Corrosion Inhibitors.....	3
2.2.2 Calcium nitrite-based corrosion-inhibitors.....	4
2.2.3 Rheocrete 222+.....	5
2.2.4 Ferrogard 901.....	6
2.2.5 Xypex Admix C-2000.....	6
2.2.6 Fly Ash.....	7
2.2.7 Silica Fume.....	9
2.2.8 Latex-Modifier.....	10
2.3 Testing.....	10
2.3.1 Air permeability test.....	10
2.3.2 Electrical tests.....	12
2.3.3 Chemical Test.....	14
2.4 Microscopy.....	15
2.4.1 Acoustic Microscopy.....	15

2.4.2	Stereozoom Microscopy	16
CHAPTER 3	- DURABILITY STUDY – CYCLIC PONDING	17
3.1	Introduction.....	17
3.2	ASTM G 109-92 Test Procedure	17
3.3	Specimens	19
3.4	Concrete Mixtures.....	21
3.5	Test Procedures.....	23
3.5.1	Half cell measurement	24
3.5.2	Macrocell current.....	25
3.5.3	Chloride samples.....	25
3.5.4	pH Level.....	26
3.5.5	Air permeability	27
CHAPTER 4	- OPTICAL MICROSCOPY	29
4.1	Introduction.....	29
4.2	Description.....	29
4.3	Procedure	29
4.3.1	Exterior Visual Inspection	30
4.3.2	Splitting of the specimens.....	31
4.3.3	Internal Examination of the Specimens	31
4.4	Visual Observation Records	32
4.4.1	Specimen Xyp4 #1 with minor corrosion.....	33
4.4.2	Specimen Con2 #6 with moderate to significant corrosion.....	36
4.4.3	Specimen FA10* #2 with moderate to significant corrosion and cracks.....	42

CHAPTER 5	- ACOUSTIC MICROSCOPY	47
5.1	Introduction.....	47
5.2	Scanning Acoustic Microscope.....	47
5.3	Procedure	49
5.3.1	Cutting the Specimens	49
5.3.2	Polishing	49
5.4	Acoustic Microscope Images.....	51
CHAPTER 6	- RESULTS.....	55
6.1	Introduction.....	55
6.2	Electrical tests.....	55
6.2.1	Marcocell Current.....	60
6.2.2	Half cell potential.....	61
6.2.3	Combined electrical results.....	62
6.3	Chemical tests.....	65
6.3.1	Chlorides.....	65
6.3.2	pH.....	66
6.3.3	Air permeability	68
CHAPTER 7	- SUMMARY AND CONCLUSIONS.....	79
7.1	Introduction.....	79
7.2	Summary	80
7.3	Conclusions.....	82
APPENDIX A	83
APPENDIX B	93

APPENDIX C	95
APPENDIX D	101
APPENDIX E	107
APPENDIX F	113
APPENDIX G	117
REFERENCES	235

LIST OF TABLES

Table 2.1: Fly ash chemical composition.....	8
Table 2.2 : Values of permeability and concrete ratings (Poroscope Plus 1998).....	12
Table 2.3: Limiting values for the interpretation of Half-cell potential results	13
Table 2.4 : Limits for water-soluble chloride-ion content in concrete (ACI 318-99).....	15
Table 3.1 : Total number of specimens.....	22
Table 3.2 : Specimens included in this study.....	22
Table 6.1 : Electrical and observational results	57
Table 6.2 : Current Percentages	60
Table 6.3 : Half cell potential percentages.....	61
Table 6.4: Shifted Half Cell Potential Percentages.....	62
Table 6.5 : Both electrical test percentages	63
Table 6.6 : New values of half-cell limits.....	63
Table 6.7 : Air permeability categories.....	69

LIST OF FIGURES

Figure 3.1: Details and dimensions (inch (mm)) of beam specimens.....	18
Figure 3.2 : Points where half cell reading were taken (left), half cell set up (right)	24
Figure 3.3 : pH sample (left), pH probe and scale (right).....	26
Figure 3.4 : Air permeability set up (left), approximate points where air permeability (small dot) and chlorides (big dot) were taken (right)	27
Figure 4.1 : Exterior visual inspection	30
Figure 4.2 : Specimen splitting	31
Figure 4.3 : Exterior visual inspection of Xyp4 #1.....	34
Figure 4.4 : Interior inspection of Xyp4 #1	35
Figure 4.5 : Bottom (left) and top (right) surfaces of top reinforcing bars	36
Figure 4.6 : Bottom of left reinforcing bar and corresponding concrete surface.....	36
Figure 4.7 : Exterior visual inspection of Con2 #6.....	38
Figure 4.8 : Interior inspection of Con2 #6.....	39
Figure 4.9 : Bottom (left) and top (right) surfaces of top reinforcing bars	40
Figure 4.10 : Left bar bottom and corresponding close up x45	40
Figure 4.11 : Right bar, bottom (left) x12, (right) x22.5	40
Figure 4.12 : Right bar, bottom inside edge (left) x22.5, (right) x45	41
Figure 4.14 : Bottom piece, right side, corrosion on concrete (left) x22.5 (right) x45.....	41
Figure 4.15 : Exterior Inspection of FA*10 #2.....	43
Figure 4.15 : Interior Inspection of FA*10 #2.....	44
Figure 4.16 : Bottom (left) and top (right) surfaces of top reinforcing bars	45
Figure 4.18 : Top surface cracks (left), left bar top, underneath cracks (right) x12	45

Figure 4.18 : Left bar bottom, (right) x12, Bottom piece left side, (left) x12	45
Figure 4.20 : Bottom piece, left side (left), Close up (right) x22.5	46
Figure 5.1 : Scanning Acoustic Microscope.....	47
Figure 5.2 : Schematic diagram of the Acoustic Microscope.....	48
Figure 5.3 : Sample cutting diagram (left), Acoustic Specimens (right).....	50
Figure 5.4 : Lapmaster	51
Figure 5.5 : Control 2 specimen #1 B-scan.....	52
Figure 5.6 : Control 2 specimen #1 C-Scan.....	53
Figure 5.7 : B-scan images (Zinin et al, 2004)	53
Figure 5.8 : C – Scan images (Zinin et al, 2004)	54
Figure 6.1 : Chlorides vs. Half cell potential	65
Figure 6.2 : Average pH vs. Half cell potential	67
Figure 6.3 : pH vs. the Chloride concentration.....	68
Figure 6.4 : Ameron Control – Air permeability	70
Figure 6.5 : Halawa Control – Air permeability	71
Figure 6.6 : Silica Fume & Fly Ash – Air permeability	72
Figure 6.7 : Latex & Xypex – Air permeability.....	73
Figure 6.8 : Rheocrete, DCI, Ferrogard – Air permeability.....	74
Figure 6.9 : All Ameron mixtures – Air permeability	75
Figure 6.10 : All Halawa Mixtures – Air permeability.....	76
Figure 6.11 : Average Figg numbers vs. ASTM G109 Cycles to Failure	77
Figure 6.12 : Figg number vs. Half-cell potential.....	78

CHAPTER 1 - INTRODUCTION

1.1 Introduction

Reinforced concrete is a widely used construction material because of its strength and durability. Corrosion of reinforcing steel in concrete is one of the main causes of concrete deterioration. Traditionally, corrosion in reinforced concrete structures has been evaluated using electrical measurements of half-cell potentials and polarization resistance. The problems with these tests are that results can vary and the values that are obtained do not give a clear picture of the degree of corrosion.

There are many methods available to protect steel from corrosion. Corrosion-inhibiting admixtures are probably the most cost-effective solution. While these admixtures provide protection, there are other factors such as type of aggregate, porosity, and water/cementitious material (w/c) ratio that also affect the rate of corrosion. It would be advantageous to be able to document different degrees of corrosion related to these factors and various corrosion-inhibiting admixtures.

This project is part of a larger on-going study on durability of concrete with Hawaiian aggregates. The first phase of the project consisted of field observations at various harbor piers on Oahu (Bola & Newton 2000). The second phase involved accelerated corrosion tests conducted in the University of Hawaii Structures Laboratory (Pham & Newton 2001, Okunaga & Robertson 2004). A total of 116 concrete mixtures with different w/c ratios, aggregates, and admixtures were tested in this study. These specimens were subjected to a 3% NaCl salt-water bath and drying cycles in accordance

with ASTM G 109 - 92. The corrosion of the reinforcement in each specimen was measured using current measurements (ASTM G 109-92) and half-cell potential measurements. This process was continued until half of the specimens for a particular mixture reached the onset of corrosion, at which point all of the specimens from that particular mixture were removed from the cycling process. The onset of corrosion is defined as the time when the macrocell current is 10 μA or greater. The specimens then underwent pH tests and a chloride concentration tests and were visually inspected to establish the extent of corrosion.

1.2 Objective

The objective of the study reported here was to use visual inspection, scanning acoustic microscopy, and optical microscopy to examine and evaluate the corrosion of steel reinforcing in concrete due to the effects of introduced chloride attack. The performance of the steel will depend on factors such as the use of different admixtures, aggregates, and w/c ratios. By comparing the visual data with the electronic measurements, these non-destructive corrosion detection methods can be evaluated. Conclusions can also be drawn regarding the effectiveness of admixtures and mixture proportions at preventing the onset of chloride induced corrosion.

CHAPTER 2 - LITERATURE REVIEW

2.1 Introduction

There are many different types of admixtures used to protect reinforcing steel in concrete. These admixtures protect against corrosion and other types of chemical attack. Tests used to identify the properties of concrete are described in this chapter. Methods of microscopy relevant to concrete are also described.

Civjan et al. (2003) evaluated the performance and economics of various combinations of corrosion-inhibiting admixtures. Their report has an extensive literature review that complements what is presented in this thesis in the areas of mineral and chemical admixtures, and electrical test methods.

2.2 Admixtures

Eight different types of corrosion-inhibiting admixtures were used in this study; namely DCI, Rheocrete CNI, Rheocrete 222+, FerroGard 901, Xypex Admix C-2000, fly ash, silica fume, and a latex-modifier. This section describes corrosion inhibitors in general and each of these admixtures in particular.

2.2.1 *Corrosion Inhibitors*

By definition a corrosion inhibitor is a substance that prevents or minimizes corrosion. Corrosion inhibitors can be classified as inorganic, organic, or vapor-phase inhibitors. In the case of reinforced concrete, corrosion-inhibiting admixtures are typically classified as anodic, cathodic, or mixed (anodic and cathodic) (Nmai et al. 1992).

Anodic inhibitors are chemicals that function by stifling the corrosion reaction at the anode. They react with an existing corrosion product to form an insoluble film adhering tightly to the metal surface. Generally, they are considered to be dangerous inhibitors because they produce increased rates of attack on unprotected areas, with the exception of sodium benzoate which causes general attack if full protection is not maintained (Griffin 1975). Anodic inhibitors are only effective when present in high concentrations and are otherwise detrimental since corrosion is intensely localized at low concentrations (Gjorv 1975). Examples of anodic inhibitors include calcium nitrite, potassium dichromate, sodium nitrite, soluble barium chromate, and stannous chloride.

2.2.2 *Calcium nitrite-based corrosion-inhibitors*

Calcium nitrite is generally considered to be an anodic inhibitor (Nmai et al. 1992). Calcium nitrite inhibits corrosion by reacting with ferrous ions to form a layer of ferric oxide, Fe_2O_3 , around the anode according to the following chemical reaction:



The additional ferric oxide enhances the passivation layer near the surface of the steel created by the highly alkaline ($\text{pH} > 12$) environment of concrete. It is believed that nitrite and chloride ions have to compete to react with the ferrous ions in the concrete. Therefore, if there are less nitrite ions than chloride ions in the vicinity of the steel surface, then the corrosion process will begin. Consequently, calcium nitrite is more effective when the concentration of the nitrite ions is high (Nmai et al. 1992).

Calcium nitrite blocks the corrosion reaction of the chloride ions by chemically reinforcing and stabilizing the passive film. The nitrite ion causes the ferric oxides to become insoluble. The chloride ions are prevented from penetrating the passive film and making contact with the steel up to a certain threshold of chloride ion. Increased levels of chloride ions require increased levels of calcium nitrite to stop corrosion. The threshold level at which corrosion starts in normal concrete with no inhibiting admixture is about 0.15% water soluble chloride ion by weight of cement (Kosmatka & Panarese 1994). Calcium nitrite admixtures increase the cost of a cubic yard of concrete about \$25 to \$30, depending on the dosage specified. Calcium nitrite also is an accelerator, so a retarder is often needed to offset the accelerating effect (Malisch and Holland 2000).

Two calcium nitrite based admixtures were used in this study. DCI, a product of W.R. Grace & Co., and Rheocrete CNI, a product of Master Builders, Inc. Both are packaged in liquid form containing a minimum of 30% calcium nitrite.

2.2.3 *Rheocrete 222+*

Rheocrete 222+ is an organic based corrosion-inhibiting admixture (OCIA) produced by Master Builders, Inc. Rheocrete 222+ is a combination of amines and esters in a water medium. According to the manufacturer, Rheocrete 222+ extends the service life of reinforced concrete by slowing the ingress of chlorides and moisture into the concrete. The admixture also forms a strong, durable protective film on the reinforcing steel to provide a second level of protection.

This protective layer prevents electrochemical reactions at both the anode and the cathode (Nmai et al. 1992). Unlike nitrite based corrosion inhibitors, there is no competing reaction between the organic corrosion inhibitor and chlorides. Therefore,

there is no need to estimate the amount of chlorides that will be present in a structure. The dosage is one gallon per cubic yard of concrete. Organic corrosion inhibitors work well in cracked concrete. The barrier that is formed continues to work even when chlorides have a direct path to reinforcing steel through a crack in the cover concrete (Holland 1992).

Research by Nmai et al. (1992) shows that OCIA do not significantly influence the plastic or hardened properties of concrete. The use of OCIA may require increasing air-entraining admixture to achieve a specific air content. Their data also suggest that chloride threshold for OCIA treated concrete is 12.0 lb/yd³.

2.2.4 Ferrogard 901

Ferrogard 901 is a liquid concrete admixture produced by Sika Corp. Ferrogard 901 uses a combination of organic and inorganic inhibitors to protect embedded reinforcing steel from corrosion. Much like Rheocrete 222+, Ferrogard 901 also influences the anodic and cathodic reaction of reinforcing steel in concrete. The product forms a film on the steel surface which delays the onset of corrosion and reduces the rate of corrosion (Sika, 2003).

2.2.5 Xypex Admix C-2000

According to the manufacturer, Xypex Admix C-2000 is a dry powder consisting of Portland cement, very fine treated silica sand and various active, proprietary chemicals. These chemicals react with the moisture in fresh concrete and with the by-products of cement hydration to cause a catalytic reaction. This reaction generates a non-soluble crystalline formation throughout the pores and capillary tracts of the concrete. The

manufacturer lists many advantages provided by their product. They claim the concrete becomes permanently sealed against penetration of water or liquids from any direction, yet allows the concrete to breath. The concrete is protected from deterioration due to harsh environmental conditions and can seal hairline cracks up to 0.0158 in. (0.4 mm) (Xypex Chemical Corp, 1999).

2.2.6 *Fly Ash*

Fly ash is the most widely used mineral admixture in concrete. Fly ash is a pozzolanic material that can be used as replacement for a portion of the cement content. Fly ash is primarily silicate glass containing silica, alumina, iron, and calcium. It is collected from the exhaust gases produced from pulverized coal in electric power generating plants. The majority of fly ash particles are solid spheres with a diameter under 0.8×10^{-3} in. ($20 \mu m$). The typical surface area is 1464.7 ft²/lb to 2441.2 ft²/lb (300 m²/kg to 500 m²/kg). There are two types of fly ash, Class F and Class C. Class F fly ash is generally low-calcium (less than 10% CaO) and usually has less than 5% carbon. In certain cases the carbon content may be as high as 10%. Class C is a high-calcium (10% to 30% CaO) fly ash with the carbon contents usually less than 2% (Kosmatka & Panarese 1994).

Replacing Portland cement with fly ash often improves later-age compressive strength if adequate moisture and free lime are present (Keck 2001). Fly ash replacement of cement provides greater hydration and less permeability. Fly ash replacement causes significant pore refinement, reduced permeability to water and chloride ions, and increased electrical resistivity. The tighter pore structure is more beneficial than the potentially negative effect of the decrease in pH of the pore solution.

The pH is a measure of the concentration of hydroxide ions. The pH is reduced because fly ash (pozzolans in general) reacts with calcium hydroxide, tying up the hydroxide ion. The decrease in pH is small, so the result is only slightly negative. Fly ash's ability to tie up chloride ions has a positive effect on corrosion protection. (Kouloumbi & Batis 1992; Hussain & Rasheeduzzafar 1994).

In studies where corrosion was measured, mixtures containing fly ash typically outperformed control mixtures. It resulted in later corrosion initiation and lower corrosion rates. The recommended dosage of fly ash, to extend the time to corrosion and reduce corrosion rates, is 30% cement replacement (Civjan et al. 2003). One study found fly ash dosages as low as 10% were advantageous in reducing corrosion activity (Lee & Lee 1997), while another study indicated that concrete with moderately high w/c values and fly ash dosages of less than 15% were not effective in preventing corrosion (Berke et al. 1991).

The fly ash used in this study did not satisfy the ASTM requirements as either Class F or Class C. The chemical composition of the fly ash used in this study is presented in Table 2.1. The specimens using fly ash had cement replacement percentages of 5, 10, and 15%. The fly ash used was collected from a Honolulu coal plant (Pham & Newtonson 2001).

Table 2.1: Fly ash chemical composition.

Chemical composition (%)		ASTM C 618-97 Specifications	
		Class F	Class C
	Hawaiian fly ash		
Total silica, aluminum, iron	56.09	70.0 Min	50.0 Min
Sulfur trioxide	9.85	5.0 Max	5.0 Max
Calcium oxide	25.99		
Moisture content	0.10	3.0 Max	3.0 Max
Loss on ignition	2.81	6.0 Max	6.0 Max
Available alkalis	1.26	1.5 Max	1.5 Max

2.2.7 *Silica Fume*

Silica fume is also a pozzolanic material. It is a product of the reduction of high purity quartz with coal in an electric arc furnace. It rises as an oxidized vapor from the furnace, cools and condenses, and is collected in filter bags. Unlike fly ash, silica fume is a very fine material with particles less than 0.04×10^{-3} in. ($1 \mu\text{m}$) in diameter. Silica fume has a surface area of $97684.5 \text{ ft}^2/\text{lb}$ ($20,000 \text{ m}^2/\text{kg}$) (Kosmatka & Panarese 1994).

Silica reacts with free lime during hydration of cement. This chemical reaction improves concrete strength and may improve aggregate-paste bonding. This reaction reduces the pH of the pore fluid in a similar manner to fly ash. While high pH provides protection of embedded reinforcing steel, silica fume is still an effective corrosion inhibitor in concrete (Wolsiefer 1993).

Reported literature showed silica fume used as an admixture or cement additive would enhance concrete's resistance to chloride induced corrosion especially at early ages. The resistance is enhanced because silica fume has the ability to improve the density of the concrete pore structure, which increases the time it takes chlorides to reach the reinforcing steel. The reduction of permeability can be improved by increasing the amount of silica fume used, reducing w/c, and increasing curing times (Civjan et al. 2003).

In long term chloride ponding tests, silica fume specimens had 90% to 98% lower chloride concentrations at the level of the reinforcing steel than the control specimens. High silica fume dosages were not necessary for maximum protection. An optimal dosage of 10% to 15% cement replacement has been indicated for moderate w/c concrete. In field application of a period of over twenty years, well-mixed silica fume concretes

with low w/c (less than 0.40) have performed very well, even in hostile environments. Proper curing is essential to prevent initial cracking. Cracking negates any benefits the silica fume provides (Civjan et al. 2003).

The silica fume used in this study is Force 10,000D, a product of W.R. Grace & Co. Silica fume was introduced into the concrete mixtures by replacing 5, 10, and 15% of cement by mass (Pham & Newton 2001).

2.2.8 Latex-Modifier

Latex is a colloidal suspension of polymer in water. It is added to concrete to produce latex-modified concrete. It is believed that the polymer forms a continuous polymer film within the paste. Latex also modifies the pore structure of concrete and reduces its permeability, increasing the corrosion-resisting capabilities of the concrete. According to Ohama (1987), the flexibility of the polymer increases the tensile strength of concrete, which reduces cracking, and improves resistance to environmental attacks (Pham & Newton, 2001).

2.3 Testing

Several tests were performed to evaluate the effectiveness of corrosion resistance properties of concrete. Both chemical and electrical tests were used. The electrical tests were used to detect the initiation of corrosion and to make sure that the results were reliable. Each of these tests are described in the following sections.

2.3.1 Air permeability test

Two methods are available to measure air permeability of concrete, output and input methods (Dhir et al. 1995). The output method is a direct measurement of

permeability of concrete using Darcy's law. Usually the output method uses a specimen with a circumferential surface that is sealed and is subjected to an external constant pressure at one end. The other end is open to normal atmospheric pressure. The flow rate is measured when the inlet flow rate equals the outlet flow rate (Dhir et al. 1989). Output methods are accurate, but time consuming. Another drawback of outputs test are that they cannot be used on in-situ concrete (Dhir et al. 1995).

Input methods are designed to measure the rate of upstream pressure change when applied pressure is removed. The first input method was proposed by Figg (1973). The input method has been altered and refined by many different authors since Figg's first proposal. Figg's method was based on applying low pressure to a drilled hole in concrete using a hand vacuum. The measure of the air permeability of the concrete was taken as the elapsed time for the pressure to increase from -7.98 psi to -7.25 psi (-55KPa to -50KPa). Input methods are fast and can be applied to in-situ concrete. Input methods also have drawbacks (Dhir et al. 1995). Some older methods do not take into account the influence of moisture content, and the techniques are partially destructive (Figg 1973). New methods continue to improve the effectiveness and ease of use, but no method has yet been developed to perfect the test.

Table 2.2 shows the categories of protection relating to the Figg number. A Figg number less than 30 indicates the protective quality to be poor. A value of 31-100 indicates the protective quality to be not very good. A value of 101-300 indicates fair protective quality. A value of 301-1000 indicates good protective quality. A value above 1000 means the concrete has excellent protective quality.

Table 2.2 : Values of permeability and concrete ratings (Poroscope Plus 1998)

Concrete Category	Protective Quality	Permeability (Figg number)
0	Poor	<30
1	Not very good	31-100
2	Fair	101-300
3	Good	301-1000
4	Excellent	>1000

2.3.2 *Electrical tests*

A series of electrical tests were performed on the concrete specimens to determine the performance of the corrosion inhibiting admixtures. These electrical tests include half-cell potential, polarization resistance, resistivity measurements, and macrocell current.

2.3.2.1 *Half-Cell Potential*

This test is a measure of the relationship between a standard reference electrode on the concrete surface and the potential difference set-up between the anodic and cathodic area (Dhir et al. 1993). In this technique, the corrosion potential of the reinforcing steel is measured with respect to a standard reference electrode such as saturated calomel electrode, copper/copper-sulphate electrode, silver-silver chloride electrode etc. (Srinivasan et al. 1994). This test is described in ASTM C876, “Standard Test Method for Half-Cell Potential of Reinforcing Steel in Concrete.” Test results indicate the likelihood of corrosion on the reinforcing steel within the concrete. One drawback of the half cell potential test is the need to access the reinforcing steel. Once the potential measurements are obtained, they can be interpreted using Table 2.3.

Table 2.3: Limiting values for the interpretation of Half-cell potential results

Measured potential (mV)	Statistical risk of corrosion occurring (%)
< -350	90
Between -350 and -200	Uncertain
> -200	10

The half-cell potential test has many advantages. It is inexpensive due to the simple equipment used, large structures can be easily and quickly surveyed, and data obtained from the test are straight forward and simple to interpret. According to some studies of corrosion in marine areas, there are some disadvantages as well. Potential measurement alone cannot give an absolute indication of the condition of reinforcing embedded in concrete (Srinivasan et al. 1994). In a study of corrosion in marine areas, Sharp et al. (1988) used both electropotential and resistivity measurements. The measurements were confirmed by physical examination of the embedded steel. The study concluded that the correlation between test results and actual corrosion was moderate, suggesting that more investigation into the accuracy of these test methods is required (Sharp et al. 1988).

2.3.2.2 *Macrocell Current*

Macrocell corrosion current is created between two layers of reinforcing steel. The current measurement provides an indication of the amount of the weight of reinforcing steel that is consumed by the corrosion process. The test measures the coupled current formed by the top layer of steel being exposed to a chloride rich environment, while the bottom reinforcement is exposed to a low chloride environment. The top steel acts as the anode, and the bottom steel is the cathode. A resistor connects

the top and bottom layers of steel, and voltage is measured across the resistor (ASTM G 109-92; Civjan et al. 2003).

The macrocell current method is a low-cost, simple, and reliable test method. Studies have found a good correlation between macrocell corrosion measured in a slab and the corresponding corrosion found on the anodic reinforcing steel after removal (Civjan et al. 2003). Other studies have noticed that the macrocell technique appears to underestimate the corrosion rate, at times by an order of magnitude (Berke et al. 1990).

2.3.3 *Chemical Test*

Two types of chemical tests were performed on the concrete specimens in this study. They are pH tests and chloride concentration tests.

2.3.3.1 *pH Test*

It is important to assess the pH of concrete surrounding the reinforcing steel because concrete has a high alkalinity ($\text{pH} > 12$), which causes it to be a natural corrosion inhibitor. The process of obtaining the pH of a concrete specimen requires that a sample of the concrete be added to an aqueous solution to form a slurry. The concrete specimen is cracked open and the concrete surrounding the reinforcing steel is ground into a powder. The powder sample is mixed with distilled water using a ratio of 1 ml of distilled water per gram of concrete powder. After the solution is uniformly mixed, a pH meter is dipped into the slurry to determine the pH.

2.3.3.2 *Chloride Concentration Test*

Two methods are available to measure chloride concentrations, measurements of water-soluble chlorides and measurements of the total-chloride. In the water-soluble

method, a sample of concrete powder is boiled in water for five minutes, and then soaked in water for 24 hours. The chloride concentration of the water solution is used to determine the chloride concentration in the concrete. In the total-chloride concentration method, concrete powder is mixed into an extraction liquid such as nitric acid, and a testing meter is placed in the solution to determine the level of chloride concentration (Pham & Newton 2001). Results are then compared to recommended safe limits of chloride content from ACI 318-99. These limits are presented in Table 2.2.

Table 2.4 : Limits for water-soluble chloride-ion content in concrete (ACI 318-99)

Type of member	Maximum water-soluble chloride ion content, percent by mass of cement
Prestressed concrete	0.06
Reinforced concrete exposed to chloride	0.15
Reinforced concrete that will be dry or protected from moisture in service	1.00
Other reinforced concrete construction	0.30

2.4 Microscopy

2.4.1 Acoustic Microscopy

Acoustic microscopy is a non-destructive method that can obtain comparable resolutions to an optical microscope. There are two advantages for using acoustic waves for producing images. Ultrasonic waves can penetrate materials that are opaque to other kinds of radiation, such as light. The second advantage is the ability to contrast mechanical properties of materials such as steels, alloys, and ceramics (Briggs 1985).

Acoustic microscopes used to describe elastic properties can be used for conventional and time-resolved microscopy. In conventional acoustic microscopy a

sound wave is focused on a specimen using an acoustic lens. The same lens is used to record the reflected signal from the sample. A liquid couplant, usually water, is put between the lens and specimen. Variations in mechanical properties with depth can be seen with different reflected signals. In time-resolved acoustic microscopy a short sound pulse is sent toward the specimen. The time of flight method uses the acoustical constraint to describe the time required for the signal sent into the specimen to return to the acoustic lens (Zinin et al. 2004)

2.4.2 Stereozoom Microscopy

The first stereozoom microscope was manufactured in the 1960's by Bausch & Lomb. Since that first design, nearly all other microscope manufacturers have created competitive models similar to the original. Stereomicroscopes have a lower upper magnification range in comparison with other microscopes. The modest magnification ranges lead to a simpler design, which means less complex optical components while being able to get useful zoom ranges (Gray 1973).

CHAPTER 3 - DURABILITY STUDY – CYCLIC PONDING

3.1 Introduction

This chapter describes the specimens and procedures used in the accelerated corrosion testing program conducted in the laboratory. The process of preparing the materials, mixing, and curing of the concrete specimens is described. The various tests performed on the specimens are also described.

3.2 ASTM G 109-92 Test Procedure

In the ASTM G 109-92 test method, three No.4 (0.5 inch diameter) reinforcement bars 14 inches long are used. The test specimens were modified slightly from the standard test procedure by installing an additional top reinforcing bar (Figure 3.1). The purpose of this modification was to allow for half cell readings of the top reinforcing bars using a GECOR-9.

The specimens were prepared according to ASTM G 109-92 guidelines. A 10% (by weight) sulfuric acid bath was used to pickle the bars. The reinforcement was dried and then wire brushed. Ends of the bars were taped for three inches from each end using non-conductive electroplater's tape. When the ends were taped there were 8 inches of exposed length. The tape was used to protect the steel from corroding during curing. The bars were inserted into molds and concrete were cast and cured. After stripping the form work, the sides were sealed with epoxy coating. Each specimen is 11 x 6 x 4.5 inches in size Figure 3.1.

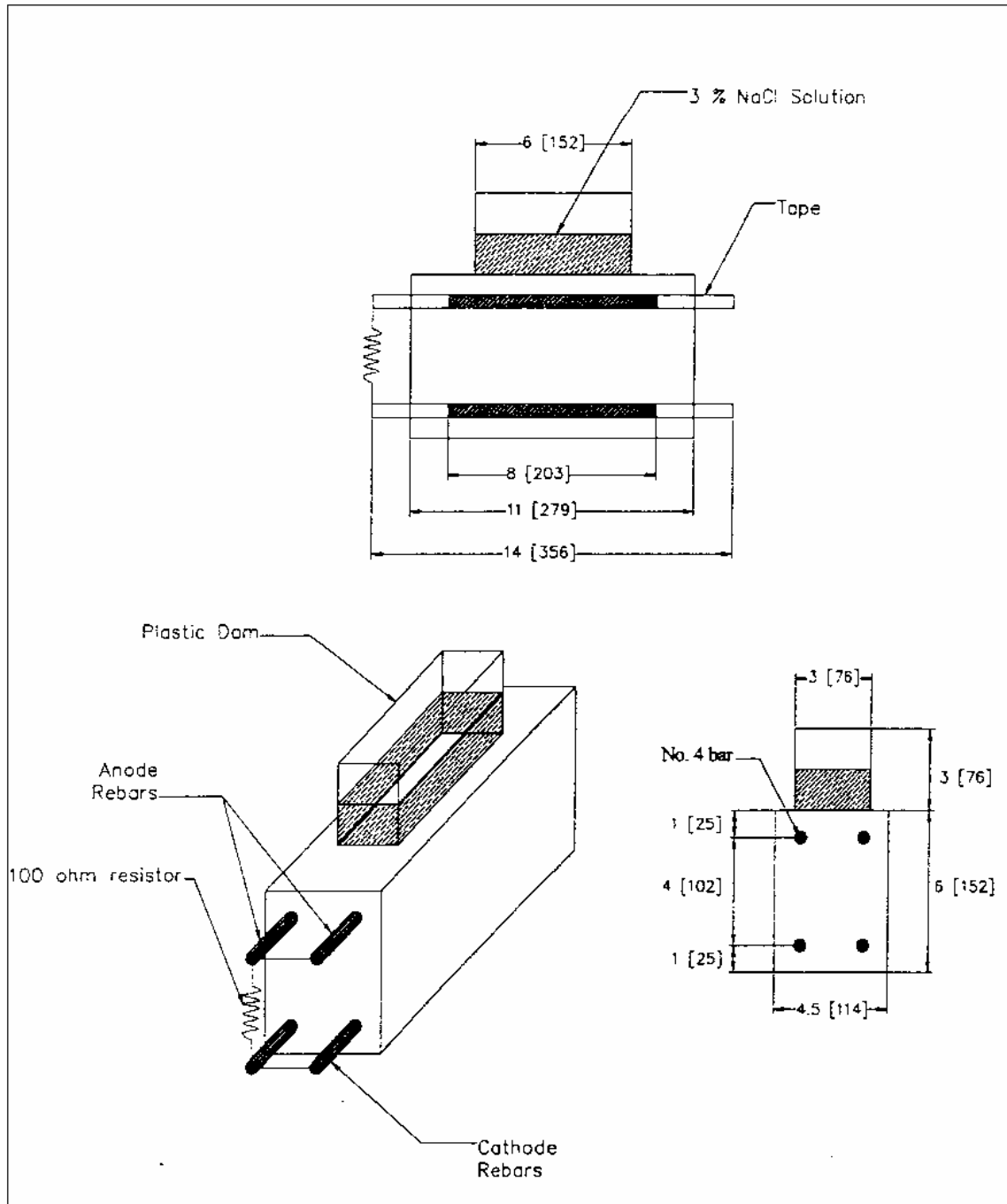


Figure 3.1: Details and dimensions (inch (mm)) of beam specimens

A plastic dam was sealed to the top of the specimen to hold approximately 400mL of a 3% NaCl solution. The plastic dams are 3 in. (76 mm) wide, 6 in. (150 mm) long, and 3 in. (76 mm) tall. Silicon glue was used on the outside of the dams to seal the top surface of the concrete to the bottom of the dam. The four vertical sides and the top surface outside of the dam were sealed with epoxy. The concrete inside the dam and the bottom of the specimen were the only surfaces not sealed with epoxy. Ground clamps were attached to each bar and a 100-ohm resistor that connects the bottom and top bars. The specimens were supported on two strips of wood or something comparable at least .5 inches thick. These supports allowed air to flow under most of the specimen. The specimen was ponded for two weeks at $23 \pm 3^{\circ}C$ ($73 \pm 3^{\circ}F$) with the salt water solution. The relative humidity fell into the range of $50 \pm 5\%$. A transparent plastic covering was placed over the dams to minimize evaporation. After two weeks the water was vacuumed off and samples were allowed to dry for two weeks. The cycle was repeated until failure. A high impedance voltmeter (at least one Mohm) was used to monitor the specimens. The current was measured every four weeks (one cycle), the first measurement occurred one week after the first introduction to the salt water solution. The specimens were monitored until the average macrocell current of the specimens is $10 \mu A$ or greater, and at least half the samples showed macrocell currents equal to or greater than $10 \mu A$. The monitoring was continued for three complete cycles to ensure the presence of enough corrosion for visual inspection.

3.3 Specimens

All of the specimens were developed, mixed, and cast at the UH Structures Laboratory (Pham & Newton 2001; Okunaga, Robertson, & Newton 2004). The

modifications include reinforcement balanced with two No. 4 bars (0.5 inches; 13 mm diameter) located 1 inch from the top and two No. 4 bars 1 inch from the bottom (Figure 3.1). Since two anode bars are required to measure the polarization resistance, the specimens were modified from the standard ASTM G 109 -92 specimen which has only one top bar. Twelve specimens were produced for the mixtures Control 1 to Control 6, DCI 1 to DCI 6, SF1 to SF7, and L1 to L6, while four specimens were produced for the other mixtures. Of the 12 specimens, 4 were used for periodic measurements of chloride concentration, permeability, and pH. The remaining 8 were used for the ponding cycling (Pham, Newtonson 2001).

After curing, the specimens were allowed to dry. Plastic dams were then added to the top of the specimens. The four vertical sides and the top surface outside of the dam were sealed with epoxy. Once the epoxy coating was dry the specimens were placed in the basement of the structures lab in Holmes Hall. The temperature and relative humidity in the basement are reasonably stable at 73°F (27.8°C) and 54%, respectively. To initiate the corrosion process 0.106 gal (400 ml) of a 3% NaCl solution was poured into each plastic dam. After two weeks the water was removed and the specimen was allowed to dry for two weeks. Two weeks of the water ponding and two weeks of the drying completed one ponding cycle. The cycle was repeated until the specimen was considered to have failed according to the ASTM G 109 test procedure, or was removed for other test reasons.

To measure the current specified in ASTM G 109, the tape at one end of each bar was cut and the end cleaned to facilitate an electrical connection. A 100-ohm resistor and two electrical wires were spot welded to the four ends of the reinforcing bars for each

concrete specimen. This circuit is shown Figure 3.1. Voltage readings are taken across this resistor to determine the macrocell current.

3.4 Concrete Mixtures

The concrete mixtures were designed using different water-cement ratios, paste content, aggregates, and admixture concentrations.

Three different types of fine aggregates were used in the concrete mixtures. The first was dune sand from an aeolian deposit of coral on the island of Maui. The second was crushed basalt from the Kapaa quarry on the island of Oahu. The third was crushed basalt from the Halawa quarry on the island of Oahu. The grain size distribution and fineness modulus for all the sands were determined according to ASTM C 136. Appendix B provides details of the aggregates used (Pham and Newton 2001).

Two types of coarse aggregate were used in the concrete mixtures. One was crushed basalt from the Kapaa quarry on the island of Oahu. The second was crushed basalt from the Halawa quarry on the island of Oahu.

Table 3.1 shows the types of admixture and number of specimens created for each mixture. On the left hand side of Table 3.1 are the types of admixtures used. The specimens that used the Kapaa quarry aggregate are located on the top half of the table. The specimens that used the Halawa aggregate are on the bottom half of the table. The right hand side of the table shows the total specimens prepared for the project. Table 3.2 shows the specimens used in this study. This study only incorporates 116 of the total 656 possible specimens.

Table 3.1 : Total number of specimens

	Agg.	Mix 1	Mix 2	Mix 3	Mix 4	Mix 5	Mix 6	Mix 7	Mix 8	Mix 9	Mix 10	Mix 11	Total
Control	Kapaa	8	8	8	8	8	8						48
DCI	Kapaa	8	8	8	8	8	8						48
CNI	Kapaa	8	8	8	8	8	8						48
Rheocrete 222+	Kapaa	8	8	8	8	8	8						48
FerroGard 901	Kapaa	8	8	8	8	8	8						48
Xypex Admix C-2000	Kapaa	8	8	8	8	8	8						48
Latex Modifier	Kapaa	8	8	8	8	8	8						48
Fly Ash	Kapaa	8	8	8	8	8	8	8	8	8	8	8	88
Silica Fume	Kapaa	8	8	8	8	8	8	8	8	8	8	8	88
Hcontrol	Halawa	4	4	4	4	4	4						24
HCNI	Halawa	4	4	4	4	4	4						24
Hrheo	Halawa	4	4	4	4	4	4						24
HFA	Halawa		4	4	4	4	4	4	4				28
HSF	Halawa	4	4	4	4	4	4						24
HSF-MB	Halawa		4	4		4	4	4					20
													656

Table 3.2 : Specimens included in this study

	Agg.	Mix 1	Mix 2	Mix 3	Mix 4	Mix 5	Mix 6	Mix 7	Mix 8	Mix 9	Mix 10	Mix 11	Total
Control	Kapaa	5	5	2	6								18
DCI	Kapaa	3	2	1	1	1	1						9
CNI	Kapaa												
Rheocrete 222+	Kapaa	1	1	1	1	1	1						6
FerroGard 901	Kapaa	1	2	1	1	5	1						11
Xypex Admix C-2000	Kapaa	4	4		4	4							16
Latex Modifier	Kapaa	7	1	2		1	1						12
Fly Ash	Kapaa					4	1			1	1		7
Silica Fume	Kapaa	1	2	1	1	3	2	2					12
Hcontrol	Halawa	4	4		1	4							13
HCNI	Halawa												0
Hrheo	Halawa				4	4							8
HFA	Halawa					4							4
HSF	Halawa												
HSF-Rh	Halawa												
													116

3.5 Test Procedures

The electrical tests that were performed for the corrosion testing include half-cell potential, and macrocell current. There were two half cell potential tests performed, the first was by a GECOR-9. The GECOR measured the polarization resistance, resistivity, and half cell values on the majority of the specimens until the machine failed and was not repaired. Those results are presented by Okunaga et al. (2004). The second half cell potential readings were taken only on specimens that were broken open to verify the extent of corrosion. A calomel reference electrode was used in the second case and the values were converted to copper-copper sulfate equivalents. The macrocell current measurements are applicable to all the specimens. All macrocell readings are presented by Okunaga et al. (2004). Macrocell readings are presented here only for the specimens related to this study.

Two chemical tests that were performed for this study were a pH test and a chloride concentration test. Because the natural alkalinity of concrete ($\text{pH} > 12$) inhibits corrosion of reinforcing steel, it is important to assess the actual pH of the concrete at the level of the top reinforcing bars. The method to obtain the pH of concrete was the same as for an aqueous solution. Concrete powder at the area surrounding reinforcing steel was collected and mixed with distilled water (1 ml of distilled water per gram of concrete powder). A pH meter was dipped in the solution to measure the pH (Pham and Newtonson 2001). The chloride concentration test was performed on dust samples collected by drilling a .039 in. (10mm) diameter hole between .75 inches and 1.25 inches deep. These samples were mixed with extraction liquid and the chloride concentration were determined using the Chloride Test System.

The last test performed was an air permeability test. A .039 in. (10mm) hole was drilled to a depth of 1.57 in. (40mm) and a .079 in. (20mm) rubber plug was inserted into the hole. A needle was inserted to vacuum air out of the hole. The value measured quantifies the porosity of the specimen.

3.5.1 *Half cell measurement*

The half cell measurements were taken with a calomel reference electrode. Six readings were taken per specimen. Three readings were taken over each of the top reinforcing bars at approximately 3 in., 5.5 in., and 8 inches from the front of the specimen (Figure 3.2). The values were recorded and later converted to a copper-copper sulfate equivalent. The conversion to convert calomel reference electrode to copper-copper sulfate is to add -0.077 mV to calomel values (Corrosion Doctors 2004).

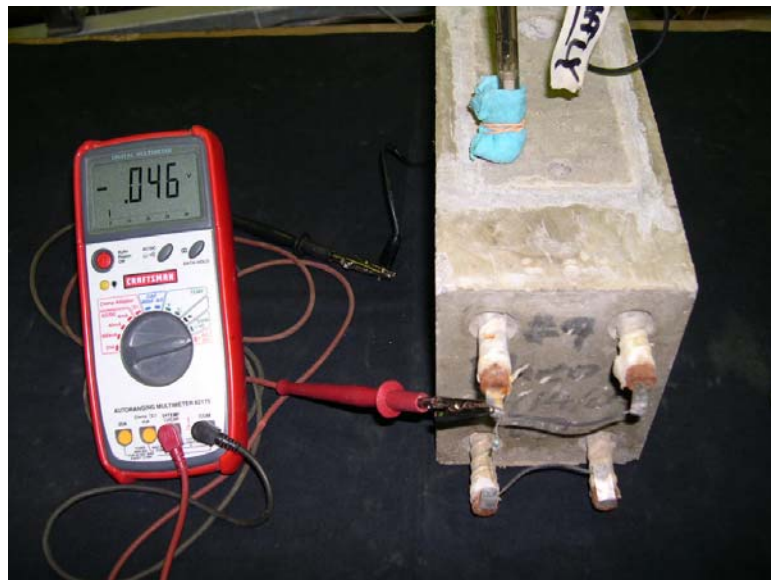
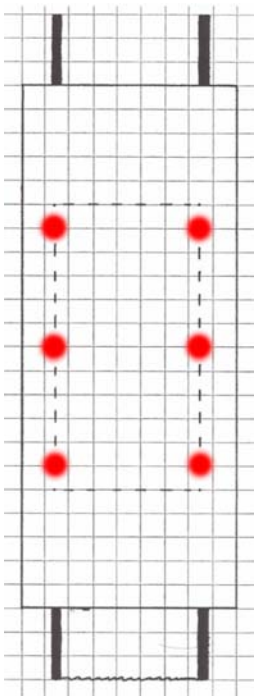


Figure 3.2 : Points where half cell reading were taken (left), half cell set up (right)

3.5.2 *Macrocell current*

Macrocell corrosion current is created between two layers of reinforcing steel. It measures the weight of reinforcing steel that is consumed by the corrosion process. The test measures the coupled current formed by the top layer of steel being exposed to a chloride rich environment, while the bottom reinforcement is exposed to a low chloride environment. The top steel acts as the anode, and the bottom steel is the cathode. A resistor connects the top and bottom layers of steel, and the voltage is measured across the resistor (ASTM G 109 1992; Civjan et al. 2003). A Fluke 45 Dual Display Multimeter was used to take all the macrocell measurements. The measurements were taken in accordance with ASTM G 109-92 until the specimens reached failure.

3.5.3 *Chloride samples*

For each specimen tested for Cl⁻ concentration, a 0.75 in. (19mm) diameter hole was drilled between the top two reinforcing bars to obtain at least 0.106 oz. (3 grams) of concrete powder. The dust was collected by drilling vertically between .75 in. and 1.25 in. in depth. The loose dust was blown out of the hole just before reaching the .75 in. depth in order to collect the right sample. Each sample was stored in a ziploc bag until all the samples were taken. The 0.106 oz. (3 gram) sample of dust was dissolved in 0.676 fl. oz. (20 ml) of extraction liquid. After allowing approximately 15 minutes for the reaction between chloride ions and the liquid acid, the chloride concentration was measured using the Chloride Test System. The system reports the chloride content in either lbs. per cu. yd. or percentage by weight (CL-2000, James Instruments, Inc.).

3.5.4 pH Level

After completing all the tests and inspections, the pH sample could be taken. A drill was used to collect dust samples for the pH test from the concrete below the top reinforcement. A 10 mm drill bit was used to drill shallow holes at the reinforcement/concrete interface (Figure 3.3). The samples were stored in ziplock plastic bags until they were tested. A typical sample consisted of 2.5 grams of concrete dust. The amount of distilled water added to the dust was a 1 to 1 ratio of 1mL distilled water to 1 gram of dust (EPA 2002). The samples and water were stirred together and the probe was inserted into the liquid and the pH was measured using a HI 8424 portable microprocessor based pH meter.

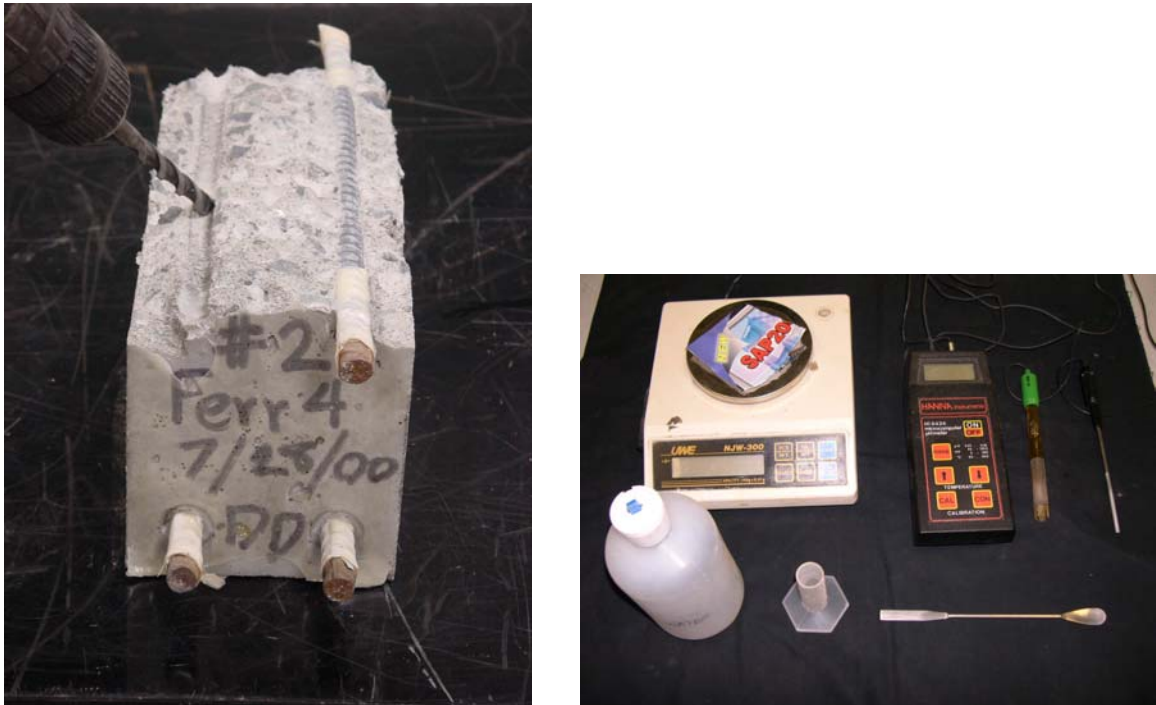


Figure 3.3 : pH sample (left), pH probe and scale (right)

3.5.5 Air permeability

To perform the air permeability test a 0.39 in. (10 mm) diameter hole was drilled to a depth of 1.58 in. (40 mm) on the top surface of each specimen. The loose dust was blown out of the hole and a molded silicon rubber plug was inserted into the hole. The top flange of the plug was secured flush to the concrete surface. Then, a needle was inserted through the plug so that the tip of the hollow needle just protrudes through the bottom of the plug. The air permeability test was performed by vacuuming the air out of the void through the needle (Figure 3.4). The air permeability test records the time it takes for the pressure in the hole to change from -7.98 psi to -7.25 psi (-55kPa to -50 kPa). The hole was drilled in the middle toward the front of the specimen. The chloride sample was drilled at the opposite end of the ponding area as shown in Figure 3.4. A Poroscope Plus was used in performing the air permeability tests (P-6050, James Instruments Inc). The testing process followed the operating instructions for the instrument.

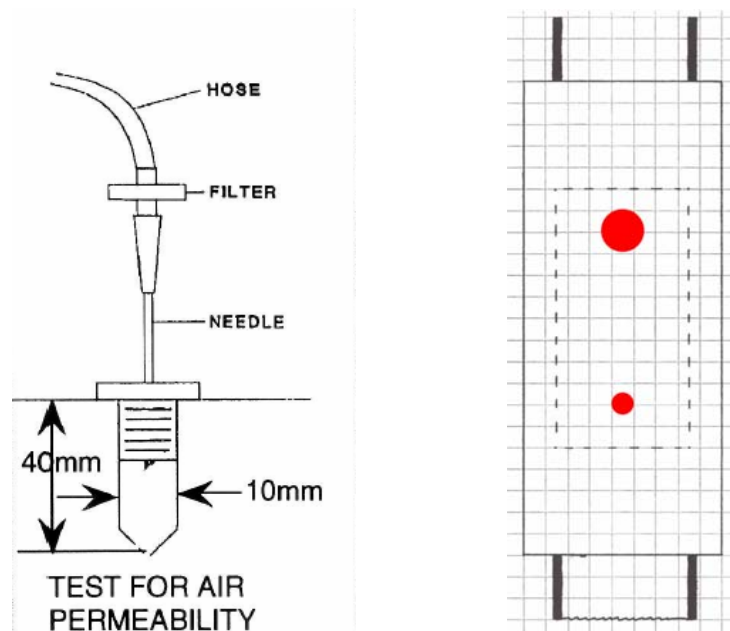


Figure 3.4 : Air permeability set up (left), approximate points were air permeability (small dot) and chlorides (big dot) were taken (right)

CHAPTER 4 - OPTICAL MICROSCOPY

4.1 Introduction

All of the specimens removed from the accelerated corrosion study, except for those used for acoustic microscopy, were inspected using a stereozoom microscope. Stereozoom microscopes do not have exceptional magnifying power. However, their design promotes simplicity while at the same time providing a useful magnification from 10X – 100X. This magnification is ample to inspect the corrosion on the reinforcing bars and the concrete macro-structure adjacent to the bars. This chapter describes the procedures for specimens inspected with optical microscopy.

4.2 Description

The majority of specimens removed from the accelerated corrosion study were inspected by carefully breaking the specimens along the top layer of reinforcing steel. A Nikon Coolpix 4300 digital camera was used with a Nikon SMZ – 2B stereoscopic microscope to examine the reinforcement/concrete interface to determine the extent of corrosion. The microscope used in this study was equipped with a 15X eyepiece, which correlates to a total magnification ranging from 12X – 75X.

4.3 Procedure

This section describes the steps taken after a specimen is removed from the corrosion study. Typically specimens were removed from the ponding cycling once a majority of the specimens had recorded macrocell currents in excess of $10 \mu A$. These specimens were then stored until final inspection. The exterior condition of each

specimen was recorded prior to splitting the specimens to inspect the top layer of reinforcing bars.

4.3.1 Exterior Visual Inspection

A thorough visual inspection was conducted of each specimen to record cracks and voids, while including side notes for future reference. Photographic records were obtained at the top surface and sides of each specimen, particularly for those with significant visual damage. The number of pictures taken depended on the amount of damage that appeared on the specimen. Figure 4.1 shows a typical specimen exterior visual record.

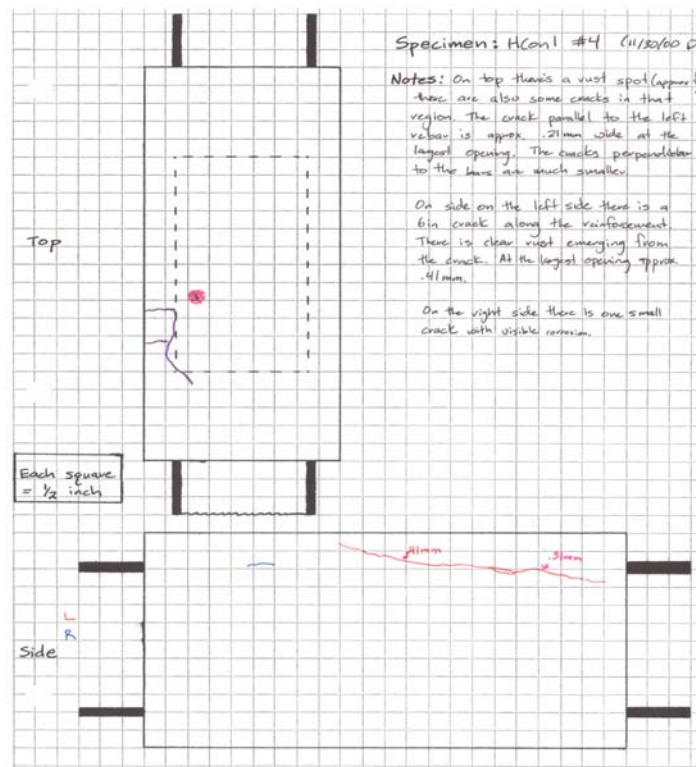


Figure 4.1 : Exterior visual inspection

4.3.2 *Splitting of the specimens*

Before the specimens were split, the top reinforcing bars and top cover were labeled to avoid confusion over orientation of the specimen pieces. The intent was to examine the interface between the steel and the concrete on both the top and the bottom of the reinforcing bars to identify corrosion and any likely causes of this corrosion. The specimens were carefully split using two channels in a compression machine (Figure 4.2). The load was increased until the specimen broke in tension along the top reinforcement layer.

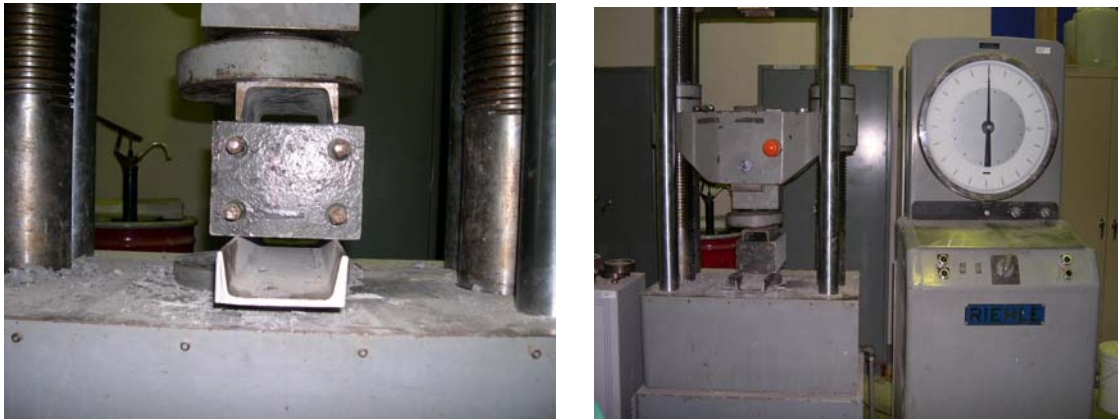


Figure 4.2 : Specimen splitting

4.3.3 *Internal Examination of the Specimens*

After the specimens were split, photographs were taken of the top piece, bottom piece, and reinforcement. A thorough visual inspection was performed and all observations recorded. Areas of particularly significant corrosion were inspected with the Nikon SMZ-2B microscope and magnified photographs taken with the Nikon Coolpix 4300 camera. The number of photographs varied with the amount of corrosion observed on the reinforcing steel.

4.4 Visual Observation Records

This section discusses the observations made during the visual and optical microscope inspections. Each specimen had two observations made, external and internal. This section describes the orientations and the nomenclature of each specimen. Figure 4.1 shows a typical exterior inspection record consisting of a top view and a side view of a particular specimen. In the top view purple lines represented cracks, light blue indicated discolorations, and red was used for both reddish discolorations and voids. On the side view, red coloring indicates cracks on the left side while blue coloring indicates cracking on the right side. In the top right hand corner the specimen label and mixing date are recorded. Areas of interest such as cracks, discolorations, and voids are described in the notes section below the specimen label.

The interior inspection was recorded in a similar manner to the external inspection. Once the specimen was split open and the bars were removed, the internal concrete could be inspected. The Figure 4.4 shows a typical interior inspection record. The block on the left side is the bottom of the specimen viewed from the above. The front of the specimen refers to the end where current measurements were taken. The top piece was oriented in the same fashion but rotated from off the bottom piece. On the right side of the page there are two full length depictions of the top reinforcing bars. The specimen label is listed below the figures along with notes about the condition of all pieces described. The interior inspection also used colors to record various observations. On the concrete section, red coloring indicates evidence of corrosion and light blue shows that voids are present at the interface between concrete and steel. On the reinforcing bars, red indicates corrosion on the top of the bar and dark blue indicates corrosion on the bottom of the bar.

In a few cases, green was also used for showing corrosion. In some specimens, the ends of the reinforcement under the electroplater's tape had corroded and were colored red. This was done for some of the early inspections because corrosion was occurring under the tape. However, after additional inspections it was noted that corrosion frequently occurred under the taped ends, so it was no longer recorded on the specimen diagrams.

Visual inspection records of both exterior and interior of all specimens are included in Appendix G. The following sections present the three selected specimens to illustrate the various degrees of corrosion observed during these inspections.

4.4.1 Specimen Xyp4 #1 with minor corrosion

The first specimen was a fairly clean sample. The external visual inspection of Xyp4 #1 is shown in Figure 4.3. The external inspection revealed cracking underneath the epoxy on the side of the specimen. In the interior inspection, there were a number of voids located on the bottom section. The majority of the voids occurred under the left reinforcing bar (Figure 4.4). The examination of the bars (Figure 4.5) revealed a small area of corrosion on the bottom of the left bar in the approximate area where a large void on the left side of the bottom piece was located (Figure 4.6). This particular specimen showed initiation of corrosion but not yet at a critical point. The specimen was removed after 31 cycles and both electrical readings fell into the lower ranges. The measured current was less than $2 \mu A$ and the half cell potential values indicated a 10% probability of corrosion.

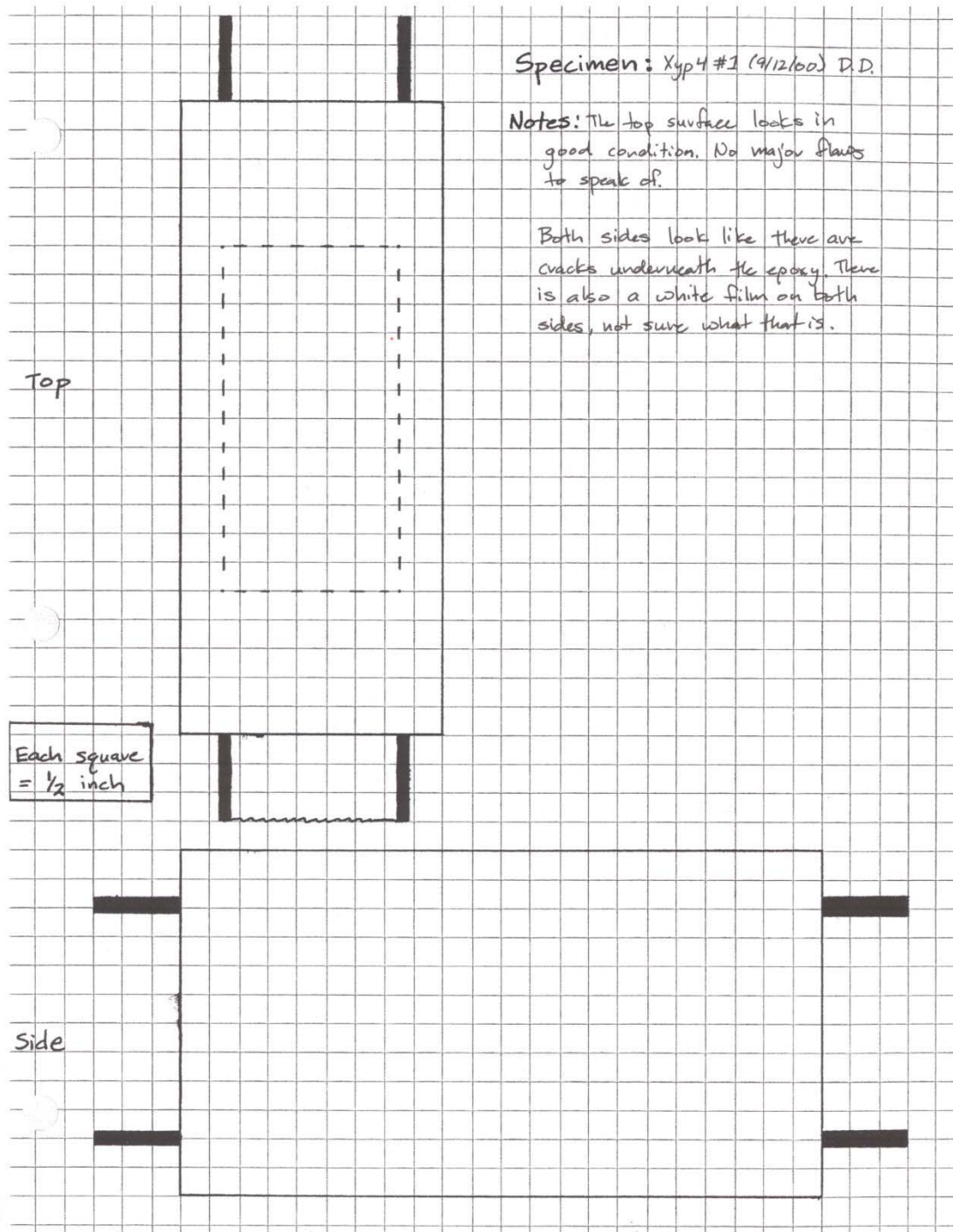
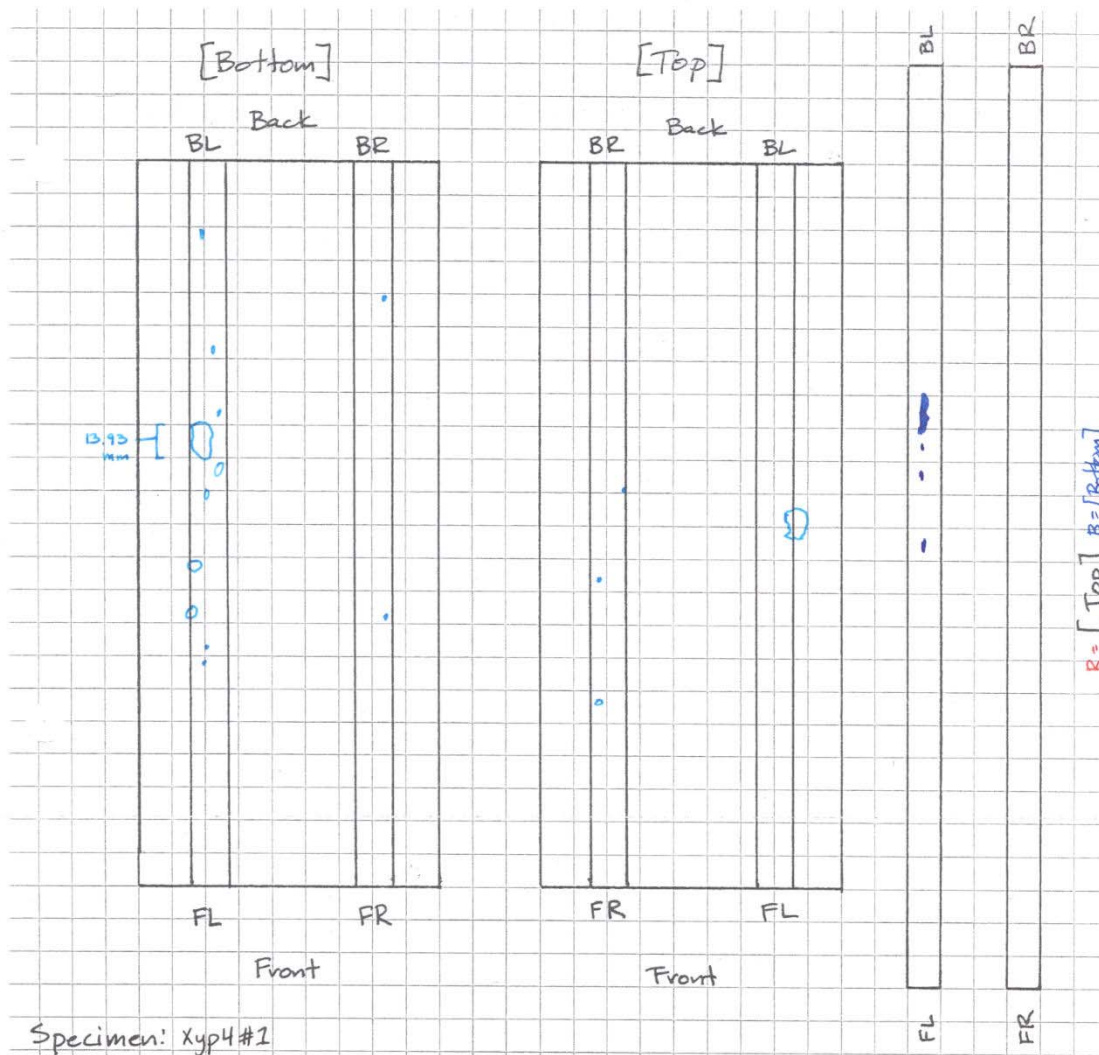


Figure 4.3 : Exterior visual inspection of Xyp4 #1



Specimen: Xyp4 #1

Notes: The top and bottom pieces are clean. The left side of both have some large voids. Only the left bar on the bottom is showing pits of orangish corrosion. The right bar is clean. Crystals and tiny voids.

Figure 4.4 : Interior inspection of Xyp4 #1

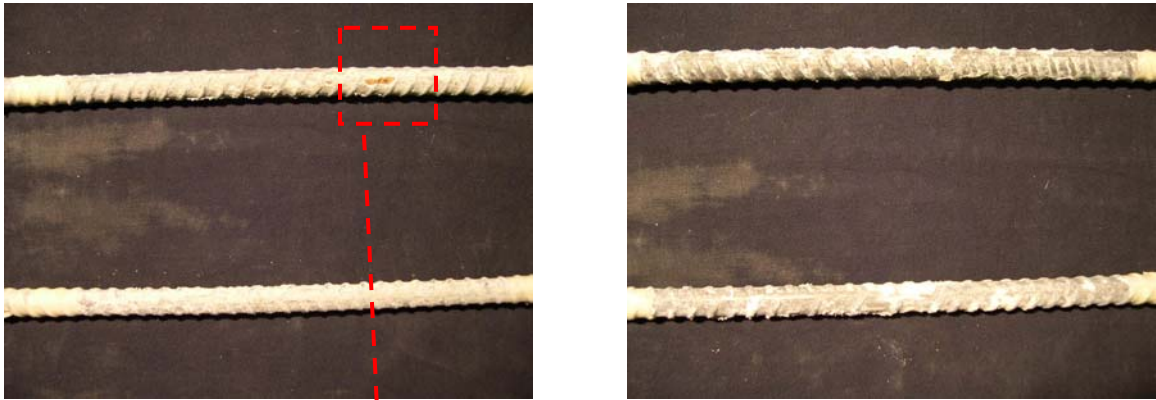


Figure 4.5 : Bottom (left) and top (right) surfaces of top reinforcing bars

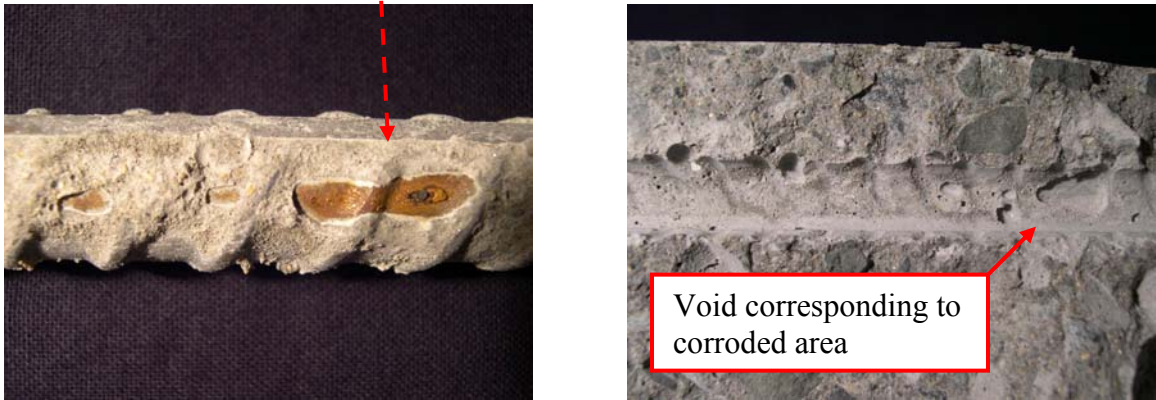


Figure 4.6 : Bottom of left reinforcing bar and corresponding concrete surface

4.4.2 Specimen Con2 #6 with moderate to significant corrosion

The second specimen was Con2 #6 which had moderate corrosion along the bottom of the reinforcing bars. The external inspection in Figure 4.7 shows that there were no major problems with the specimen. There were some blue discolorations on the left side and a few voids also on the left side. The blue discolorations were probably from the blue sponges used to take half cell readings. The internal inspection in Figure 4.8 shows numerous voids below the reinforcing bars on the bottom piece. The bottom piece was also stained by the corrosion on the bottom of the right bar. Both reinforcing

bars experienced corrosion. The bulk of the corrosion appeared on the bottom of the bars (Figure 4.9). The bottom of the left bar had multiple pits distributed along the bar. The bottom of the right bar was almost completely covered in corrosion for the full length of the bar. The top of the bar also contained some areas of corrosion along the edges and toward the front edge of the tape/bar interface (Figure 4.10).

Figure 4.9 to Figure 4.12 show examples of the corrosion occurring on both bars. Figure 4.9 shows overall views of the bottom and top view of both bars. Figure 4.10 shows the bottom of the left bar and a close up of a corrosion pit. Figure 4.11 and Figure 4.12 show close-ups of two different areas located on the bottom and inside edge of the right reinforcing bar. Figure 4.13 shows the transfer of corrosion on the bottom piece. The mixture of Con2 #6 had a water-cement ratio of 0.45 and had no admixtures to protect against corrosion. There were no cracks on the outside surface to indicate localized corrosion. There were voids on both sides of the bottom piece that appeared to contribute to the initiation of corrosion. The electrical current measured for Con2 #6 was less than $2 \mu A$ and the half cell potential readings fell into the uncertain region. The electrical results did not seem to characterize the specimen as failed but the visual results showed extensive corrosion.

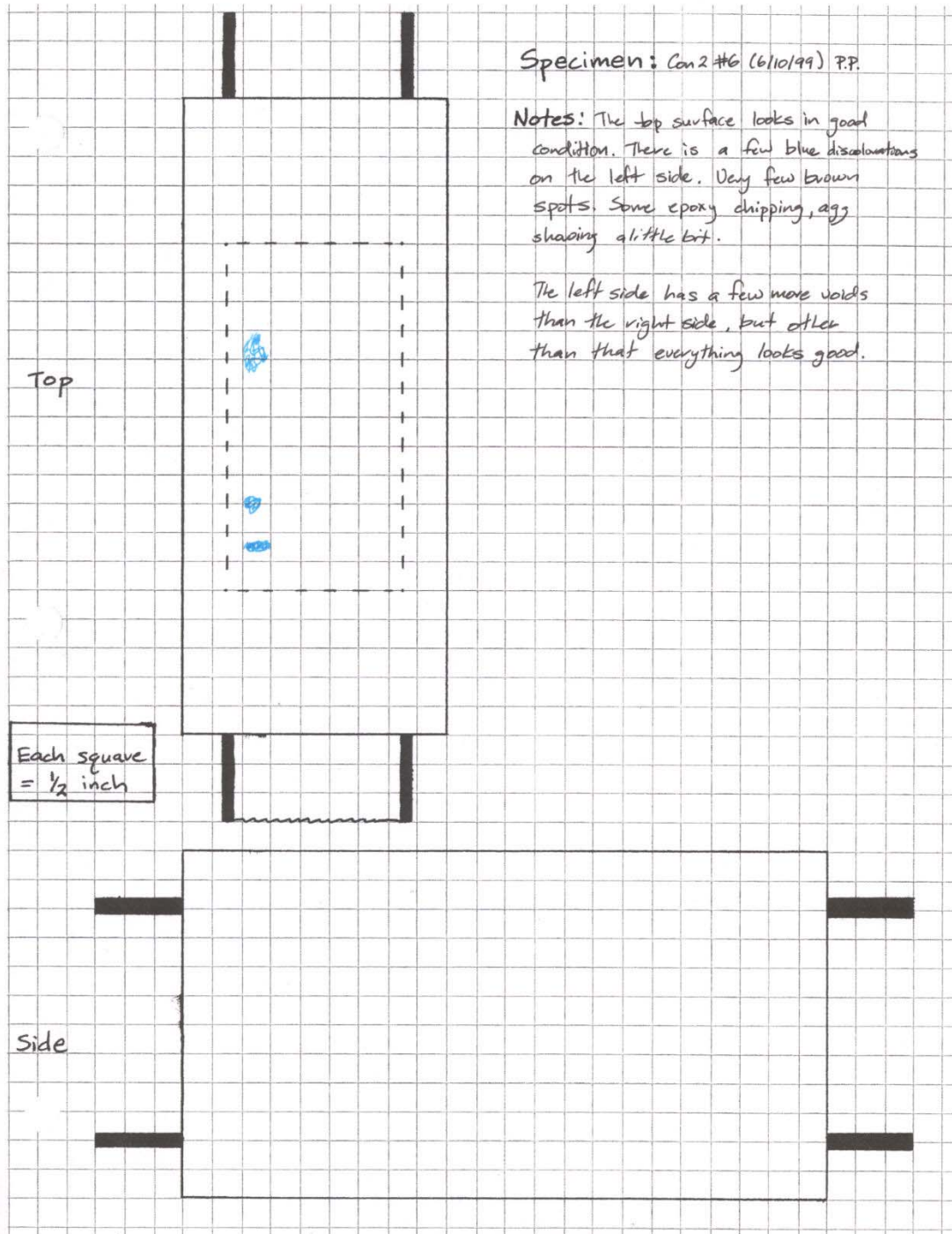
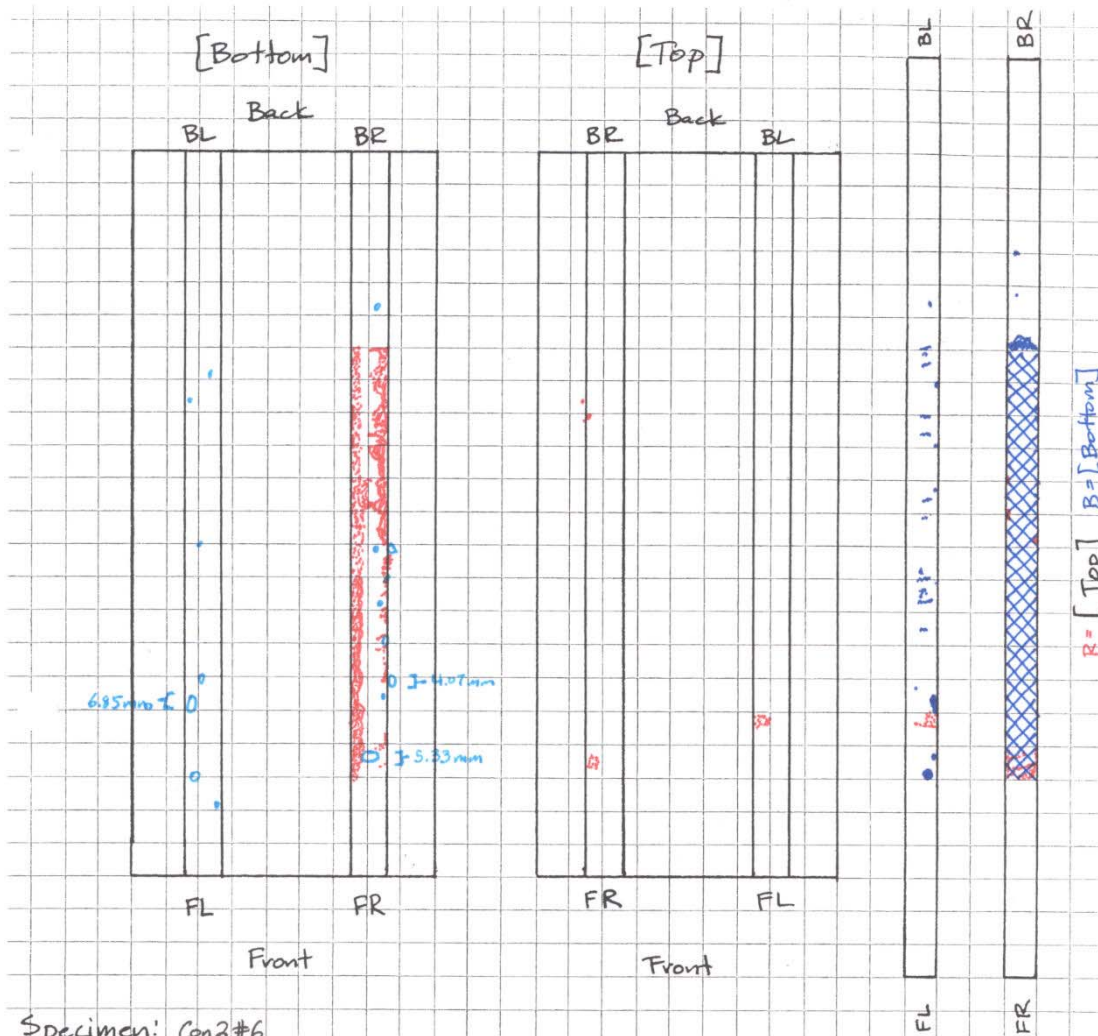


Figure 4.7 : Exterior visual inspection of Con2 #6



Specimen: Con2 #6

Notes: The bottom piece has a good variation of voids on both sides, but only the right side has corrosion. Toward the front it's light brown, as you move to the back it gets darker. The top piece has a few light spots. The left (bottom) bar has some pitting, light orange coloring. The top of the right bar has some light haze at the front face, the bottom is almost completely covered.

Figure 4.8 : Interior inspection of Con2 #6

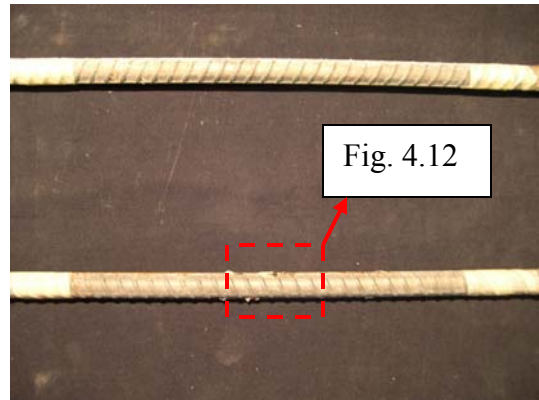
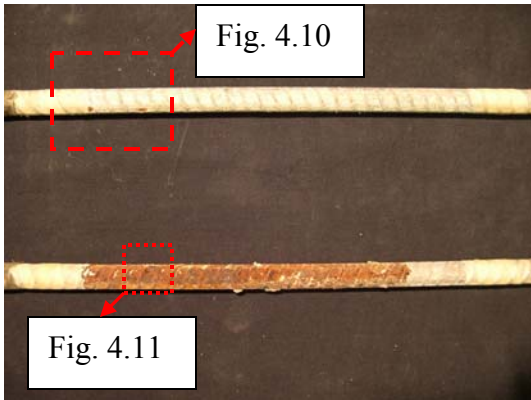
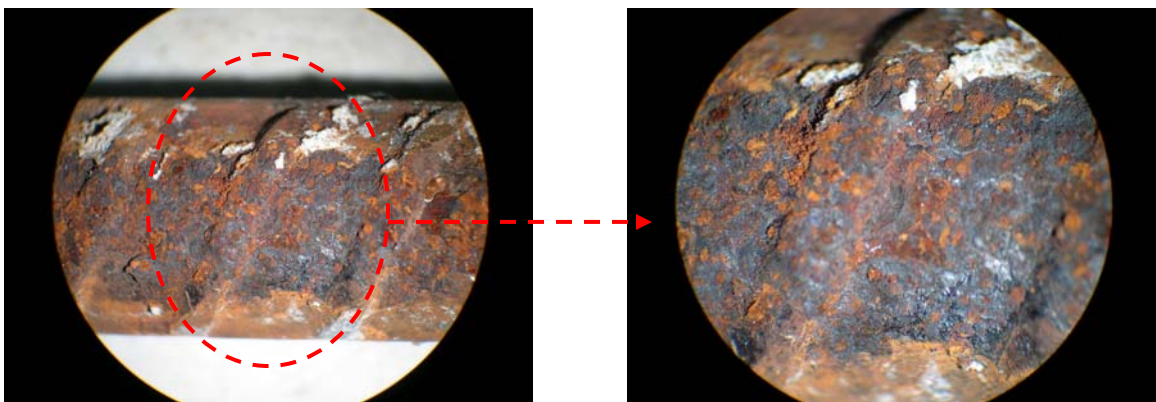
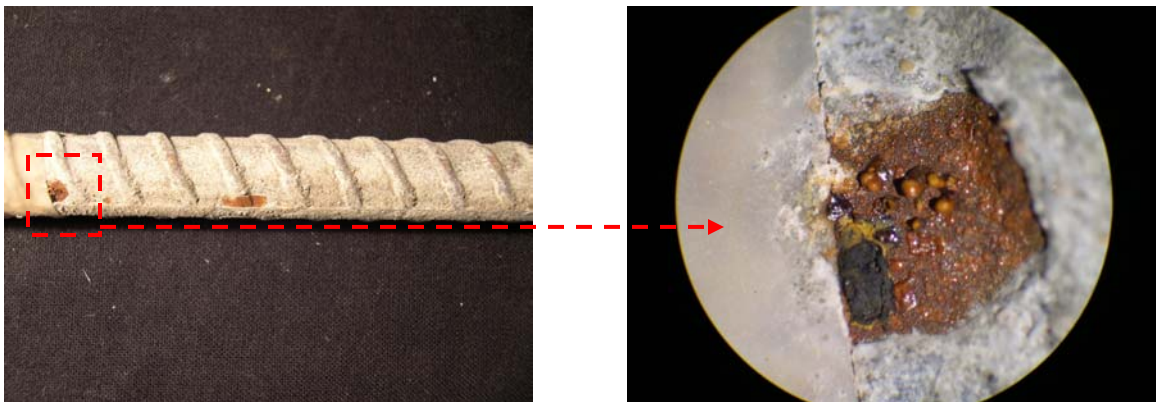


Figure 4.9 : Bottom (left) and top (right) surfaces of top reinforcing bars



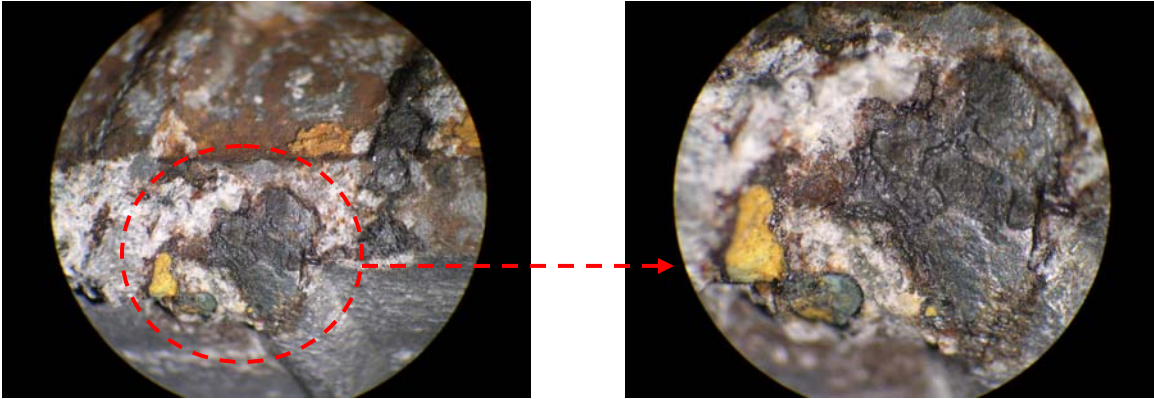


Figure 4.12 : Right bar, bottom inside edge (left) x22.5, (right) x45

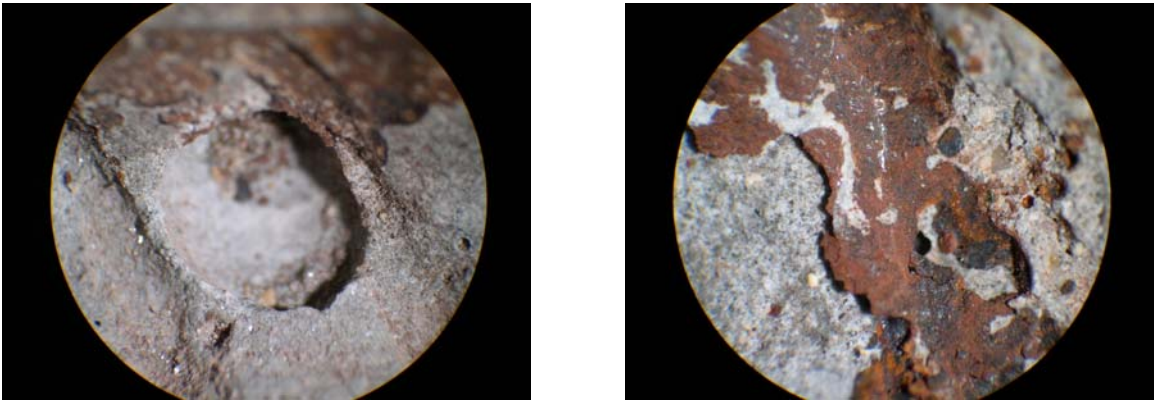


Figure 4.13 : Bottom piece, right side, corrosion on concrete (left) x22.5 (right) x45

4.4.3 Specimen FA10* #2 with moderate to significant corrosion and cracks

The exterior inspection of this specimen had cracks on the left of the top surface (Figure 4.14 and Figure 4.17). The left side of the specimen also had some small cracks underneath the epoxy (Figure 4.14). The interior inspection showed that the area where the cracks were located corresponded to significant corrosion on both the top and bottom surfaces of the left bar (Figure 4.15). The right bar had some corrosion along the bottom surface. Figure 4.16 shows the top and bottom of the reinforcing bars. Significant corrosion was noted on the left bar as shown in the magnified images in Figure 4.17 and Figure 4.18. In Figure 4.17, a close-up of the cracks can be seen on the top surface. Figure 4.19 shows the left side of the bottom piece and some of the corrosion toward the inside of the specimen. This specific mixture contained a water to cementitious material (cement + fly ash) ratio of 0.45 with 10% fly ash replacement of cement. Both electrical tests provided suspicions of corrosion. The macrocell current measured over $10 \mu A$ and the half cell potential gave readings indicating 90% probability of corrosion.

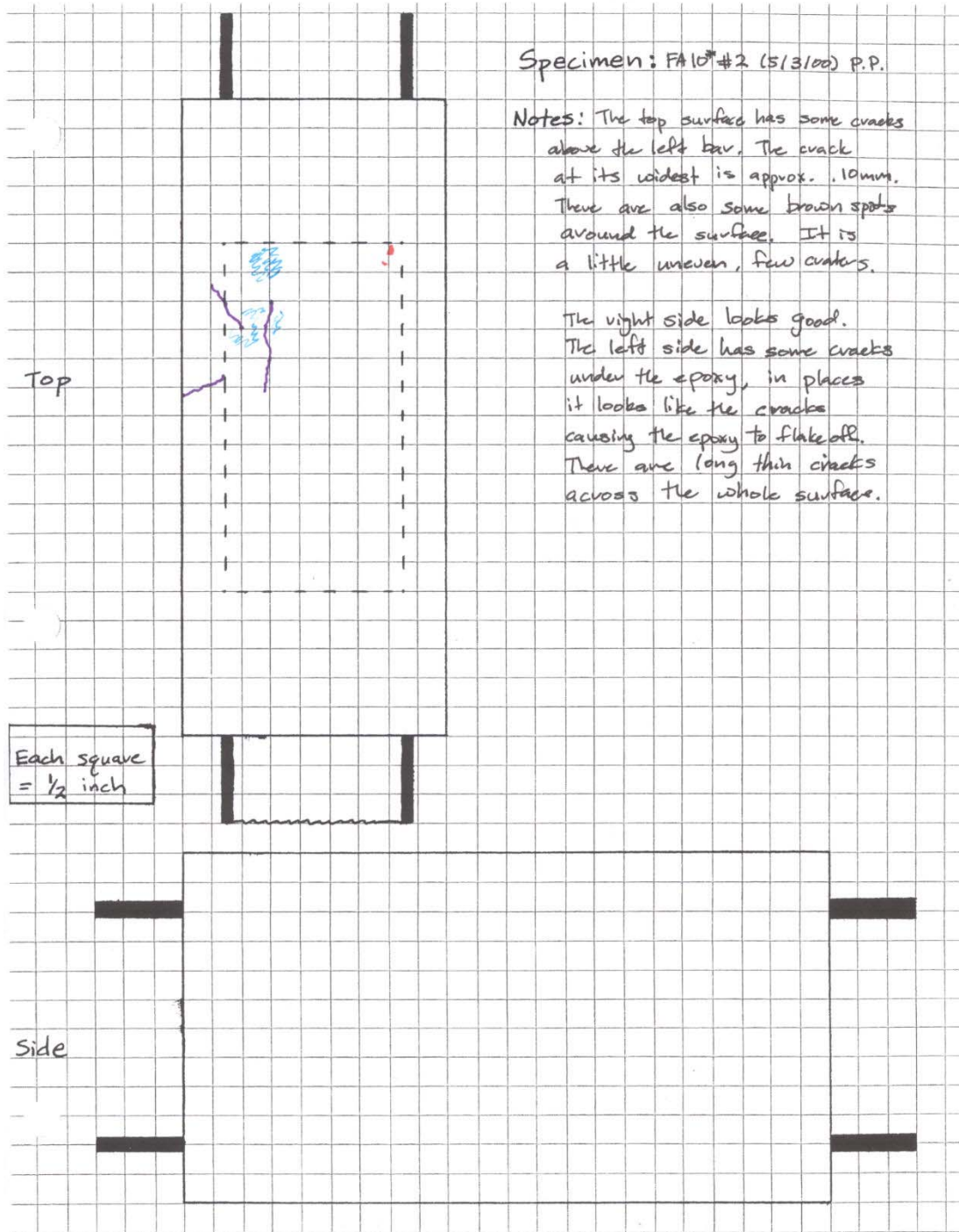
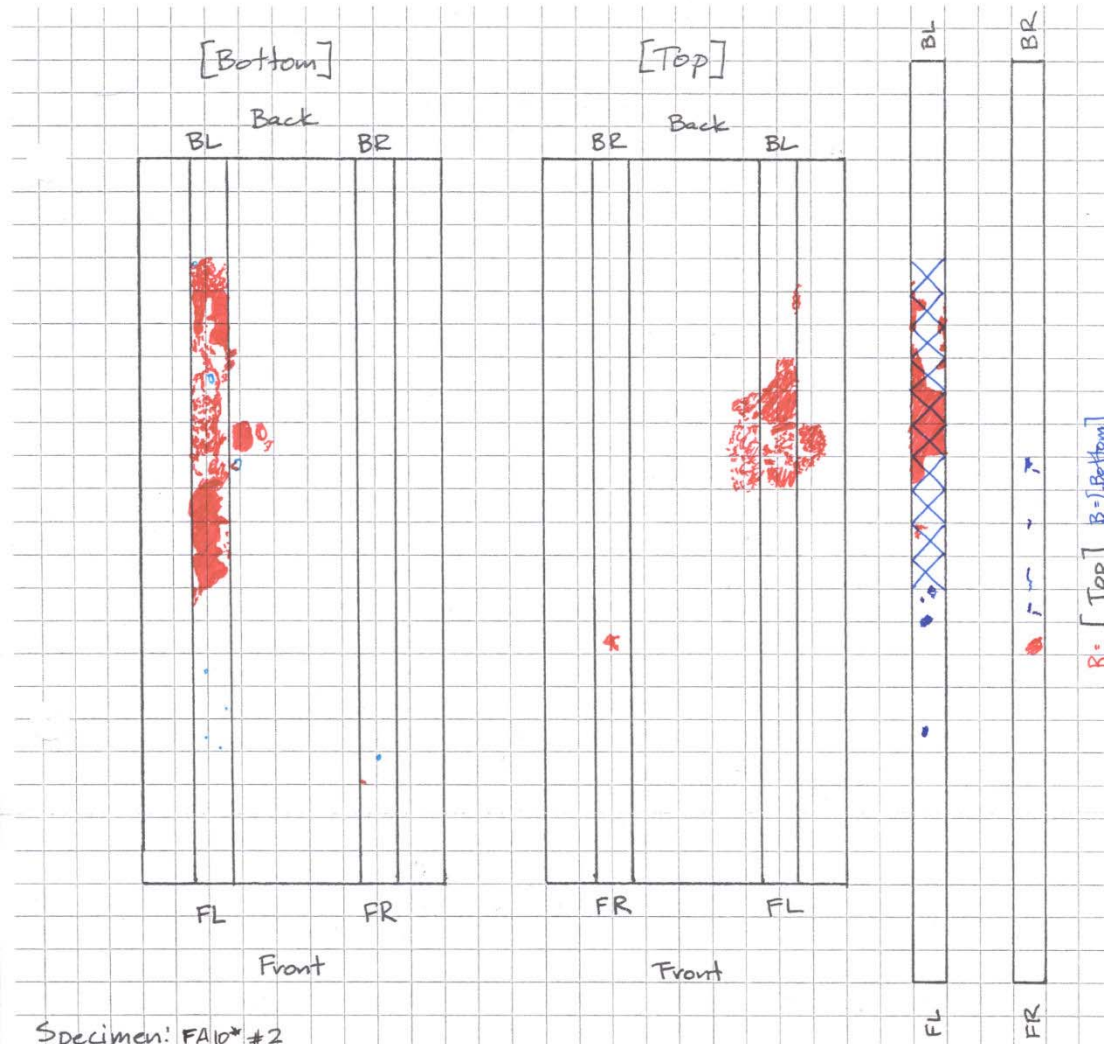


Figure 4.14 : Exterior Inspection of FA*10 #2



Specimen: FA10* #2

Notes: The bottom piece has a few tiny voids. On the left side there is dark brown, and a few black spots (tiny). There is one big spot on the inside of the left bar indentation. The top piece has a large area of corrosion on the left side, it goes to the inside as well as the outside edge. It is dark brown and orange in color. The top of the left bar is black with a few more pits toward the back. The bottom is fairly well covered in brown and black spots, from the middle toward the back. The right bar has one spot on the top (black). The bottom has a few light pits, light orange.

Figure 4.15 : Interior Inspection of FA*10 #2

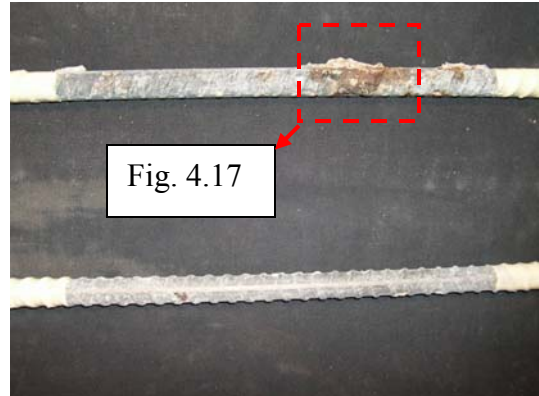
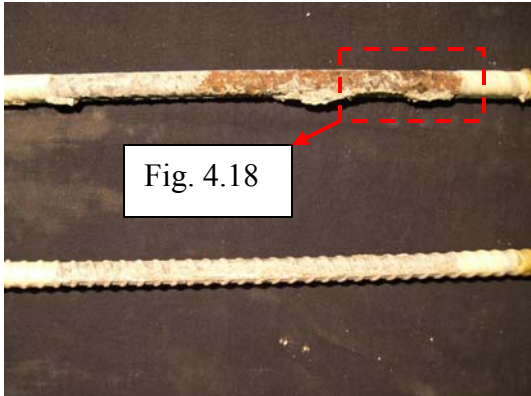


Figure 4.16 : Bottom (left) and top (right) surfaces of top reinforcing bars

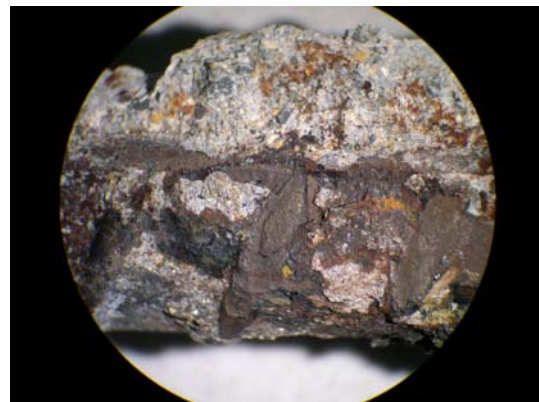


Figure 4.17 : Top surface cracks (left), left bar top, underneath cracks (right) x12

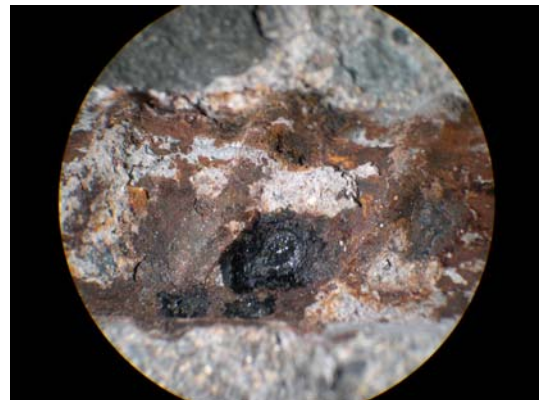


Figure 4.18 : Left bar bottom, (right) x12, Bottom piece left side, (left) x12

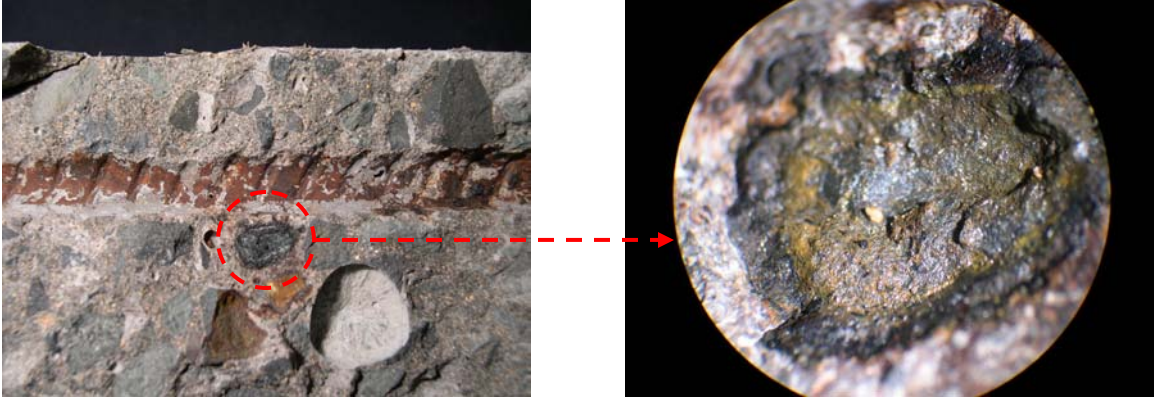


Figure 4.19 : Bottom piece, left side (left), Close up (right) x22.5

CHAPTER 5 - ACOUSTIC MICROSCOPY

5.1 Introduction

Scanning acoustic microscopy (SAM) is a relatively new technique that is becoming established as a method for non-destructive evaluation of engineering materials. The idea behind SAM is to use a focused acoustic beam to measure velocities of different types of acoustic waves propagating in solid media (Zinin et al. 2000). This chapter describes the SAM used in this study, discusses the steps for preparing specimens for acoustic microscopy and presents some of the resulting images.

5.2 Scanning Acoustic Microscope

The acoustic microscope used in this study is part of the Department of Geophysics material identification laboratory. The acoustic microscope used in this study was a Kramer Scientific Instrument SAM 50 (Figure 5.1).



Figure 5.1 : Scanning Acoustic Microscope

For layered materials the reflected signals represent a train of pulses, or A-scan. The first pulse is the reflection from the liquid/specimen interface. The second pulse is due to the reflection from an internal interface. The time between pulses and the amplitudes provide hints about the elastic properties and reduction in the acoustic signal in the specimen. Time resolved images obtained by mechanical scanning along a line are called B-scans. The B-scan provides a section view through the specimen. C-scan images are a planar scan at a particular depth in the specimen. From the A-scan, a particular reflected signal is selected and the focal length gated to focus at that signal depth. By changing the gate position, multiple layers can be viewed within the sample (3-D imaging). A gate position of zero corresponds to the pulse coming from the top surface. Increasing the gate position investigates deeper layers below the surface.

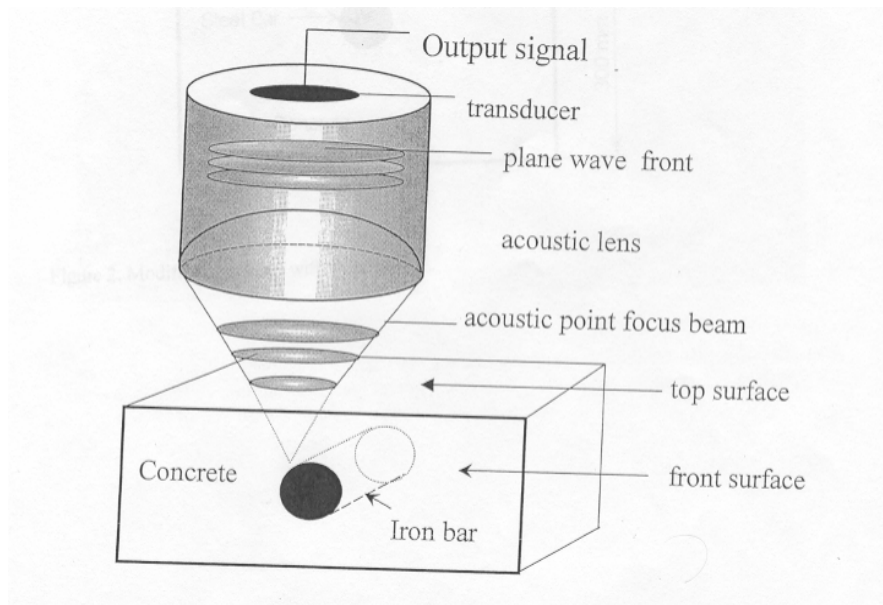


Figure 5.2 : Schematic diagram of the Acoustic Microscope

5.3 Procedure

Two mixtures were selected for the investigation by SAM, the Control #5 and Control #2 mixtures. These mixtures were selected because the electrical readings indicated a range of corrosion levels in these specimens and it was hoped that the scanning acoustic microscope could be used to identify the extent of corrosion at the steel/concrete interface.

5.3.1 *Cutting the Specimens*

The acoustic microscope is not able to scan an 11 x 4.5 x 6 inch specimen. The specimens had to be cut into smaller pieces approximately 2 x 1 x 1 inches. These smaller samples were taken from the middle of the specimen directly below the salt water dam. The specimens were cut to size using a concrete saw. An approximately 1 inch thick plate was cut horizontally out of a typical specimen. This plate was then cut into the 2 x 1 x 1 in. acoustic specimens. Four acoustic specimens were obtained from each laboratory specimen (Figure 5.3).

5.3.2 *Polishing*

The sawn surfaces are too rough for imaging with the SAM. To improve the image, the smaller samples were polished using an open face flat lapping machine called a Lap Master model 20 (Figure 5.4). The top surface of each specimen was polished to allow for acoustic imaging. After a number of unsuccessful attempts to scan through the top cover of concrete, it was apparent that the acoustic signal could not penetrate adequately to provide an image of the reinforcing bar. The distance between the top

surface and the top reinforcement therefore was reduced to 1-2 mm to image the steel/concrete interface.

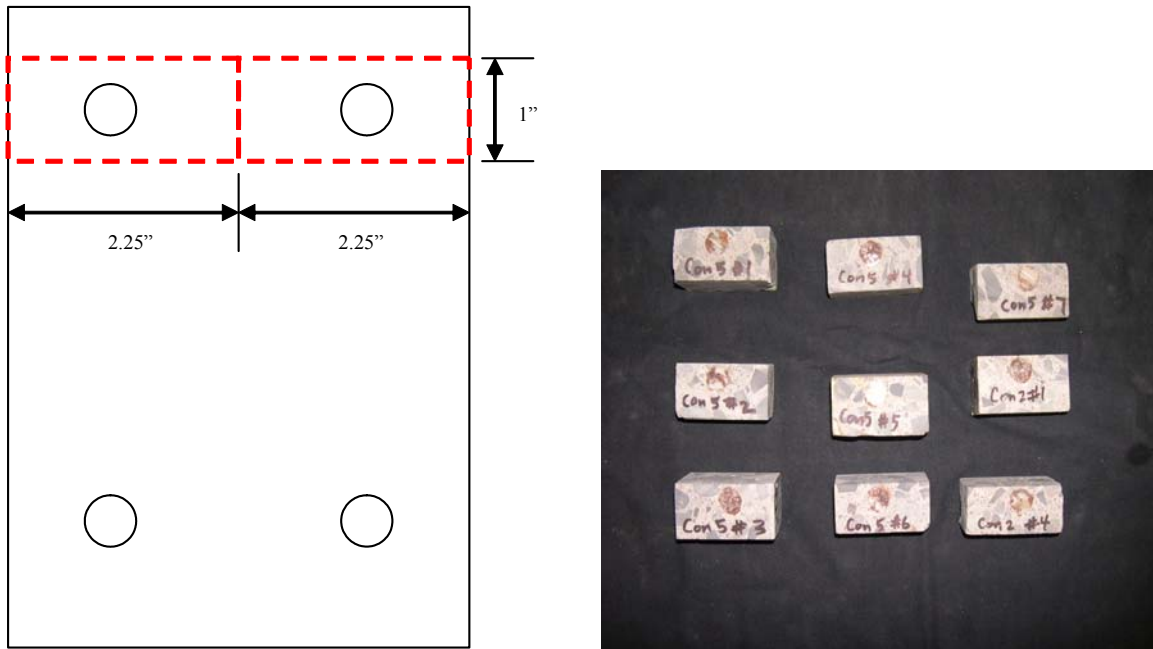


Figure 5.3 : Sample cutting diagram (left), Acoustic Specimens (right)

The lapmaster uses a lapping vehicle (water based) to apply the abrasive dust to the desired surface to be polished. The lapping vehicle came in a concentrated form and had to be diluted by a 4 to 1 ratio with water. The lapmaster uses 2 ounces of abrasive per quart of diluted lapping vehicle to help facilitate the polishing process. There were three different types of abrasives used on the specimens. The abrasives are made with Silicon Carbide that removes coatings on hard or soft materials. The three that were used were 2220, 2320, and 2600. They had micron sizes of 75, 35, and 17.5, respectively.

There were not many specimens, so each was polished individually by hand. The specimens were held against the polishing plate and were checked periodically to check if

they were square. The first objective was to remove the roughness caused by the saw cuts; the second was to remove cover concrete so that the surface was close to the reinforcing bar. After this was done, the specimens were labeled and were ready for the acoustic microscope. It is possible that the polishing process could affect the imaging process.



Figure 5.4 : Lapmaster

5.4 Acoustic Microscope Images

After the specimens were cut and polished they were brought to the Department of Geology and Geophysics, for SAM analysis. The microscope was used to take acoustic images of 8 different types of specimens. Two images were taken for each specimen. The first was a B-scan which represents a vertical section through the specimen. The

second was a C-scan which represents a horizontal section across the specimen at a pre-selected depth.

Examples of both B- and C-scans of Control 2 specimen #1 are shown in Figure 5.5 and

Figure 5.6, respectively. The B-scan shows a slight hump toward the left of the center of the picture, presumably representing the top of the reinforcing bar. The SAM can only capture signals that are reflected back at the lens located directly above the bar. Consequently the sides of the bar are not evident in the scan. It was hoped that a more distinctive difference would be evident at the concrete and steel interface.

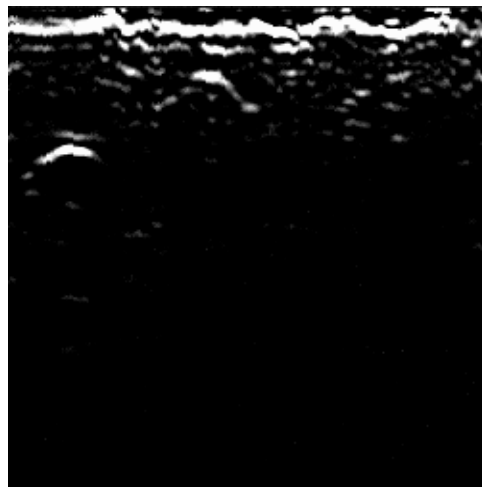


Figure 5.5 : Control 2 specimen #1 B-scan

In

Figure 5.6, showing a C-scan (plan view) of the same specimen, the lighter portion in the middle of the image is presumed to represent the ribs on the top of the reinforcing bar.

Any voids or evidence of corrosion adjacent to the reinforcing bar were not clearly visible.

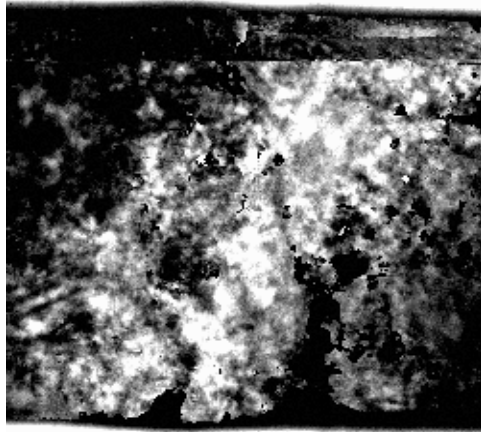


Figure 5.6 : Control 2 specimen #1 C-Scan

Figure 5.7 and Figure 5.8 show previous images taken by the SAM (Zinin, et al, 2004).

Those attempts show better results than were obtained in this study.

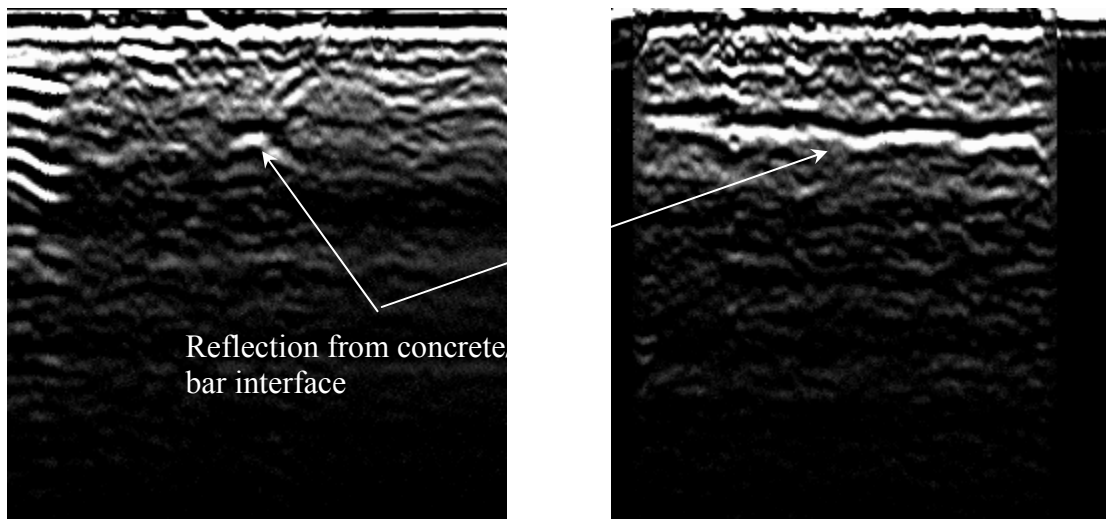


Figure 5.7 : B-scan images (Zinin et al, 2004)

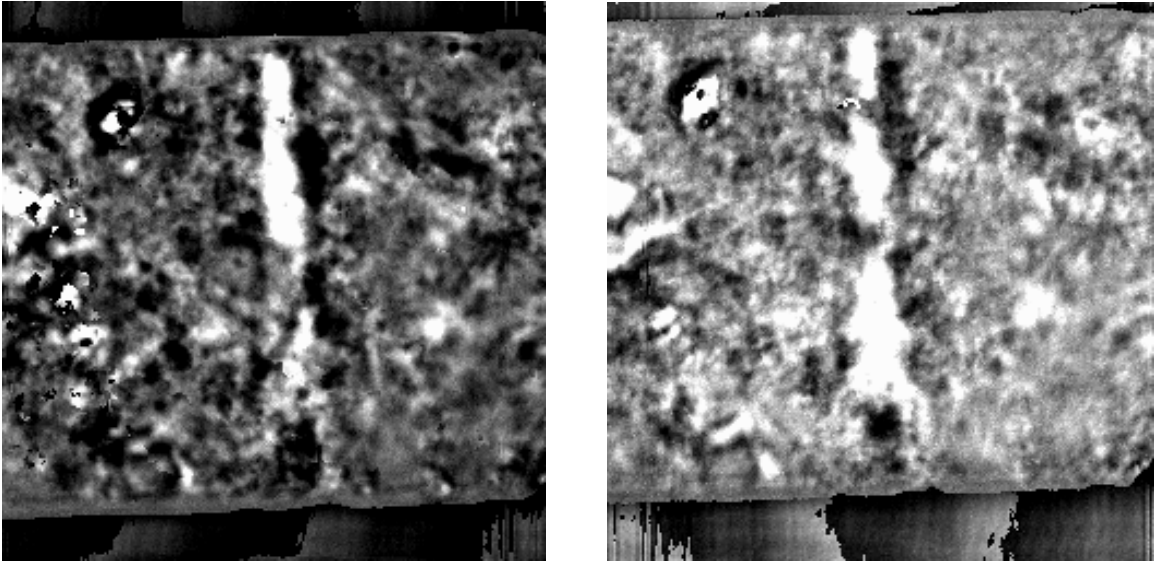


Figure 5.8 : C – Scan images (Zinin et al, 2004)

The pictures from acoustic microscopy were not very helpful. The hope of this inspection was to get an image of the extent of the corrosion on the bar. From the images the extent of what is seen is uncertain. There are various reasons why SAM did not provide better images. One was because sound travels poorly through concrete. The SAM equipment used in this study was not sensitive enough in distinguishing the difference between cement paste and aggregate. Other reasons include inadequate resolution, high frequency range, and small wave lengths.

CHAPTER 6 - RESULTS

6.1 Introduction

This chapter presents a discussion of the electrical and chemical tests performed on the laboratory specimens. Results from each of the electrical tests were evaluated to determine whether or not corrosion would be expected in the specimen. These results were then compared with the visual inspections to assess the validity of the test method. The air permeability, chloride, and pH tests results were also compared to the visual inspections to identify any trends or threshold values.

6.2 Electrical tests

Two electrical tests were performed on each specimen. The macrocell current between the top and bottom reinforcing bars was measured according to the ASTM standard G 109-92. If this current exceeds $10 \mu A$, it is anticipated that corrosion has been initiated. The second measurement was the half cell potential on the specimen's top surface, using a calomel reference electrode. The potential was measured at six locations on each specimen; three measurements over each top reinforcement bar. The largest negative value measured was the value used in the evaluation.

Table 6.1 presents the electrical results along with the results of the visual inspection. The table lists the specimens, the number of cycles until the specimen was removed from cycling, current results, half cell potentials, and observations of the inside and outside of the specimen. The macrocell current measurements were separated into these categories: a value above $10 \mu A$ was given a purple coloring, values between $2 \mu A$

and $10 \mu A$ were given an orange color coding, and values below $2 \mu A$ were given a light blue coding.

The same color coding was used for the half cell readings. Any value that was below -350 mV indicates a 90% probability of corrosion (90%, purple). Any value that fell between -350 mV and -200 mV was considered uncertain for corrosion (Uncertain, orange). If the value was greater than -200 mV then there was a 10% probability of corrosion (10%, light blue).

The observations of the inside of the specimens were identified with a similar color coding. If the reinforcing bars exhibit substantial overall corrosion or major pitting corrosion, the bars were considered moderately to substantially corroded (purple). If small areas of corrosion or less severe pitting were observed, the specimen was categorized as “minor” corrosion (orange). The light blue designation meant either negligible corrosion or the reinforcing bars were completely clean.

Table 6.1 : Electrical and observational results

Specimen	Cycles	Current	Half Cell	Reinforcement	Comments
Con1 #1	31	$i > 10 \mu a$	UN	Mod - significant	Outside in good condition
Con1 #2	31	$2 < i < 10 \mu a$	UN	Mod - significant	Outside in good condition
Con1 #3	31	$i > 10 \mu a$	UN	Mod - significant	Cracks on the right side
Con1 #4	31	$i > 10 \mu a$	10%	Mod - significant	Outside in good condition
Con1 #7	31	$i < 2 \mu a$	UN	Mod - significant	Outside in good condition
Con2 #2	31	$i > 10 \mu a$	UN	Mod - significant	Outside in good condition
Con2 #3	31	$i > 10 \mu a$	UN	Mod - significant	Outside in good condition
Con2 #5	31	$i > 10 \mu a$	UN	Mod - significant	Outside in good condition
Con2 #6	31	$i < 2 \mu a$	UN	Mod - significant	Outside in good condition
Con2 #7	31	$2 < i < 10 \mu a$	UN	Mod - significant	Outside in good condition
Con3 #5	46	$i > 10 \mu a$	90%	Mod - significant	Cracks on top & right
Con3 #6	24	$2 < i < 10 \mu a$	UN	Mod - significant	Outside in good condition
Con4 #1	24	$i > 10 \mu a$	UN	Mod - significant	Cracks on top & left
Con4 #2	29	$i > 10 \mu a$	UN	Mod - significant	Cracks on top & right
Con4 #3	29	$i > 10 \mu a$	UN	Mod - significant	Outside in good condition
Con4 #4	29	$i > 10 \mu a$	10%	Mod - significant	Some discolorations
Con4 #6	24	$i > 10 \mu a$	UN	Mod - significant	Some discolorations
Con4 #7	29	$i > 10 \mu a$	UN	Mod - significant	Outside in good condition
HCon1 #1	27	$i > 10 \mu a$	10%	Mod - significant	Outside in good condition
HCon1 #2	27	$2 < i < 10 \mu a$	10%	Minor	Outside in good condition
HCon1 #3	27	$i > 10 \mu a$	90%	Mod - significant	Cracks on top & right
HCon1 #4	27	$i > 10 \mu a$	90%	Mod - significant	Cracks on top & left
HCon2 #1	13	$i > 10 \mu a$	90%	Mod - significant	Cracks on top & left
HCon2 #2	13	$i > 10 \mu a$	10%	Minor	Outside in good condition
HCon2 #3	13	$i > 10 \mu a$	UN	Mod - significant	Small crack on top
HCon2 #4	13	$i > 10 \mu a$	UN	Mod - significant	Cracks on top & left
HCon4 #1	28	$i > 10 \mu a$	90%	Mod - significant	Outside in good condition
HCon5 #1	28	$2 < i < 10 \mu a$	UN	Mod - significant	Outside in good condition
HCon5 #2	28	$i > 10 \mu a$	UN	Mod - significant	Cracks on top & right
HCon5 #3	28	$i > 10 \mu a$	UN	Mod - significant	Outside in good condition
HCon5 #4	28	$2 < i < 10 \mu a$	UN	Mod - significant	Outside in good condition
Xyp1 #1	25	$i > 10 \mu a$	UN	Mod - significant	Cracks on top surface
Xyp1 #2	25	$i < 2 \mu a$	10%	None	Web cracking on top
Xyp1 #3	25	$i > 10 \mu a$	UN	Mod - significant	Cracks on top & right
Xyp1 #4	25	$i > 10 \mu a$	10%	Minor	Discolorations on right

Specimen	Cycles	Current	Half Cell	Reinforcement	Comments
Xyp2 #1	31	$i > 10 \mu a$	UN	Mod - significant	Few voids on top
Xyp2 #2	31	$i > 10 \mu a$	UN	Mod - significant	Outside in good condition
Xyp2 #3	31	$i > 10 \mu a$	10%	Mod - significant	Outside in good condition
Xyp2 #4	31	$i > 10 \mu a$	UN	Mod - significant	Cracks on top & left
Xyp4 #1	31	$i < 2 \mu a$	10%	Minor	Cracks under epoxy
Xyp4 #2	31	$2 < i < 10 \mu a$	UN	Minor	Outside in good condition
Xyp4 #3	31	$i > 10 \mu a$	90%	Mod - significant	Cracks on left side
Xyp4 #4	31	$i > 10 \mu a$	UN	Mod - significant	Outside in good condition
Xyp5 #1	16	$i > 10 \mu a$	UN	Mod - significant	Cracks on top & right
Xyp5 #2	16	$i > 10 \mu a$	10%	Mod - significant	Cracks on top & left
Xyp5 #3	16	$i > 10 \mu a$	UN	Mod - significant	Cracks on top & right
Xyp5 #4	16	$i > 10 \mu a$	UN	Mod - significant	Cracks on top & right
HRh4 #1	21	$i > 10 \mu a$	10%	Mod - significant	Cracks on top & left
HRh4 #2	27	$i > 10 \mu a$	UN	Mod - significant	Cracks on top & right
HRh4 #3	27	$i > 10 \mu a$	10%	Minor	Some small voids
HRh4 #4	27	$i > 10 \mu a$	90%	Mod - significant	Cracks on top
HRh5 #1	24	$i > 10 \mu a$	90%	Mod - significant	Outside in good condition
HRh5 #2	24	$2 < i < 10 \mu a$	UN	Mod - significant	Outside in good condition
HRh5 #3	24	$i > 10 \mu a$	90%	Mod - significant	Some small voids
HRh5 #4	24	$i > 10 \mu a$	90%	Mod - significant	Outside in good condition
HFA5 #1	17	$i < 2 \mu a$	10%	None	Web cracking on top
HFA5 #2	17	$i > 10 \mu a$	UN	Mod - significant	Web cracking on top
HFA5 #3	17	$i > 10 \mu a$	90%	Mod - significant	Cracks on top & left
HFA5 #4	17	$2 < i < 10 \mu a$	10%	None	Web cracking on top
DCI1 #2	31	$i > 10 \mu a$	10%	Mod - significant	Outside in good condition
DCI1 #6	31	$i > 10 \mu a$	UN	Mod - significant	Outside in good condition
DCI1 #8	31	$i > 10 \mu a$	UN	Mod - significant	Outside in good condition
DCI2 #4	31	$i > 10 \mu a$	UN	Mod - significant	Outside in good condition
DCI2 #8	34	$i < 2 \mu a$	10%	Mod - significant	Outside in good condition
DCI3 #8	34	$i < 2 \mu a$	10%	None	Outside in good condition
DCI4 #8	33	$i < 2 \mu a$	10%	Minor	Outside in good condition
DCI5 #8	33	$2 < i < 10 \mu a$	10%	None	Discolorations on right
DCI6 #8	32	$i < 2 \mu a$	10%	Minor	Outside in good condition
LA1 #1	22	$i < 2 \mu a$	UN	Mod - significant	Outside in good condition
LA1 #2	22	$i > 10 \mu a$	UN	Mod - significant	Cracks on top & right
LA1 #3	22	$i > 10 \mu a$	UN	Mod - significant	Cracks under epoxy
LA1 #4	22	$i < 2 \mu a$	UN	Mod - significant	Web cracking on top
LA1 #5	22	$i > 10 \mu a$	UN	Mod - significant	Cracks on top & left
LA1 #6	22	$i > 10 \mu a$	UN	Mod - significant	Outside in good condition
LA1 #8	22	$i > 10 \mu a$	UN	Mod - significant	Web cracking on top
LA2 #8	27	$i < 2 \mu a$	10%	None	Light discolorations
LA3 #7	24	$i > 10 \mu a$	UN	Minor	Outside in good condition
LA3 #8	25	$i < 2 \mu a$	UN	Mod - significant	Outside in good condition
LA5 #8	26	$i < 2 \mu a$	10%	None	Outside in good condition
LA6 #8	24	$2 < i < 10 \mu a$	10%	Minor	Light discolorations

Specimen	Cycles	Current	Half Cell	Reinforcement	Comments
Ferr1 #8	21	$i > 10 \mu a$	10%	Mod - significant	Crack on left
Ferr2 #5	35	$i > 10 \mu a$	UN	Mod - significant	Cracks on right side
Ferr2 #8	21	$i < 2 \mu a$	10%	None	Outside in good condition
Ferr3 #8	20	$i < 2 \mu a$	10%	None	Outside in good condition
Ferr4 #1	32	$i > 10 \mu a$	UN	Mod - significant	Outside in good condition
Ferr5 #1	25	$i > 10 \mu a$	10%	Mod - significant	Outside in good condition
Ferr5 #3	25	$i > 10 \mu a$	90%	Mod - significant	Cracks on top & left
Ferr5 #5	25	$i > 10 \mu a$	UN	Mod - significant	Outside in good condition
Ferr5 #7	25	$i > 10 \mu a$	UN	Mod - significant	Outside in good condition
Ferr5 #8	19	$i < 2 \mu a$	UN	Minor	Outside in good condition
Ferr6 #8	19	$i < 2 \mu a$	10%	None	Web cracking on top
FA5 #1	44	$i > 10 \mu a$	90%	Mod - significant	Cracks on top & right
FA5 #2	44	$2 < i < 10 \mu a$	UN	Mod - significant	Outside in good condition
FA5 #3	28	$i > 10 \mu a$	10%	Mod - significant	Outside in good condition
FA5 #4	44	$2 < i < 10 \mu a$	UN	Mod - significant	Outside in good condition
FA6 #3	28	$i > 10 \mu a$	UN	Mod - significant	Outside in good condition
FA9 #3	27	$i < 2 \mu a$	10%	Minor	Outside in good condition
FA10^ #2	36	$i > 10 \mu a$	90%	Mod - significant	Cracks on top
Rheo1 #8	20	$2 < i < 10 \mu a$	10%	Minor	Cracks on top
Rheo2 #8	24	$i < 2 \mu a$	10%	None	Few voids on top
Rheo3 #8	23	$i < 2 \mu a$	10%	Minor	Web cracking on top
Rheo4 #8	22	$i < 2 \mu a$	10%	None	Outside in good condition
Rheo5 #8	22	$i < 2 \mu a$	10%	Minor	Outside in good condition
Rheo6 #8	20	$i < 2 \mu a$	10%	None	Outside in good condition
SF1 #8	32	$i < 2 \mu a$	10%	None	Outside in good condition
SF2 #8	31	$i < 2 \mu a$	10%	None	Outside in good condition
SF2^ #8	31	$i < 2 \mu a$	10%	Minor	Outside in good condition
SF3 #8	32	$2 < i < 10 \mu a$	10%	Minor	Discolorations
SF4 #8	32	$i < 2 \mu a$	UN	Minor	Outside in good condition
SF5 #5	45	$i > 10 \mu a$	UN	Mod - significant	Cracks on top & right
SF5 #7	29	$i > 10 \mu a$	UN	Mod - significant	Outside in good condition
SF5 #8	29	$i > 10 \mu a$	10%	Mod - significant	Outside in good condition
SF6 #6	45	$i > 10 \mu a$	90%	Mod - significant	Cracks on top & right
SF6 #8	32	$2 < i < 10 \mu a$	10%	Minor	Outside in good condition
SF7 #3	45	$i > 10 \mu a$	90%	Mod - significant	Cracks on top
SF7 #8	31	$2 < i < 10 \mu a$	10%	Minor	Outside in good condition

6.2.1 *Macrocell Current*

Comparisons can now be made between the current readings and the visual inspection results presented in Table 6.1. Table 6.2 shows a comparison between the macrocell current readings and the severity of corrosion observed during the visual inspections. The percentages show the probability of a certain level of corrosion if a particular current is measured.

Table 6.2 : Current Percentages

Current	Mod - substantial	Minor	None
$i > 10 \mu a$	94%	6%	0
$2 < i < 10 \mu a$	47%	41.2%	11.8%
$i < 2 \mu a$	21%	32%	46%

For example, if a $10 \mu A$ or greater macrocell current was measured; these data indicated that there was a 94% chance of substantial corrosion; 6% chance of minor corrosion, and a 0% chance of no corrosion. This confirms the ASTM G109 threshold of $10 \mu A$ for certainty of corrosion initiation. If the current fell between $2 \mu A$ and $10 \mu A$ there was a 47% chance of substantial corrosion, 41.2% chance of minor corrosion, and 11.8% of none. These values indicate that if moderate to high currents ($>2 \mu A$) are measured, corrosion was initiated in 88% of the specimens. If the current is below $2 \mu A$ then there was a 53% chance that corrosion had already been initiated.

Current measurements of $10 \mu A$ or greater consistently indicated corrosion was present, with substantial corrosion in most cases. Values that fell below $2 \mu A$ showed that nothing conclusive could be inferred with almost half the specimens showing no sign

of corrosion. The current measurements prove to be a good predictor of corrosion when values above 10 μA are measured.

6.2.2 Half cell potential

Half cell potential readings indicate the probability of corrosion occurring. Table 6.3 presents the half cell readings compared with the severity of corrosion observed during the visual inspections. The left hand side of Table 6.3 shows the break down of the half cell readings. The top lists the severity of corrosion starting with moderate to significant on the top left, minor, then none. The percentages in the table show the correlation between a certain level of corrosion and the half-cell prediction.

Table 6.3 : Half cell potential percentages

Half cell	Mod - substantial	Minor	None
<-350 mV	100%	0	0
-200 to -350mV	93%	7%	0
>-200 mV	28%	37%	35%

For all specimens where the half-cell readings indicated a 90% probability of corrosion there was moderate to significant corrosion. If the value fell in the uncertain range, there was a 93% chance of substantial corrosion and 7% chance of minor corrosion. These values indicate that if uncertain values were measured, then the majority of the time there was substantial corrosion present. If half cell potential readings fell in the 10% probability of corrosion range there was a 28% chance of substantial corrosion, 37% minor corrosion, and 35% none.

The half-cell values are consistent for the 90% probability range. If a potential below -350 mV was measured then considerable corrosion was always present. When the half-cell values were in the uncertain range there was also corrosion present in all cases, with substantial corrosion 93% of the time. Values that fell in the 10% range were evenly spread into all corrosion categories. 65% of specimens had some type of corrosion present when only 10% would be expected. The half-cell measurements tended to underestimate the amount of corrosion present in all cases. It would appear that the half-cell measurement criteria could be shifted to limits of -100 mV and -200 mV in place of the standard -200 mV and -350 mV respectively. The resulting half-cell potential percentages are shown in Table 6.4.

Table 6.4: Shifted Half Cell Potential Percentages

Half cell	Mod - substantial	Minor	None
<-200 mV	95%	5%	0
-200 to -100mV	40%	33%	27%
>-100 mV	0%	46%	54%

All specimens with a half-cell reading less than -200 mV had minor to significant corrosion. The specimens in the undecided range are now evenly split between no corrosion, minor and moderate to significant corrosion. Finally, none of the specimens with half-cell readings above -100 mV displayed moderate to significant corrosion, while half showed minor corrosion and the other half no corrosion.

6.2.3 Combined electrical results

The two previous sections attempted to compare the electrical tests with the observed condition of a sample. This section investigates the value of using both tests

together to evaluate corrosion. In Table 6.5, column 1 lists the current readings and column 2 lists the three possible half cell readings based on the standard -200 mV and -350 mV limits. Columns 3 to 5 show the probability of a certain degree of corrosion if both the current and half cell measurements are known.

Table 6.5 : Both electrical test percentages

		Mod - substantial	Minor	None
	<-350 mV	100%	0%	0%
i > 10 µa	-200 to -350mV	98%	2%	0%
	>-200 mV	77%	23%	0%
		Mod - substantial	Minor	None
	<-350 mV	0%	0%	0%
2 < i < 10µa	-200 to -350mV	89%	11%	0%
	>-200 mV	0%	75%	25%
		Mod - substantial	Minor	None
	<-350 mV	0%	0%	0%
i < 2µa	-200 to -350mV	71%	29%	0%
	>-200 mV	5%	33%	62%

Table 6.6 : New values of half-cell limits

		Mod - substantial	Minor	None
	<-200 mV	98%	2%	0%
i > 10 µa	-200 to -100mV	79%	21%	0%
	>-100 mV	0%	0%	0%
		Mod - substantial	Minor	None
	<-200 mV	89%	11%	0%
2 < i < 10µa	-200 to -100mV	0%	71%	29%
	>-100 mV	0%	100%	0%
		Mod - substantial	Minor	None
	<-200 mV	71%	29%	0%
i < 2µa	-200 to -100mV	11%	22%	67%
	>-100 mV	0%	42%	58%

Table 6.5 reveals that if the current is greater than $10 \mu A$ and half-cell measurements indicate a 90% probability of corrosion, there will be substantial corrosion 100% of the time. When $10 \mu A$ were measured and the half cell indicated uncertain probability there was 98% substantial corrosion and 2% minor corrosion. When $10 \mu A$ were measured and the half cell indicated 10% probability there was 77% substantial corrosion and 23% minor corrosion. For the range from $2 \mu A$ to $10 \mu A$, there were no half cell values in the 90% range. In the $2 \mu A$ to $10 \mu A$ range with an uncertain half-cell reading, there was substantial corrosion 89% of the time and 11% minor corrosion. When the half cell values fell in the 10% range there was minor corrosion 75% of the time and no corrosion the other 25% of the time. When the current fell under $2 \mu A$ there were half cell measurements in the uncertain and 10% probability range. In the uncertain range there was substantial corrosion 71% of the time with minor corrosion 29% of the time. In the 10% region substantial corrosion occurred 5% of the time, minor corrosion 33%, and none 62% of the time. Table 6.6 shows the comparison between both tests if the shifted half-cell readings were used.

Using both test results together provides an improved prediction. Any current measurement above $10 \mu A$ always means corrosion and in most cases substantial corrosion. When the current was between $2 \mu A$ and $10 \mu A$ or less than $2 \mu A$, and the half-cell reading was uncertain then corrosion was occurring. In 3/4 of the cases the corrosion was considerable. When the current was lower than $2 \mu A$ and the half-cell indicated 10% probability of corrosion the chance of corrosion was 38%, with only 5% classified as moderate to substantial.

6.3 Chemical tests

Tests that were conducted to measure chloride concentration, pH level, and air permeability of all test specimens. This section presents the data collected from these tests and compares them with the electrical tests and visual inspections described earlier.

6.3.1 Chlorides

Figure 6.1 below shows chloride concentrations (% by mass of cement) versus the maximum half cell potential value measured on each specimen. The points on the figure are color coded with the same, light blue indicating no corrosion, orange indicating minor corrosion, and purple indicating moderate to substantial corrosion. The figure also indicates the limits for the probability of corrosion from the half cell potential readings.

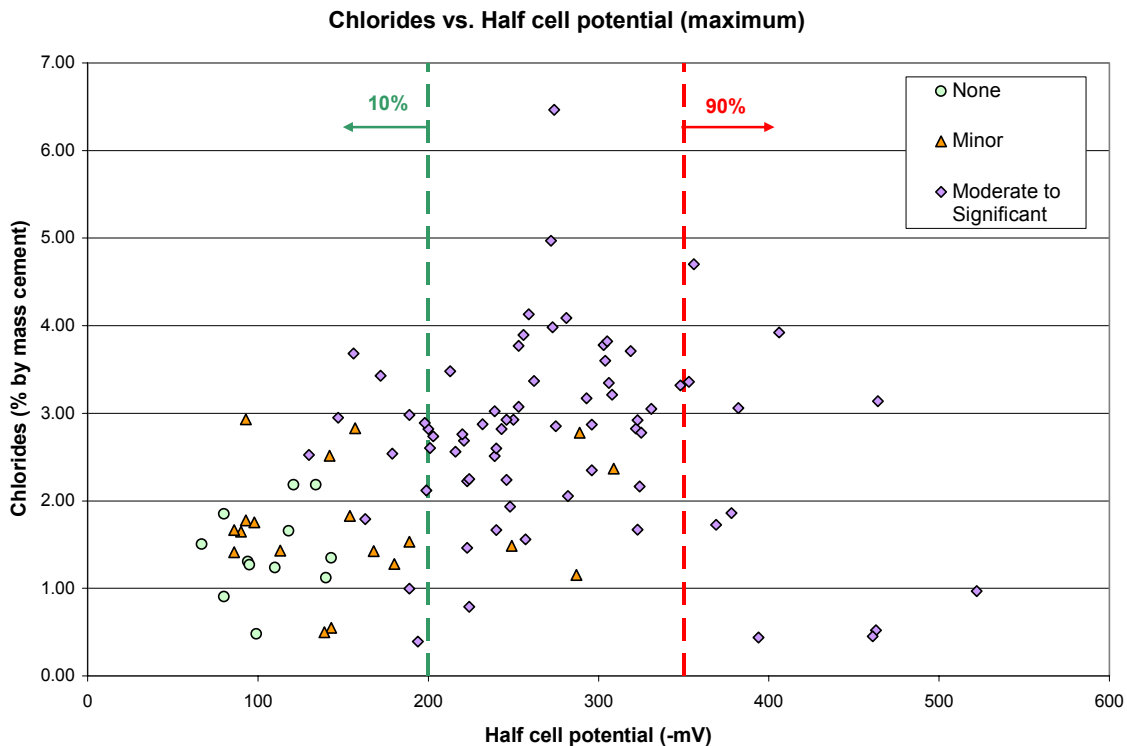


Figure 6.1 : Chlorides vs. Half cell potential

The specimens with no corrosion all fell in the 10% probability corrosion area and the majority had less than 2% chloride content. Most of the specimens with minor corrosion fell into the 10% probability range and had less than 3% chlorides. The specimens with substantial corrosion were spread out all over the figure. The majority of the specimens with substantial corrosion were in the uncertain half cell range. Values for specimens with substantial corrosion fell into every single category of chloride content and half-cell range, making it difficult to draw an encompassing conclusion. Figure 6.1 seems to show the lower limit of guaranteed substantial corrosion. Substantial corrosion always occurred when the chlorides values were over 3% or the half-cell readings were in the 90% probability range.

6.3.2 *pH*

The pH of the concrete was measured at the level of the top reinforcing steel as described in section 3.5.4. The resulting pH values of both left and right reinforcing bars are listed in Appendix F for all specimens, along with the average value for each specimen. Figure 6.2 plots the average pH versus the maximum half-cell readings obtained from the six readings on each specimen. Specimens in Figure 6.2 are colored to indicate the three different corrosion levels resulting from the visual inspection. The figure also indicates the limits for the probabilities of corrosion from the half-cell potential readings.

The high alkalinity of the concrete ($\text{pH} > 12$) creates a passivating layer which protects against corrosion. One would expect that a low pH would indicate a higher probability of corrosion. There is no apparent correlation between the pH level and the extent of corrosion on the reinforcing steel. For specimens with no corrosion the pH

values ranged from 12-12.6. For specimens with minor corrosion the pH values of the minor corrosion specimens were between 12 and 12.6. The specimens with moderate to substantial corrosion had pH values between 11.9 and 12.9. Figure 6.2 also indicates no significant correlation between the pH and the half cell readings.

Figure 6.3 compares the pH to the chloride content. The chloride content does not appear to have a correlation to the pH. The majority of the pH values are between 12 and 12.6 regardless of the chloride content.

The pH appears to be negligible in determining when corrosion is a factor. Knowledge of the pH does not appear to provide an indication of the likelihood of corrosion and chloride content. However, a very small range of pH values were observed in this study.

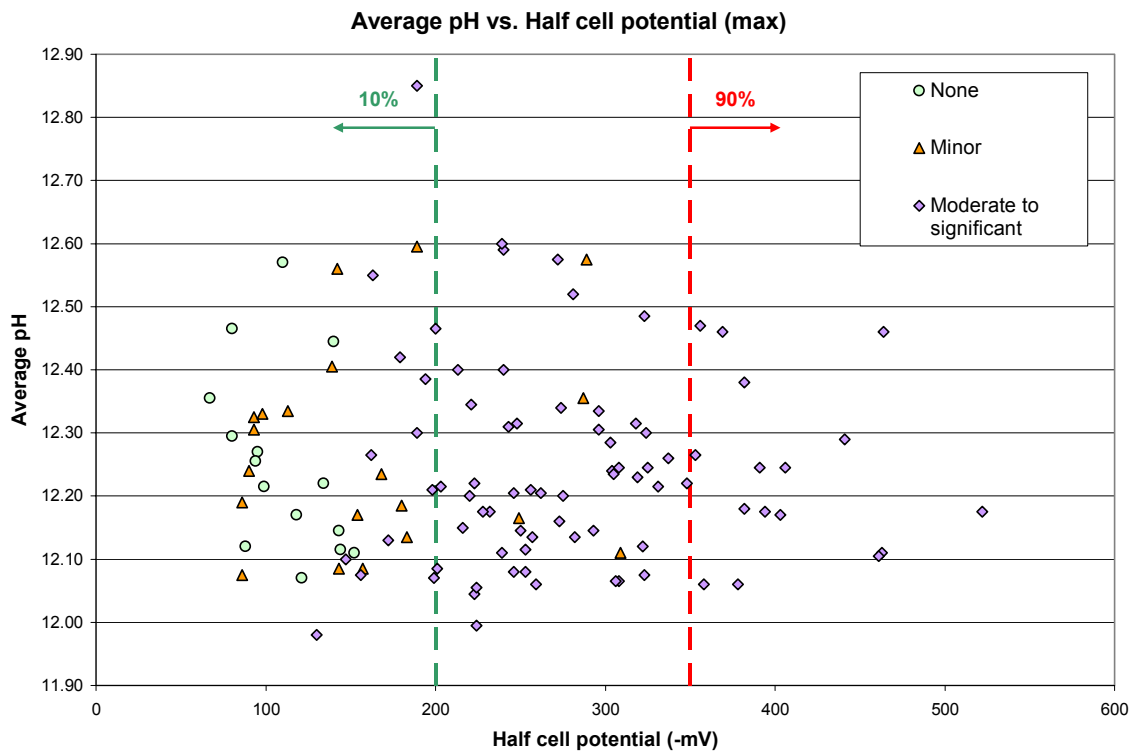


Figure 6.2 : Average pH vs. Half cell potential

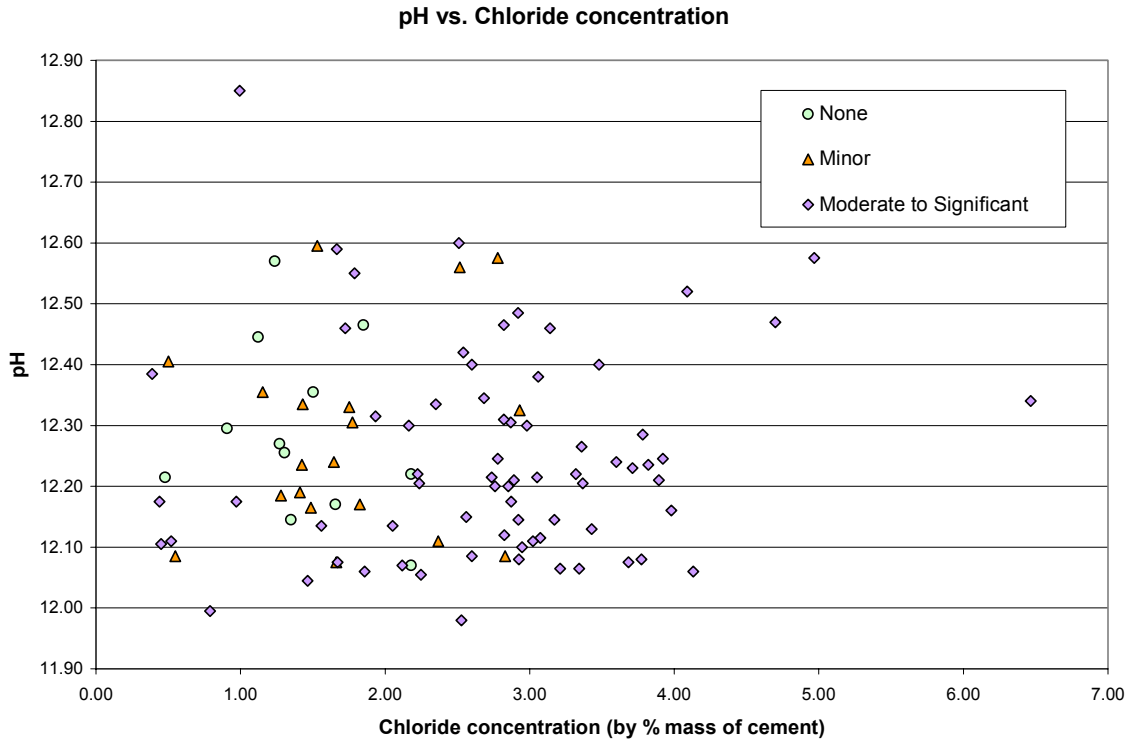


Figure 6.3 : pH vs. the Chloride concentration

6.3.3 Air permeability

The air permeability gives a measure of the concrete porosity. The test used in this study results in a Figg number which can be used to assign protective quality of the concrete into different categories according to Table 6.7.

Only specimens with moderate to significant corrosion are considered in this section so as to compare the effect of air permeability. The plots below compare the number of ponding cycles for a specimen to first reach a macrocell reading of $10 \mu A$, with the Figg number for that specimen. The Ameron control and Halawa control mixtures were plotted separately. Silica Fume and Fly Ash specimens were plotted

together because their effect on the concrete is believed to be similar. They both decrease porosity by filling voids between the other concrete materials. Latex and Xypex values were also grouped together because both admixtures attempt to modify the pore structure and reduce permeability in a similar manner. The other Halawa aggregate mixtures of Rheocrete, DCI, and Ferrogard were plotted together. These admixtures are not expected to affect the pore size or the pore structure.

Table 6.7 : Air permeability categories

Concrete Category	Protective Quality	Permeability (Figg number)
0	Poor	<30
1	Not very good	31-100
2	Fair	101-300
3	Good	301-1000
4	Excellent	>1000

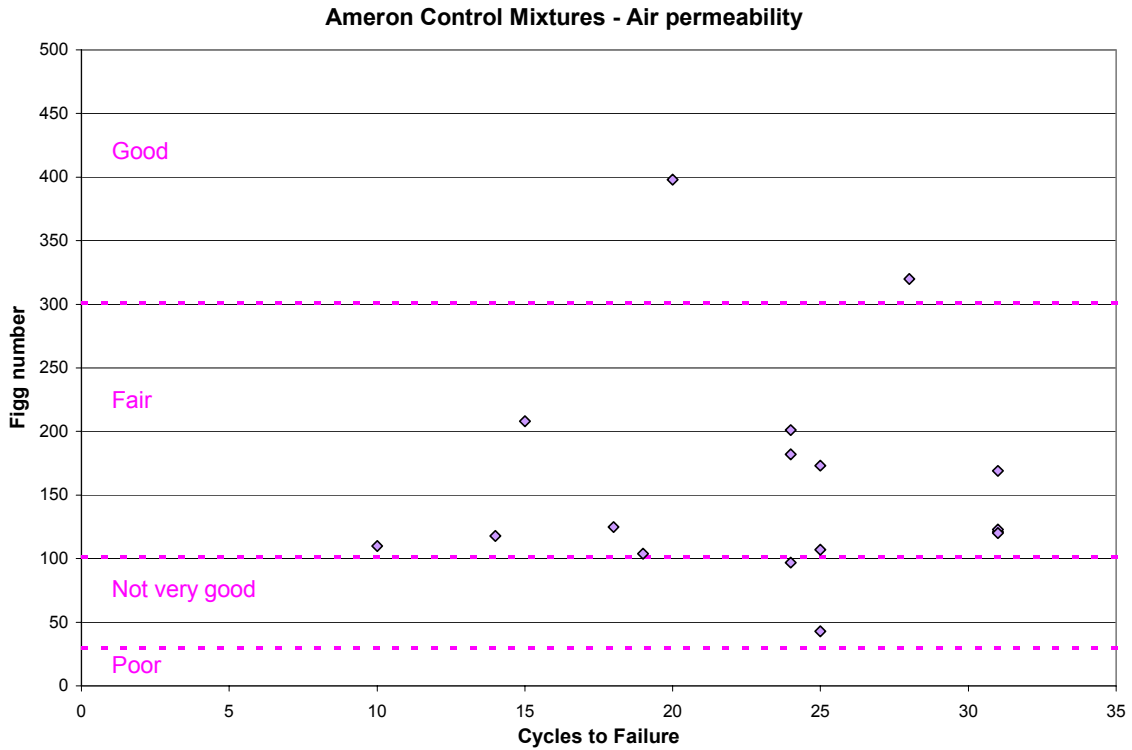


Figure 6.4 : Ameron Control – Air permeability

Figure 6.4 plots the Ameron Control mixture Figg numbers versus the number of cycles to failure. The graph shows a slight trend to increasing cycles to failure as the Figg number increases, however there are a number of specimens with very low Figg numbers that took over 20 ponding cycles to reach failure. One would expect the number of cycles to failure to increase as the Figg number increases.

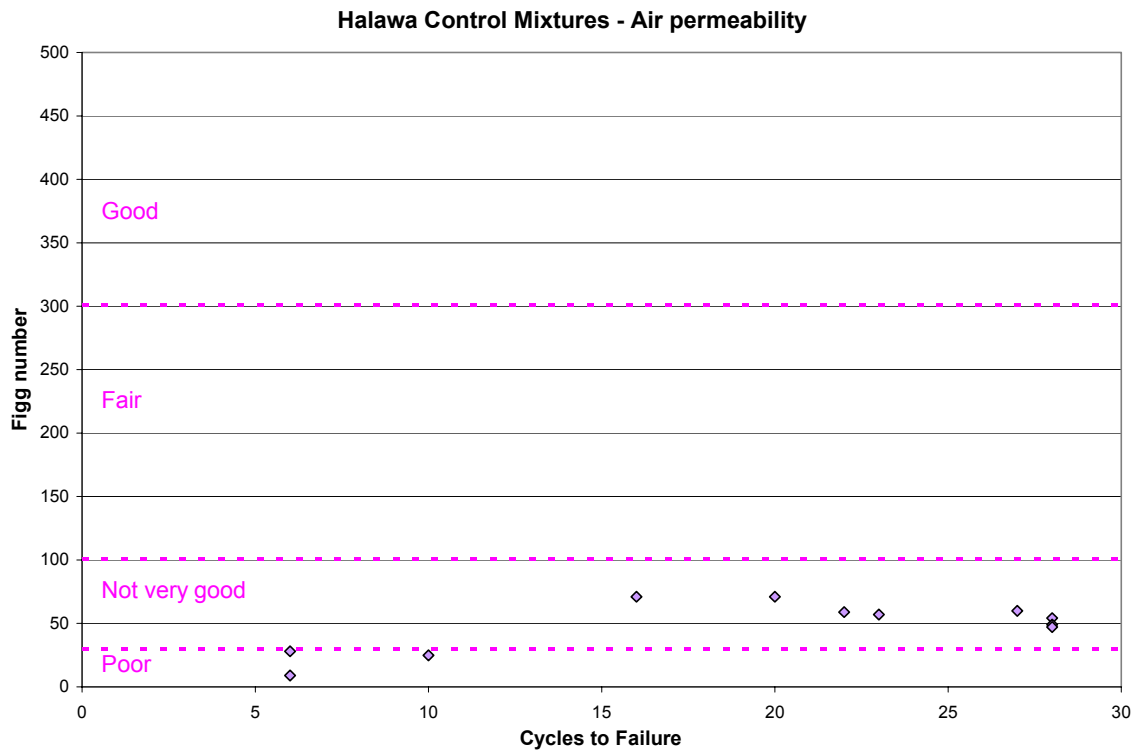


Figure 6.5 : Halawa Control – Air permeability

Figure 6.5 plots the Halawa Control mixture Figg numbers versus the number of cycles to failure. The graph shows a trend of a higher Figg number (less permeability) corresponding to a greater number of cycles until first corrosion. One concern about the Halawa control mixtures is the low values of the Figg numbers. All of the values fall into either the “not very good” or “poor” range.

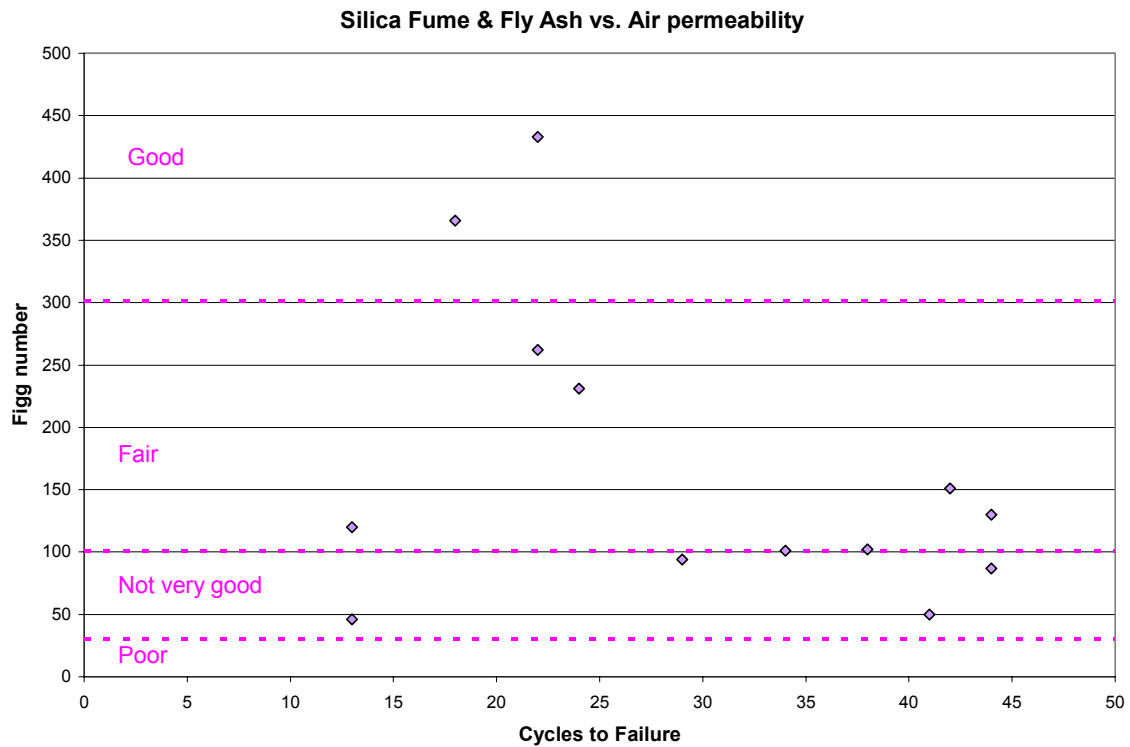


Figure 6.6 : Silica Fume & Fly Ash – Air permeability

Figure 6.6 shows how silica fume and fly ash specimen air permeability varied against the number of cycles to failure. From the plot there is a slight trend of increased permeability (low Figg number) and a longer of time until the specimen measures $10 \mu A$. This is not what was expected, but the correlation was not very strong.

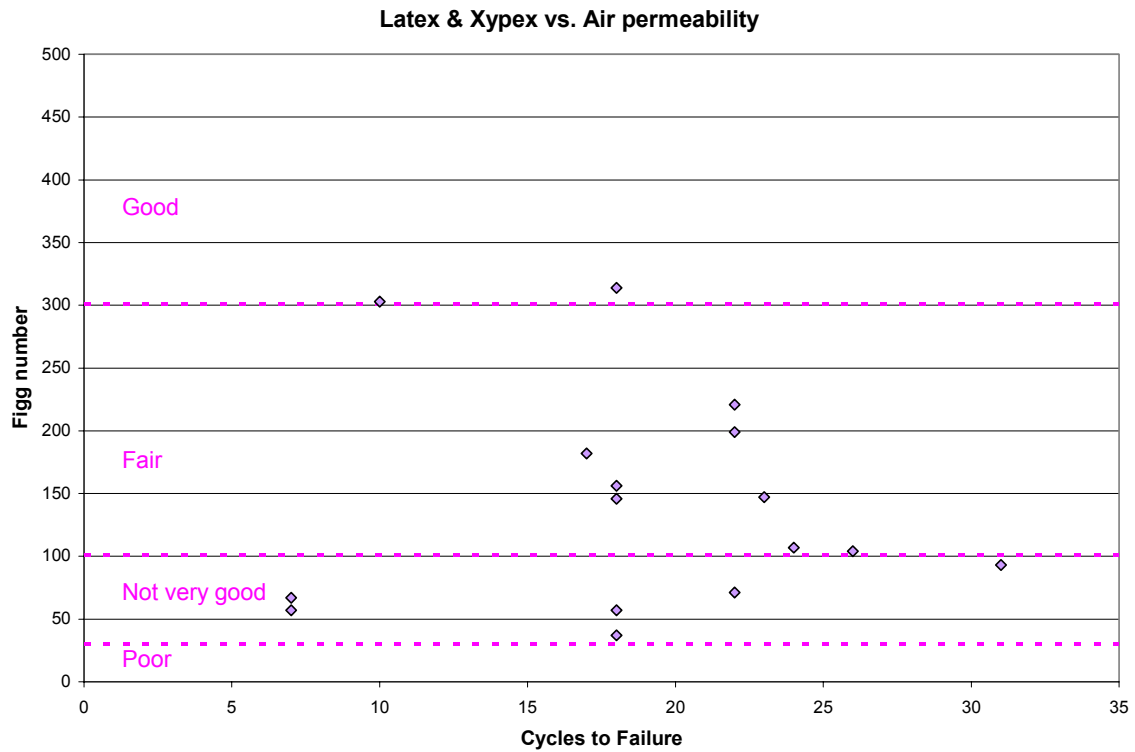


Figure 6.7 : Latex & Xypex – Air permeability

Figure 6.7 plots the Figg number of the Latex and Xypex admixtures versus the number of cycles to failure. There is no apparent correlation between permeability and cycles to failure for these specimens.

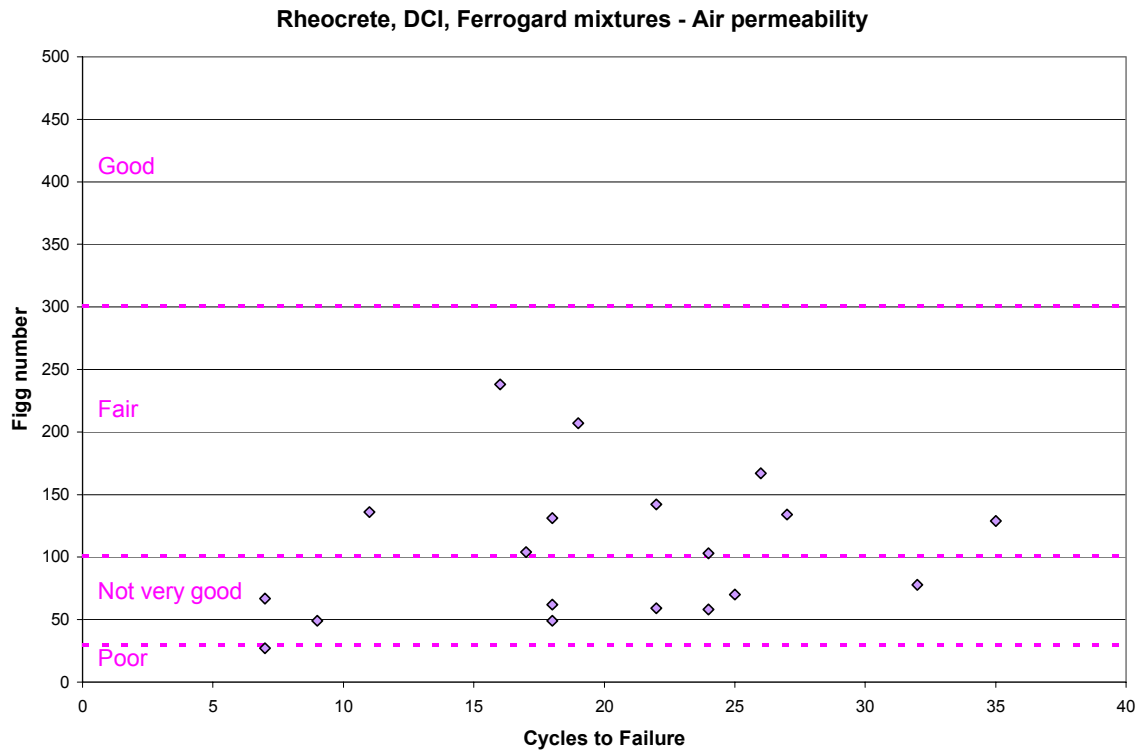


Figure 6.8 : Rheocrete, DCI, Ferrogard – Air permeability

Figure 6.8 plots Rheocrete, DCI, and Ferrogard mixture Figg numbers versus the number of cycles to failure. The graph shows a weak trend of a higher Figg number (less permeability) relating to a greater number of cycles until first corrosion. The trend is one that would be expected but it is also a weak correlation.

All Ameron Mixtures - Air permeability

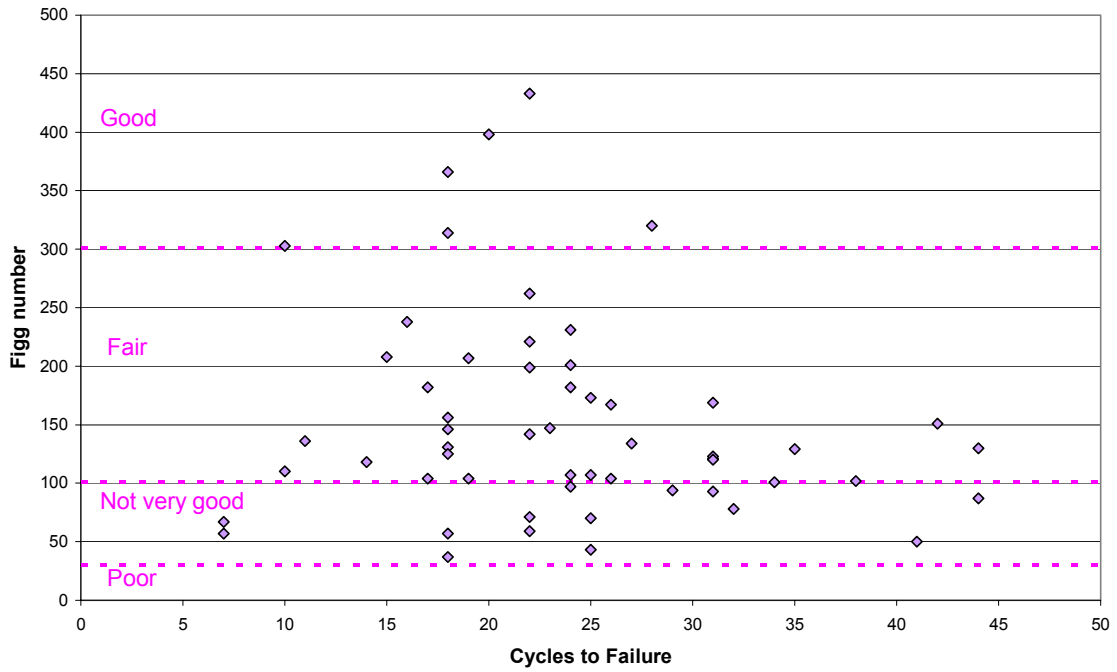


Figure 6.9 : All Ameron mixtures – Air permeability

All Halawa Mixtures - Air permeability

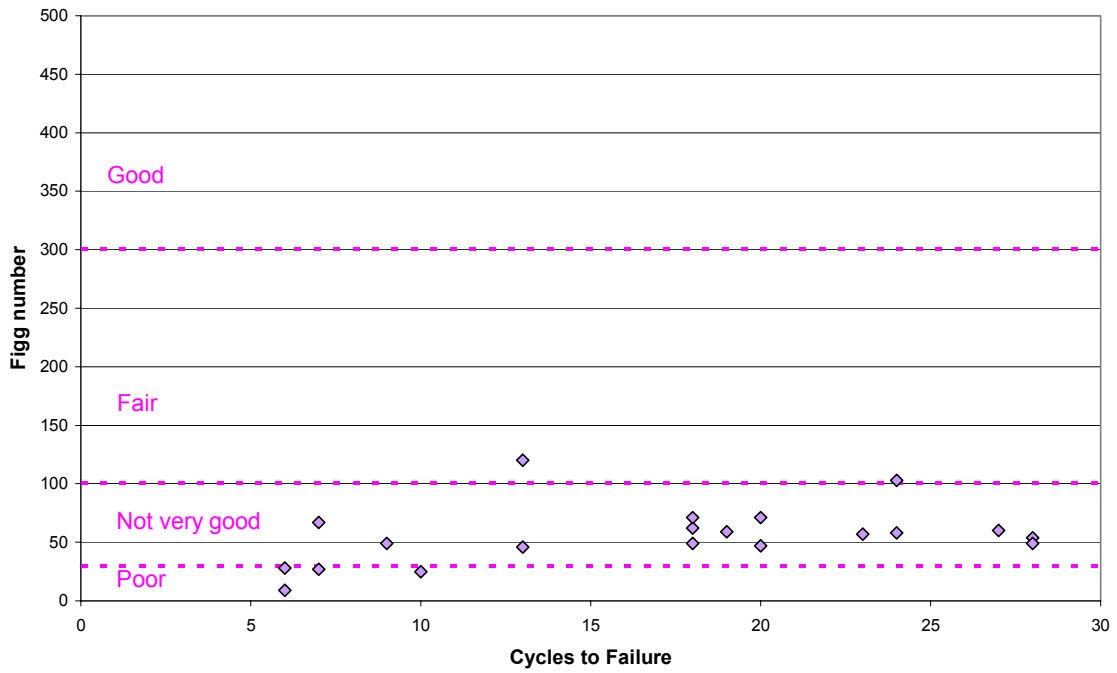


Figure 6.10 : All Halawa Mixtures – Air permeability

Figure 6.9 shows all the Ameron mixtures Figg numbers versus cycles to failure. Figure 6.10 shows all the Halawa mixtures Figg numbers versus cycles to failure. The cumulative results do not indicate any trend. The Halawa aggregate are more permeable than the Ameron aggregate.

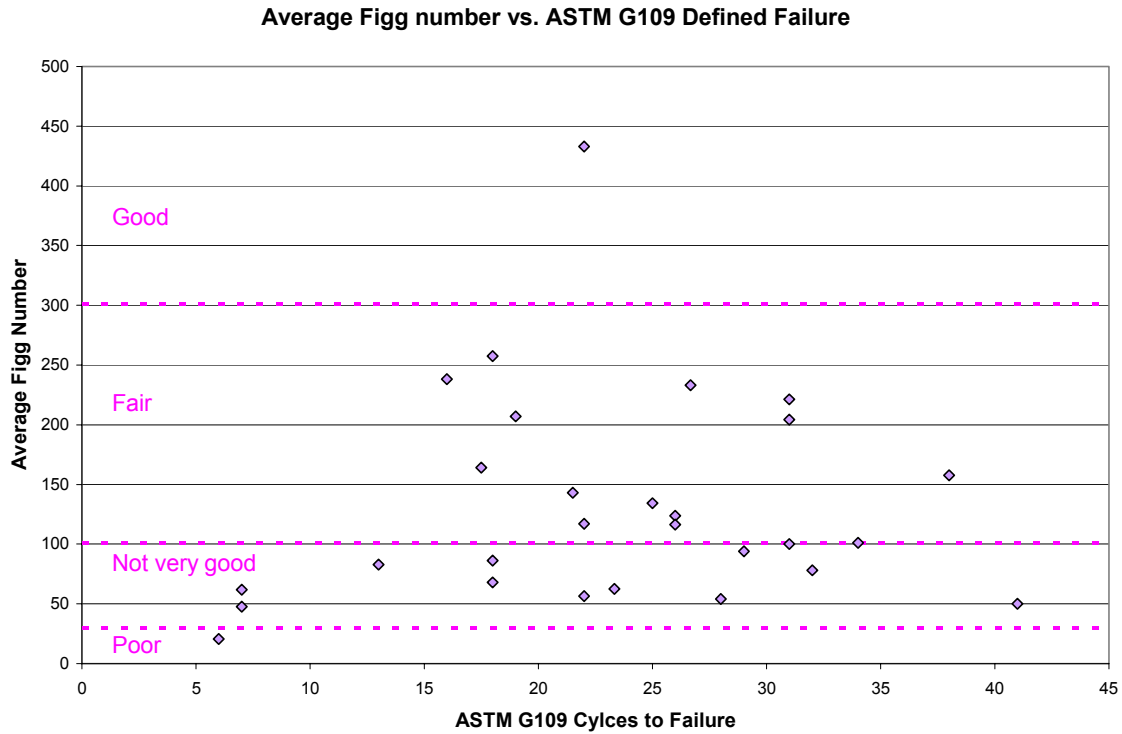


Figure 6.11 : Average Figg numbers vs. ASTM G109 Cycles to Failure

Figure 6.11 shows the average Figg numbers versus the ASTM G109 cycles to failure. The mixes with multiple specimens that failed were all averaged. The figure incorporates all of the admixtures. The averaged results do not indicate any trend or conclusion.

The air permeability values do not seem to give useful information regarding the time to corrosion for the specimens tested in this study. Only the Halawa Control mixtures showed a slight trend of less permeability leading to longer time until corrosion occurs.

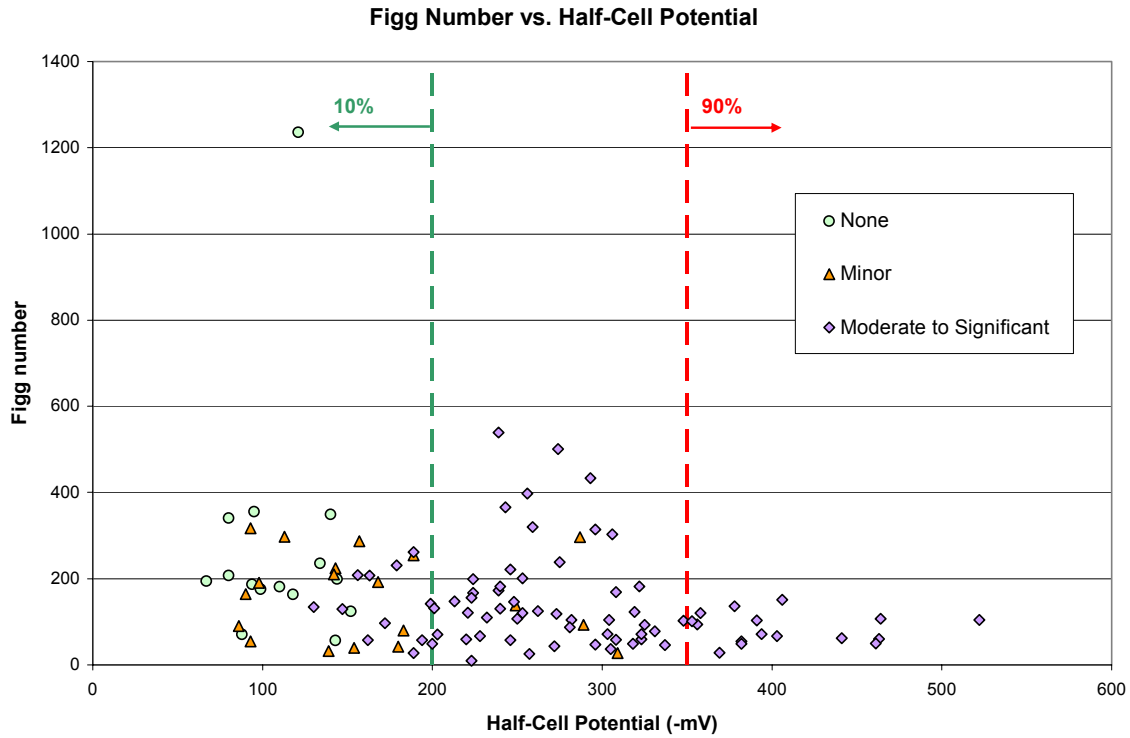


Figure 6.12 : Figg number vs. Half-cell potential

Figure 6.12 shows the relationship between Figg number and half-cell potential for all specimens in this study. The degree of corrosion observed in each specimen is indicated by the symbol color. Permeability relates to corrosion because high permeability increases the ability of chlorides to attack the reinforcing steel. Figure 6.12 does not show any clear correlation between the Figg number and the half-cell potential.

At best the air permeability test proves to be a poor predictor of how well concrete performs against corrosion. However, air permeability has a large variation because the test hole is small and the reading can be largely influenced by a single void or aggregate particle.

CHAPTER 7 - SUMMARY AND CONCLUSIONS

7.1 Introduction

The objective of this research was to use visual inspection, optical microscopy and acoustic scanning microscopy to evaluate the extent of corrosion on reinforcing bars in corrosion test specimens. The visual inspections of both exterior and interior of each corrosion specimen were used to characterize the extent of corrosion on the reinforcing bars. These observations were augmented by the use of an optical stereo-microscope. The scanning acoustic microscope used in this study was not able to image the reinforcing steel with enough resolution to identify the extent of corrosion. Based on these inspections, all specimens were classified as having “no corrosion”, “minor corrosion”, or “moderate to substantial corrosion”. The extent of corrosion was then used to evaluate the performance of two electrical tests meant to identify the presence of corrosion in concrete specimens, and for comparison with air permeability, pH level and chloride content of the specimens.

The test specimens used in this study were part of a larger project investigating the performance of various corrosion-inhibiting admixtures in concrete subjected to a marine environment. Eight corrosion-inhibiting admixtures were used including, DCI, Rheocrete CNI, Rheocrete 222+, FerroGard 901, Xypex Admix C-2000, fly ash, silica fume, and a latex-modifier.

7.2 Summary

As part of the overall durability project, each specimen was monitored for macrocell current during ponding cycling according to ASTM G109-92. All specimens that were removed from the cycling test were tested for air permeability, half-cell potential, and pH and chloride concentration at the level of the top reinforcing bars. The specimens were visually inspected externally and internally. These inspections were documented and photographic records taken using an optical stereo-microscope. Selected specimens were also prepared and examined using a scanning acoustic microscope.

According to the ASTM G109 procedures, a macrocell reading exceeding $10 \mu A$ indicates the presence of corrosion. In this study, 94% of specimens which recorded a current exceeding $10 \mu A$ had moderate to substantial corrosion while the remaining 6% had minor corrosion. When the maximum macrocell current fell between $2 \mu A$ and $10 \mu A$ there was a 47% occurrence of moderate to substantial corrosion, a 41.2% occurrence of minor corrosion, and 11.8% of no corrosion. When the macrocell current remained below $2 \mu A$, then 21% of the specimens exhibited moderate to substantial corrosion, 32% exhibited minor corrosion, and 46% exhibited no corrosion.

Half-cell readings below -350 mV are expected to indicate a 90% probability of corrosion. In this study, 100% of the specimens with half-cell readings below -350 mV exhibited moderate to substantial corrosion. For half-cell readings between -200 and -350 mV, corrosion is uncertain. In this study, 93% of specimens falling in this range had moderate to substantial corrosion and 7% had minor corrosion. Half-cell potential readings above -200 mV are expected to indicate a 10% probability of corrosion, or 90%

probability of no corrosion. In this study, 28% of specimens falling in this range had moderate to substantial corrosion, while 37% had minor corrosion, and 35% had none. It appears that the probability range has shifted from that suggested by current practice. Based on the results of this study, more accurate results would be obtained if the half-cell limits were modified to -100 mV and -200 mV instead of -200 mV and -350 mV respectively.

Specimens using the control mixture with Halawa aggregates indicated a trend of greater permeability leading to earlier initiation of corrosion. The air permeability results for specimens using Ameron aggregates and DCI, Rheocrete CNI, Rheocrete 222+, FerroGard 901, Xypex Admix C-2000, fly ash, and silica fume, showed either very weak or no correlation between permeability and time to initiation of corrosion.

The chloride concentration at the level of the reinforcing steel did not show a strong correlation with observed corrosion. Specimens with low chloride levels experienced all levels of corrosion, however, higher chloride levels were associated with more substantial corrosion. Specimens with no corrosion had chloride levels from 0.5 to 2.2% by weight of cement. Specimens with minor corrosion had chloride levels from 0.5 to 3.0%, while those with moderate to substantial corrosion had chloride levels from 0.5 to 6.5%.

There was no apparent correlation between the pH level and the extent of corrosion on the reinforcing steel for the specimens investigated in this study. The specimens with no corrosion had pH values ranging from 12 to 12.6. The specimens with minor corrosion had pH values between 12 and 12.6. The specimens with moderate to substantial corrosion had pH values between 11.9 and 12.9.

7.3 Conclusions

1. Corrosion was observed in all specimens that had recorded a macrocell current exceeding $10 \mu A$. This current measurement is therefore an accurate predictor of the presence of corrosion.
2. Based on the results of this study, it would appear that the potential limits for the half-cell measurements have shifted. More accurate results were obtained if the half-cell limits were modified from -200 mV and -350 mV to -100 mV and -200 mV , respectively.
3. Specimens using the control mixture with Halawa aggregates indicated a trend of greater permeability leading to earlier initiation of corrosion. The air permeability results for all other specimens showed either very weak or no correlation between permeability and time to initiation of corrosion.
4. The chloride concentration at the level of the reinforcing steel did not show a strong correlation with observed corrosion. Chloride levels ranged from 0.5% to 6.5%.
5. The pH level at the top reinforcement did not show any correlation with the severity of corrosion of the reinforcement. All specimens in this study had pH levels between 12 and 13.
6. The scanning acoustic microscope used in this study was not able to map the extent of corrosion around the steel reinforcing bars.

APPENDIX A

Mix Designs

Table A.1. Mixture proportions for control mixtures (Ameron?)

Material or property	CON1 C2	CON2 C3	CON3 C1	CON4 C5	CON5 C6	CON6 C4
W/c	0.4	0.45	0.35	0.4	0.45	0.35
Paste volume (%)	31.2	31.2	31.2	32.5	32.5	32.5
Design Slump (in)	4	4	4	4	4	4
(mm)	100	100	100	100	100	100
Coarse aggregate (lb/yd ³)	1576	1576	1576	1576	1576	1576
(kg/m ³)	935	935	935	935	935	935
Dune sand (lb/yd ³)	431	431	431	411.5	411.5	411.5
(kg/m ³)	255.7	255.7	255.7	244.1	244.1	244.1
Concrete sand (lb/yd ³)	825.6	825.6	825.6	788.2	788.2	788.2
(kg/m ³)	489.8	489.8	489.8	467.6	467.6	467.6
Cement (lb/yd ³)	733.2	683.7	786.1	762.5	712.8	819.6
(kg/m ³)	435	405.6	466.4	452.4	422.9	486.3
Water (lb/yd ³)	292.1	307.7	275.1	305	320.8	286.9
(kg/m ³)	173.3	182.6	163.2	181	190.3	170.2
Daratard (oz./sk)	3	3	3	3	3	3
(ml/sk)	88.7	88.7	88.7	88.7	88.7	88.7
Darex (oz./sk)	2	2	2	2	2	2
(ml/sk)	59.1	59.1	59.1	59.1	59.1	59.1
Design air content (%)	4	4	4	4	4	4

Table A.2 Mixture Proportions for DCI and CNI mixtures

Material or property	DCI1	DCI2	DCI3	DCI4	DCI5	DCI6
	D4	D5	D6	D1	D2	D3
	CNI1	CNI2	CNI3	CNI4	CNI5	CNI6
W/c	0.4	0.4	0.4	0.35	0.35	0.35
Paste volume (%)	31.2	31.2	31.2	32.5	32.5	32.5
Design Slump (in)	4	4	4	4	4	4
(mm)	100	100	100	100	100	100
Coarse aggregate (lb/yd ³)	1576	1576	1576	1576	1576	1576
(kg/m ³)	935	935	935	935	935	935
Dune sand (lb/yd ³)	431.4	431.4	431.4	411.5	411.5	411.5
(kg/m ³)	256	256	256	244.1	244.1	244.1
Concrete sand (lb/yd ³)	826.5	826.5	826.5	788.2	788.2	788.2
(kg/m ³)	490.4	490.4	490.4	467.6	467.6	467.6
Cement (lb/yd ³)	733.2	733.2	733.2	819.6	819.6	819.6
(kg/m ³)	435	435	435	486.3	486.3	486.3
Water (lb/yd ³)	275.4	258.7	242	270.2	253	236.8
(kg/m ³)	163.4	153.5	143.6	160.3	150.4	140.5
Liquid DCI or CNI (gal/yd ³)	2	4	6	2	4	6
(l/m ³)	9.9	19.8	29.7	9.9	19.8	29.7
Daratard (oz./sk)	3	3	3	3	3	3
(ml/sk)	88.7	88.7	88.7	88.7	88.7	88.7
Darex (oz./sk)	2	2	2	2	2	2
(ml/sk)	59.1	59.1	59.1	59.1	59.1	59.1
Design air content (%)	4	4	4	4	4	4

Table A.3. Mixture Proportions for Rheocrete mixtures

Material or property	RHEO1 RHE2	RHEO2 RHE3	RHEO3 RHE1	RHEO4 RHE5	RHEO5 RHE6	RHEO6 RHE4
W/c	0.4	0.45	0.35	0.4	0.45	0.35
Paste volume (%)	31.2	31.2	31.2	32.5	32.5	32.5
Design Slump (in)	4	4	4	4	4	4
(mm)	100	100	100	100	100	100
Coarse aggregate (lb/yd ³)	1576	1576	1576	1576	1576	1576
(kg/m ³)	935	935	935	935	935	935
Dune sand (lb/yd ³)	431	431	431	411.5	411.5	411.5
(kg/m ³)	255.7	255.7	255.7	244.1	244.1	244.1
Concrete sand (lb/yd ³)	825.6	825.6	825.6	788.2	788.2	788.2
(kg/m ³)	489.8	489.8	489.8	467.6	467.6	467.6
Cement (lb/yd ³)	733.2	683.7	786.1	762.5	712.8	819.6
(kg/m ³)	435	405.6	466.4	452.4	422.9	486.3
Water (lb/yd ³)	292.1	307.7	275.1	305	320.8	286.9
(kg/m ³)	173.3	182.6	163.2	181	190.3	170.2
Rheocrete 222+ (gal/yd ³)	1	1	1	1	1	1
(l/m ³)	4.95	4.95	4.95	4.95	4.95	4.95
Daratard (oz./sk)	3	3	3	3	3	3
(ml/sk)	88.7	88.7	88.7	88.7	88.7	88.7
Darex (oz./sk)	2	2	2	2	2	2
(ml/sk)	59.1	59.1	59.1	59.1	59.1	59.1
Design air content (%)	4	4	4	4	4	4

Table A.4. Mixture Proportions for FerroGard mixtures

Material or property	FERR1 FER2	FERR2 FER3	FERR3 FER1	FERR4 FER5	FERR5 FER6	FERR6 FER4
W/c	0.4	0.45	0.35	0.4	0.45	0.35
Paste volume (%)	31.2	31.2	31.2	32.5	32.5	32.5
Design Slump (in)	4	4	4	4	4	4
(mm)	100	100	100	100	100	100
Coarse aggregate (lb/yd ³)	1576	1576	1576	1576	1576	1576
(kg/m ³)	935	935	935	935	935	935
Dune sand (lb/yd ³)	431	431	431	411.5	411.5	411.5
(kg/m ³)	255.7	255.7	255.7	244.1	244.1	244.1
Concrete sand (lb/yd ³)	825.6	825.6	825.6	788.2	788.2	788.2
(kg/m ³)	489.8	489.8	489.8	467.6	467.6	467.6
Cement (lb/yd ³)	733.2	683.7	786.1	762.5	712.8	819.6
(kg/m ³)	435	405.6	466.4	452.4	422.9	486.3
Water (lb/yd ³)	267.1	282.7	250.1	280	295.8	262
(kg/m ³)	158.5	167.7	148.4	166.1	175.5	155.4
FerroGard 901 (gal/yd ³)	3	3	3	3	3	3
(l/m ³)	14.85	14.85	14.85	14.85	14.85	14.85
Darex (oz./sk)	2	2	2	2	2	2
(ml/sk)	59.1	59.1	59.1	59.1	59.1	59.1
Design air content (%)	4	4	4	4	4	4

Table A.5. Mixture Proportions for Xypex mixtures

Material or property	Xypex1 XYP2	Xypex2 XYP3	Xypex3 XYP1	Xypex4 XYP5	Xypex5 XYP6	Xypex6 XYP4
W/c	0.4	0.45	0.35	0.4	0.45	0.35
Paste volume (%)	31.2	31.2	31.2	32.5	32.5	32.5
Design Slump (in)	4	4	4	4	4	4
(mm)	100	100	100	100	100	100
Coarse aggregate (lb/yd ³)	1576	1576	1576	1576	1576	1576
(kg/m ³)	935	935	935	935	935	935
Dune sand (lb/yd ³)	431	431	431	411.5	411.5	411.5
(kg/m ³)	255.7	255.7	255.7	244.1	244.1	244.1
Concrete sand (lb/yd ³)	825.6	825.6	825.6	788.2	788.2	788.2
(kg/m ³)	489.8	489.8	489.8	467.6	467.6	467.6
Cement (lb/yd ³)	718.5	670	770.4	746.7	698.5	803.2
(kg/m ³)	426.3	397.5	457.1	443	414.4	476.5
Water (lb/yd ³)	292.1	307.7	275.1	305	320.8	286.9
(kg/m ³)	173.3	182.6	163.2	181	190.3	170.2
Xypex (lb/yd ³)	14.7	13.7	15.72	15.8	14.3	16.4
(kg/m ³)	8.72	8.13	9.33	9.37	8.48	9.73
Darex (oz./sk)	2	2	2	2	2	2
(ml/sk)	59.1	59.1	59.1	59.1	59.1	59.1
Design air content (%)	4	4	4	4	4	4

Table A.6. Mixture Proportions for latex-modified mixtures

Material or property	LA1	LA2	LA3	LA4	LA5	LA6
	L4	L5	L6	L1	L2	L3
W/c	0.4	0.4	0.4	0.35	0.35	0.35
Paste volume (%)	34.6	31.2	32.2	31.2	32.3	33.4
Coarse aggregate (lb/yd ³)	1576	1576	1576	1576	1576	1576
(kg/m ³)	935	935	935	935	935	935
Dune sand (lb/yd ³)	415.2	399.5	383.8	414.2	397.3	380.5
(kg/m ³)	246.3	237	227.7	245.7	235.7	225.8
Concrete sand (lb/yd ³)	795.3	765.2	735.1	793.4	761.1	728.9
(kg/m ³)	471.8	454	436.1	470.7	451.6	432.4
Cement (lb/yd ³)	733.2	733.2	733.2	786.1	786.1	786.1
(kg/m ³)	435	435	435	466.4	466.4	466.4
Water (lb/yd ³)	237.1	182.1	127.1	216.2	157.2	98.3
(kg/m ³)	140.7	108	75.4	128.3	93.3	58.3
Latex liquid (lb/yd ³)	73.3	146.6	220	78.6	157.2	235.8
(kg/m ³)	43.5	87	130.5	46.6	93.3	140
Design air content (%)	4	4	4	4	4	4

Table A.7. Mixture Proportions for silica fume

Material or property	SF1	SF2	SF3	SF4	SF5	SF6	SF7	SF8	SF9	SF10	SF11
w/(c+sf)	0.36	0.36	0.36	0.36	0.36	0.36	0.45	0.45	0.45	0.45	0.45
Paste volume (%)	32.6	32.9	33.3	33.6	32.9	32.9	34.7	35	35.3	34.7	34.7
D.Slump (in)	8 ~ 10	8 ~ 10	8 ~ 10	8 ~ 10	8 ~ 10	8 ~ 10	8 ~ 10	8 ~ 10	8 ~ 10	8 ~ 10	8 ~ 10
(mm)	(200-250)	(200-250)	(200-250)	(200-250)	(200-250)	(200-250)	(200-250)	(200-250)	(200-250)	(200-250)	(200-250)
Coarse agg. (lb/yd ³)	1668	1668	1668	1668	1668	1668	1668	1668	1668	1668	1668
(kg/m ³)	989.6	989.6	989.6	989.6	989.6	989.6	989.6	989.6	989.6	989.6	989.6
Dune sand (lb/yd ³)	537.6	531.3	525.4	519.2	531.3	531.3	497.9	492.2	486.5	497.9	497.9
(kg/m ³)	319	315.2	311.7	308	315.2	315.2	295.4	292	288.6	295.4	295.4
Concrete sand (lb/yd ³)	712.6	704.3	696.4	688.2	704.3	704.3	660.1	652.5	644.8	660.1	660.1
(kg/m ³)	422.8	417.9	413.2	408.3	417.9	417.9	391.6	387.1	382.6	391.6	391.6
Cement (lb/yd ³)	811	771	729.9	689.4	722.6	675.8	717.8	680	642.2	674	631.1
(kg/m ³)	481.2	457.4	433	409	428.7	401	425.9	403.4	381	400	374.4
Water (lb/yd ³)	292	292	292	292	289.1	286.2	340	340	340	337	334.1
(kg/m ³)	173.2	173.2	173.2	173.2	171.5	169.8	201.7	201.7	201.7	200	198.2
Silica fume (lb/yd ³)	0	40	81.1	121.65	80.29	119.25	37.78	75.56	113.33	74.89	111.36
(kg/m ³)	0	23.73	48.12	72.17	47.64	70.75	22.42	44.83	67.24	44.43	66.07
Design air content (%)	1	1	1	1	1	1	1	1	1	1	1

Table A.8. Mixture Proportions of Fly Ash Mixtures

Material or property	FA2	FA3	FA4	FA5	FA6	FA7	FA8	FA9	FA10	FA11
w/(c+sf)	0.36	0.36	0.36	0.36	0.36	0.45	0.45	0.45	0.45	0.45
Paste volume (%)	32.6	32.8	33	33.2	32.8	32.8	34.6	34.8	35	34.6
D.Slump (in) (mm)	8 ~ 10 (200- 250)									
Coarse agg. (lb/yd ³) (kg/m ³)	1668 989.6									
Dune sand (lb/yd ³) (kg/m ³)	533.9 316.8	530.2 314.6	526.4 312.3	533.9 316.8	533.9 316.8	500.4 296.9	496.9 294.8	493.5 292.8	500.4 296.9	500.4 296.9
Concrete sand (lb/yd ³) (kg/m ³)	707.7 419.9	702.8 417	697.8 414	707.7 419.9	707.7 419.9	663.3 393.5	658.7 390.8	654.1 388.1	663.3 393.5	663.3 393.5
Cement (lb/yd ³) (kg/m ³)	771 457.4	729.9 433	689.4 409	725.5 430.4	681.1 404.1	717.8 425.9	680 403.4	642.2 381	676.4 401.3	635.4 377
Water (lb/yd ³) (kg/m ³)	292 173.2	292 173.2	292 173.2	290.2 172.2	288.5 171.2	340 201.7	340 201.7	340 201.7	338.2 200.6	336.4 199.6
Fly Ash (lb/yd ³) (kg/m ³)	40 23.73	81.1 48.12	121.65 72.17	80.61 47.82	120.19 71.31	37.78 22.42	75.56 44.83	113.33 67.24	75.15 44.59	112.13 66.53
Design air content (%)	1	1	1	1	1	1	1	1	1	1

APPENDIX B

Materials

Table B.1. Particle size distribution for fine aggregates

Sieve Size	Percent passing by weight			
	Maui Dune Sand	Basalt sand	Blended Sand	ASTM C 33 requirement
3/8 in. (9.5 mm)	100	100	100	100
No. 4 (4.75 mm)	98.8	97.5	98	95 to 100
No. 8 (2.36 mm)	97.5	90.9	93.2	80 to 100
No. 16 (1.18 mm)	95	56.7	69.8	50 to 85
No. 30 (600 μ m)	91.2	32.4	52.6	25 to 60
No. 50 (300 μ m)	66.6	11.6	30.5	10 to 30
No. 150 (150 μ m)	9	2.1	4.5	2 to 10

Table B.2. Fineness modulus of fine aggregates

	Maui Dune Sand	Basalt sand	Blended sand	ASTM C33 requirement
Fineness modulus	1.42	2.61	2.52	2.3 to 3.1

Table B.3. Specific gravity and absorption for fine aggregates

	Bulk specific gravity	Absorption (%)
Maui dune sand	2.42	2.78
Crushed basalt sand	2.83	5.01
Blended sand	2.54	--

Table B.4. Particle size distribution for coarse aggregate

Sieve Size	Percent passing by weight (%)	
	Crushed coarse basalt	ASTM C 33 Requirement
1" (25 mm)	100	100
³ / ₄ " (19 mm)	99.2	90 to 100
¹ / ₂ " (12.5 mm)	66.3	NA
3/8" (9.5 mm)	33.3	25 to 55
No. 4 (4.75 mm)	4.6	0 to 10

Table B.5. Specific gravity and absorption for coarse aggregate

	Bulk specific gravity	Absorption (%)
Coarse aggregate	2.63	2.75

APPENDIX C

Material Properties

Table C.1. Tests performed for each concrete mixture

	Compressive strength	Elastic modulus	Poisson's ratio	Slump	Concrete permeability	pH	Chloride concentration	Air entrained
C1	x	x		x	x	x	x	
C2	x	x	x	x	x	x	x	
C3	x	x		x	x	x	x	
C4	x	x		x	x	x	x	
C5	x	x	x	x	x	x	x	
C6	x	x	x	x	x	x	x	
D1 - D6	x	x	x	x	x	x	x	
CNI1- CNI6	x	x	x	x				x
FER1	x	x	x	x				
FER2	x	x	x	x				
FER3	x	x	x	x				
FER4	x	x	x	x				x
FER5	x	x	x	x				x
FER6	x	x	x	x				x
RHE1- RHE6	x	x	x	x				x
XYP1- XYP6	x	x	x	x				x
L1 - L6	x	x	x	x	x	x	x	
SF1 - SF11	x	x	x	x	x	x	x	
FA2 - FA11	x	x	x	x				

Table C.2. Slump, average compressive strength, elastic modulus, and Poisson's ratio of control mixtures.

	C1	C2	C3	C4	C5	C6
w/c	0.35	0.4	0.45	0.35	0.4	0.45
Paste content (%)	31.2	31.2	31.2	32.5	32.5	32.5
Slump (in.)	3.75	4.25	8.5	3.75	5.5	8.5
(mm)	95	108	216	95	140	216
Compressive strength (psi)	7,620	7,050	5,780	8,140	6,530	6,440
(MPa)	52.6	48.6	39.8	56.2	45	44.4
Elastic modulus (ksi)	3,900	3,200	3,750	4,100	3,850	3,750
(MPa)	26,890	22,064	25,856	28,270	26,546	25,856
Poisson's ratio		0.17			0.17	0.22

Table C.3. Slump, average compressive strength, elastic modulus, and Poisson's ratio of DCI mixtures.

	C4	D1	D2	D3	C2	D4	D5	D6
w/c	0.35	0.35	0.35	0.35	0.4	0.4	0.4	0.4
DCI (gal/yd ³)	0	2	4	6	0	2	4	6
(1/m ³)	0	9.9	19.8	29.7	0	9.9	19.8	29.7
Paste content (%)	32.48	32.48	32.48	32.48	31.15	31.15	31.15	31.15
Slump (in.)	3.75	4.5	5	5	4.25	6	5.75	3.5
(mm)	95	114	127	127	108	152	146	89
Compressive strength (psi)	8,140	8,220	9,010	9,380	7,050	7,260	8,040	10,250
(MPa)	56.2	56.7	62.1	64.6	48.6	50	55.4	70.7
Elastic modulus (ksi)	4,100	4,000	4,150	4,400	3,200	4,100	4,350	4,200
(MPa)	28,270	27,580	28,614	30,338	22,064	28,270	29,993	28,959
Poisson's ratio		0.23	0.26	0.26	0.17	0.2	0.15	0.26

Table C.4. Slump, average compressive strength, elastic modulus, Poisson's ratio, and air content of CNI mixtures.

	C4	CNI1	CNI2	CNI3	C2	CNI4	CNI5	CNI6
w/c	0.35	0.35	0.35	0.35	0.4	0.4	0.4	0.4
CNI (gal/yd ³)	0	2	4	6	0	2	4	6
(1/m ³)	0	9.9	19.8	29.7	0	9.9	19.8	29.7
Paste content (%)	32.5	32.5	32.5	32.5	31.2	31.2	31.2	31.2
Slump (in.)	3.75	7.5	7	6.75	4.25	6.25	8.5	8.75
(mm)	95	190	178	172	108	159	216	222
Compressive strength (psi)	8,140	8,760	9,400	7,630	7,050	7,590	7,560	8,240
(MPa)	56.2	60.4	64.8	52.6	48.6	52.3	52.2	56.8
Elastic modulus (ksi)	4,100	3,850	3,900	3,800	3,200	3,900	3,800	3,500
(MPa)	28,270	26,546	26,890	26,201	22,064	26,890	26,201	24,133
Poisson's ratio		0.21	0.27	0.2	0.17	0.24	0.18	0.21
Air content (%)		2.7	2.8	5.4		3.6	3.5	4.2

Table C.5. Slump, average compressive strength, elastic modulus, Poisson's ratio, and air content of FerroGarrd mixtures.

	FER1	FER2	FER3	FER4	FER5	FER6
w/c	0.35	0.4	0.45	0.35	0.4	0.45
FER content (gal/yd ³) (1/m ³)	3 14.85	3 14.85	3 14.85	3 14.85	3 14.85	3 14.85
Paste content (%)	31.2	31.2	31.2	32.5	32.5	32.5
Slump (in.) (mm)	4.5 114	7.5 190	9.25 235	6 152	7.25 184	9.25 235
Compressive strength (psi) (MPa)	8,160 56.3	6,540 45	6,120 42.2	7,560 52.1	6,230 43	5,750 39.7
Elastic modulus (ksi) (MPa)	3,900 26,890	3,500 24,132	3,450 23,788	3,950 27,235	3,500 24,132	3,150 21,719
Poisson's ratio	0.18	0.22	0.16	0.24	0.23	0.27
Air content (%)	3.75			4.3	5.3	5.0

Table C.6. Slump, average compressive strength, elastic modulus, Poisson's ratio, and air content of Rheocrete 222+ mixtures.

	RHE1	RHE2	RHE3	RHE4	RHE5	RHE6
w/c	0.35	0.4	0.45	0.35	0.4	0.45
RHE content (gal/yd ³) (1/m ³)	1 4.95	1 4.95	1 4.95	1 4.95	1 4.95	1 4.95
Paste content (%)	31.2	31.2	31.2	32.5	32.5	32.5
Slump (in.) (mm)	4.25 108	5.25 133	9.5 241	5.5 140	8.5 216	10 254
Compressive strength (psi) (MPa)	8,240 56.8	6,530 45	5,960 41.1	7,270 50.1	6,640 45.8	6,460 44.6
Elastic modulus (ksi) (MPa)	3,650 25,167	3,650 25,167	3,650 25,167	4,000 27,580	3,500 24,132	3,200 22,064
Poisson's ratio	0.22	0.22	0.22	0.23	0.23	0.22
Air content (%)	2.8	6.5	2.6	4.8	3.6	1.5

Table C.7. Slump, average compressive strength, elastic modulus, Poisson's ratio, and air content of Xypex mixtures.

	XYP1	XYP2	XYP3	XYP4	XYP5	XYP6
w/c	0.35	0.4	0.45	0.35	0.4	0.45
XYP (% of cement wt.)	2	2	2	2	2	2
Paste content (%)	31.2	31.2	31.2	32.5	32.5	32.5
Slump (in.)	3	6	7	4	6.5	8
(mm)	76	152	178	102	165	203
Compressive strength (psi)	6,690	5,460	4,380	6,590	4,270	4,260
(MPa)	46.1	37.7	30.2	45.4	29.4	29.4
Elastic modulus (ksi)	3,750	3,150	2,800	3,800	3,000	3,100
(MPa)	25,856	21,719	19,306	26,201	20,685	21,374
Poisson's ratio	0.3	0.19	0.22	0.23	0.26	0.3
Air content (%)	5.5	4.75	8.0	5.25	8.0	7.75

Table C.8. Slump, average compressive strength, elastic modulus, and Poisson's ratio of Latex-modified mixtures.

	C1	L1	L2	L3	C2	L4	L5	L6
w/c	0.35	0.35	0.35	0.35	0.4	0.4	0.4	0.4
Latex (% of cement wt.)	0	2.5	5	7.5	0	2.5	5	7.5
Paste content (%)	31.2	32.3	33.4	34.6	31.2	32.2	33.3	34.4
Slump (in.)	3.75	5.25	8.5	9.25	4.25	8.5	9.75	9.75
(mm)	95	133	216	235	108	216	248	248
Compressive strength (psi)	7,620	6,320	4,080	6,160	7,050	3,060	4,490	4,800
(MPa)	52.6	43.6	28.1	42.5	48.6	21.1	31	33.1
Elastic modulus (ksi)	3,900	3,500	2,850	3,350	3,200	2,650	3,025	3,000
(MPa)	26,890	24,132	19,651	23,098	22,064	18,272	21,374	20,685
Poisson's ratio		0.24	0.23	0.24	0.17	0.19	0.24	0.23

Table C.9. Slump, average compressive strength, elastic modulus, and Poisson's ratio of Silica fume mixtures.

	SF1	SF2	SF3	SF4	SF5	SF6	SF7	SF8	SF9	SF10	SF11
w/c	0.36	0.36	0.36	0.36	0.36	0.36	0.45	0.45	0.45	0.45	0.45
Silica fume content (%)	0	5	10	15	10	15	5	10	15	10	15
Paste content (%)	32.6	32.9	33.3	33.6	32.9	32.9	34.7	35.0	35.3	34.7	34.7
Slump (in.)	8	8	8.25	8.25	8.25	8.25	8.5	8	8	8	8
(mm)	203	203	210	210	210	210	216	203	203	203	203
Compressive strength (psi)	7,800	9,210	8,990	9,770	9,700	9,260	6,560	7,230	7,130	6,740	6,730
(MPa)	53.8	63.5	62	67.4	66.9	63.9	45.2	49.8	49.2	46.5	46.4
Elastic modulus (ksi)	3,900	4,700	3,800	4,000	4,350	4,600	3,600	3,950	3,850	3,850	3,850
(MPa)	26,890	32,406	26,201	27,580	29,993	31,717	24,822	27,235	26,546	26,546	26,546
Poisson's ratio	0.24	0.27	0.22	0.22	0.21	0.28	0.21	0.24	0.24	0.23	0.26

Table C.10. Slump, average compressive strength, elastic modulus, and Poisson's ratio of Fly ash mixtures.

	SF1	FA2	FA3	FA4	FA5	FA6	FA7	FA8	FA9	FA10	FA11
w/c	0.36	0.36	0.36	0.36	0.36	0.36	0.45	0.45	0.45	0.45	0.45
Fly Ash content (%)	0	5	10	15	10	15	5	10	15	10	15
Paste content (%)	32.6	32.8	33.0	33.2	32.8	32.8	34.6	34.8	35.0	34.6	34.6
Slump (in.)	8	8.5	8.5	8.75	8.75	8.25	8.5	8.25	8.5	8.5	8
(mm)	203	216	216	222	222	210	216	210	216	216	203
Compressive strength (psi)	7,800	7,750	7,370	7,610	8,200	7,780	5,950	6,110	6,020	6,840	6,810
(MPa)	53.8	53.4	50.8	52.5	56.6	53.6	41.0	42.1	41.5	47.2	47
Elastic modulus (ksi)	3,900	4,300	4,300	4,100	3,950	4,100	3,500	3,950	3,600	3,400	3,450
(MPa)	26,890	29,648	29,648	28,269	27,235	28,269	24,132	27,235	24,822	23,443	23,788
Poisson's ratio	0.24	0.22	0.23	0.25	0.25	0.25	0.21	0.24	0.22	0.10	0.21

APPENDIX D

Air permeability, Chloride and Ph values

Table D.1. Values of permeability and concrete ratings (Poroscope Plus 1998).

Concrete Category	Protective Quality	Permeability (Figg number)
0	Poor	<30
1	Not very good	30-100
2	Fair	100-300
3	Good	301-1000
4	Excellent	>1000

Table D.2. Air permeability for control, DCI, latex-modified, and silica fume mixtures

Mix	Air permeability (Figg number)	Standard Deviation	Variation (%)	Protective quality
C1	613	346	56.4	Good
C2	899	281	31.2	Good
C3	596	86	14.5	Good
C4	784	364	46.5	Good
C5	421	237	56.1	Good
C6	769	382	49.6	Good
D1	625	308	49.2	Good
D2	556	363	65.3	Good
D3	1139	671	58.9	Excellent
D4	460	171	37.2	Good
D5	286	144	50.3	Fair
D6	603	327	54.2	Good
L1	1351	907	67.1	Excellent
L2	833	264	31.7	Good
L3	2061	697	33.8	Excellent
L4	253	62	24.5	Fair
L5	2150	657	30.6	Excellent
L6	1967	299	15.2	Excellent
SF1	2387	1228	51.5	Excellent
SF2	926	589	63.6	Good
SF3	1574	618	39.2	Excellent
SF4	1354	404	29.9	Excellent
SF7	1496	1004	67.1	Excellent
SF8	1174	531	45.2	Excellent
SF9	3435	1258	36.6	Excellent

Table D.3. Chloride concentrations for control and DCI mixtures (%by mass of cement).

Control	C1		C2		C3		C4		C5		C6
Cycles	%	Cycles	%	Cycles	%	Cycles	%	Cycles	%	Cycles	%
0	0.021	0	0.032	0	0.035	0	0.017	0	0.028	0	0.03
3	0.426	3	0.028	3	0.716	3	0.204	3	0.539	3	0.604
5	0.228	5	0.753	5	0.823	4	0.261	4	0.635	4	1.069
7	0.991	7	1.053	7	1.511	6	0.483	6	1.008	6	1.176
16	1.487	16	3.476	16	3.134	16	1.563	16	2.319	16	2.672
DCI	D1		D2		D3		D4		D5		D6
Cycles	%	Cycles	%	Cycles	%	Cycles	%	Cycles	%	Cycles	%
0	0.036	0	0.041	0	0.044	0	0.05	0	0.045	0	0.04
3	0.218	3	0.298	3	0.369	3	0.284	3	0.648	3	0.453
5	0.706	5	0.583	5	0.45	4	0.695	4	0.432	4	0.558
7	0.876	8	0.621	7	0.706	6	1.053	6	1.106	6	1.022

Table D.4. Chloride concentrations for latex-modified and silica fume mixtures.

Latex	L1		L2		L3		L4		L5		L6		
Cycles	%	Cycles	%	Cycles	%	Cycles	%	Cycles	%	Cycles	%		
0	0.038	0	0.024	0	0.029	0	0.034	0	0.028	0	0.029		
3	0.295	2	0.083	2	0.126	3	0.392	2	0.311	2	0.201		
4	0.393	4	0.341	4	0.276	4	0.366	4	0.871	4	0.463		
6	0.531	6	1.171	7	0.775	6	1.097	6	0.944	7	0.772		
Silica fume	SF1		SF2		SF3		SF4		SF7		SF8		SF9
Cycles	%	Cycles	%	Cycles	%	Cycles	%	Cycles	%	Cycles	%	Cycles	%
0	0.039	0	0.057	0	0.115	0	0.104	0	0.082	0	0.086	0	0.115
3	0.506	3	0.278	3	0.109	2	0.104	2	0.24	2	0.08	2	0.121
5	0.635	4	0.345	5	0.148	4	0.121	4	0.743	4	0.362	4	0.127
7	0.620	6	0.360	7	0.563	6	0.156	6	1.038	6	0.701	6	0.576

Table D.5. pH test results for control and DCI mixtures.

Control	C1		C2		C3		C4		C5		C6
Cycles	pH	Cycles	pH	Cycles	pH	Cycles	pH	Cycles	pH	Cycles	pH
0	12.65	0	12.72	0	12.60	0	12.78	0	12.68	0	12.73
3	12.65	3	12.64	3	12.62	3	12.74	3	12.67	3	12.7
5	12.69	5	12.70	5	12.61	4	12.76	4	12.67	4	12.67
7	12.66	7	12.60	7	12.65	6	12.68	6	12.65	6	12.59
16	12.77	16	12.68	16	12.75	16	12.80	16	12.73	16	12.73
DCI	D1		D2		D3		D4		D5		D6
Cycles	pH	Cycles	pH	Cycles	pH	Cycles	pH	Cycles	pH	Cycles	pH
0	12.80	0	12.79	0	12.74	0	12.72	0	12.69	0	12.66
3	12.84	3	12.76	3	12.75	3	12.70	3	12.66	3	12.62
4	12.80	4	12.75	4	12.72	5	12.72	5	12.64	5	12.68
6	12.82	6	12.75	6	12.70	7	12.67	8	12.63	7	12.66

Table D.6. pH test results for latex-modified and silica fume mixtures.

Latex	L1		L2		L3		L4		L5		L6		
Cycles	pH	Cycles	pH	Cycles	pH	Cycles	pH	Cycles	pH	Cycles	pH		
0	13.01	0	13.05	0	13.02	0	13.06	0	12.89	0	0.029		
2	12.98	2	13.07	3	13.03	2	12.95	2	12.89	3	0.201		
4	13	5	13.06	4	13.02	4	12.95	4	12.89	4	0.463		
6	12.96	7	13.05	6	13.02	6	12.94	7	12.89	6	0.772		
Silica fume	SF1		SF2		SF3		SF4		SF7		SF8		SF9
Cycles	pH	Cycles	pH	Cycles	pH	Cycles	pH	Cycles	pH	Cycles	pH	Cycles	pH
0	12.93	0	12.87	0	12.89	0	12.87	0	12.90	0	12.90	0	12.89
3	12.88	3	12.87	3	12.89	2	12.89	2	12.89	2	12.90	2	12.88
5	12.92	4	12.87	5	12.90	4	12.87	4	12.90	4	12.89	4	12.89
7	12.88	6	12.81	7	12.88	6	12.84	6	12.87	6	12.89	6	12.88

APPENDIX E

Half cell potential and current measurements

Raw values

Current	Mod - substantial	Minor	None
$i > 10 \mu\text{a}$	67	4	0
$2 < i < 10 \mu\text{a}$	8	7	2
$i < 2 \mu\text{a}$	6	9	13

Half cell	Mod - substantial	Minor	None
$< -350 \text{ mV}$	16	0	0
$-200 \text{ to } -350 \text{ mV}$	53	4	0
$> -200 \text{ mV}$	12	16	15

Probability tree raw

		Mod - substantial	Minor	None
	$< -350 \text{ mV}$	16	0	0
$i > 10 \mu\text{a}$	$-200 \text{ to } -350 \text{ mV}$	41	1	0
	$> -200 \text{ mV}$	10	3	0
		Mod - substantial	Minor	None
	$< -350 \text{ mV}$	0	0	0
$2 < i < 10 \mu\text{a}$	$-200 \text{ to } -350 \text{ mV}$	8	1	0
	$> -200 \text{ mV}$	0	6	2
		Mod - substantial	Minor	None
	$< -350 \text{ mV}$	0	0	0
$i < 2 \mu\text{a}$	$-200 \text{ to } -350 \text{ mV}$	5	2	0
	$> -200 \text{ mV}$	1	7	13

		Mod - substantial	Minor	None
	$< -200 \text{ mV}$	56	1	0
$i > 10 \mu\text{a}$	$-200 \text{ to } -100 \text{ mV}$	11	3	0
	$> -100 \text{ mV}$	0	0	0
		Mod - substantial	Minor	None
	$< -200 \text{ mV}$	8	1	0
$2 < i < 10 \mu\text{a}$	$-200 \text{ to } -100 \text{ mV}$	0	5	2
	$> -100 \text{ mV}$	0	1	0
		Mod - substantial	Minor	None
	$< -200 \text{ mV}$	5	2	0
$i < 2 \mu\text{a}$	$-200 \text{ to } -100 \text{ mV}$	1	2	6
	$> -100 \text{ mV}$	0	5	7

Converted Half cell potential values

		Left	Right			Left	Right
HCon1 #1	1	-0.152	-0.15	Xyp1 #1	1	-0.217	-0.248
	2	-0.191	-0.158		2	-0.216	-0.212
	3	-0.194	-0.179		3	-0.212	-0.222
HCon1 #2	1	-0.114	-0.103	Xyp1 #2	1	-0.06	-0.06
	2	-0.117	-0.116		2	-0.062	-0.059
	3	-0.11	-0.139		3	-0.067	-0.06
HCon1 #3	1	-0.311	-0.339	Xyp1 #3	1	-0.218	-0.232
	2	-0.336	-0.457		2	-0.22	-0.23
	3	-0.357	-0.463		3	-0.233	-0.24
HCon1 #4	1	-0.325	-0.312	Xyp1 #4	1	-0.154	-0.14
	2	-0.39	-0.336		2	-0.147	-0.139
	3	-0.394	-0.374		3	-0.154	-0.135
HCon2 #1	1	-0.303	-0.301	Xyp2 #1	1	-0.176	-0.213
	2	-0.369	-0.316		2	-0.175	-0.199
	3	-0.359	-0.326		3	-0.211	-0.211
HCon2 #2	1	-0.171	-0.129	Xyp2 #2	1	-0.271	-0.289
	2	-0.18	-0.133		2	-0.278	-0.304
	3	-0.173	-0.133		3	-0.294	-0.289
HCon2 #3	1	-0.215	-0.184	Xyp2 #3	1	-0.132	-0.151
	2	-0.257	-0.191		2	-0.142	-0.129
	3	-0.221	-0.199		3	-0.151	-0.162
HCon2 #4	1	-0.221	-0.179	Xyp2 #4	1	-0.301	-0.269
	2	-0.223	-0.176		2	-0.305	-0.241
	3	-0.181	-0.18		3	-0.279	-0.269
HCon4 #1	1	-0.294	-0.331	Xyp4 #1	1	-0.081	-0.093
	2	-0.304	-0.382		2	-0.075	-0.078
	3	-0.292	-0.295		3	-0.073	-0.082
HCon5 #1	1	-0.189	-0.185	Xyp4 #2	1	-0.289	-0.268
	2	-0.197	-0.2		2	-0.283	-0.277
	3	-0.176	-0.2		3	-0.279	-0.274
HCon5 #2	1	-0.254	-0.296	Xyp4 #3	1	-0.464	-0.399
	2	-0.268	-0.303		2	-0.451	-0.384
	3	-0.275	-0.27		3	-0.361	-0.398
HCon5 #3	1	-0.297	-0.279	Xyp4 #4	1	-0.309	-0.315
	2	-0.296	-0.286		2	-0.295	-0.285
	3	-0.323	-0.294		3	-0.103	-0.325
HCon5 #4	1	-0.268	-0.277	Xyp5 #1	1	-0.142	-0.216
	2	-0.251	-0.296		2	-0.148	-0.192
	3	-0.27	-0.248		3	-0.15	-0.214
Rheo1 #8	1	-0.167	-0.156	Xyp5 #2	1	-0.218	-0.208
	2	-0.161	-0.133		2	-0.21	-0.246
	3	-0.168	-0.148		3	-0.19	-0.201
Rheo2 #8	1	-0.134	-0.128	Xyp5 #3	1	-0.184	-0.197
	2	-0.144	-0.133		2	-0.192	-0.198
	3	-0.119	-0.127		3	-0.188	-0.183
Rheo3 #8	1	-0.124	-0.143	Xyp5 #4	1	-0.19	-0.21
	2	-0.128	-0.143		2	-0.214	-0.228
	3	-0.133	-0.14		3	-0.206	-0.225

Rheo 4 #8	1	-0.083	-0.08	FA5 #1	1	-0.375	-0.388
	2	-0.099	-0.088		2	-0.369	-0.406
	3	-0.097	-0.087		3	-0.401	-0.46
Rheo5 #8	1	-0.104	-0.131	FA5 #2	1	-0.24	-0.221
	2	-0.117	-0.142		2	-0.236	-0.239
	3	-0.105	-0.134		3	-0.218	-0.217
Rheo6 #8	1	-0.08	-0.079	FA5 #3	1	-0.164	-0.186
	2	-0.079	-0.074		2	-0.167	-0.189
	3	-0.079	-0.078		3	-0.166	-0.177
SF1 #8	1	-0.115	-0.121	FA5 #4	1	-0.269	-0.281
	2	-0.109	-0.112		2	-0.266	-0.258
	3	-0.103	-0.114		3	-0.252	-0.268
SF2 #8	1	-0.094	-0.086	FA6 #3	1	-0.244	-0.25
	2	-0.088	-0.084		2	-0.252	-0.268
	3	-0.09	-0.091		3	-0.264	-0.293
SF2^ #8	1	-0.082	-0.081	FA9 #3	1	-0.083	-0.088
	2	-0.082	-0.077		2	-0.093	-0.08
	3	-0.086	-0.081		3	-0.086	-0.082
SF3 #8	1	-0.113	-0.103	FA10^ #2	1	-0.351	-0.349
	2	-0.108	-0.107		2	-0.353	-0.356
	3	-0.12	-0.105		3	-0.344	-0.353
SF4 #8	1	-0.255	-0.23	HRh4 #1	1	-0.149	-0.167
	2	-0.265	-0.242		2	-0.177	-0.172
	3	-0.287	-0.256		3	-0.189	-0.171
SF5 #5	1	-0.324	-0.332	HRh4 #2	1	-0.268	-0.284
	2	-0.334	-0.347		2	-0.268	-0.318
	3	-0.344	-0.348		3	-0.255	-0.305
SF5 #7	1	-0.243	-0.215	HRh4 #3	1	-0.161	-0.157
	2	-0.204	-0.208		2	-0.183	-0.16
	3	-0.209	-0.211		3	-0.163	-0.171
SF5 #8	1	-0.164	-0.157	HRh4 #4	1	-0.322	-0.305
	2	-0.179	-0.173		2	-0.403	-0.305
	3	-0.165	-0.159		3	-0.312	-0.292
SF6 #6	1	-0.295	-0.32	HRh5 #1	1	-0.318	-0.327
	2	-0.312	-0.322		2	-0.329	-0.391
	3	-0.33	-0.353		3	-0.297	-0.29
SF6 #8	1	-0.143	-0.085	HRh5 #2	1	-0.241	-0.308
	2	-0.149	-0.081		2	-0.234	-0.232
	3	-0.157	-0.077		3	-0.226	-0.231
SF7 #3	1	-0.359	-0.446	HRh5 #3	1	-0.34	-0.346
	2	-0.442	-0.382		2	-0.408	-0.441
	3	-0.461	-0.409		3	-0.364	-0.408
SF7 #8	1	-0.189	-0.168	HRh5 #4	1	-0.3	-0.283
	2	-0.18	-0.182		2	-0.339	-0.311
	3	-0.181	-0.171		3	-0.382	-0.325
Con1 #1	1	-0.182	-0.199	LA1 #1	1	-0.241	-0.21
	2	-0.199	-0.21		2	-0.241	-0.212
	3	-0.206	-0.256		3	-0.246	-0.205
Con1 #2	1	-0.212	-0.161	LA1 #2	1	-0.267	-0.262
	2	-0.214	-0.175		2	-0.235	-0.3
	3	-0.221	-0.181		3	-0.262	-0.306
Con1 #3	1	-0.212	-0.219	LA1 #3	1	-0.151	-0.219
	2	-0.225	-0.262		2	-0.164	-0.164
	3	-0.218	-0.301		3	-0.195	-0.223

Con1 #4	1	-0.139	-0.143	LA1 #4	1	-0.306	-0.323
	2	-0.134	-0.156		2	-0.298	-0.281
	3	-0.145	-0.154		3	-0.31	-0.293
Con1 #7	1	-0.29	-0.27	LA1 #5	1	-0.296	-0.254
	2	-0.308	-0.285		2	-0.257	-0.243
	3	-0.289	-0.259		3	-0.24	-0.238
Con2 #2	1	-0.263	-0.262	LA1 #6	1	-0.205	-0.225
	2	-0.273	-0.274		2	-0.226	-0.225
	3	-0.26	-0.265		3	-0.239	-0.233
Con2 #3	1	-0.231	-0.23	LA1 #8	1	-0.175	-0.218
	2	-0.246	-0.245		2	-0.182	-0.2
	3	-0.245	-0.259		3	-0.187	-0.224
Con2 #5	1	-0.242	-0.247	LA2 #8	1	-0.139	-0.14
	2	-0.272	-0.26		2	-0.124	-0.143
	3	-0.268	-0.261		3	-0.134	-0.132
Con2 #6	1	-0.319	-0.34	LA3 #7	1	-0.285	-0.284
	2	-0.299	-0.305		2	-0.309	-0.287
	3	-0.286	-0.284		3	-0.289	-0.281
Con2 #7	1	-0.238	-0.242	LA3 #8	1	-0.301	-0.324
	2	-0.251	-0.246		2	-0.293	-0.295
	3	-0.253	-0.252		3	-0.284	-0.31
Con 3 #5	1	-0.393	-0.39	LA5 #8	1	-0.102	-0.098
	2	-0.392	-0.484		2	-0.122	-0.117
	3	-0.412	-0.522		3	-0.14	-0.129
Con3 #6	1	-0.193	-0.322	LA6 #8	1	-0.072	-0.077
	2	-0.197	-0.321		2	-0.062	-0.09
	3	-0.217	-0.319		3	-0.067	-0.085
Con4 #1	1	-0.221	-0.205	HFA5 #1	1	-0.071	-0.088
	2	-0.219	-0.202		2	-0.065	-0.068
	3	-0.232	-0.219		3	-0.069	-0.062
Con4 #2	1	-0.253	-0.226	HFA5 #2	1	-0.292	-0.276
	2	-0.243	-0.232		2	-0.306	-0.337
	3	-0.225	-0.241		3	-0.289	-0.29
Con4 #3	1	-0.229	-0.25	HFA5 #3	1	-0.284	-0.284
	2	-0.222	-0.248		2	-0.358	-0.303
	3	-0.211	-0.241		3	-0.335	-0.315
Con4 #4	1	-0.172	-0.158	HFA5 #4	1	-0.138	-0.126
	2	-0.158	-0.15		2	-0.144	-0.152
	3	-0.151	-0.158		3	-0.141	-0.138
Con4 #6	1	-0.273	-0.15	DCI1 #2	1	-0.14	-0.129
	2	-0.259	-0.14		2	-0.122	-0.13
	3	-0.248	-0.131		3	-0.115	-0.12
Con4 #7	1	-0.217	-0.222	DCI1 #6	1	-0.202	-0.183
	2	-0.239	-0.217		2	-0.188	-0.193
	3	-0.221	-0.218		3	-0.203	-0.186
Ferr1 #8	1	-0.142	-0.134	DCI1 #8	1	-0.217	-0.198
	2	-0.144	-0.148		2	-0.223	-0.199
	3	-0.163	-0.163		3	-0.224	-0.205
Ferr2 #5	1	-0.239	-0.282	DCI2 #4	1	-0.216	-0.222
	2	-0.242	-0.275		2	-0.248	-0.231
	3	-0.265	-0.268		3	-0.282	-0.255
Ferr2 #8	1	-0.125	-0.131	DCI2 #8	1	-0.145	-0.143
	2	-0.114	-0.134		2	-0.144	-0.139
	3	-0.108	-0.124		3	-0.147	-0.144

Ferr3 #8	1	-0.094	-0.097	DCI3 #8	1	-0.074	-0.075
	2	-0.094	-0.102		2	-0.076	-0.077
	3	-0.094	-0.11		3	-0.08	-0.071
Ferr4 #1	1	-0.318	-0.275	DCI4 #8	1	-0.092	-0.089
	2	-0.331	-0.306		2	-0.093	-0.096
	3	-0.325	-0.285		3	-0.098	-0.093
Ferr5 #1	1	-0.193	-0.199	DCI5 #8	1	-0.109	-0.102
	2	-0.194	-0.198		2	-0.118	-0.116
	3	-0.196	0.049		3	-0.118	-0.11
Ferr5 #3	1	-0.256	-0.258	DCI6 #8	1	-0.083	-0.076
	2	-0.378	-0.273		2	-0.083	-0.082
	3	-0.347	-0.291		3	-0.077	-0.086
Ferr5 #5	1	-0.181	-0.216				
	2	-0.204	-0.22				
	3	-0.197	-0.197				
Ferr5 #7	1	-0.191	-0.183				
	2	-0.199	-0.196				
	3	-0.201	-0.199				
Ferr5 #8	1	-0.14	-0.236				
	2	-0.151	-0.223				
	3	-0.173	-0.249				
Ferr6 #8	1	-0.095	-0.09				
	2	-0.087	-0.086				
	3	-0.089	-0.09				

APPENDIX F

Chlorides, pH, and cycles

Specimen	Cycles	Air perm.	Half Cell (max)	Chloride	pH left	pH right	Avg. pH
Con1 #1	31	398	256	3.89	12.18	12.24	12.21
Con1 #2	31	121	221	2.68	12.35	12.34	12.35
Con1 #3	31	125	262	3.37	12.18	12.23	12.21
Con1 #4	31	208	156	3.68	12.04	12.11	12.08
Con1 #7	31	169	308	3.21	12.05	12.08	12.07
Con2 #2	31	501	274	6.47	12.26	12.42	12.34
Con2 #3	31	320	259	4.13	11.99	12.13	12.06
Con2 #5	31	43	272	4.97	12.93	12.22	12.58
Con2 #6	31	123	319	3.71	12.22	12.24	12.23
Con2 #7	31	120	253	3.77	11.91	12.25	12.08
Con3 #5	46	104	522	0.97	12.19	12.16	12.18
Con3 #6	24	182	322	2.82	12.21	12.03	12.12
Con4 #1	24	110	232	2.87	12.13	12.22	12.18
Con4 #2	29	201	253	3.07	12.16	12.07	12.12
Con4 #3	29	107	250	2.92	12.15	12.14	12.15
Con4 #4	29	97	172	3.43	12.13	12.13	12.13
Con4 #6	24	118	273	3.98	12.23	12.09	12.16
Con4 #7	29	173	239	3.02	12.09	12.13	12.11
HCon1 #1	27	57	194	0.39	12.37	12.4	12.39
HCon1 #2	27	32	139	0.5	12.36	12.45	12.41
HCon1 #3	27	60	463	0.52	12.14	12.08	12.11
HCon1 #4	27	71	394	0.44	12.14	12.21	12.18
HCon2 #1	13	28	369	1.72	12.31	12.61	12.46
HCon2 #2	13	42	180	1.28	12.18	12.19	12.19
HCon2 #3	13	25	257	1.56	12.06	12.21	12.14
HCon2 #4	13	9	223	2.23	12.21	12.23	12.22
HCon4 #1	28	54	382	3.06	12.46	12.3	12.38
HCon5 #1	28	49	200	2.82	12.47	12.46	12.47
HCon5 #2	28	71	303	3.78	12.28	12.29	12.29
HCon5 #3	28	59	323	2.92	12.45	12.52	12.49
HCon5 #4	28	47	296	2.87	12.32	12.29	12.31
Xyp1 #1	25	146	248	1.93	12.32	12.31	12.32
Xyp1 #2	25	194	67	1.50	12.76	11.95	12.36
Xyp1 #3	25	182	240	1.66	12.63	12.55	12.59
Xyp1 #4	25	39	154	1.83	12.21	12.13	12.17
Xyp2 #1	31	147	213	3.48	12.36	12.44	12.40
Xyp2 #2	31	104	304	3.6	12.28	12.2	12.24
Xyp2 #3	31	57	162		12.31	12.22	12.27
Xyp2 #4	31	37	305	3.82	12.26	12.21	12.24
Xyp4 #1	31	54	93	2.93	12.35	12.3	12.33
Xyp4 #2	31	93	289	2.78	12.57	12.58	12.58
Xyp4 #3	31	107	464	3.14	12.58	12.34	12.46
Xyp4 #4	31	93	325	2.78	12.25	12.24	12.25
Xyp5 #1	16		216	2.56	12.13	12.17	12.15
Xyp5 #2	16	57	246	2.24	12.21	12.2	12.21

Xyp5 #3	16		198	2.89	12.21	12.21	12.21
Xyp5 #4	16	67	228		12.17	12.18	12.18
HRh4 #1	21	27	189	0.99	12.89	12.81	12.85
HRh4 #2	27	49	318		12.32	12.31	12.32
HRh4 #3	27	80	183		12.13	12.14	12.14
HRh4 #4	27	67	403		12.16	12.18	12.17
HRh5 #1	24	103	391		12.24	12.25	12.25
HRh5 #2	24	58	308		12.22	12.27	12.25
HRh5 #3	24	62	441		12.21	12.37	12.29
HRh5 #4	24	49	382		12.17	12.19	12.18
HFA5 #1	17	70	88		12.15	12.09	12.12
HFA5 #2	17	46	337		12.29	12.23	12.26
HFA5 #3	17	120	358		12.03	12.09	12.06
HFA5 #4	17	124	152		12.14	12.08	12.11
DCI1 #2	31	134	130	2.53	11.96	12	11.98
DCI1 #6	31	70	203	2.74	12.27	12.16	12.22
DCI1 #8	31	167	224	0.79	11.98	12.01	12.00
DCI2 #4	31	104	282	2.05	12.13	12.14	12.14
DCI2 #8	34	129	147	2.95	12.11	12.09	12.10
DCI3 #8	34	340	80	1.85	12.46	12.47	12.47
DCI4 #8	33	190	98	1.75	12.37	12.29	12.33
DCI5 #8	33	163	118	1.66	12.16	12.18	12.17
DCI6 #8	32	90	86	1.66	12.04	12.11	12.08
LA1 #1	22	221	246	2.93	12.07	12.09	12.08
LA1 #2	22	303	306	3.34	12.08	12.05	12.07
LA1 #3	22	156	223	1.46	12.15	11.94	12.05
LA1 #4	22	71	323	1.67	12.08	12.07	12.08
LA1 #5	22	314	296	2.35	12.33	12.34	12.34
LA1 #6	22	539	239	2.51	12.61	12.59	12.60
LA1 #8	22	199	224	2.25	12.15	11.96	12.06
LA2 #8	27	56	143	1.35	12.1	12.19	12.15
LA3 #7	24	27	309	2.37	12.1	12.12	12.11
LA3 #8	25		324	2.16	12.39	12.21	12.30
LA5 #8	26	349	140	1.12	12.34	12.55	12.45
LA6 #8	24	164	90	1.646	12.3	12.18	12.24
Ferr1 #8	21	207	163	1.79	12.49	12.61	12.55
Ferr2 #5	35	238	275	2.85	12.3	12.1	12.20
Ferr2 #8	21	235	134	2.18	12.17	12.27	12.22
Ferr3 #8	20	181	110	1.24	12.52	12.62	12.57
Ferr4 #1	32	78	331	3.05	12.13	12.3	12.22
Ferr5 #1	25	142	199	2.12	12.06	12.08	12.07
Ferr5 #3	25	136	378	1.86	12.05	12.07	12.06
Ferr5 #5	25	59	220	2.76	12.17	12.23	12.20
Ferr5 #7	25	131	201	2.60	12.05	12.12	12.09
Ferr5 #8	19	138	249	1.49	12.15	12.18	12.17
Ferr6 #8	19	355	95	1.27	12.11	12.43	12.27
FA5 #1	44	151	406	3.92	12.23	12.26	12.25
FA5 #2	44	130	240	2.6	12.52	12.28	12.40

FA5 #3	28	262	189	2.98	12.29	12.31	12.30
FA5 #4	44	87	281	4.09	12.53	12.51	12.52
FA6 #3	28	433	293	3.17	12.14	12.15	12.15
FA9 #3	27	317	93	1.78	12.52	12.09	12.31
FA10^ #2	36	94	356	4.7	12.47	12.47	12.47
Rheo1 #8	20	192	168	1.42	12.2	12.27	12.24
Rheo2 #8	24	199	144		12.11	12.12	12.12
Rheo3 #8	23	224	143	0.55	12.04	12.13	12.09
Rheo4 #8	22	175	99	0.48	12.18	12.25	12.22
Rheo5 #8	22	210	142	2.52	12.55	12.57	12.56
Rheo6 #8	20	207	80	0.91	12.27	12.32	12.30
SF1 #8	32	1236	121	2.18	12.06	12.08	12.07
SF2 #8	31	187	94	1.31	12.28	12.23	12.26
SF2^ #8	31		86	1.41	12.18	12.2	12.19
SF3 #8	32	297	113	1.43	12.35	12.32	12.34
SF4 #8	32	296	287	1.15	12.31	12.4	12.36
SF5 #5	45	102	348	3.32	12.28	12.16	12.22
SF5 #7	29	366	243	2.82	12.19	12.43	12.31
SF5 #8	29	231	179	2.54	12.35	12.49	12.42
SF6 #6	45	101	353	3.36	12.27	12.26	12.27
SF6 #8	32	287	157	2.83	12.06	12.11	12.09
SF7 #3	45	50	461	0.45	12.07	12.14	12.11
SF7 #8	31	254	189	1.53	12.2	12.99	12.60

APPENDIX G

Records of Specimen Visual Inspection

CONTROL MIXTURES

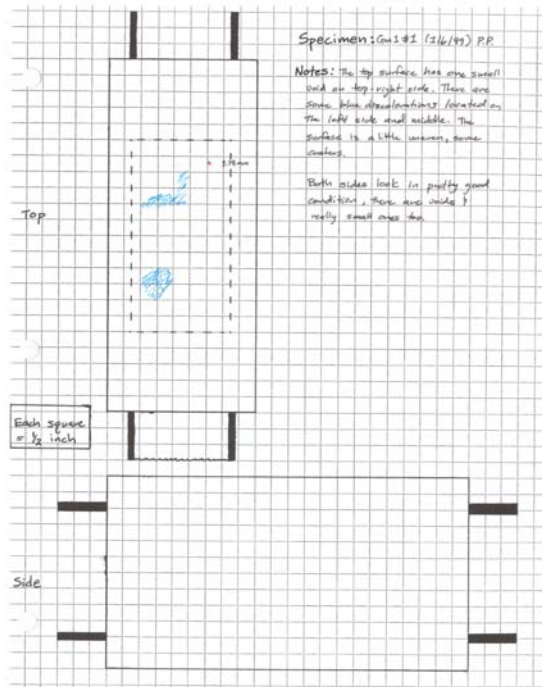


Figure 7.1 : Control 1 #1A

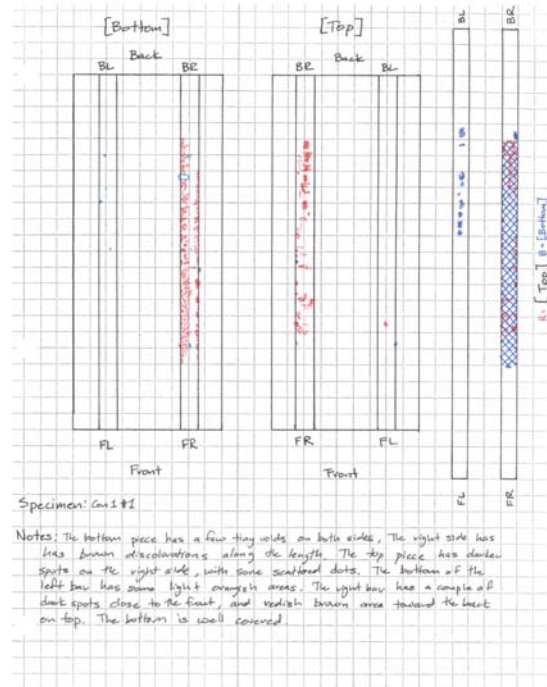


Figure 7.2 : Control 1 #1B

Con1 #1 – The visual inspection did not show much on the outside. On the inside of the right bar it was almost completely covered with corrosion on the bottom. The top of the bar had a few areas of corrosion. The left bar has a pits on the bottom of the bar. The half cell potential results all fell into the uncertain range. The voltage readings show the specimen had failed. The inspection concluded the corrosion to be moderate to significant.



Figure 7.3- Bars, bottom



Figure 7.4 - Bars, top

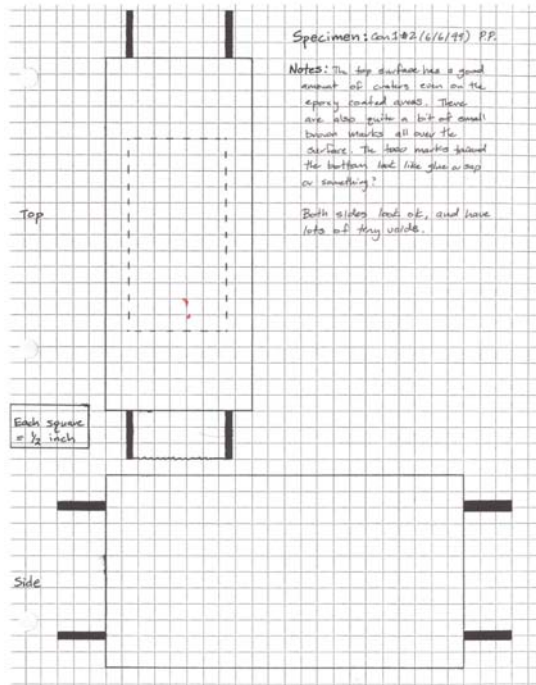


Figure 7.5 : Control 1 #2A

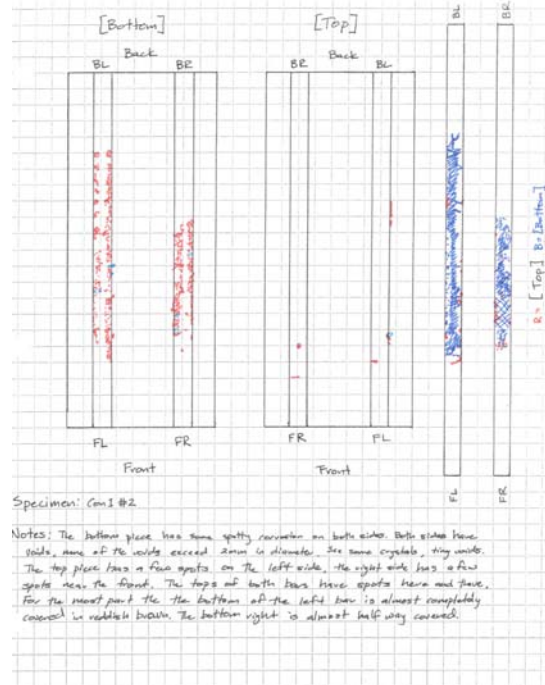


Figure 7.6 : Control 1 #2B

Con1 #2 – The outside of the specimen looked to be in good condition. On the inside there was significant corrosion on the bottoms of both bars. The tops of both of the bars had very few discolorations. The half cells potential readings indicate that all the reading were in the uncertain range. The voltage readings illustrate that the specimen had not yet reached failure mode. The inspection concluded the corrosion to be moderate to significant.



Figure 7.7 - Bars, bottom



Figure 7.8 - Bars, top

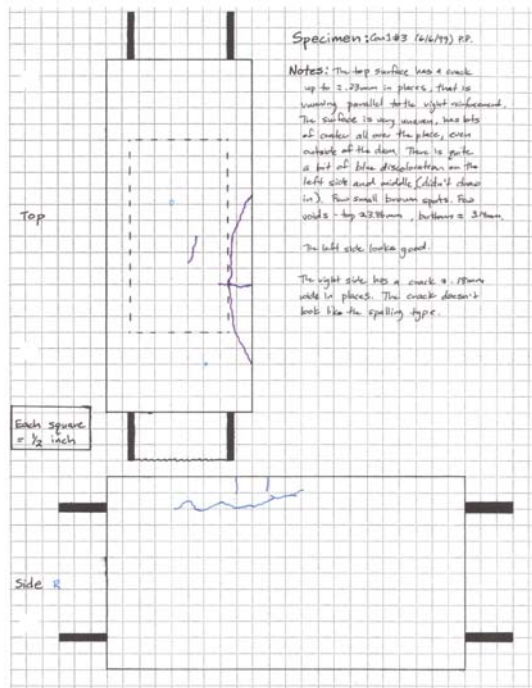


Figure 7.9 : Control 1 #3A

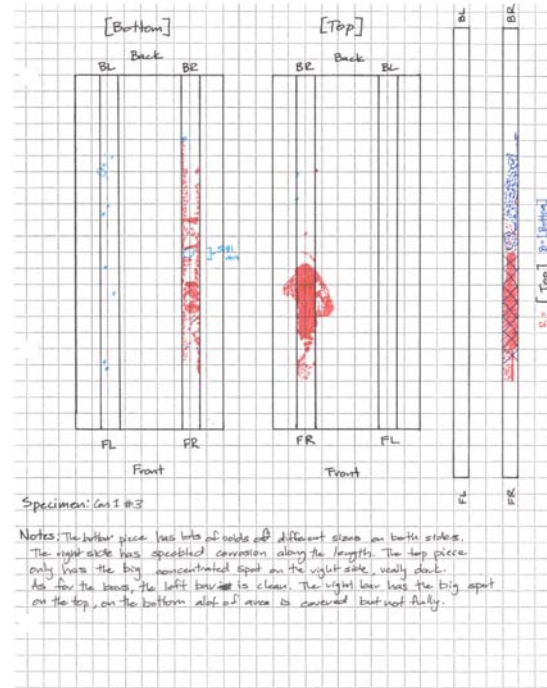


Figure 7.10 : Control 1 #3B

Con1 #3 – The visual inspection showed a few cracks on the right side on both the top surface and the side surface. The cracks mostly above the right bar, there was also a small crack in the middle of the specimen. All of the corrosion inside the specimen was located on the right bar. The bottom of the right bar was covered in hazy corrosion while the top of the bar has a smaller area of corrosion it was more concentrated and darker in color. The half cell potential readings show that all of the values were in the uncertain range. The voltage readings show that the specimen has reached the failure mode. The inspection concluded the corrosion to be moderate to significant.



Figure 7.11 - Bars, bottom



Figure 7.12 - Bars, top

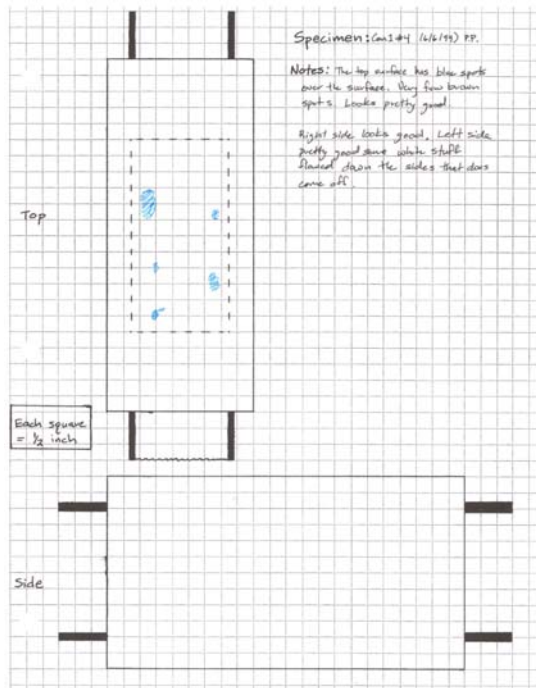


Figure 7.13 : Control 1 #4A

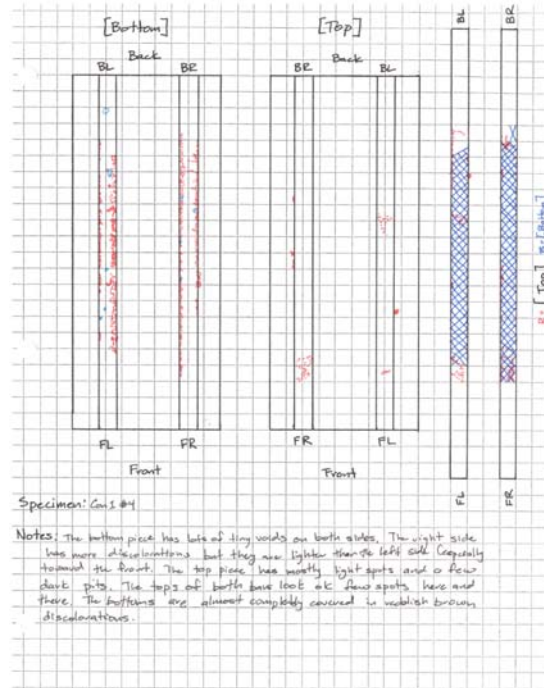


Figure 7.14 : Control 1 #4B

Con1 #4 – The visual inspection showed the specimen was in good condition. In the inside of the specimen both bars were completely covered on the bottoms. The top of the bars had some corrosion areas scattered along the edges. The half cell potential values show that all of the values fell into the 10% of probability range. The voltage numbers indicated that the specimen had reached failure. The inspection concluded the corrosion to be moderate to significant.



Figure 7.15 - Bars, bottom



Figure 7.16 - Bars, top

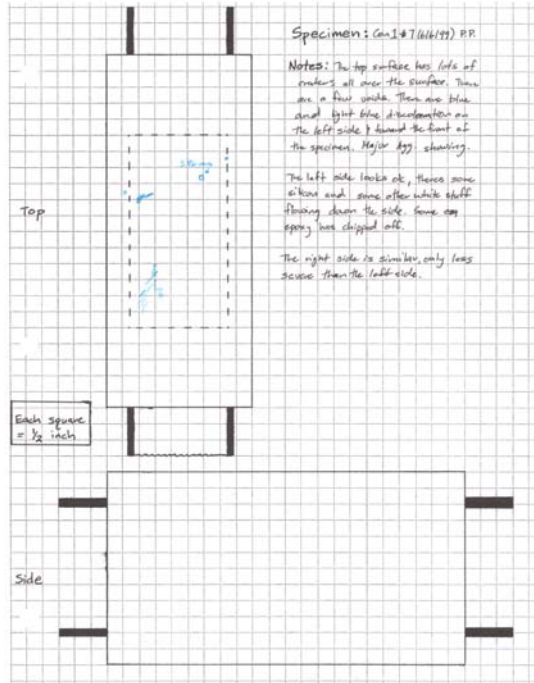


Figure 7.17 : Control 1 #7A

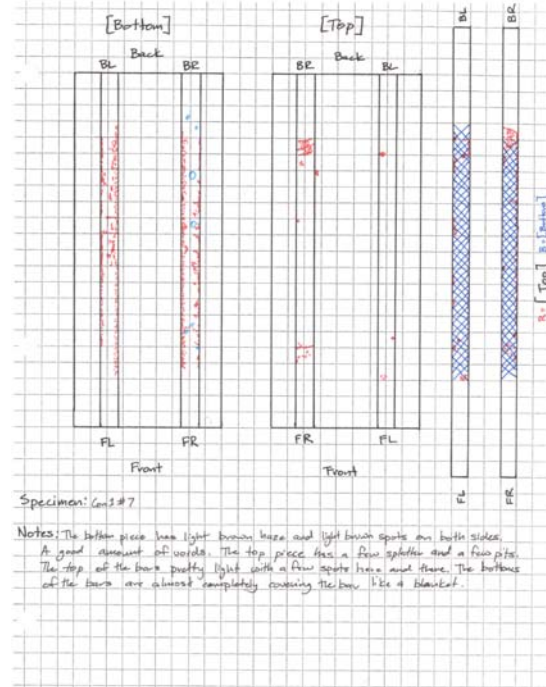


Figure 7.18 : Control 1 #7B

Con1 #7 – The visual inspection did not show any major flaws in the specimen. The inside of the specimen had lots of corrosion on the bottom of both bars. The bottoms of both bars are almost completely covered with the tops having some corrosion along the edges. The half cell potential readings indicate that all of the values fell into the uncertain range. The voltage results show that the specimen was not close to failure. The inspection concluded the corrosion to be moderate to significant.



Figure 7.19 - Bars, bottom



Figure 7.20 - Bars, top

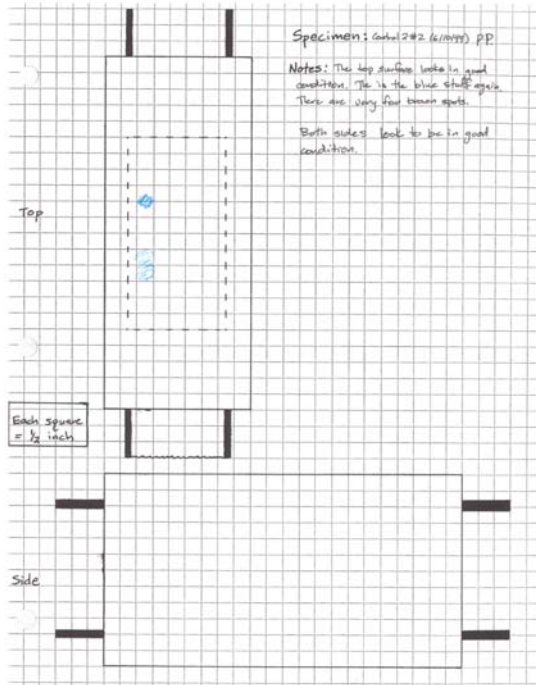


Figure 7.21 : Control 2 #2A

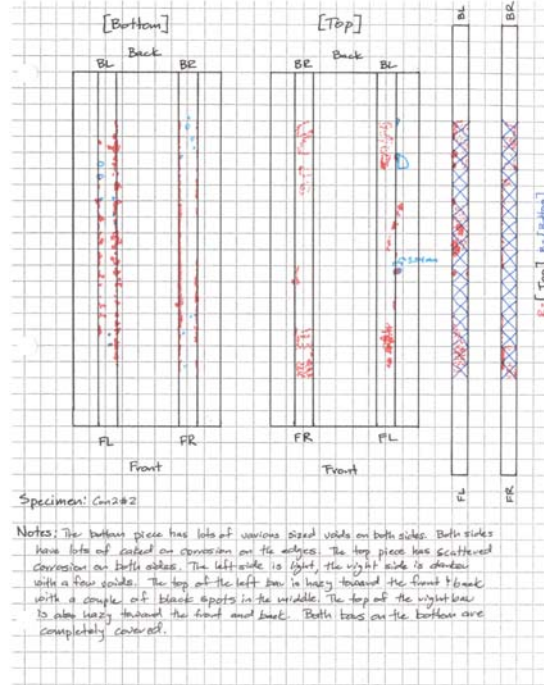


Figure 7.22 : Control 2 #2B

Con2 #2 – The visual inspection did not provide any useful additional information. The inside of the specimen showed multiple areas of corrosion. The bottoms of both bars were completely covered in corrosion. The tops of the bars had multiple corrosion spots. The half cell potential numbers show that all of the values were in the uncertain range. The voltage readings show that the specimen had failed. The inspection concluded the corrosion to be moderate to significant.



Figure 7.23 - Bars, bottom



Figure 7.24 - Bars, top

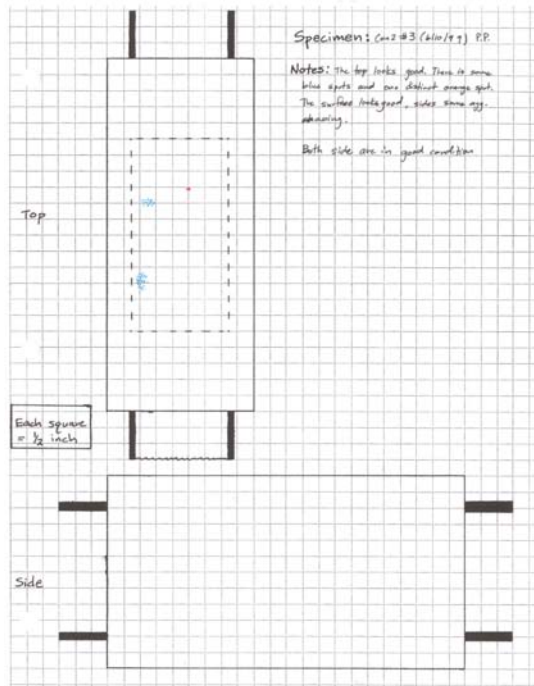


Figure 7.25 : Control 2 #3A

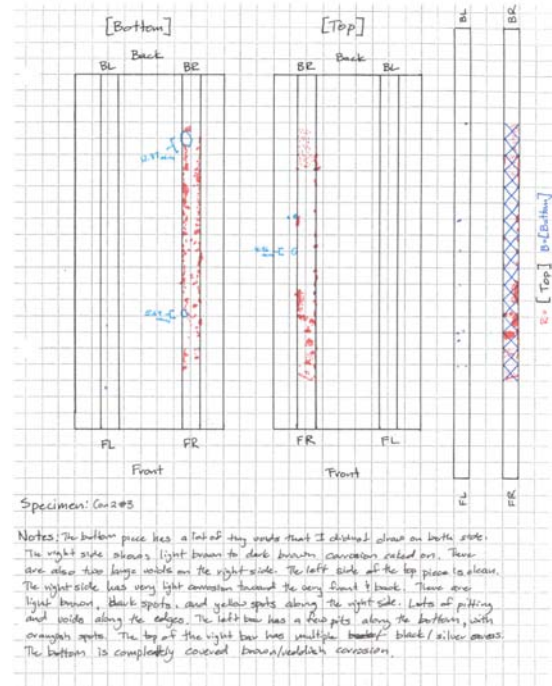


Figure 7.26 : Control 2 #3B

Con2 #3 – The specimen looked in good condition from the outside. On the inside the majority of the corrosion was located on the bottom of the right bar. On the top of the right bar there were multiple black and silver pits. The left bar had a few pits on the bottom. The half cell potential values all fell into the uncertain range. The voltage readings show that the specimen had failed. The inspection concluded the corrosion to be moderate to significant.



Figure 7.27 - Bars, bottom



Figure 7.28 - Bars, top

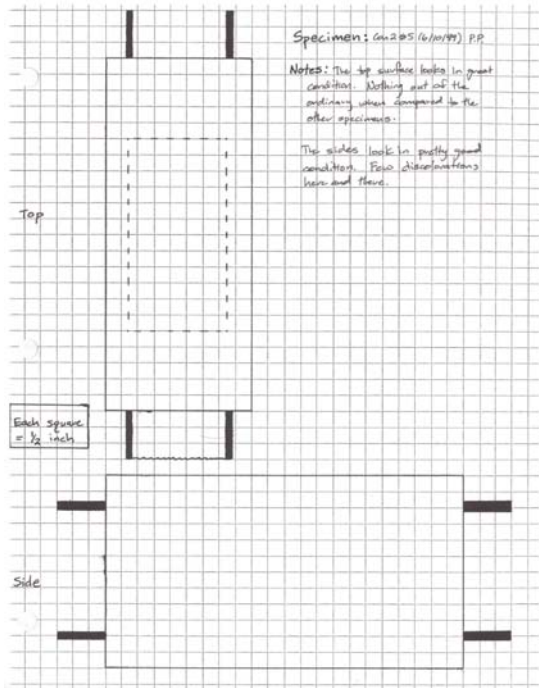


Figure 7.29 : Control 2 #5A

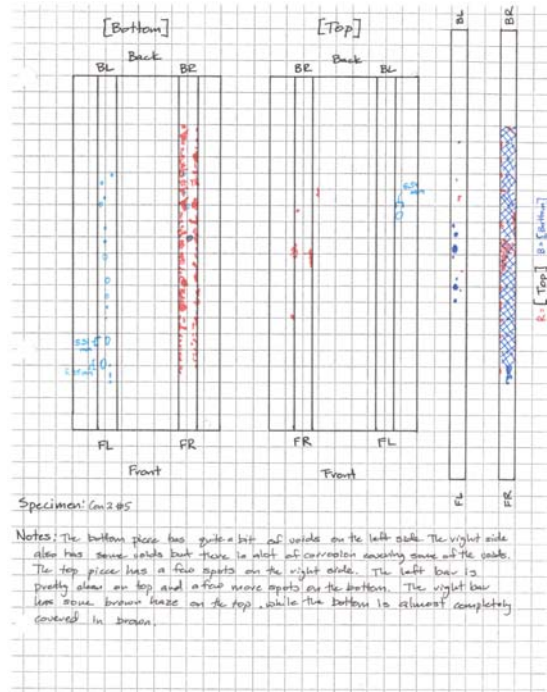


Figure 7.30 : Control 2 #5B

Con2 #5 – The visual inspection did not show any major cracks or voids on the outside. On the inside the majority of the corrosion was located on the bottom of the right bar. The right bar also had some spots on the top. The left bar had some pits on the bottom. The half cell potential numbers show that all of the values fell into the uncertain range. The voltage readings show that the specimen was considered to be failed. The inspection concluded the corrosion to be moderate to significant.



Figure 7.31 - Bars, bottom

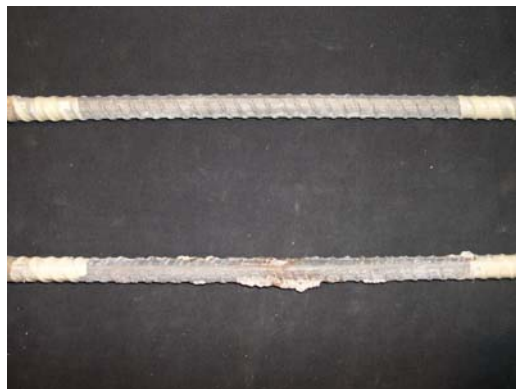


Figure 7.32 - Bars, top

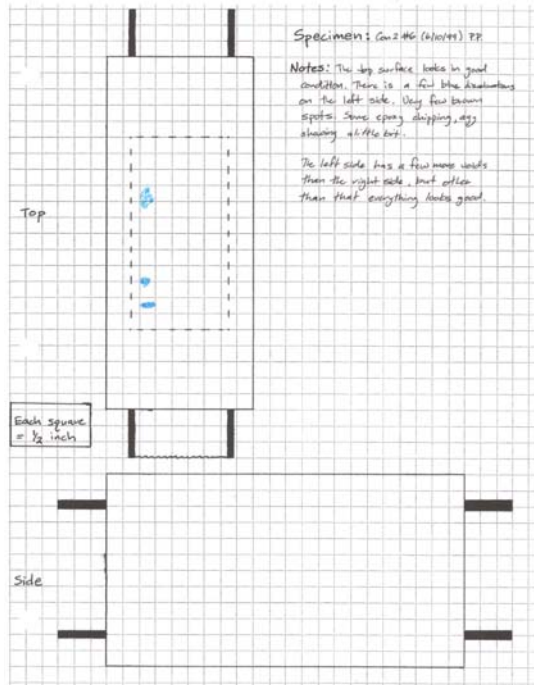


Figure 7.33 : Control 2 #6A

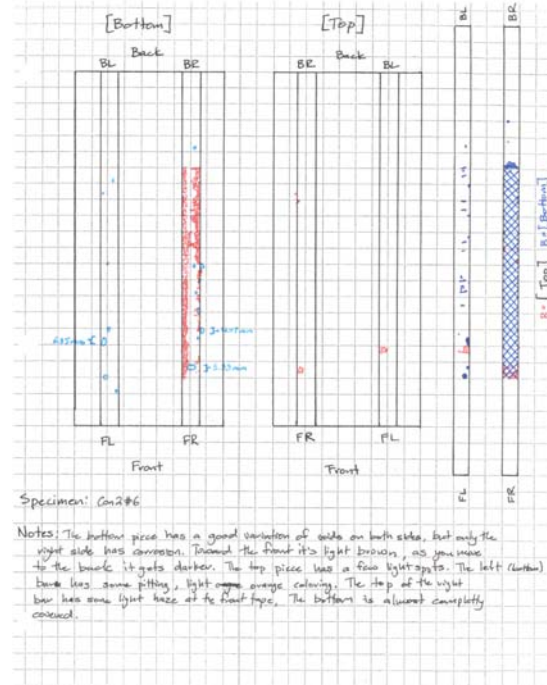


Figure 7.34 : Control 2 #6B

Con2 #6 – The visual inspection of the outside of the specimen showed that there were no major flaws. The inside of the specimen contained corrosion on the bottom of the right bar. The right bar was completely covered in corrosion and the top had a few spots. The bottom of the left bar had pits along the length of the bar. The half cell potential numbers all fell into the uncertain range. The voltage results show that the specimen was not close to being considered as a failure. The inspection concluded the corrosion to be moderate to significant.



Figure 7.35 - Bars, bottom



Figure 7.36 - Bars, top

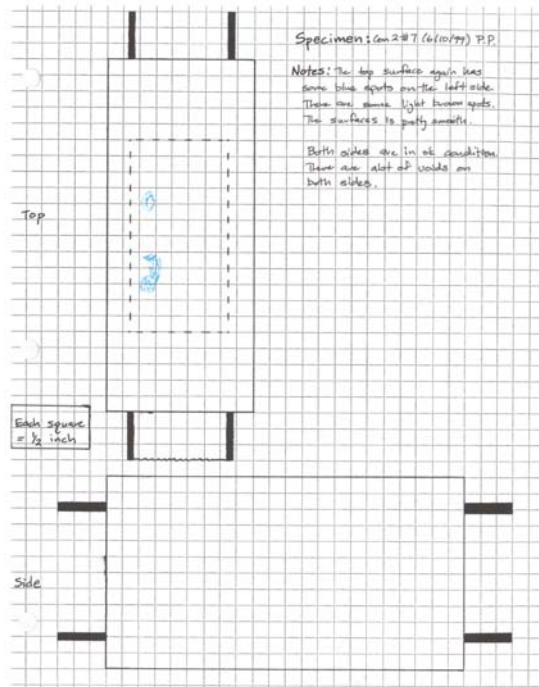


Figure 7.37 : Control 2 #7A

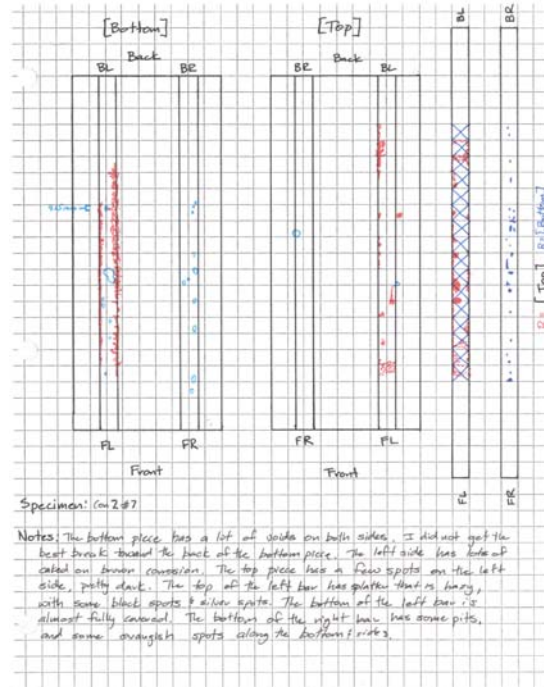


Figure 7.38 : Control 2 #7B

Con2 #7 – From the outside the specimen looked very clean. From the inside the bottom of the left bar was covered in corrosion. The top of the left bar had some black and silver spots on the edges. The right bar had multiple pits and spots on the bottom. The half cell potential values were found in the range of uncertain. The voltage readings show that the specimen was getting close to the failure threshold. The inspection concluded the corrosion to be moderate to significant.



Figure 7.39 - Bars, bottom



Figure 7.40 - Bars, top

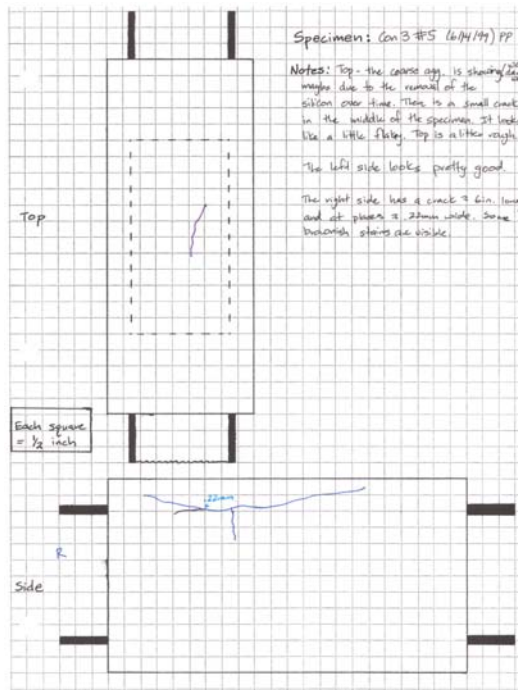


Figure 7.41 : Control 3 #5A

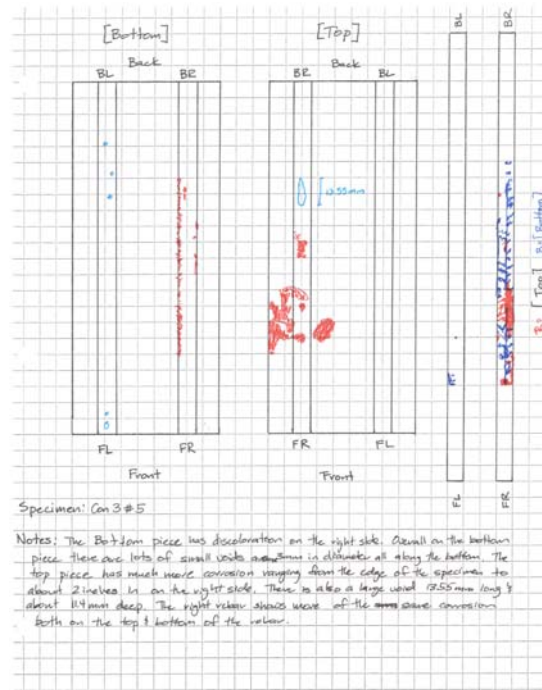


Figure 7.42 : Control 3 #5B

Con3 #5 – The visual inspection showed a crack on the top surface. The crack is in the middle but more to the right than left. There was also a long crack along the right side that was parallel to the right reinforcement. On the inside of the specimen the majority of the corrosion was located on the right bar. The corrosion on the bottom covers the ribs of the steel, while the corrosion on the top is a concentrated black area. The half cell potential values were all in the 90% probability range. The right side values were much higher than the left side. The voltage readings show that the specimen had reached failure. The inspection concluded the corrosion to be moderate to significant.



Figure 7.43 - Bars, bottom



Figure 7.44 - Bars, top

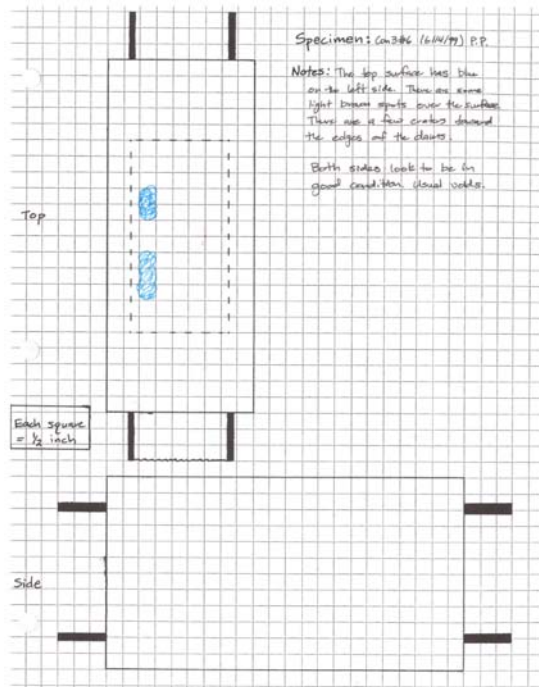


Figure 7.45 : Control 3 #6A

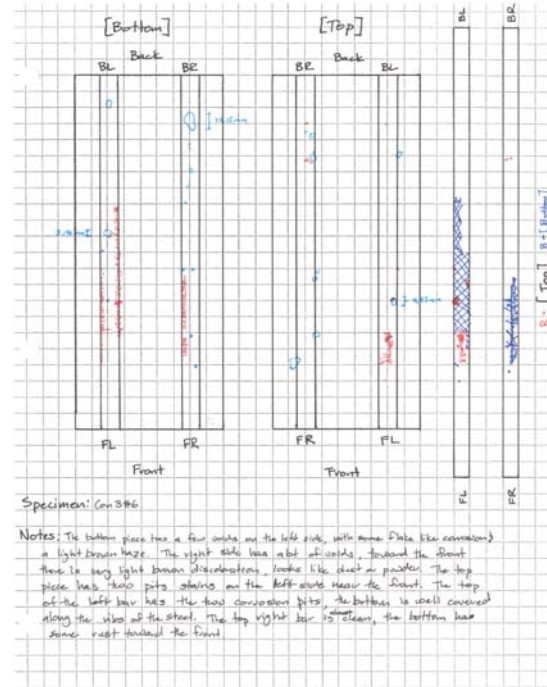


Figure 7.46 : Control 3 #6B

Con3 #6 – The visual inspection of the specimen showed no major flaws on the outside. On the inside of the specimen the bottoms of both bars had some corrosion more towards the front of the bar. The left bar has more corrosion on the bottom and has a few spots on the top. The half cell potential numbers show that all of the values fell into the uncertain range, but the numbers on the right side was higher than the left side. The voltage results show that the specimen had not failed. The inspection concluded the corrosion to be moderate to significant.



Figure 7.47 - Bars, bottom



Figure 7.48 - Bars, top

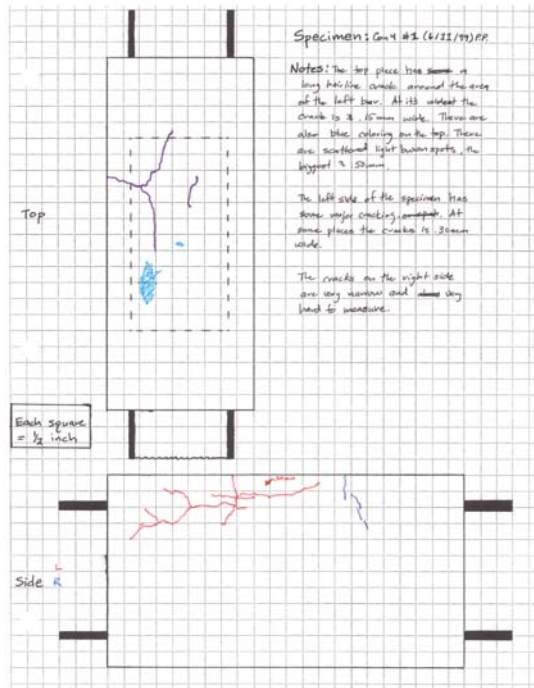


Figure 7.49 : Control 4 #1A

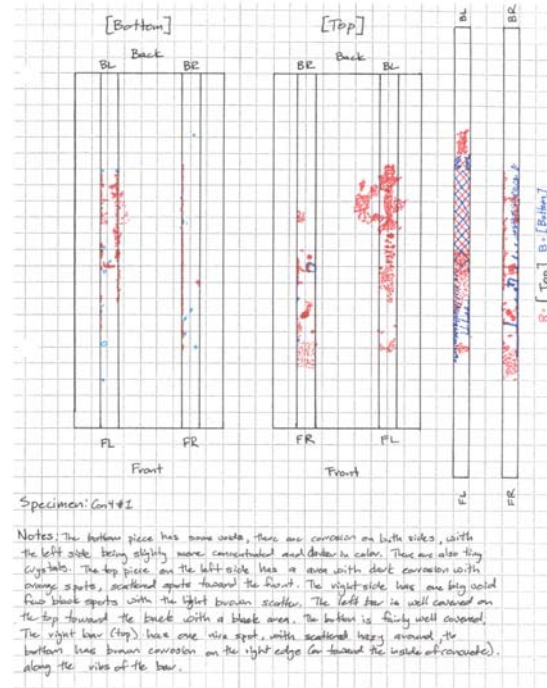


Figure 7.50 : Control 4 #1B

Con4 #1 – The visual inspection showed multiple cracks above the left bar. The cracks spanned parallel to the left reinforcement on the top surface and on the left side. There was also a crack in the middle of the specimen and two small cracks on the right side. On the inside of the specimen there was lots of corrosion on both bars. The left bar has more corrosion on the top and bottom than the right bar. The right bar had corrosion on the edges. The half cell potential readings showed all the values in the uncertain range. The voltage readings showed that the specimen reached the failure. The inspection concluded the corrosion to be moderate to significant.



Figure 7.51 - Bars, bottom



Figure 7.52 - Bars, top

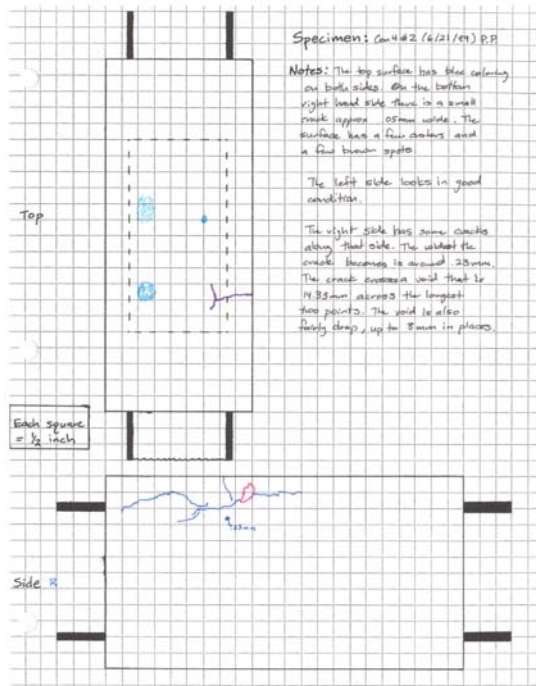


Figure 7.53 : Control 4 #2A

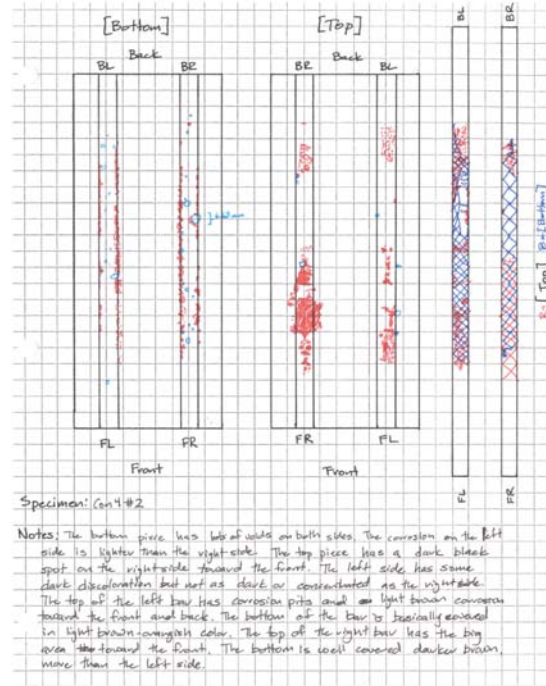


Figure 7.54 : Control 4 #2B

Con4 #2 – The visual inspection showed that there were cracks on the right side on the top and side surface. On the inside of the surface both bars looked bad. Both bars were almost covered on the bottom and had some scattered areas on the top. According to the half cell potential readings all fell into the uncertain category. The voltage readings show that the specimen had reached failure. The inspection concluded the corrosion to be moderate to significant.



Figure 7.55 - Bars, bottom



Figure 7.56 - Bars, top

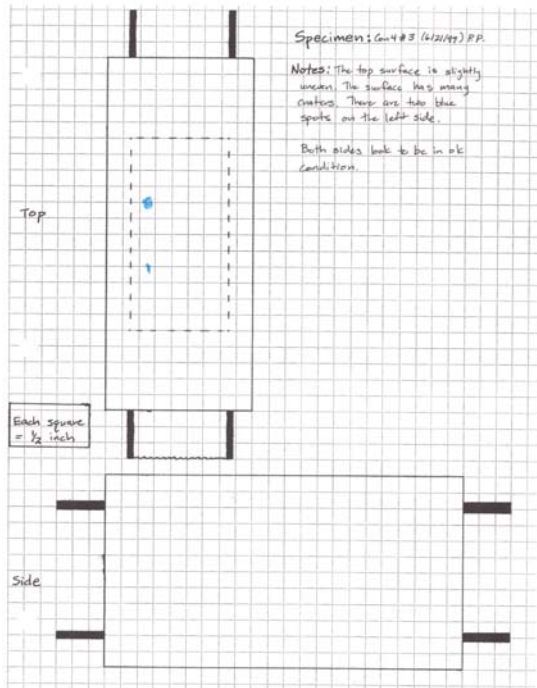


Figure 7.57 : Control 4 #3A

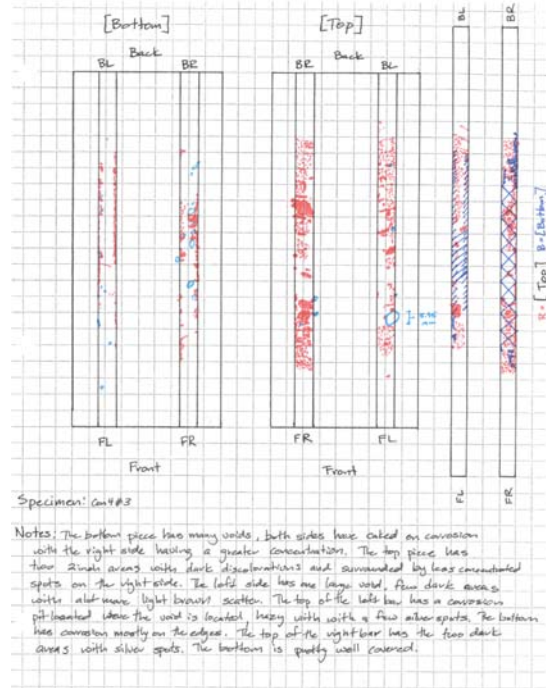


Figure 7.58 : Control 4 #3B

Con4 #3 – The visual inspection showed that there were no major flaws on the outside of the specimen. On the inside of the specimen both bars were well covered in corrosion on both top and bottom of the bars. The half cell potential results show that all the values were in the uncertain range. The voltage readings showed the specimen had reached the failure threshold. The inspection concluded the corrosion to be moderate to significant.



Figure 7.59 - Bars, bottom



Figure 7.60 - Bars, top

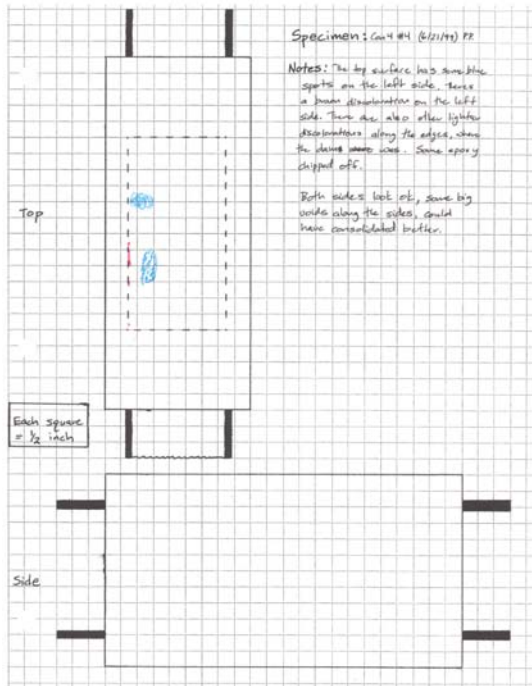


Figure 7.61 : Control 4 #4A

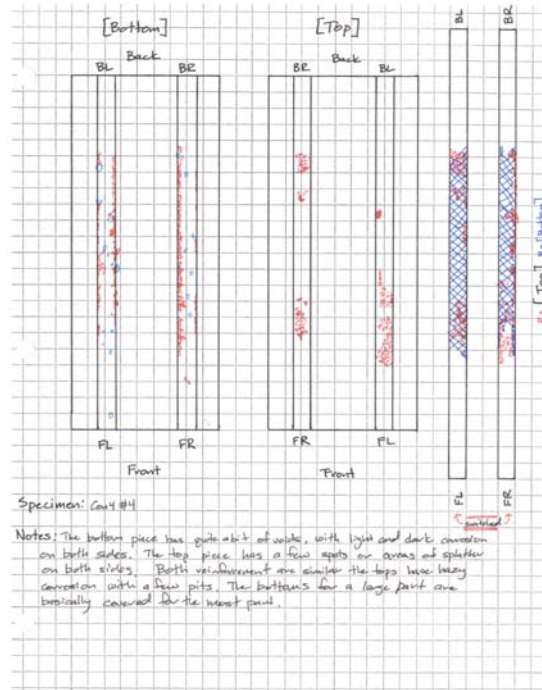


Figure 7.62 : Control 4 #4B

Con4 #4 – The visual inspection did not show any cracks, but it did show some light brown discolorations on the top surface above the left reinforcement. Both reinforcement bars were well covered on their bottoms with corrosion. The tops of the bars had areas of scattered corrosion with some pits. The half cell potential numbers indicate that all the values fell into the 10% probability of corrosion range. The voltage readings showed the specimen had reached failure. The inspection concluded the corrosion to be moderate to significant.



Figure 7.63 - Bars, bottom



Figure 7.64 - Bars, top

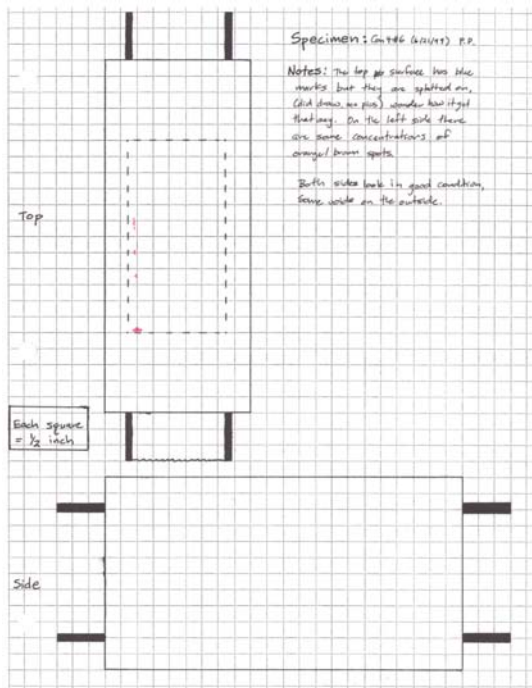


Figure 7.65 : Control 4 #6A

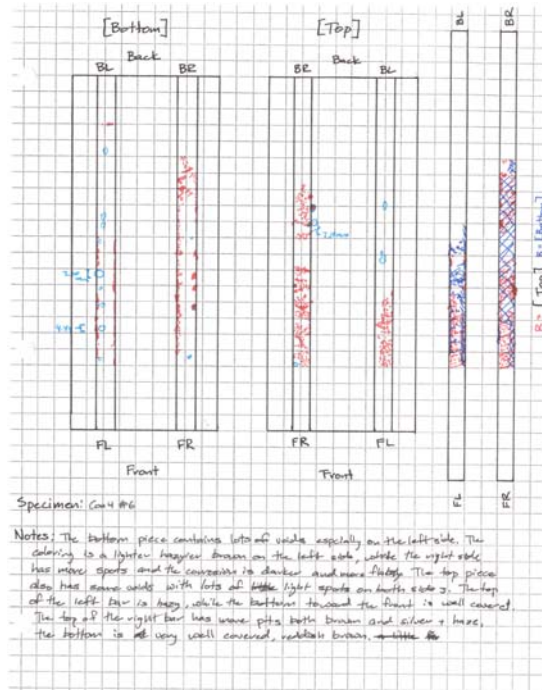


Figure 7.66 : Control 4 #6B

Con4 #6 – The visual inspection on the outside of the specimen showed no critical flaws. There were some brown concentrations on the top surface on the left side. There was corrosion on both bars on the top and bottom. The corrosion on the right bar was more extensive than the left side. The half cell potential readings showed that the values on the left fell into the uncertain range, while the values on the right side all fell into the 10% probability range. The voltage reveals that the specimen had reached failure. The inspection concluded the corrosion to be moderate to significant.



Figure 7.67 - Bars, bottom



Figure 7.68 - Bars, top

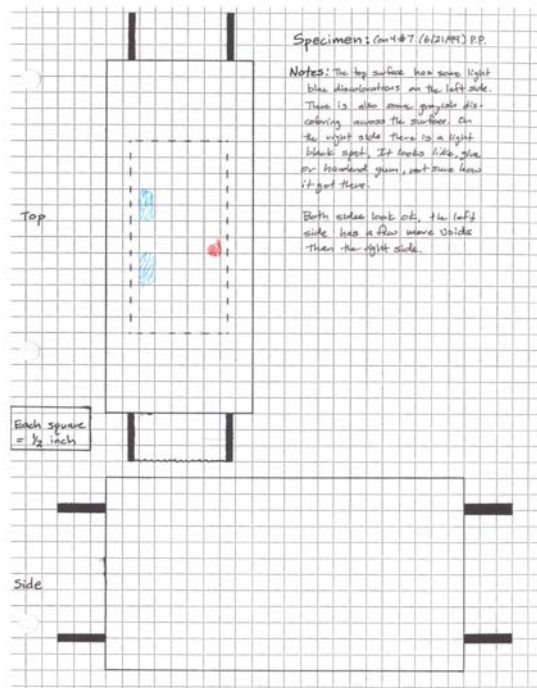


Figure 7.69 : Control 4 #7A

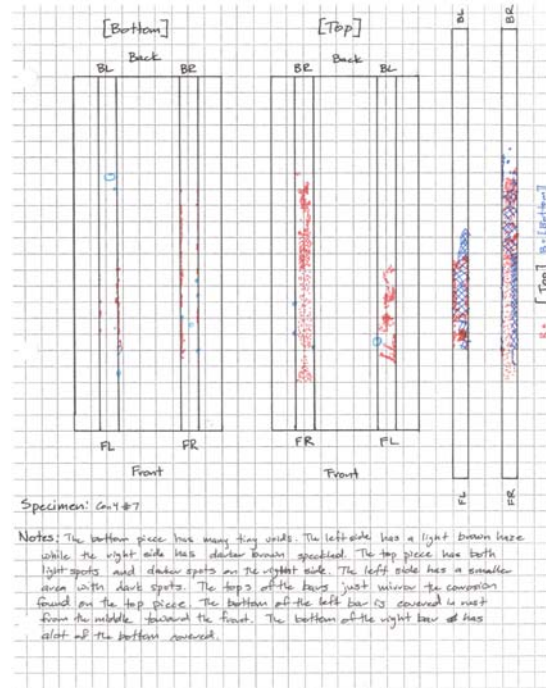


Figure 7.70 : Control 4 #7B

Con4 #7 – Overall the visual inspection of the outside showed no major flaws. The examination of the bars showed that there was corrosion on both bars. The corrosion on the bottom of both bars was more concentrated than the corrosion located on the top. The half cell potential tests reveal that all the numbers fell into the uncertain range. The voltage readings showed that the specimen had reached failure. The inspection concluded the corrosion to be moderate to significant.



Figure 7.71 - Bars, bottom



Figure 7.72 - Bars, top

DAREX CORROSION INHIBITOR

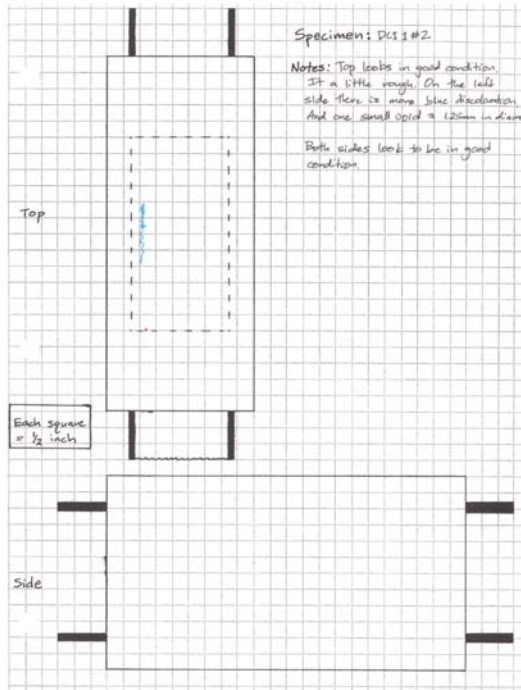


Figure 7.73 : DCI 1 #2 A

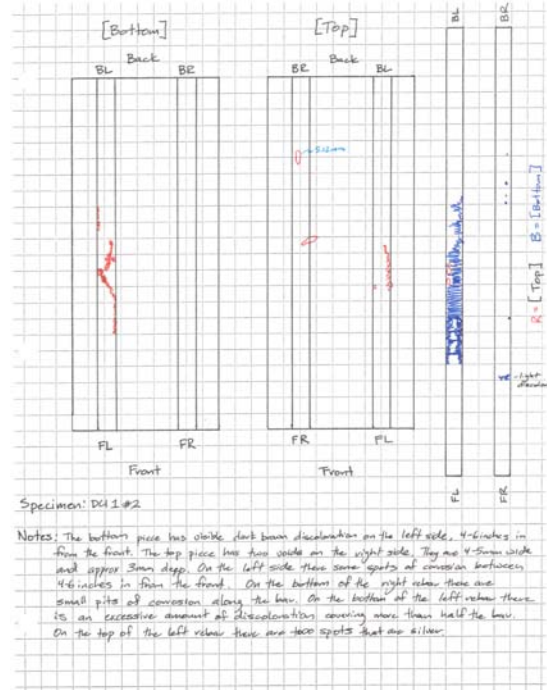


Figure 7.74 : DCI 1 #2 B

DCI1 #2 – The outside of the specimen appears to be in good condition. There is one small void on the top surface that was toward the front and to the left. The majority of the corrosion appears on the bottom of the left bar. The top of the left bar has a couple of pits. The bottom of the right bar has some pits as well. The half cell potential values all fell into the 10% probability range. The voltage data showed that the specimen was close to failure but did not reach that point. The inspection concluded the corrosion to be moderate to significant.



Figure 7.75 - Bars, bottom



Figure 7.76 - Bars, top

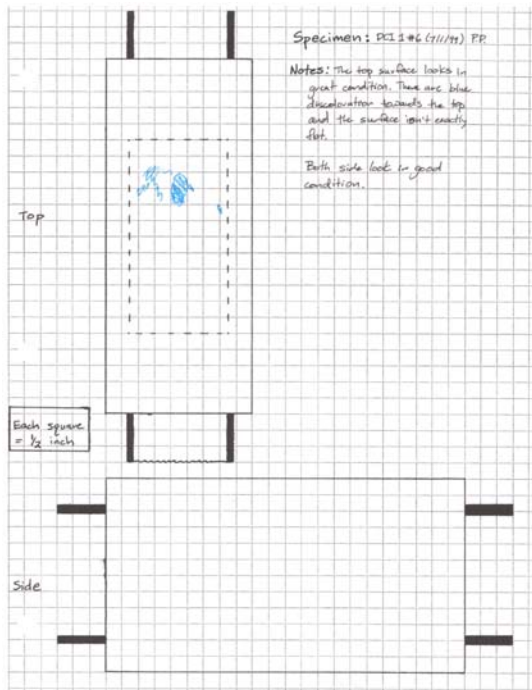


Figure 7.77 : DCI 1 #6A

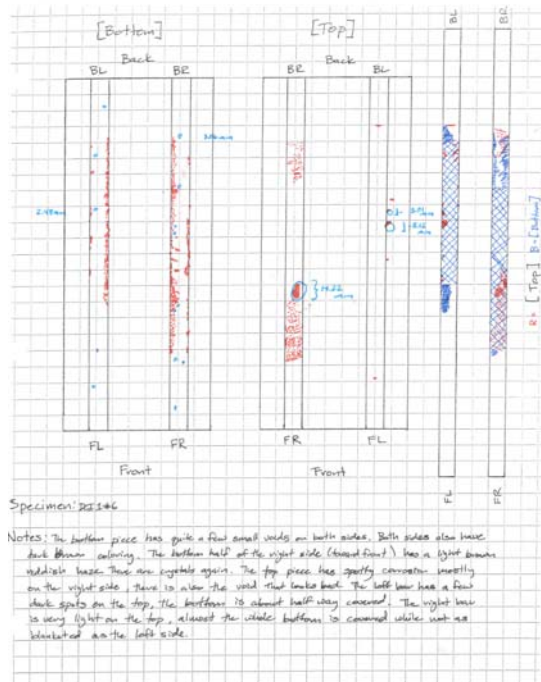


Figure 7.78 : DCI 1 #6B

DCI1 #6 – From the outside the specimen looked in great condition. Both bars are well covered in corrosion on their bottoms. The bottom of the right bar covers more area on the bottom than the left. On the top both bars had pits and other scattered areas of corrosion. The half cell potential values showed that left side had two numbers in the uncertain range. All the other values fell into the 10% probability range. The voltage results showed the specimen had failed. The inspection concluded the corrosion to be moderate to significant.



Figure 7.79 - Bars, bottom



Figure 7.80 - Bars, top

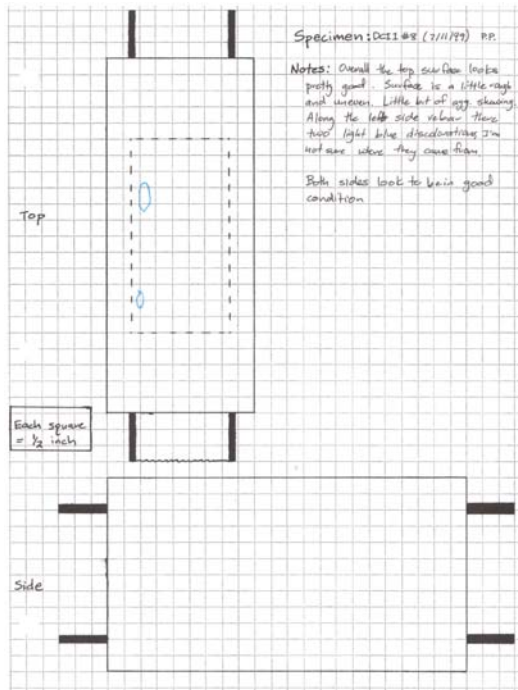


Figure 7.81 : DCI 1 #8A

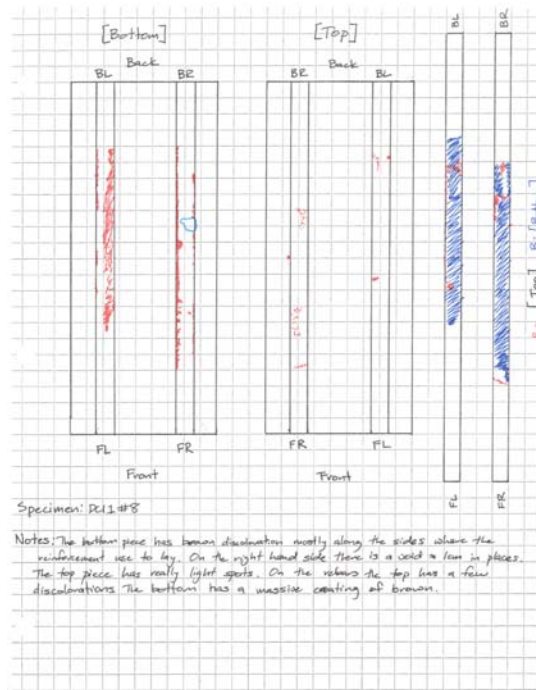


Figure 7.82 : DCI 1 #8B

DCI1 #8 – The visual inspection showed no detrimental flaws to the specimen. Both bars are well covered in corrosion on their bottoms. The bottom of the right bar covers more area on the bottom than the left. On the top both bars had pits and other scattered areas of corrosion. The half cell potential values on the left side and one on the right fell into the uncertain range. The other two values fell into the 10% probability range. The voltage data showed that the specimen had not failed, but was getting close. The inspection concluded the corrosion to be moderate to significant.



Figure 7.83 - Bars, bottom



Figure 7.84 - Bars, top

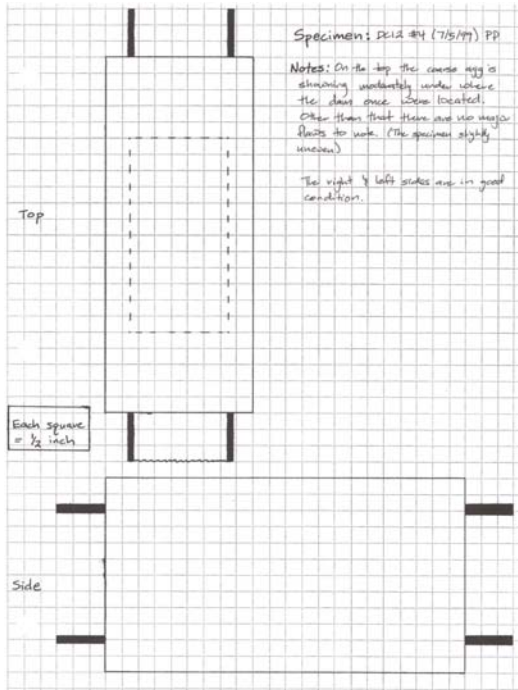


Figure 7.85 : DCI 2 #4A

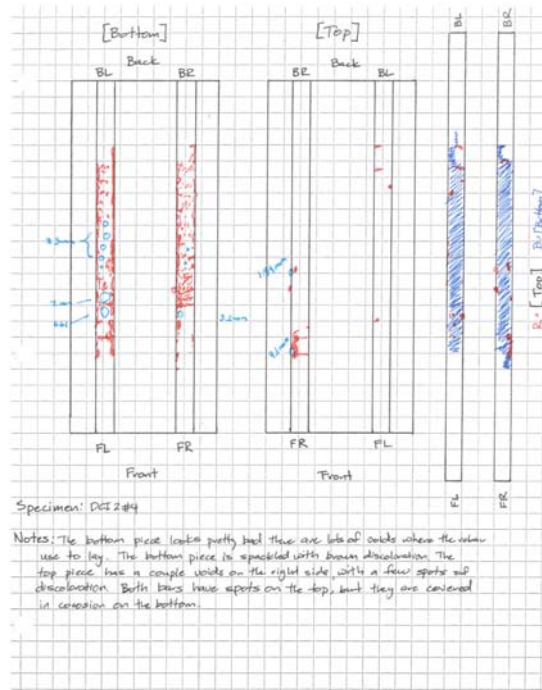


Figure 7.86 : DCI 2 #4B

DCI2 #4 – From the outside the specimen showed no discernable problems. The bottoms of both bars were well covered in corrosion. There were a large amount of voids that may have contributed to the corrosion. The tops of the bars had pits and spots on the edges. The half cell potential values all fell into the uncertain range. The voltage readings showed the specimen was very close to failure but it did not reach the failure threshold. The inspection concluded the corrosion to be moderate to significant.



Figure 7.87 - Bars, bottom



Figure 7.88 - Bars, top

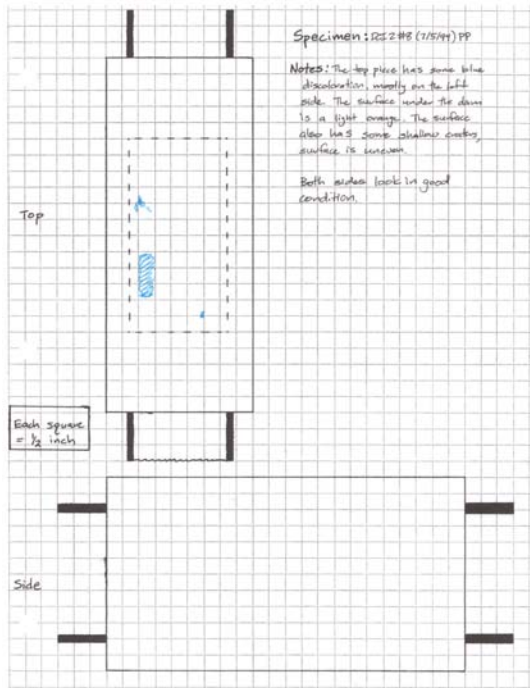


Figure 7.89 : DCI 2 #8 A

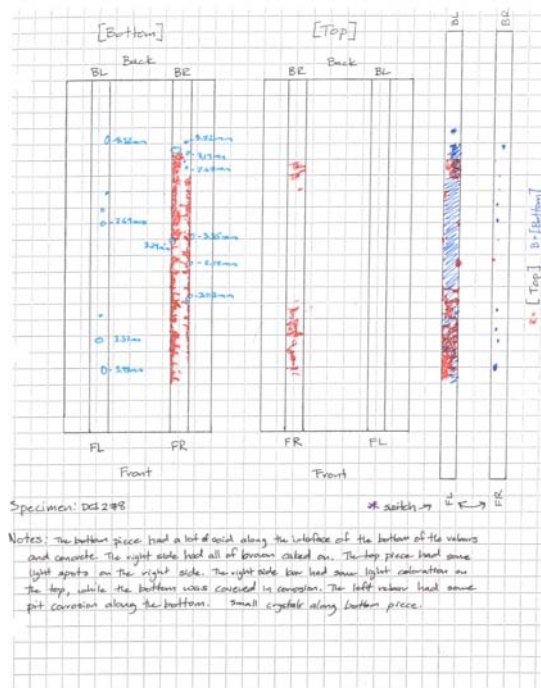


Figure 7.90 : DCI 2 #8 B

DCI2 #8 – The visual inspection showed no major flaws on the outside. The right bar was well covered in corrosion on the bottom. The top of the right bar has a 2 inch area of corrosion near the front with pits toward the back. The left bar has pits on the bottom along the length of the bar. The half cell potential values all fell into the 10% probability range. The voltage data showed that the specimen had not failed. The inspection concluded the corrosion to be moderate to significant.



Figure 7.91 - Bars, bottom



Figure 7.92 - Bars, top

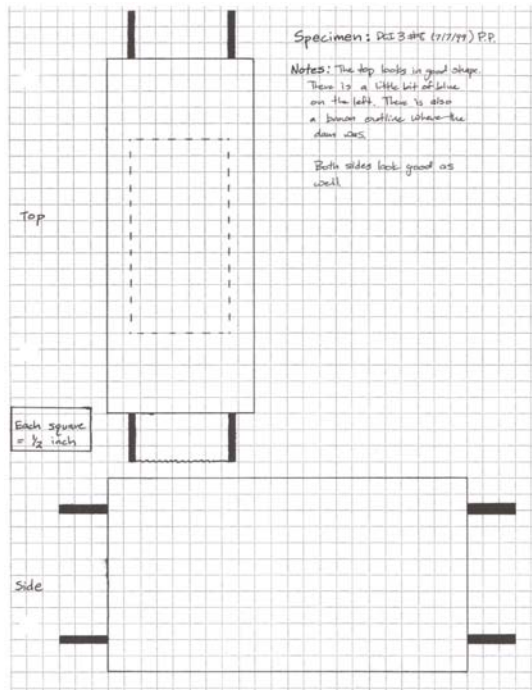


Figure 7.93 : DCI 3 #8 A

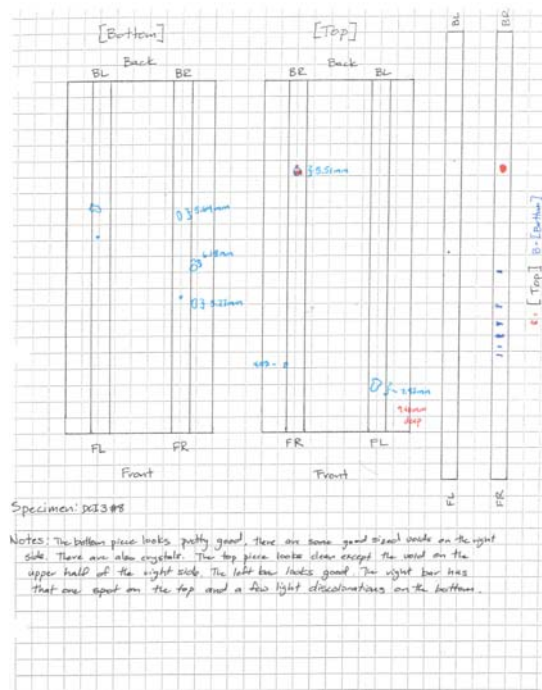


Figure 7.94 : DCI 3 #8 B

DCI3 #8 – The visual inspection showed that the specimen was in good condition. The inside of the specimen was fairly clean. There were some spots here and there. The half cell potential values all fell into the 10% probability range. The voltage readings showed that the specimen had not failed. The inspection concluded the corrosion to be none.



Figure 7.95 - Bars, bottom



Figure 7.96 - Bars, top

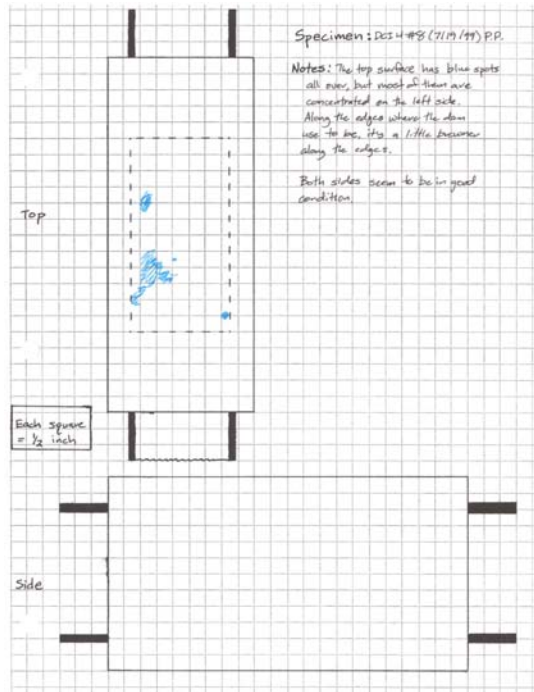


Figure 7.97 : DCI 4 #8 A

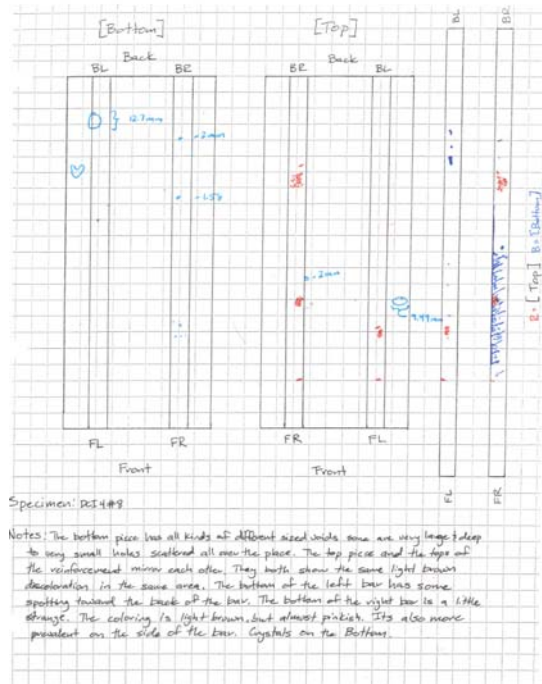


Figure 7.98 : DCI 4 #8 B

DCI4 #8 – The visual inspection does not show any major flaws on the outside. Both bars had corrosion on the tops and bottoms. The corrosion was either spots or not well concentrated. The half cell potential values all fell into the 10% probability range. The voltage data showed that the specimen had not failed. The inspection concluded the corrosion to be minor.



Figure 7.99 - Bars, bottom



Figure 7.100 - Bars, top

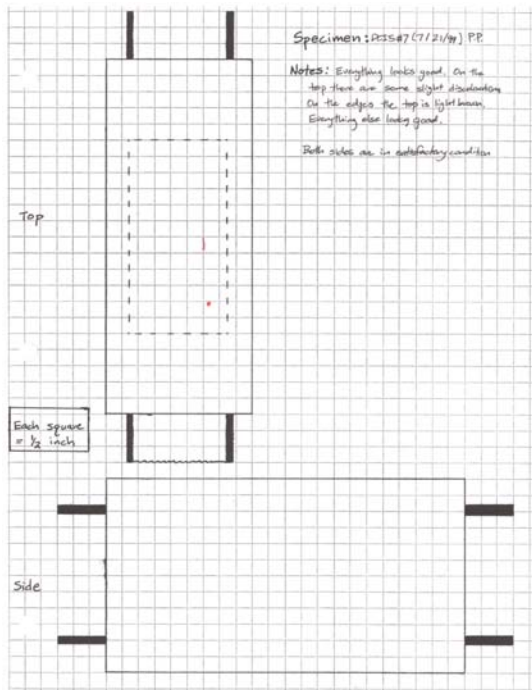


Figure 7.101 : DCI 5 #8A

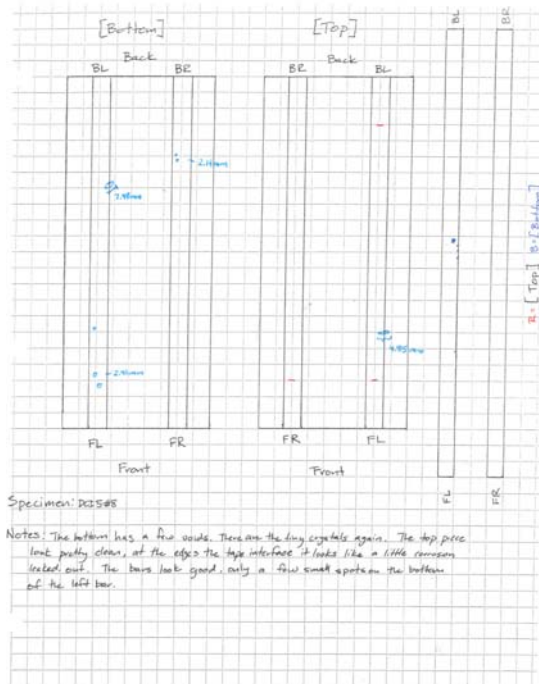


Figure 7.102 : DCI 5 #8B

DCI5 #8 – The top surface showed some light discoloration on the right side. There was very little corrosion on the inside. There were only a few spots on the bottom of the left bar. The half cell potential values all fell into the 10% probability range. The voltage numbers indicated that the specimen had not failed. The inspection concluded the corrosion to be none.



Figure 7.103 - Bars, bottom



Figure 7.104 - Bars, top

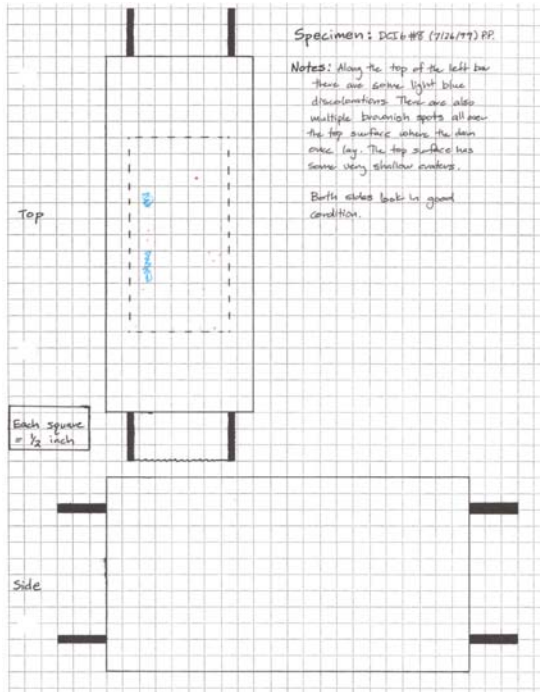


Figure 7.105 : DCI 6 #8A

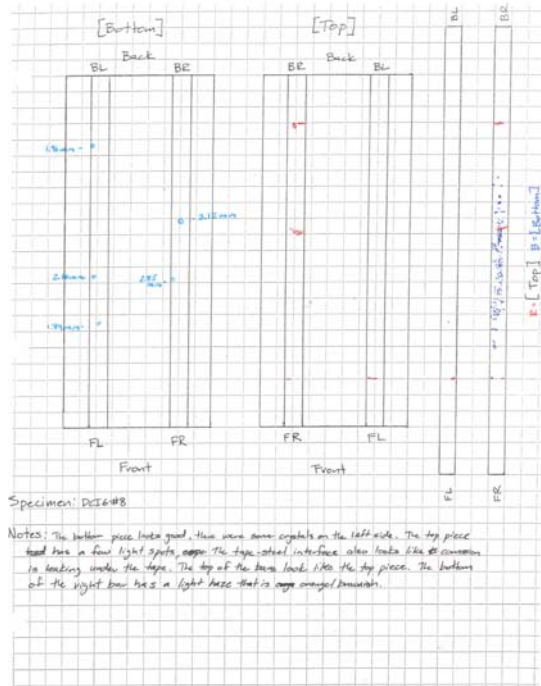


Figure 7.106 : DCI 6 #8B

DCI6 #8 – The specimen from the outside looked in fair condition. The majority of corrosion occurred on the bottom of the right bar. The corrosion was scattered over a large area. There were also some spots on the top of the right bar. The half cell potential values all fell into the 10% probability range. The voltage data showed the specimen did not meet the failure criteria. The inspection concluded the corrosion to be minor.



Figure 7.107 - Bars, bottom

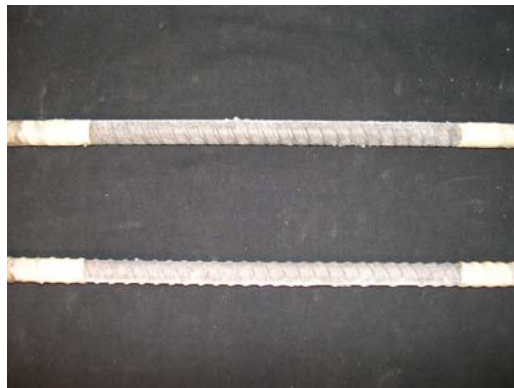


Figure 7.108 - Bars, top

FLY ASH

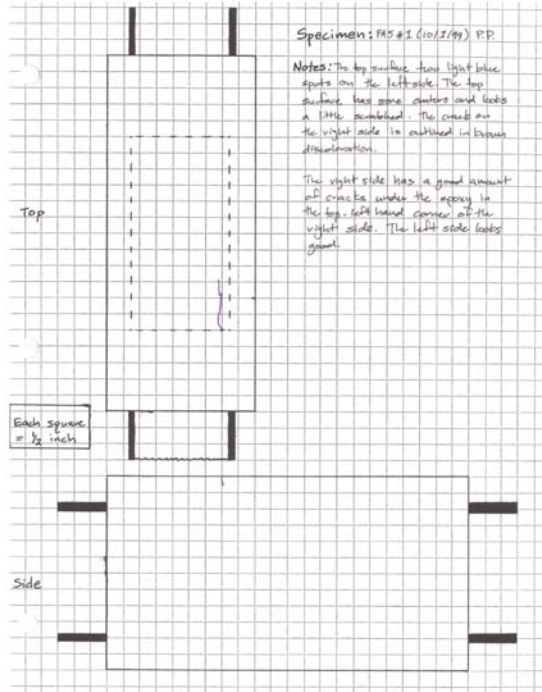


Figure 7.109 : FA5 #1A

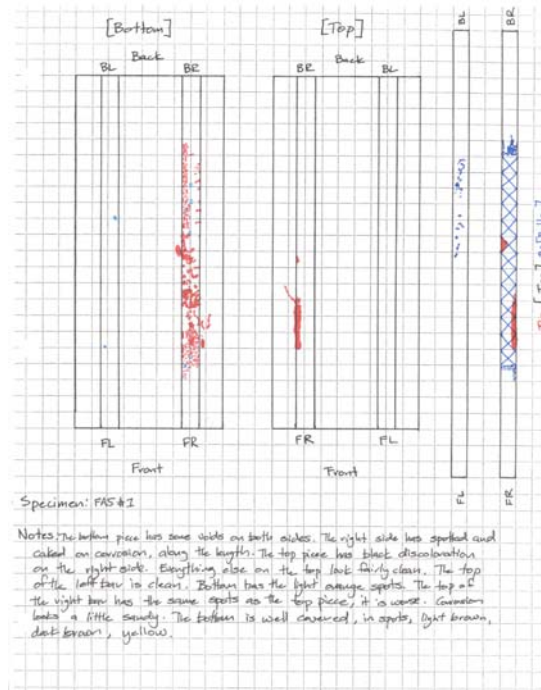


Figure 7.110 : FA5 #1B

FA5 #1 – The visual inspection showed a crack on the top surface above the right bar. There were also many cracks underneath the epoxy coating on the right side. Inside the specimen the majority of the corrosion occurred on the bottom of the right bar. There were two large areas of corrosion on the top of the right bar. The left bar had a few pits and spots on the bottom. The half cell potential values indicated 90% probability of corrosion. The voltage readings showed the specimen had failed. The inspection concluded the corrosion to be moderate to significant.



Figure 7.111 - Bars, bottom



Figure 7.112 - Bars, top

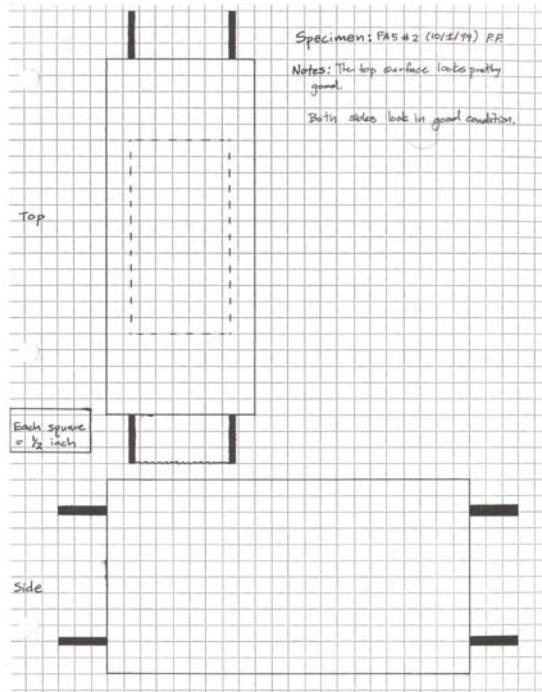


Figure 7.113 : FA5 #2 A

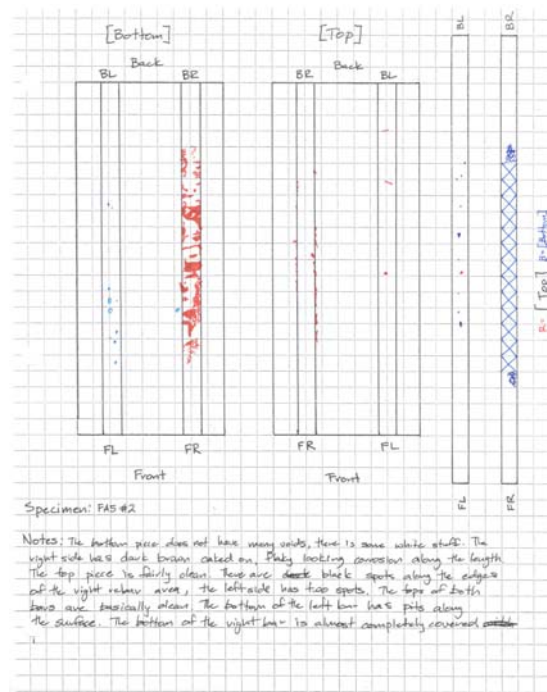


Figure 7.114 : FA5 #2 B

FA5 #2 – The visual inspection from the outside showed no flaws. The inside showed the bottom of the right bar covered in corrosion. There were pits of corrosion scattered along the bottom of the left bar. The half cell potential testing showed that all the values fell into the uncertain range. The voltage readings indicated that the specimen was half way toward failure. The inspection concluded the corrosion to be moderate to significant.



Figure 7.115 - Bars, bottom



Figure 7.116 - Bars, top

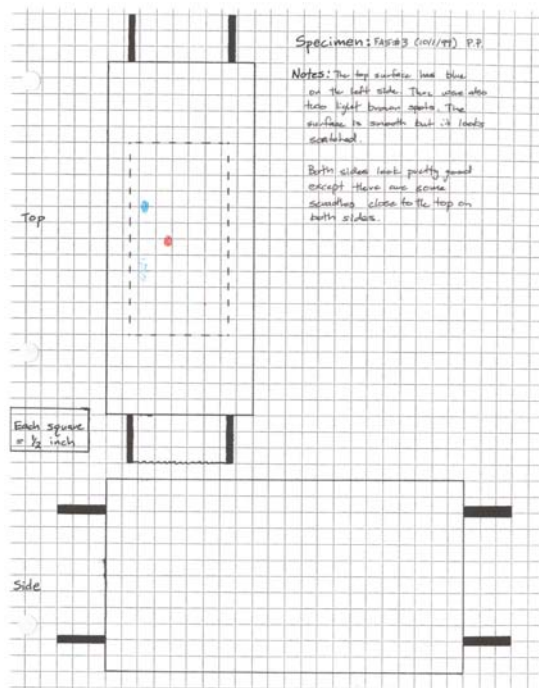


Figure 7.117 : FA5 #3 A

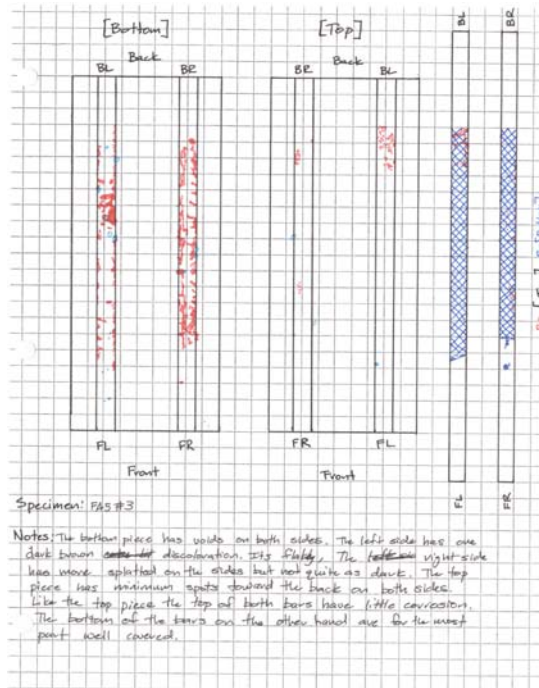


Figure 7.118 : FA5 #3 B

FA5 #3 – The visual inspection did not show any critical flaws of the specimen. Both bars were covered in corrosion on the bottom over the length of the bars. The tops of both bars have scattered spots in a few areas. The half cell potential values showed that all the values fell into the 10% probability of corrosion range. The voltage readings indicated the specimen was extremely close to failure. The inspection concluded the corrosion to be moderate to significant.



Figure 7.119 - Bars, bottom



Figure 7.120 - Bars, top

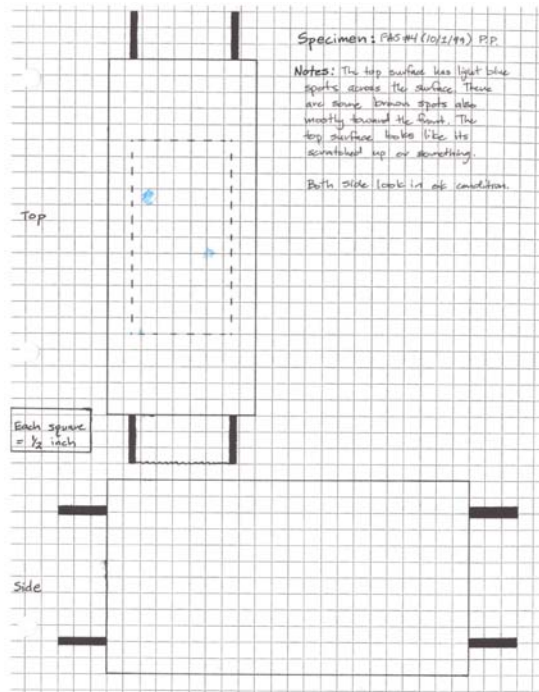


Figure 7.121 : FA5 #4 A

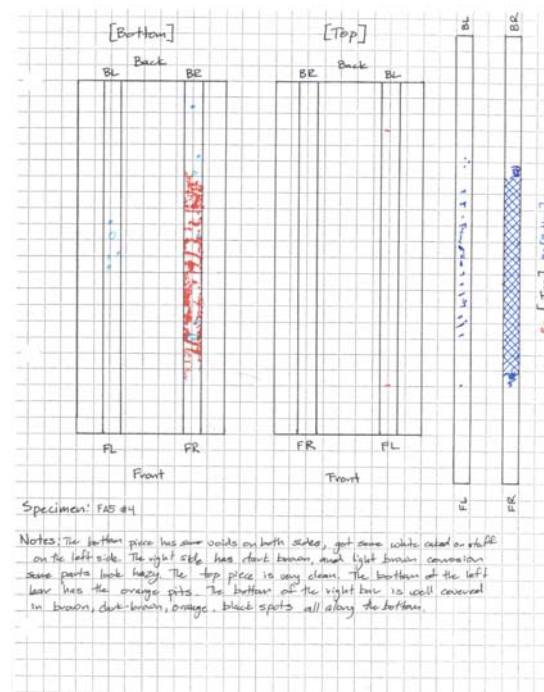


Figure 7.122 : FA5 #4 B

FA5 #4 – The visual inspection of the outside of the specimen showed that the specimen was in good condition. The right bar was covered in corrosion along the bottom of the bar. The left bar also had pits along the bottom. The half cell potential test showed that all the values fell into the uncertain range. The voltage readings showed that the specimen had not reached failure. The inspection concluded the corrosion to be moderate to significant.



Figure 7.123 - Bars, bottom



Figure 7.124 - Bars, top

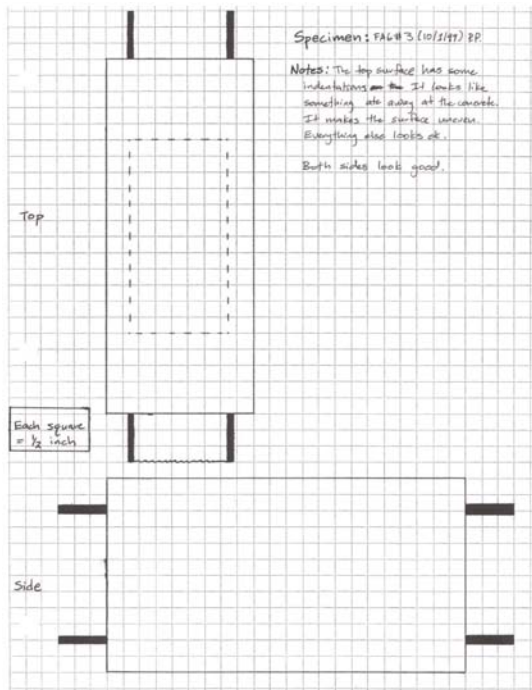


Figure 7.125 : FA6 #3 A

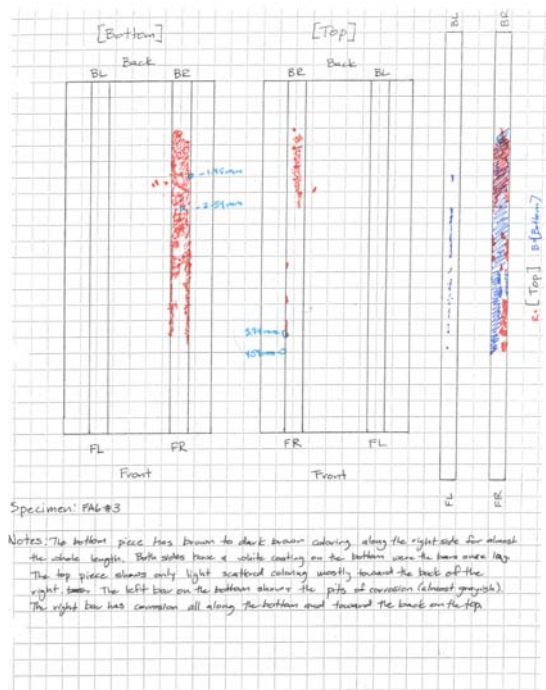


Figure 7.126 : FA6 #3 B

FA6 #3 – The top surface looked uneven but no major flaws. The right bar was covered in corrosion for the majority of the bottom of the bar. The top of the bar had a few concentrated areas of corrosion. The left bar had some spots along the bottom of the bar. The half cell potential readings showed all of the values fell into the uncertain range. The voltage readings indicated that the specimen had failed. The inspection concluded the corrosion to be moderate to significant.



Figure 7.127 - Bars, bottom



Figure 7.128 - Bars, top

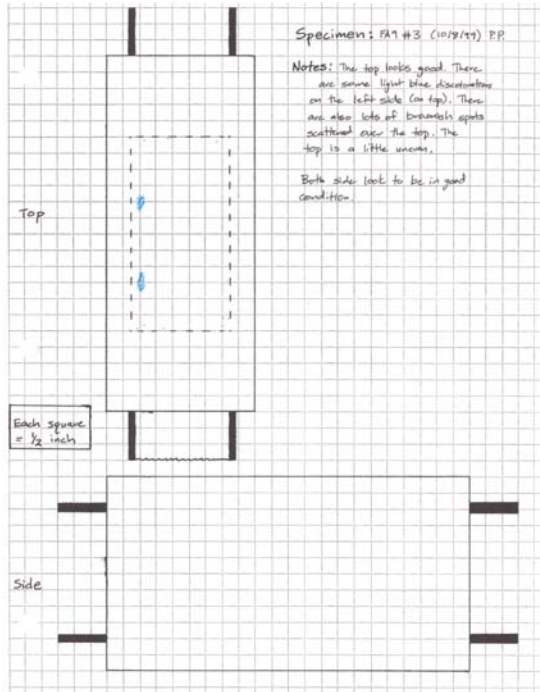


Figure 7.129 : FA9 #3A

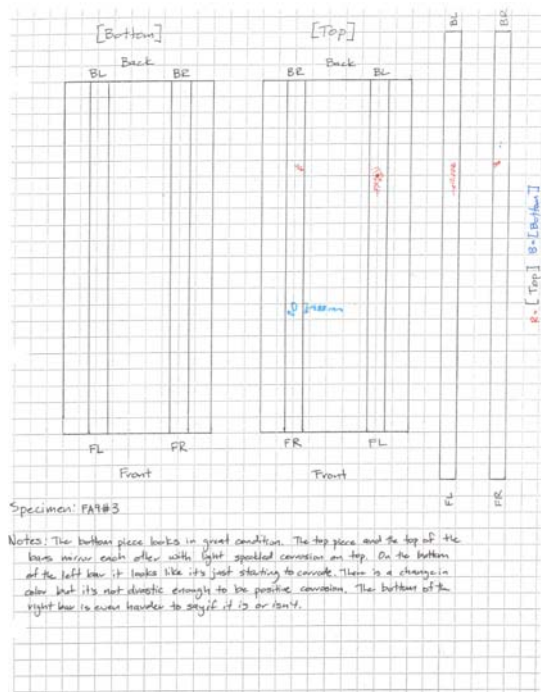


Figure 7.130 : FA9 #3B

FA9 #3 – The visual inspection did not reveal any serious problems. There was very little corrosion located on the bars. Both bars had a small area of spotted corrosion. The half cell testing indicated that all the values fell into the 10% probability range. The voltage readings showed that the specimen had not failed. The inspection concluded the corrosion to be minor.



Figure 7.131 - Bars, bottom



Figure 7.132 - Bars, top

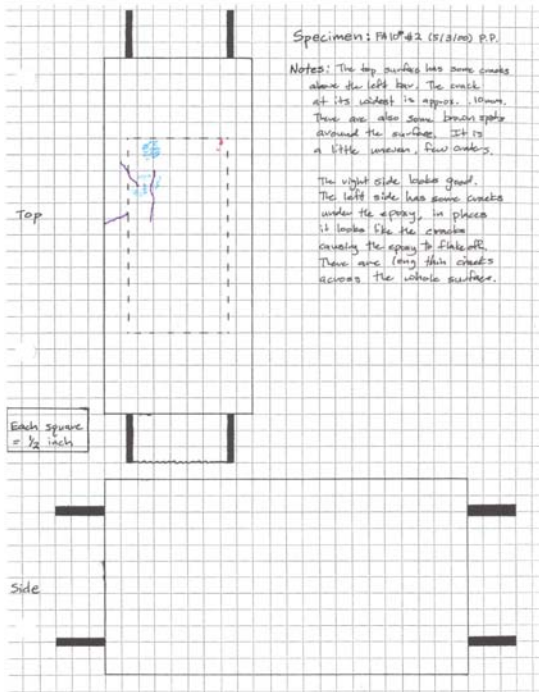


Figure 7.133 : FA10* #2A

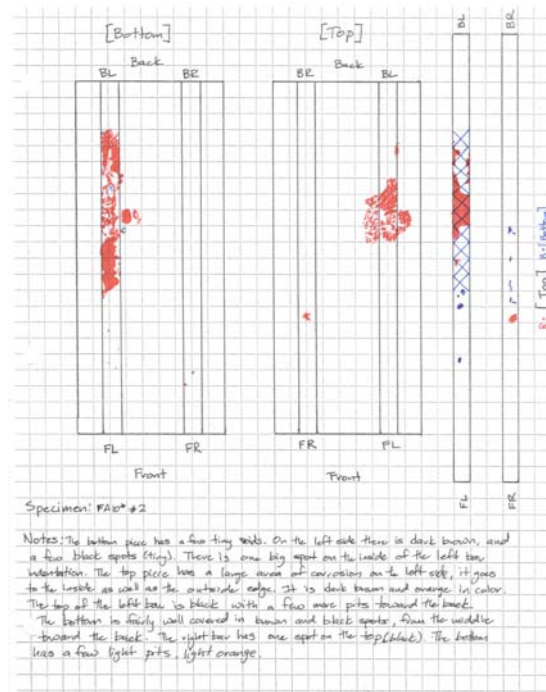


Figure 7.134 : FA10* #2B

FA10* #2 – There are three cracks located on the top surface above the left bar. The left bar was covered in corrosion on the bottom for most of the bar. The top of the left bar had a large concentrated area of corrosion. The right bar had a few spot here and there. The half cell potential values showed that two values on the right and left side fell into the 90% probability range. The other two values left fell into the uncertain range. The voltage readings showed the specimen has failed. The inspection concluded the corrosion to be moderate to significant.



Figure 7.135 - Bars, bottom



Figure 7.136 - Bars, top

FERROGARD 901

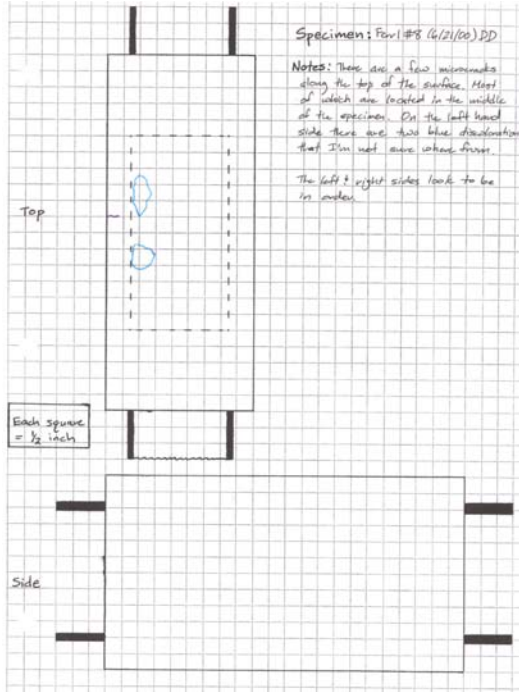


Figure 7.137 : Ferr1 #8A

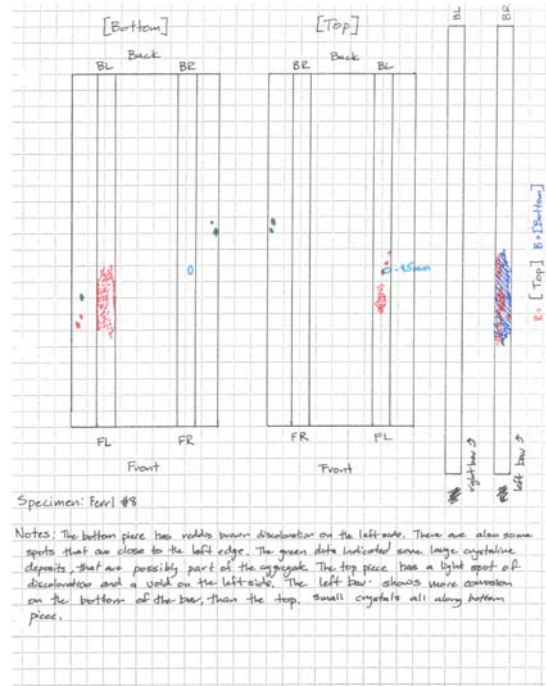


Figure 7.138 : Ferr1 #8B

Ferr1 #8 – The visual inspection showed a tiny crack on the edge of the top surface on the left side. The left bar had corrosion on the top and the bottom of the bar. The half cell potential values all fell into the 10% probability range. The voltage results showed that the specimen had failed. The inspection concluded the corrosion to be moderate to significant.



Figure 7.139 - Bars, bottom



Figure 7.140 - Bars, top

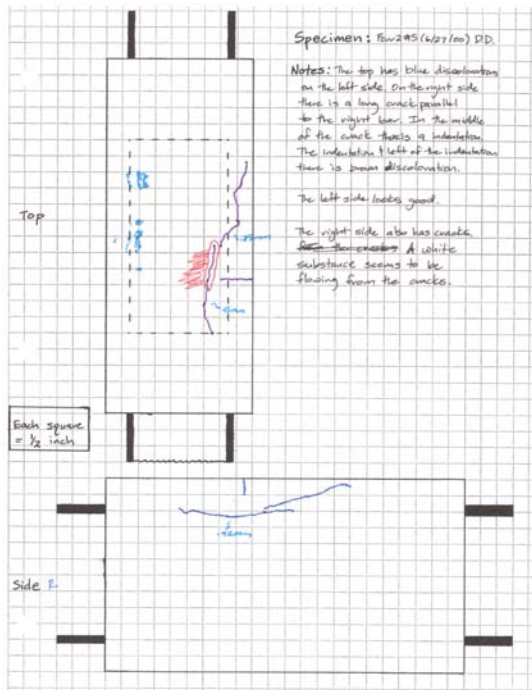


Figure 7.141 : Ferr2 #5A

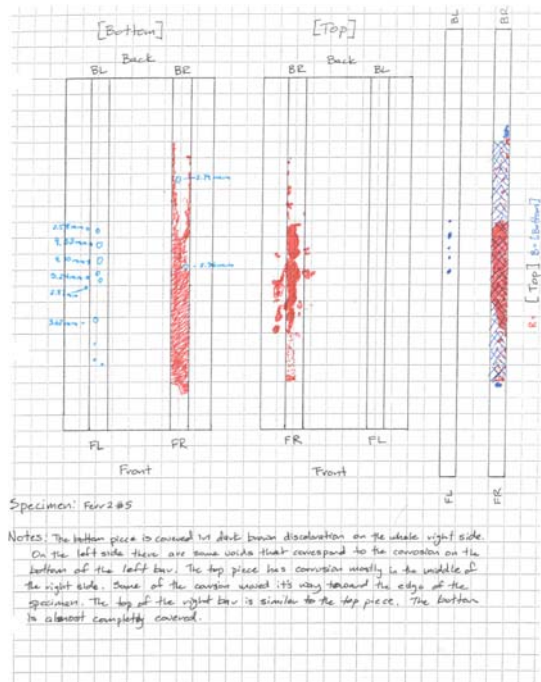


Figure 7.142 : Ferr2 #5B

Ferr2 #5 – The visual inspection showed a large crack along the right side of the specimen. Around the crack there was brown discoloration. There was a few cracks on the right side of the specimen. The right bar was completely covered in corrosion on the bottom. The top of the bar also has a large area of corrosion. The bottom of the left bar has a few pits. The half cell potential numbers showed all the values fell in the uncertain range. The voltage readings indicated that the specimen had failed. The inspection concluded the corrosion to be moderate to significant.



Figure 7.143 - Bars, bottom



Figure 7.144 - Bars, top

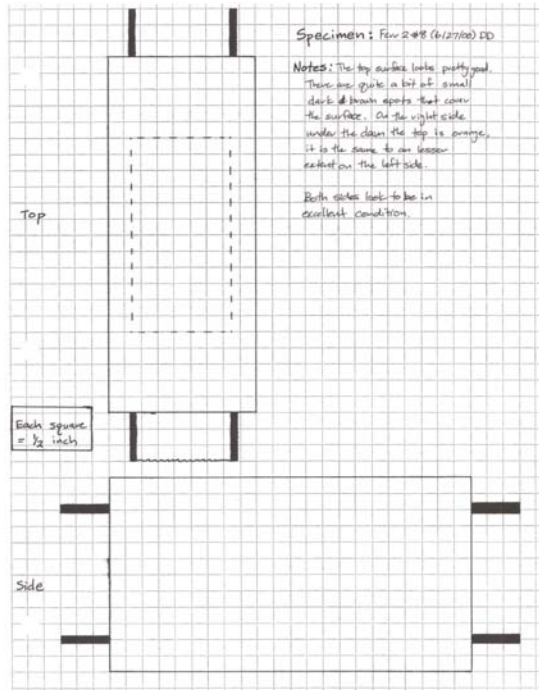


Figure 7.145 : Ferr2 #8 A

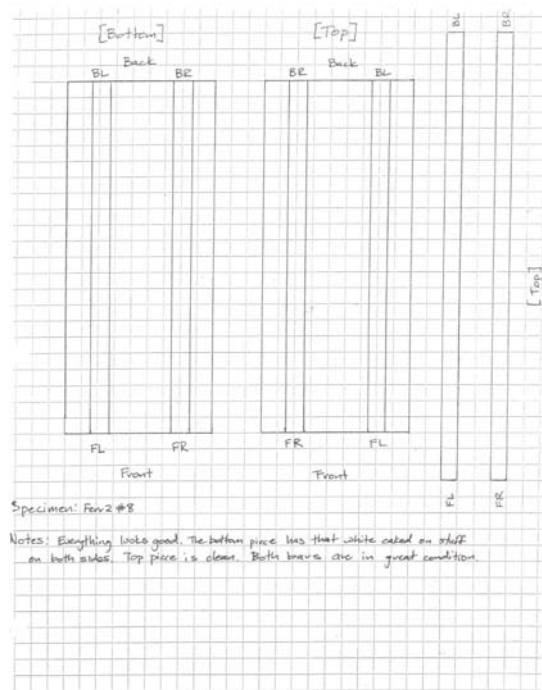


Figure 7.146 : Ferr2 #8 B

Ferr2 #8 – The outside of the specimen looked to be in excellent condition. There was no corrosion on the inside of the specimen. The half cell potential numbers were in the 10% probability range. The voltage readings showed that the specimen was not close to failure. The inspection concluded the corrosion to be none.



Figure 7.147 - Bars, bottom



Figure 7.148 - Bars, top

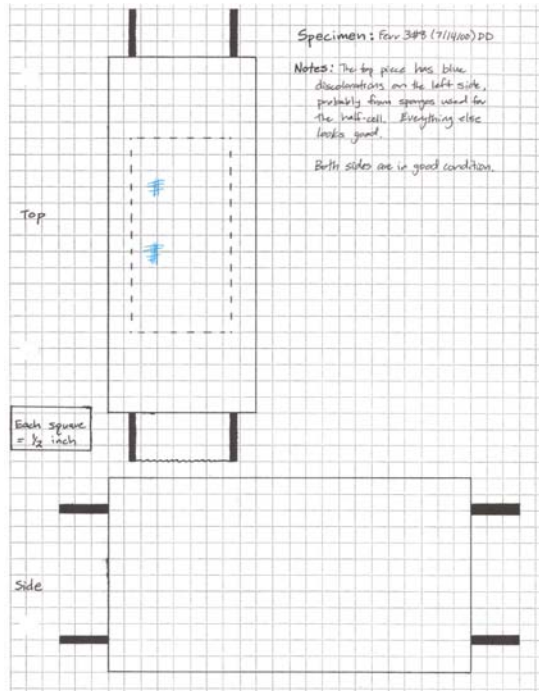


Figure 7.149 : Ferr3 #8A

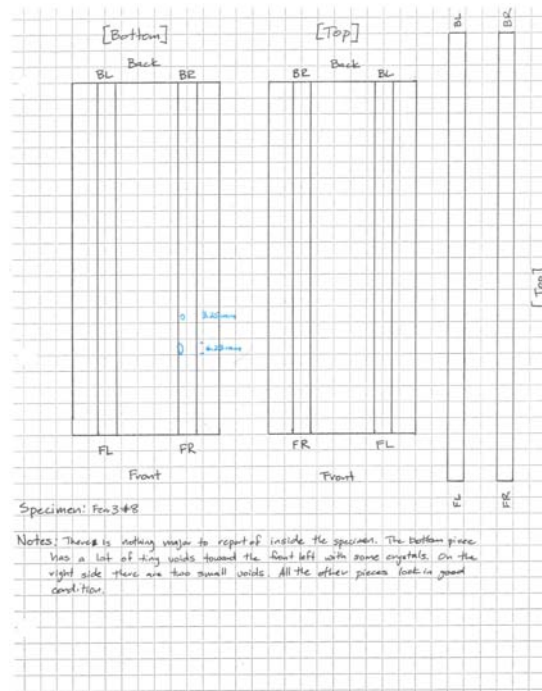


Figure 7.150 : Ferr3 #8B

Ferr3 #8 – The visual showed no flaws of significance on the outside of the specimen. The inside of the specimen was clean. The half cell potential values were all in the 10% probability range. The voltage readings showed that the specimen was not near failure. The inspection concluded the corrosion to be none.



Figure 7.151 - Bars, bottom



Figure 7.152 - Bars, top

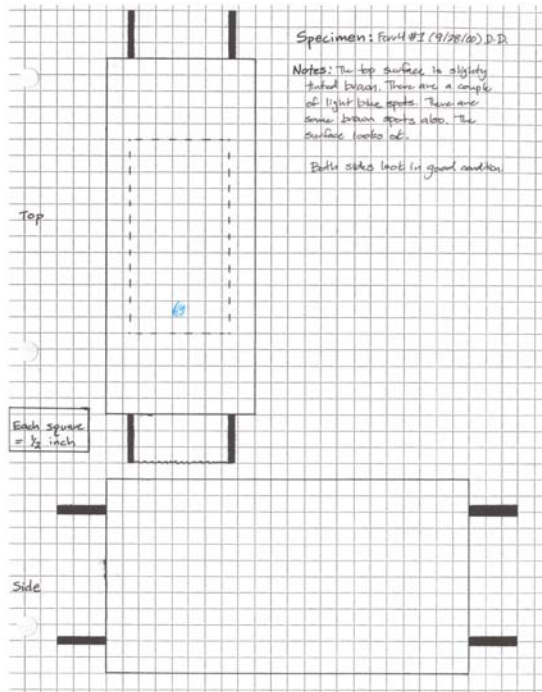


Figure 7.153 : Ferr4 #1A

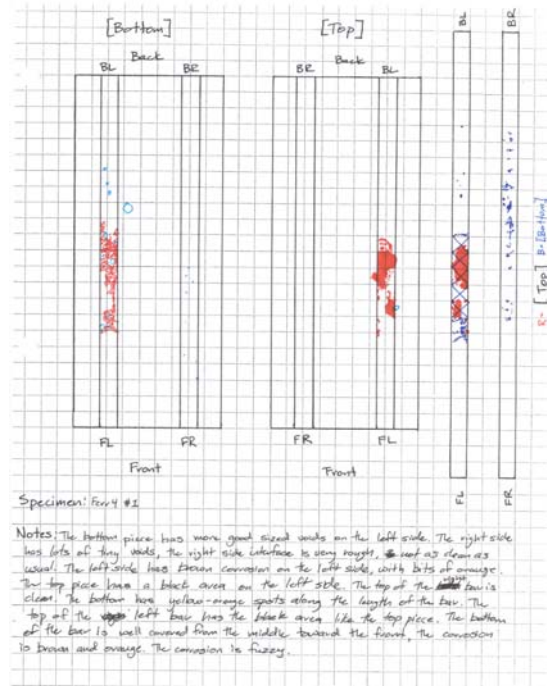


Figure 7.154 : Ferr4 #1B

Ferr4 #1 – The outside of the specimen looked to be in great condition. The left bar had corrosion toward the front of the bar on both the top and the bottom. The right bar had pits and spots along the length of the bottom. The half cell potential readings fell into the uncertain region. The voltage readings showed that the specimen had failed. The inspection concluded the corrosion to be moderate to significant.



Figure 7.155 - Bars, bottom



Figure 7.156 - Bars, top

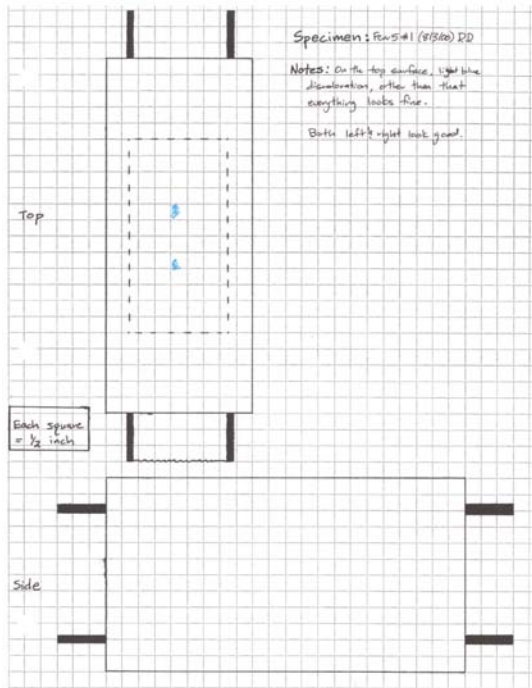


Figure 7.157 : Ferr5 #1A

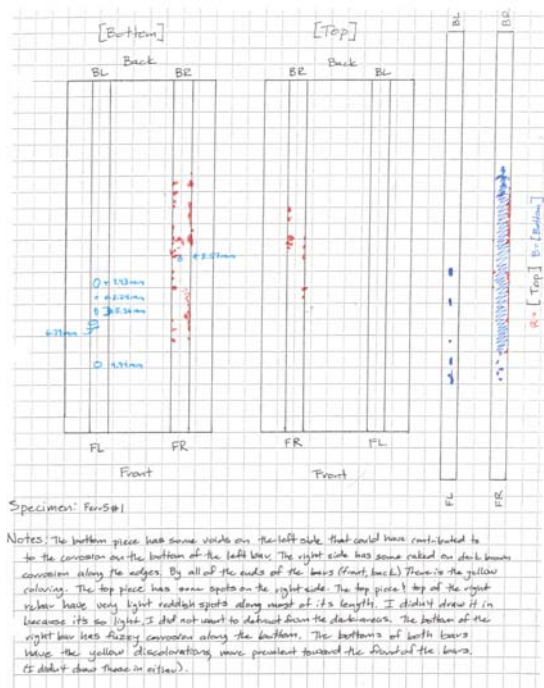


Figure 7.158 : Ferr5 #1B

Ferr5 #1 – The visual inspection of the outside of the specimen turned up nothing suspicious. The right bar was well covered in corrosion on the bottom. On the top of the right bar there were corrosion along the edges. The bottom of the left bar had pits and other small corrosion spots. The half cell potential indicated that all the values fell into the 10% probability range. The voltage readings showed that the specimen had failed. The inspection concluded the corrosion to be moderate to significant.



Figure 7.159 - Bars, bottom



Figure 7.160 - Bars, top

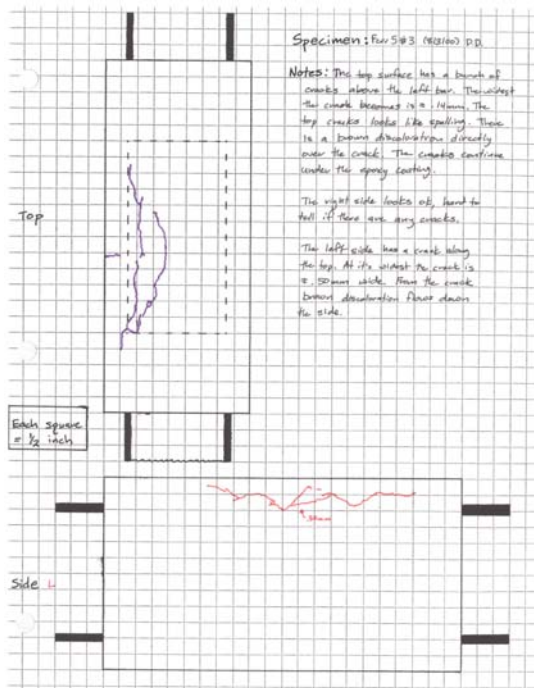


Figure 7.161 : Ferr5 #3 A

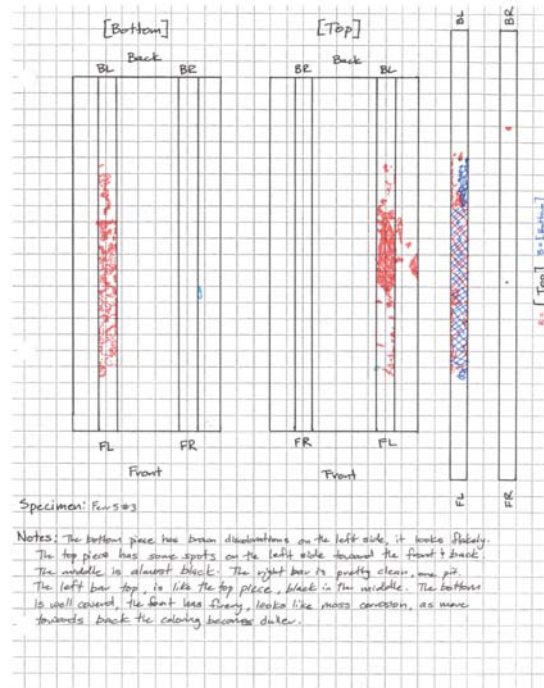


Figure 7.162 : Ferr5 #3 B

Ferr5 #3 – The visual inspection showed multiple cracks on the left of the top surface of the specimen. There were also cracks on the left side of the specimen. All of the corrosion occurred on the left bar. The left bar was basically covered on the top and bottom in corrosion. The half cell potential results indicated that two values on the left side fell into the 90% probability range. The other values all fell into the uncertain range. The voltage results showed that the specimen had failed. The inspection concluded the corrosion to be moderate to significant.



Figure 7.163 - Bars, bottom



Figure 7.164 - Bars, top

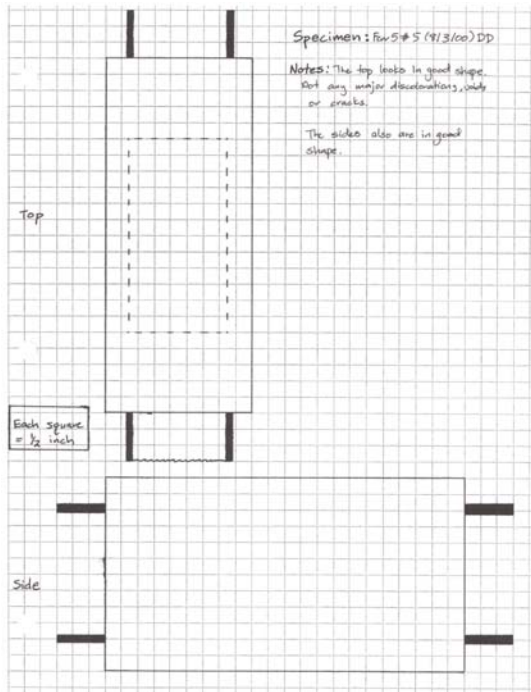


Figure 7.165 : Ferr5 #5A

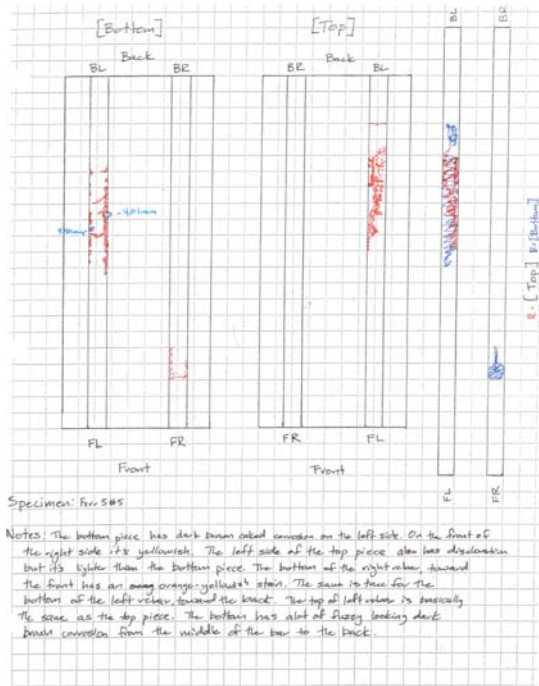


Figure 7.166 : Ferr5 #5B

Ferr5 #5 – The specimen looked in great condition from the outside. On the inside the left bar had a three inch area of corrosion located on both the top and the bottom. The right bar had a small area toward the front and bottom of the bar. The half cell potential readings showed two readings on the left and one on the right fell into the 10% probability range, the others fell into the uncertain range. The voltage data indicated the specimen had failed. The inspection concluded the corrosion to be moderate to significant.



Figure 7.167 - Bars, bottom



Figure 7.168 - Bars, top

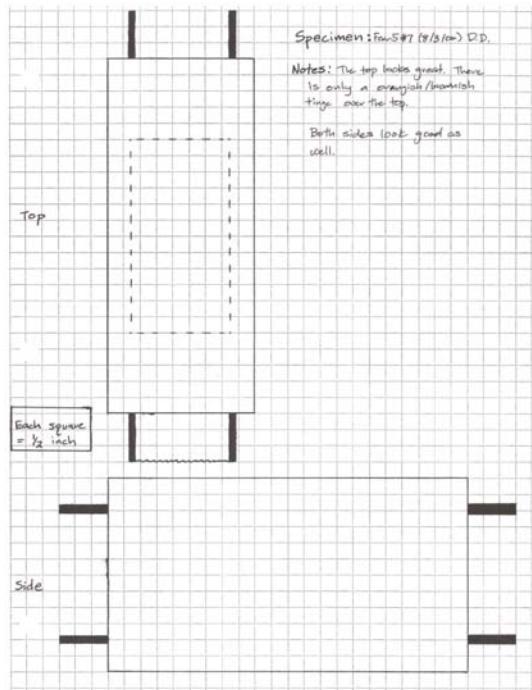


Figure 7.169 : Ferr5 #7A

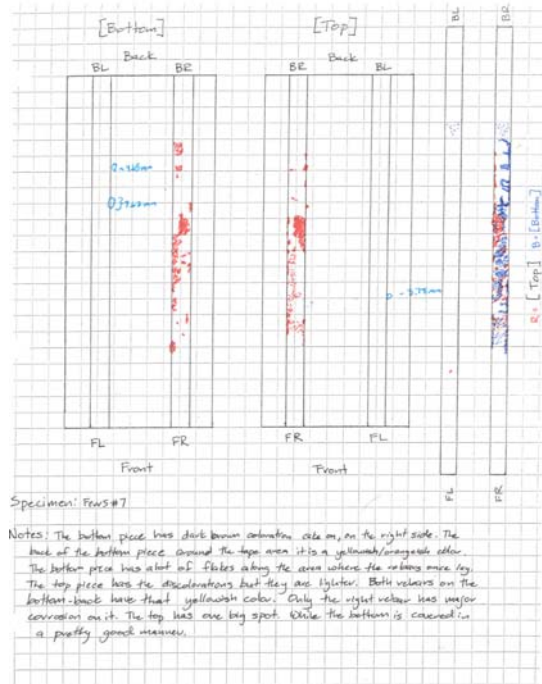


Figure 7.170 : Ferr5 #7B

Ferr5 #7 – From the outside the specimen looked in great condition. The right bar had lots of scattered corrosion on both the top and bottom of the bar. The half cell potential numbers showed one left side values in the uncertain range and all the rest in the 10% probability range. The voltage readings indicated that the specimen had failed. The inspection concluded the corrosion to be moderate to significant.



Figure 7.171 - Bars, bottom



Figure 7.172 - Bars, top

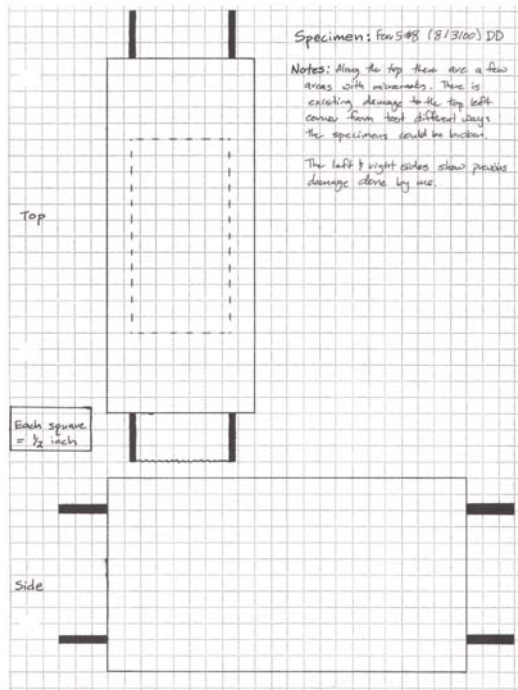


Figure 7.173 : Ferr5 #8 A

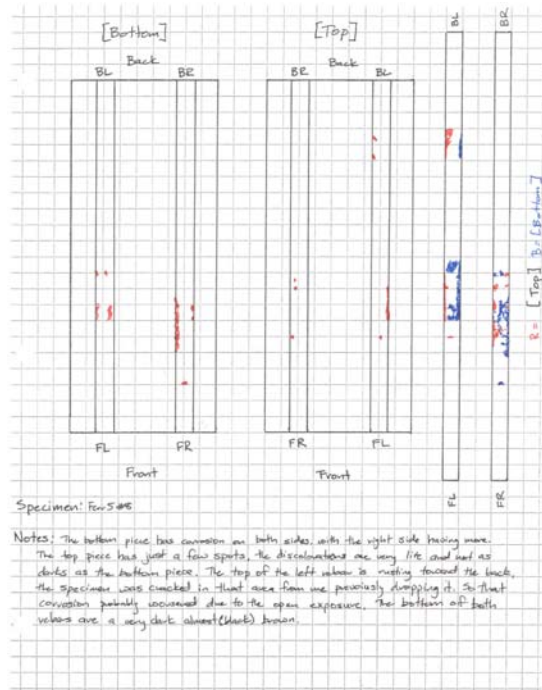


Figure 7.174 : Ferr5 #8 B

Ferr5 #8 – The visual inspection of the specimen did not turn up any fatal flaws. The specimen contained light areas of corrosion on both bars, and corrosion appearing on the top and bottom of both. The half cell potential results showed all the left side values fell into the 10% probability range. All the right side values fell into the uncertain range. The voltage data showed that the specimen did not reach failure. The inspection concluded the corrosion to be minor.



Figure 7.175 - Bars, bottom



Figure 7.176 - Bars, top

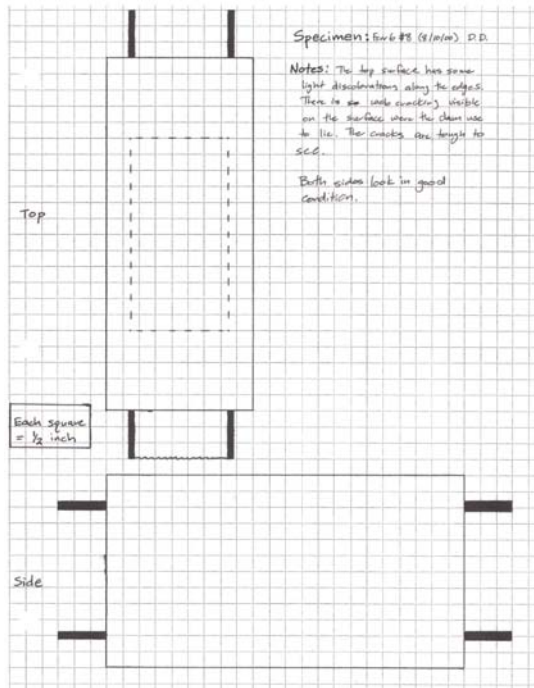


Figure 7.177 : Ferr6 #8 A

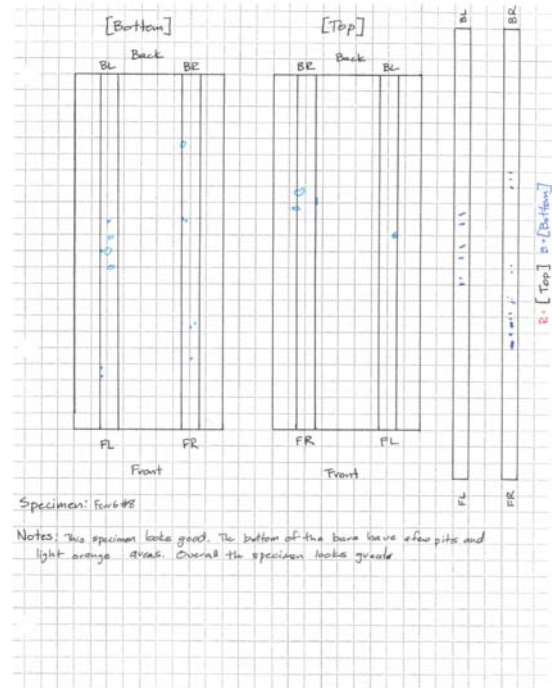


Figure 7.178 : Ferr6 #8 B

Ferr6 #8 – There was some web cracking on the surface of the specimen but it was very hard to see. The bars contained minimum corrosion. Corrosion pits appeared on the bottoms of both bars. The half cell potential readings showed all of the values were in the 10% probability range. The voltage data showed the specimen had not failed. The inspection concluded the corrosion to be none.



Figure 7.179 - Bars, bottom



Figure 7.180 - Bars, top

HALAWA CONTROL MIXTURE

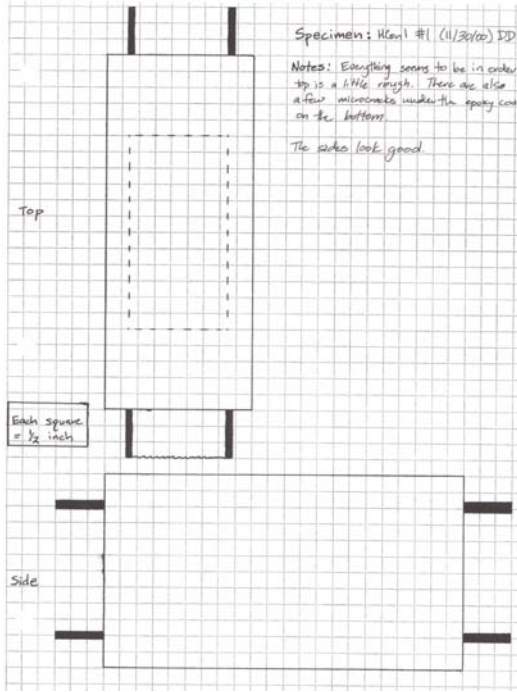


Figure 7.181 : HCon1 #1A

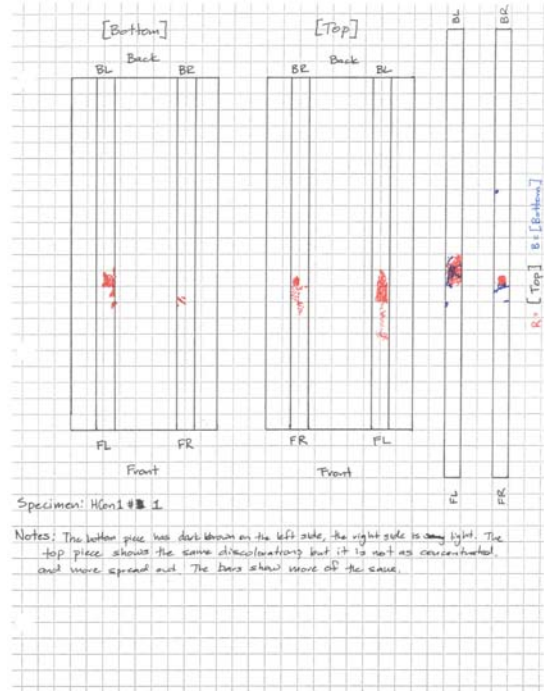


Figure 7.182 : HCon1 #1B

HCon1 #1 - On the outside, of the specimen there was no real visual damage. The inside of the specimen had small areas of corrosion on both rebar, on both the top and the bottom (top looks in worse condition). The half cell potential was almost to the uncertain range, but falls in the 10% range. The voltage results were getting very close to being considered to being failed. The inspection concluded the corrosion to be moderate to significant.



Figure 7.183 - Bars, bottom



Figure 7.184 - Bars, top

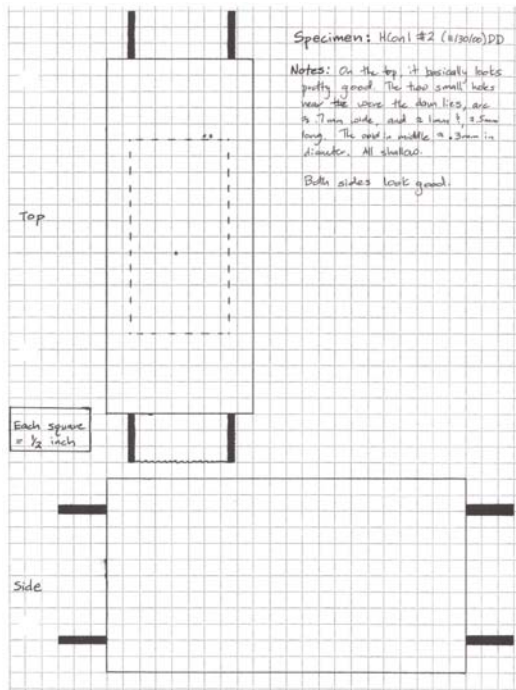


Figure 7.185 : HCon1 #2A

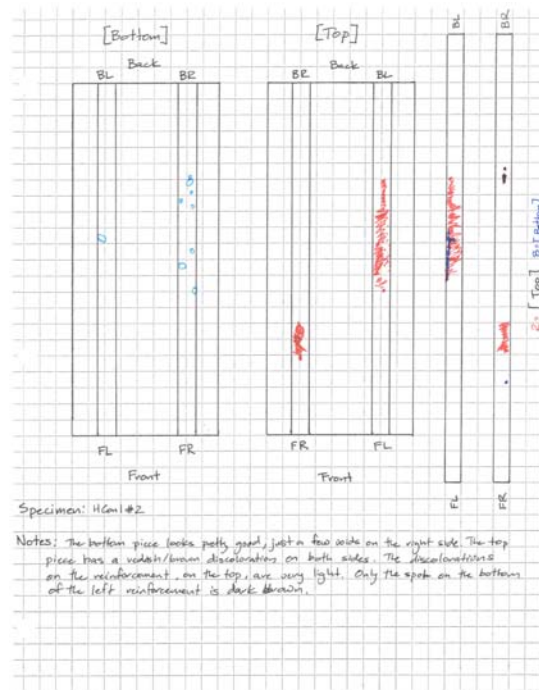


Figure 7.186 : HCon1 #2B

HCon1 #2 – The visual inspection on the outside did not show any particular flaws. The inside of the specimen the top of both bars have a light reddish haze on the top and a few spots on the bottom of the bars (more so on the left side). The half cell potential was very low, indicating that there is only a 10% of corrosion. The voltage results were also fairly low. The inspection concluded the corrosion to be minor.



Figure 7.187 – Bars, bottom



Figure 7.188 – Bars, top

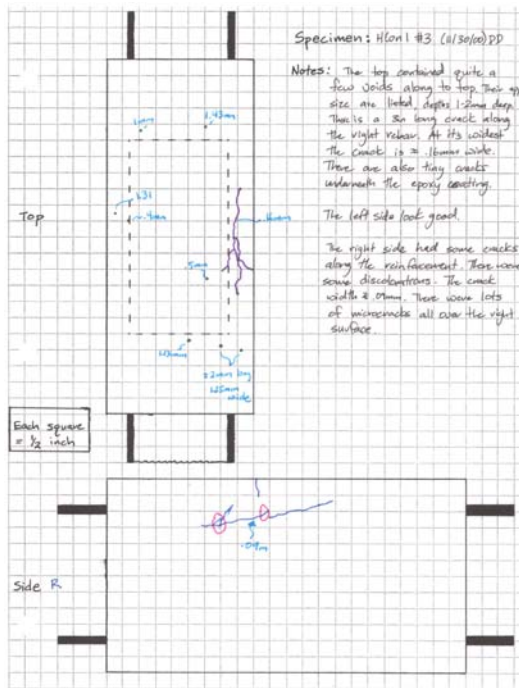


Figure 7.189 : HCon1 #3 A

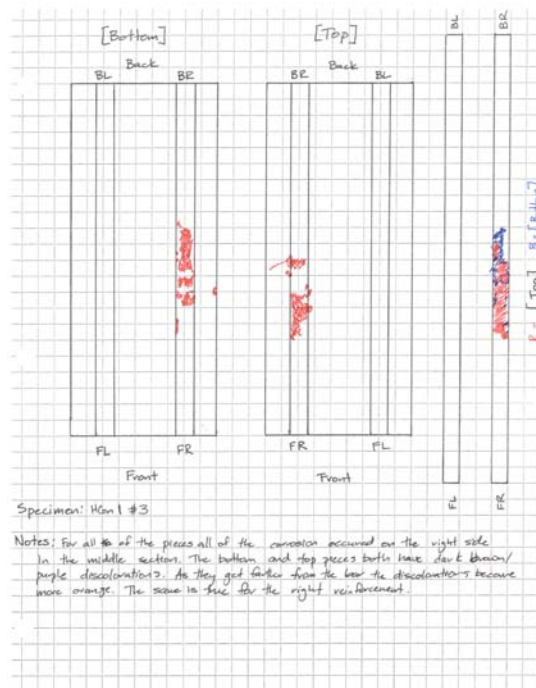


Figure 7.190 : HCon1 #3 B

HCon1 #3 – The visual inspection showed that there were cracks on the right side of the specimen, both on the top and the right side. As expected there was a large area of corrosion in the areas of the cracks, the corrosion was located on both the top and the bottom. The half cell potential numbers were fairly high on both sides. The left side had one reading in the 90% probability range and the other two being very close. The right side has all the values being in the 90% probability range. The voltage results were also high, with the specimen failing. The inspection concluded the corrosion to be moderate to significant.



Figure 7.191 – Bars, bottom



Figure 7.192 – Bars, top

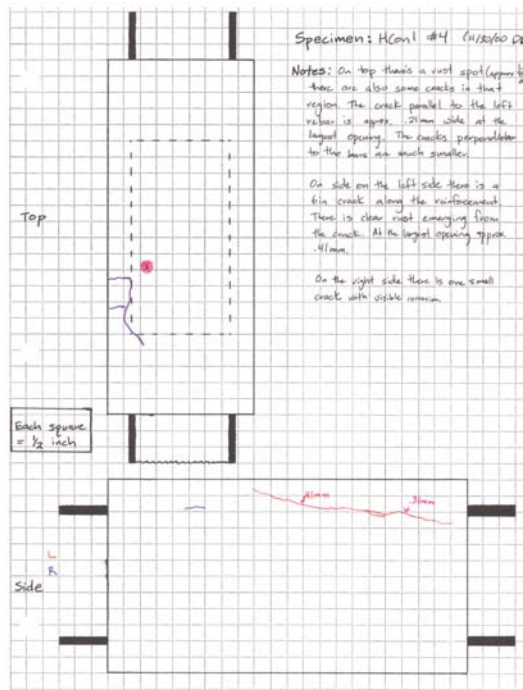


Figure 7.193 : HCon1 #4A

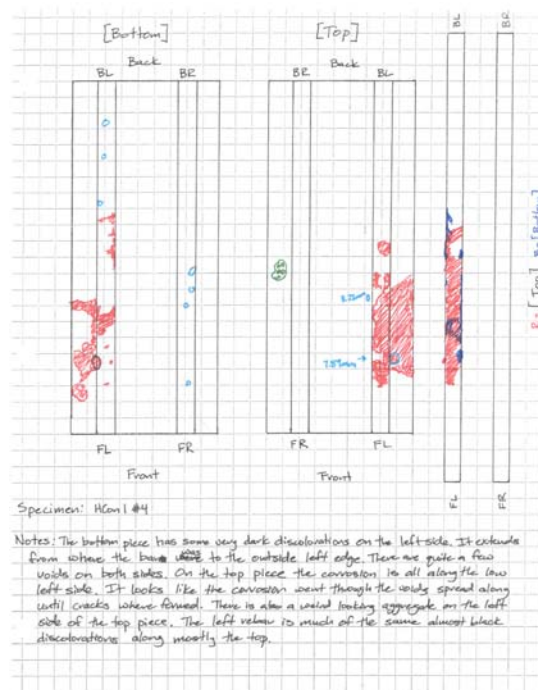


Figure 7.194 : HCon1 #4B

HCon1 #4 – The visual inspection showed cracks on the left side, on both the top and side of the specimen. The corrosion only appeared in the area of the cracks on the left side. The corrosion appeared more severe on the top of the left bar than on the bottom. The half cell potential numbers were high on both sides, but the highest numbers appeared on the left side toward the front. There were two values on the left side that were in the 90% range and one on the right. The voltage results were the highest of all the HCon1 specimens. The inspection concluded the corrosion to be moderate to significant.



Figure 7.195 - Bars, bottom



Figure 7.196 - Bars, top

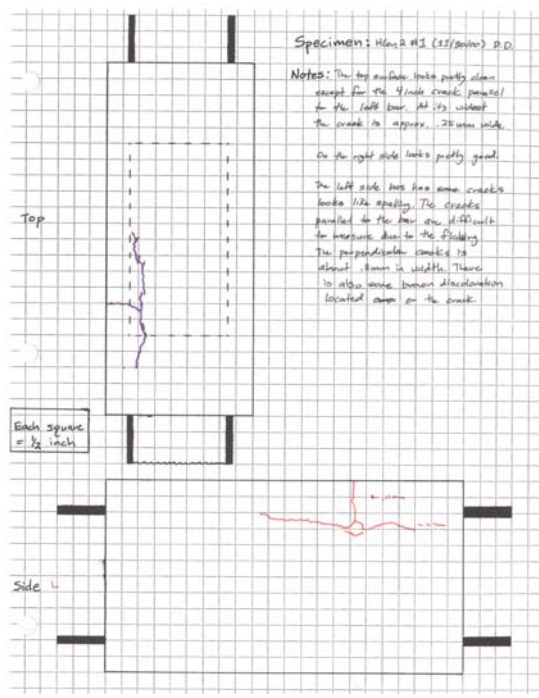


Figure 7.197 : HCon2 #1A

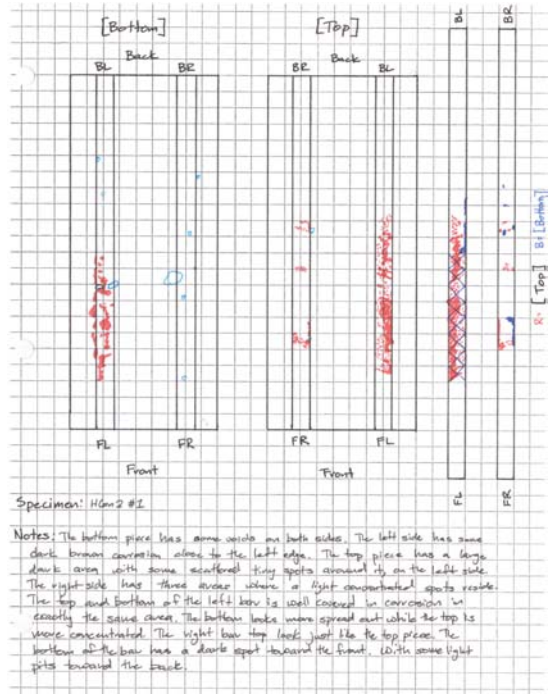


Figure 7.198 : HCon2 #1B

HCon2 #1 – The visual inspection showed cracks on the left side, on both the top and front side of the specimen. The majority of the corrosion appeared on the left side, but there were a few spots on the right side also. The corrosion seems more severe on the bottom of the left bar. The half cell potential numbers were high, more so on the left side. The left side had two values in the 90% range, with the other values being high but in the uncertain designation. The voltage results showed that the specimen had failed. The inspection concluded the corrosion to be moderate to significant.



Figure 7.199 - Bars, bottom



Figure 7.200 - Bars, top

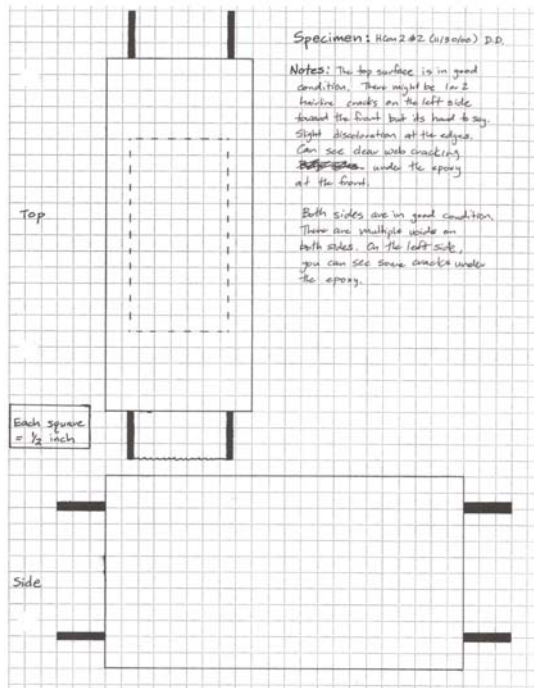


Figure 7.201 : HCon2 #2A

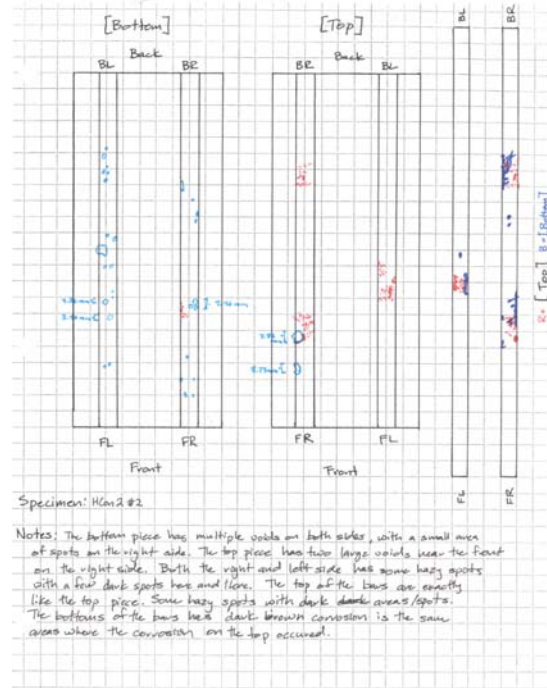


Figure 7.202 : HCon2 #2B

HCon2 #2 – The visual inspection showed no major flaws on the outside of the specimen. Inside of the specimen there are a few corrosion areas on both the left and right side. The right side had a little bit more corrosion than the left side. The corrosion on the top and the bottom seems to be of similar degrees. The half cell potentials numbers are on the low side. All the values fell within the 10% probability of corrosion range. The voltage numbers were just beginning to get to the point of failure. The inspection concluded the corrosion to be minor.



Figure 7.203 - Bars, bottom



Figure 7.204 - Bars, top

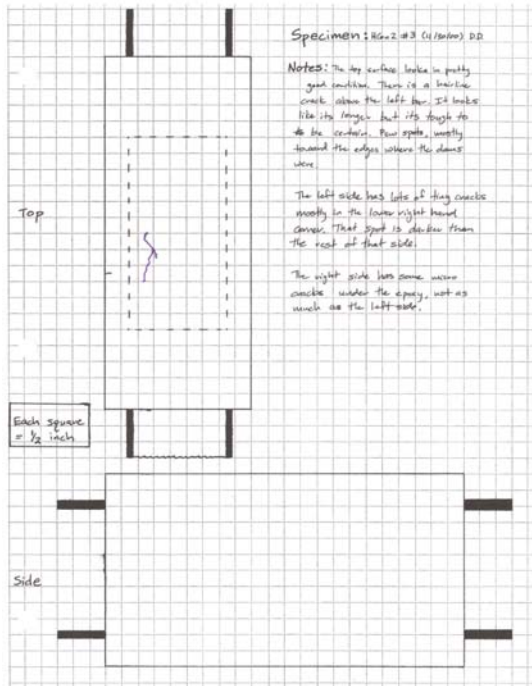


Figure 7.205 : HCon2 #3A

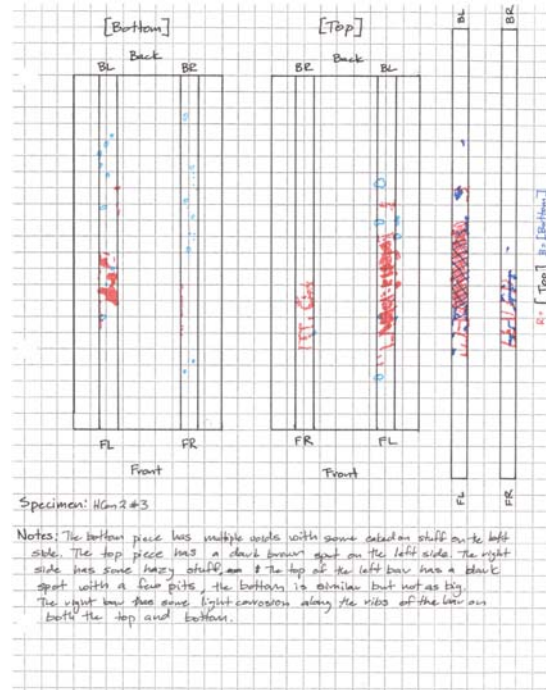


Figure 7.206 : HCon2 #3B

HCon2 #3 – The visual inspection showed a small crack on the top of the specimen, above the left bar. The inside of the specimen showed the majority of the corrosion on the left side. There was also a small area of corrosion on the right side. The corrosion on the top of the left bar looked harsher than the bottom. The half cell potential readings on the left side fell in the uncertain range, while the values on the right side are all in the 10% corrosion range. The voltage numbers were very close to being considered for failure. The inspection concluded the corrosion to be moderate to significant.



Figure 7.207 - Bars, bottom



Figure 7.208 - Bars, top

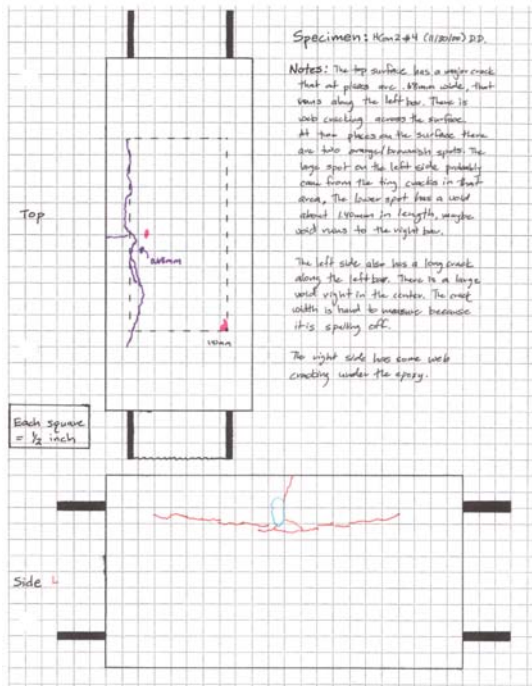


Figure 7.209 : HCon2 #4A

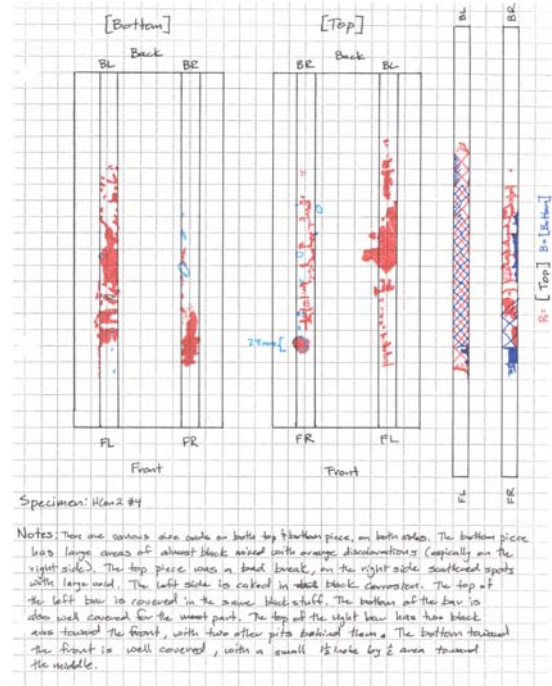


Figure 7.210 : HCon2 #4B

HCon2 #4 – The visual inspection showed a large crack above the left bar, there was also a large crack on the left side. On the inside the left bar was well covered in corrosion on both the top and the bottom. The right bar was fairly well covered on the bottom and there are a few spots on the top. The half cell potential results showed two values on the left side fell in the uncertain range. All the other values fell in the 10% probability of corrosion range. The voltage results were the worst of the group, the specimen was considered failed. The inspection concluded the corrosion to be moderate to significant.



Figure 7.211 - Bars, bottom



Figure 7.212 - Bars, top

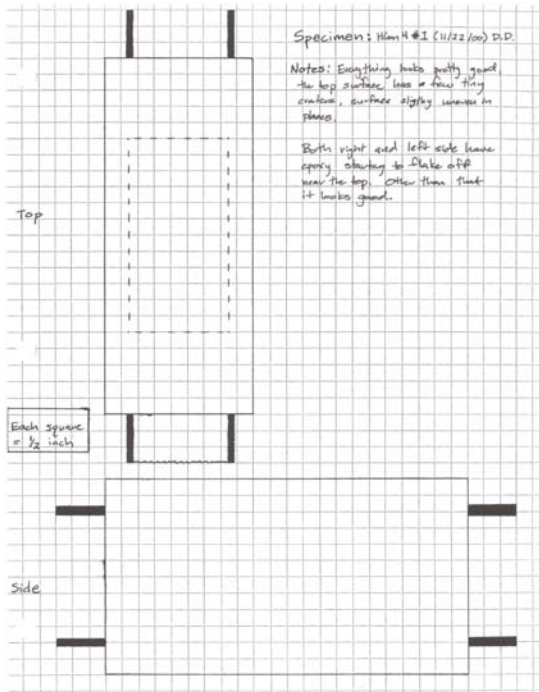


Figure 7.213 : HCon4 #1A

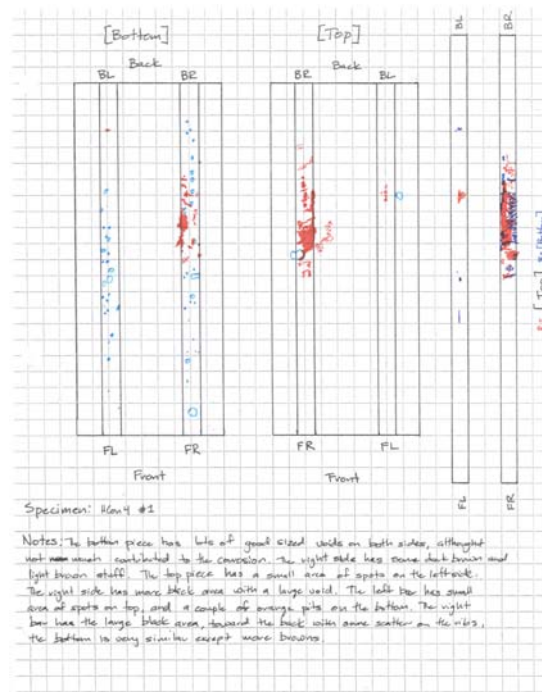


Figure 7.214 : HCon4 #1B

HCon4 #1 – The visual inspection did not show any suspicious voids or cracks on the outside. On the inside there was a medium sized area of corrosion on the top and the bottom of the right bar. The left bar had a small corrosion area on the top and a few orange pits on the bottom. The half cell potential results indicate on the left side the values were in the uncertain range. There was one value on the right side that lands in the 90% probability of corrosion range. This specimen was the only one of the group that met the criteria for failure. The inspection concluded the corrosion to be moderate to significant.



Figure 7.215 - Bars, bottom



Figure 7.216 - Bars, top

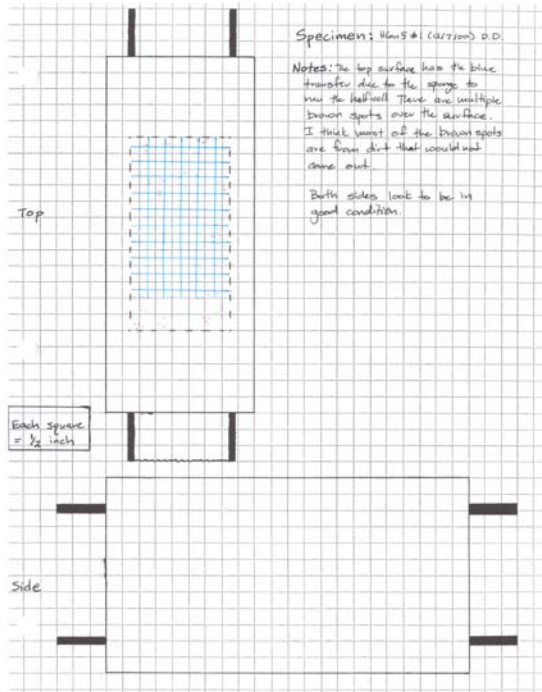


Figure 7.217 : HCon5 #1A

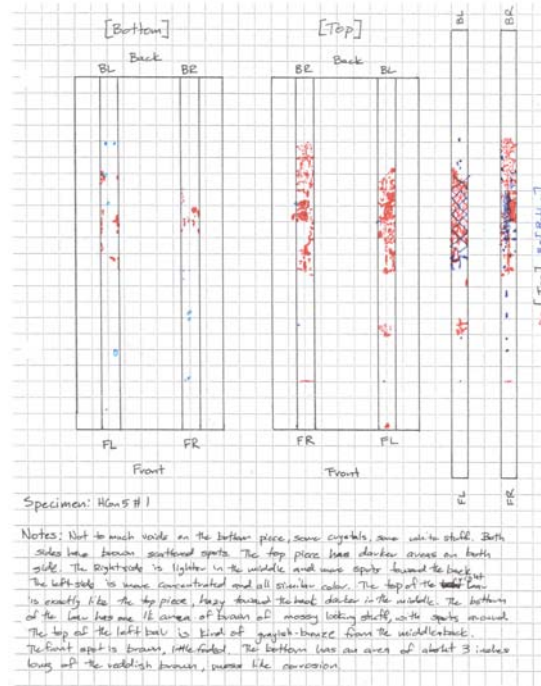


Figure 7.218 : HCon5 #1B

HCon5 #1 – The visual inspection did not show anything suspicious. The inside contained corrosion on both bars from the middle to the back. There was a greater amount of corrosion on the top of the bars, but the corrosion located on the bottom looked to be more detrimental. The corrosion was worse on the left bar. The half cell potential reading showed that all the values on the left side were in the 10% probability range. Two of the values on the right fell into the uncertain range. The voltage readings did not reach failure. The inspection concluded the corrosion to be moderate to significant.



Figure 7.219 - Bars, bottom



Figure 7.220 - Bars, top

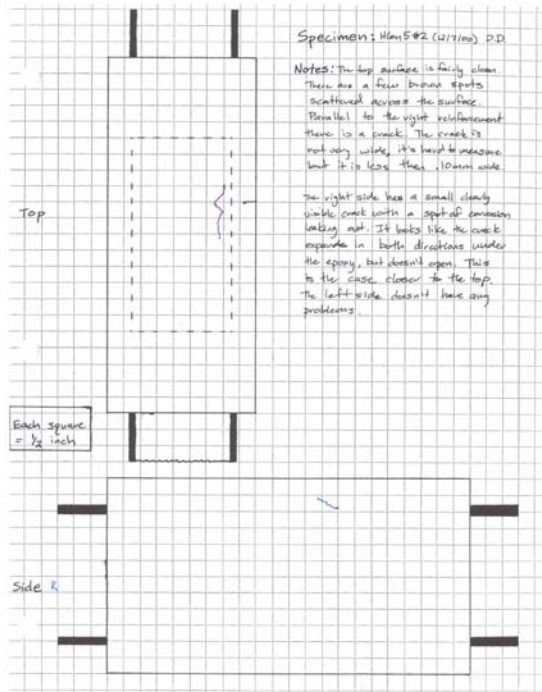


Figure 7.221 : HCon5 #2A

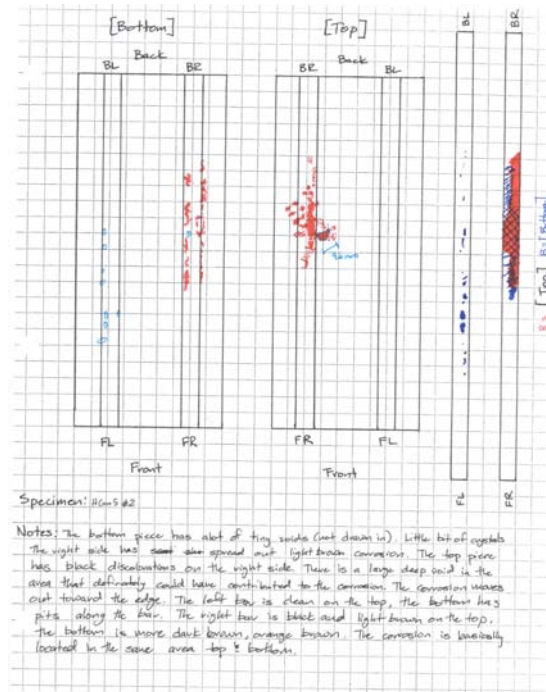


Figure 7.222 : HCon5 #2B

HCon5 #2 – The visual inspection showed a crack about 1.5 inches long on the top surface, above and parallel to the right reinforcement. There is also a small crack on the right side of the specimen. Inside the specimen the most of the corrosion was on the right bar, on both the top and bottom. The left bar had pits along the length of the bottom of the bar. The half cell potential reading show that all the values fell in the uncertain range. The voltage readings indicated failure. The inspection concluded the corrosion to be moderate to significant.



Figure 7.223- Bars, bottom



Figure 7.224 - Bars, top

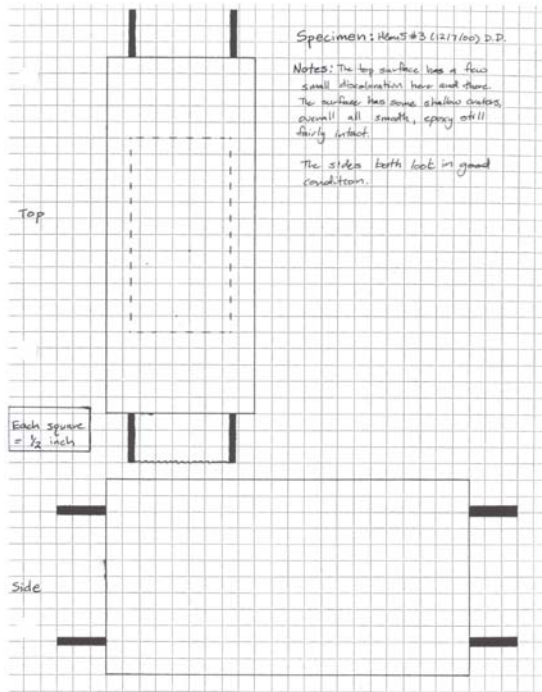


Figure 7.225 : HCon5 #3A

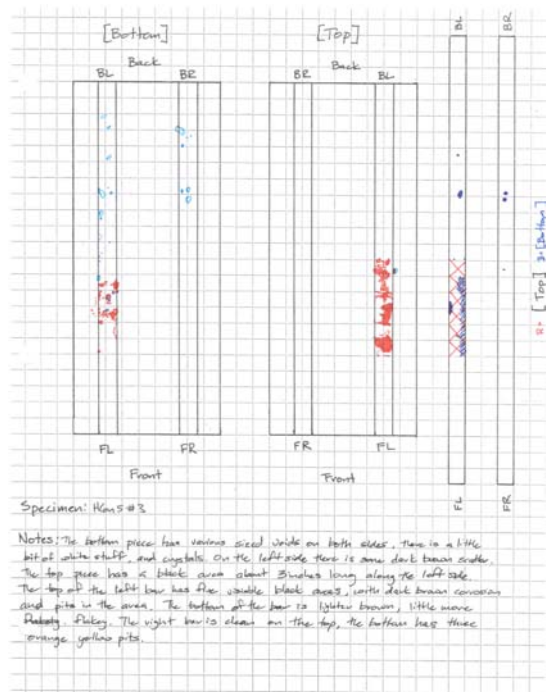


Figure 7.226 : HCon5 #3B

HCon5 #3 – The specimen looked to be in good condition on the outside. On the inside the majority of the corrosion was located on the left bar. The corrosion on the top of the left bar was more concentrated than on the bottom. The right bar had only a few pits on the bottom of the bar. The half cell potential readings show that all of the values were in the uncertain range. The voltage readings indicated the specimen has failed. The inspection concluded the corrosion to be moderate to significant.



Figure 7.227 - Bars, bottom



Figure 7.228 - Bars, top

HALAWA FLY ASH

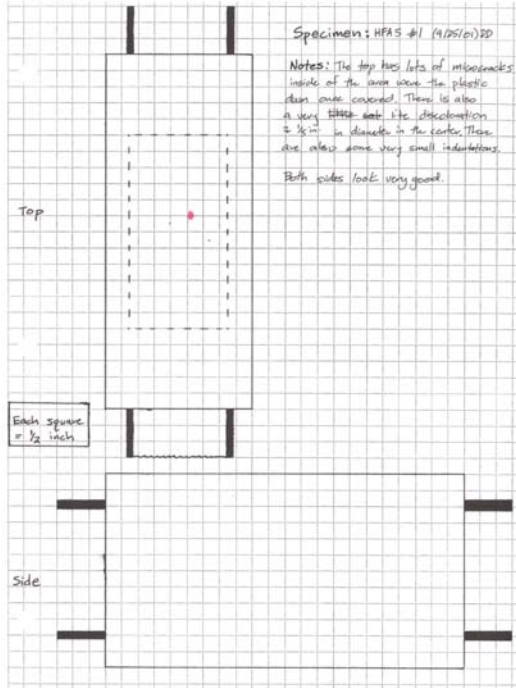


Figure 7.233 : HFA5 #1A

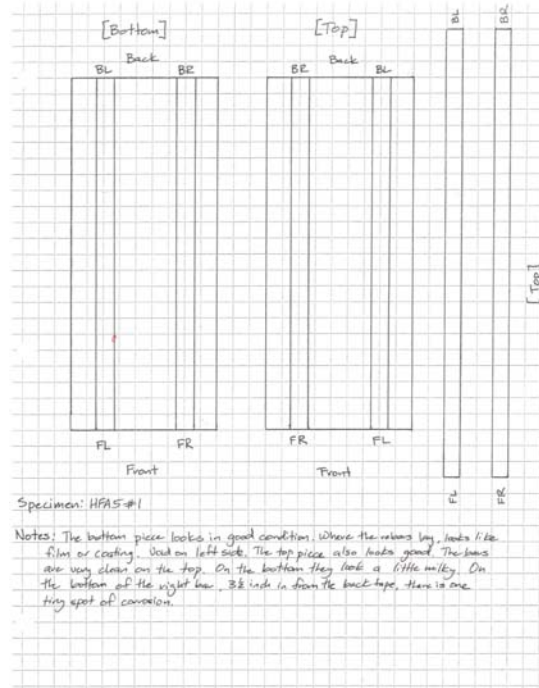


Figure 7.234 : HFA5 #1B

HFA5 #1 – The top surface has some web cracking occurring. There are also some small indentations and discolorations. The bars on the inside have absolutely no corrosion on them. The half cell potential values all fell into the 10% probability range. The voltage results showed that the specimen had not failed. The inspection concluded the corrosion to be none.



Figure 7.235 - Bars, bottom

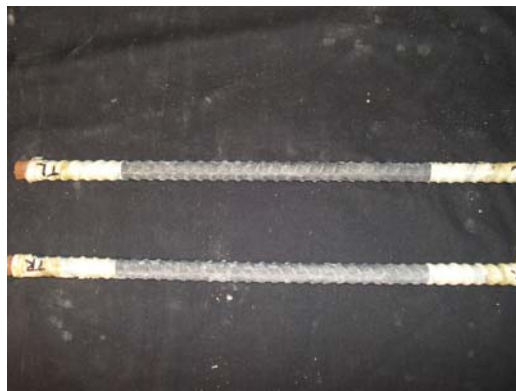


Figure 7.236 - Bars, top

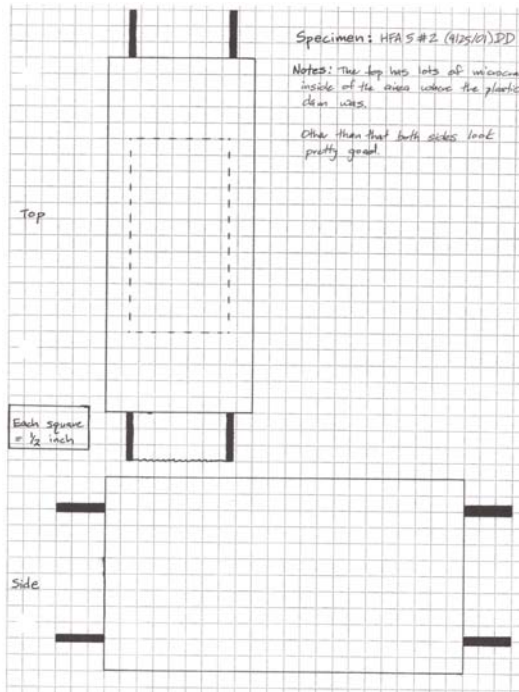


Figure 7.237 : HFA5 #2 A

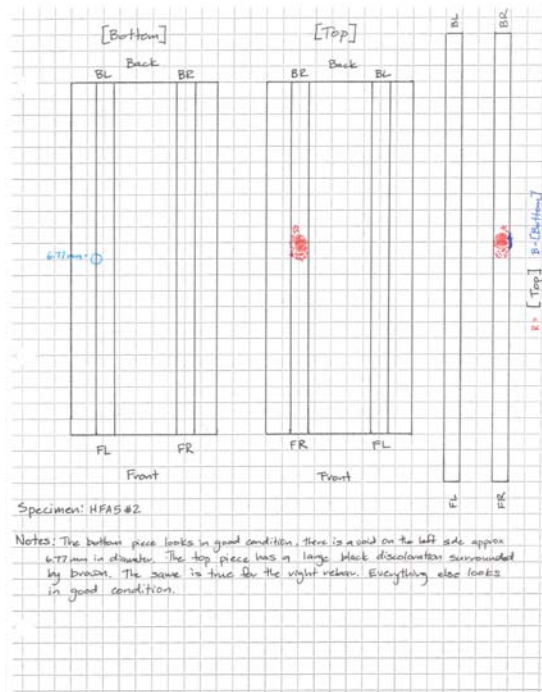


Figure 7.238 : HFA5 #2 B

HFA5 #2 – The top surface has web cracking occurring. The right bar has a small area of corrosion on the top. The area of corrosion spills off to the bottom of the bar as well. The half cell potential readings all fell into the uncertain range. The voltage data showed that the specimen had failed. The inspection concluded the corrosion to be moderate to significant.



Figure 7.239 - Bars, bottom



Figure 7.240 - Bars, top

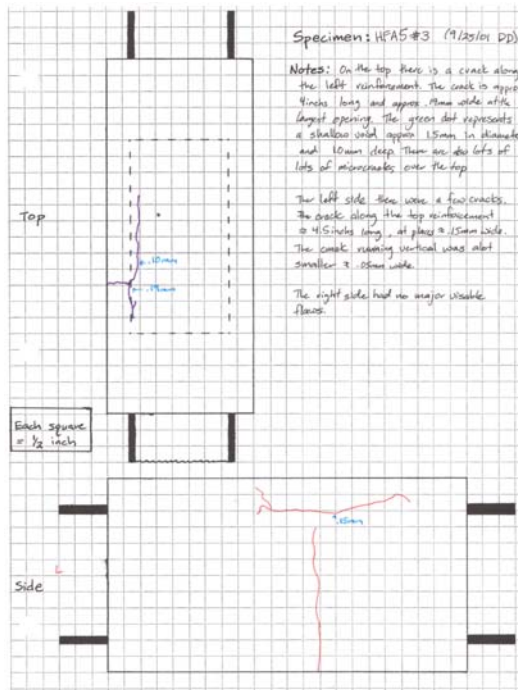


Figure 7.241 : HFA5 #3 A

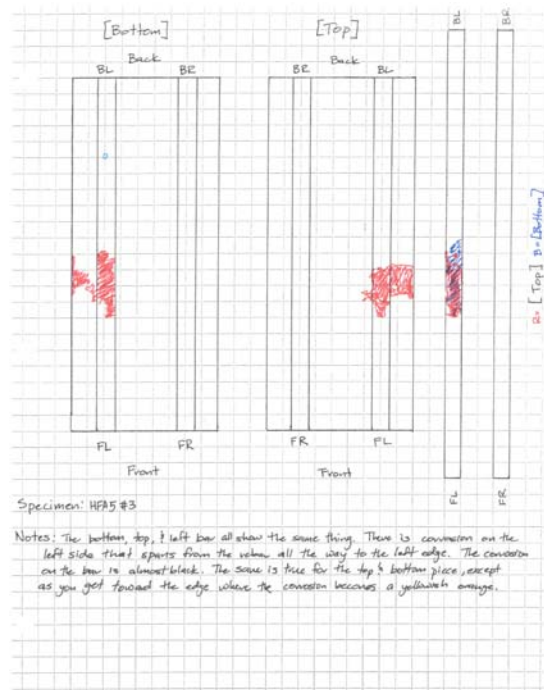


Figure 7.242 : HFA5 #3 B

HFA5 #3 – There was a crack on the top surface above the left bar. There were also cracks on the left side of the specimen. The left bar has a 2.5 inch area of corrosion on the top and bottom of the bar. The half cell potential results showed that one value on the left side fell into the 90% probability range. All the other results fell into the uncertain range. The voltage data showed that the specimen had failed. The inspection concluded the corrosion to be moderate to significant.



Figure 7.243 - Bars, bottom



Figure 7.244 - Bars, top

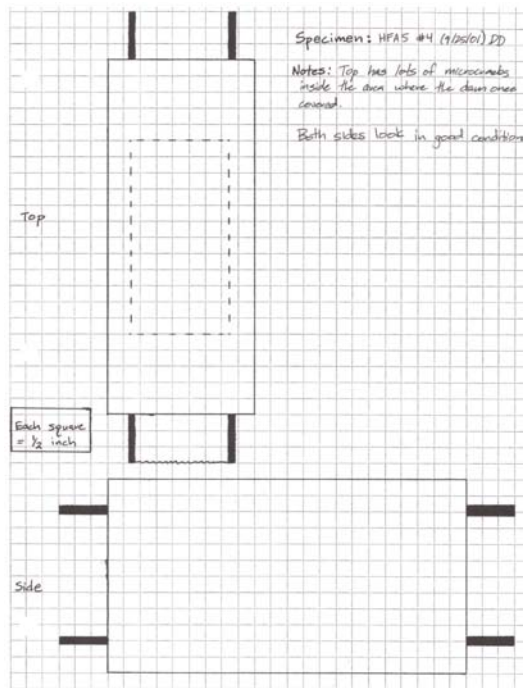


Figure 7.245 : HFA5 #4A

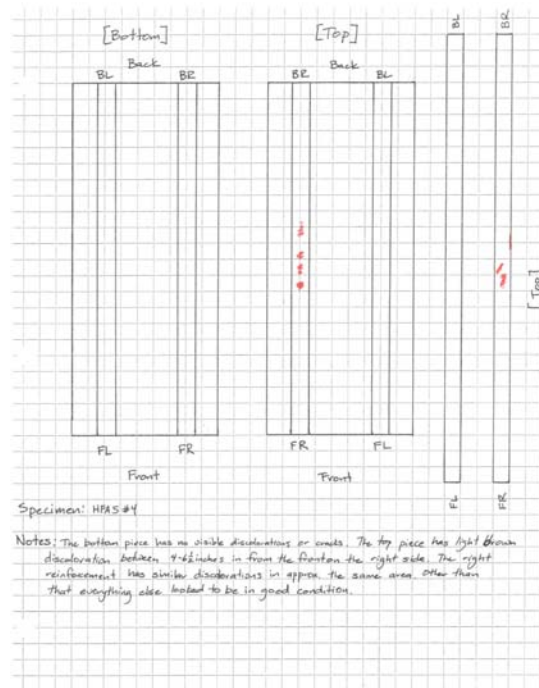


Figure 7.246 : HFA5 #4B

HFA5 #4 – There was clear web cracking on the top surface. There were a few spot of corrosion on the top of the right bar. There were no other areas of corrosion located on both bars. The half cell potential values all fell into the 10% probability range. The voltage data concluded that the specimen had not failed. The inspection concluded the corrosion to be none.



Figure 7.247 - Bars, bottom



Figure 7.248 - Bars, top

HALAWA RHEOCRETE 222+

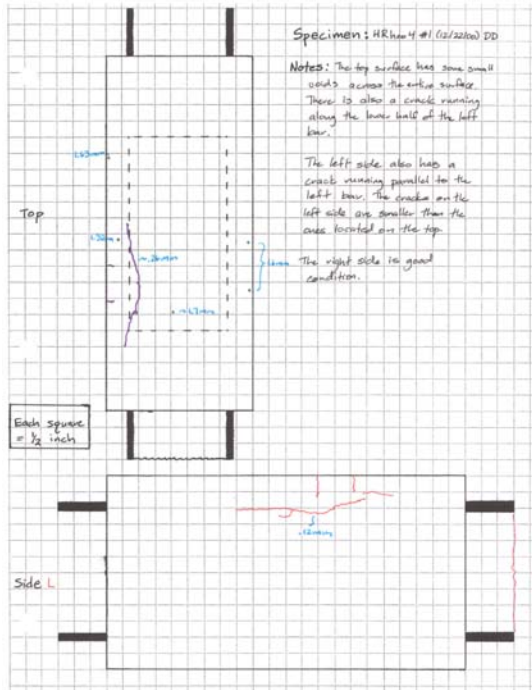


Figure 7.249 : HRrheo4 #1A

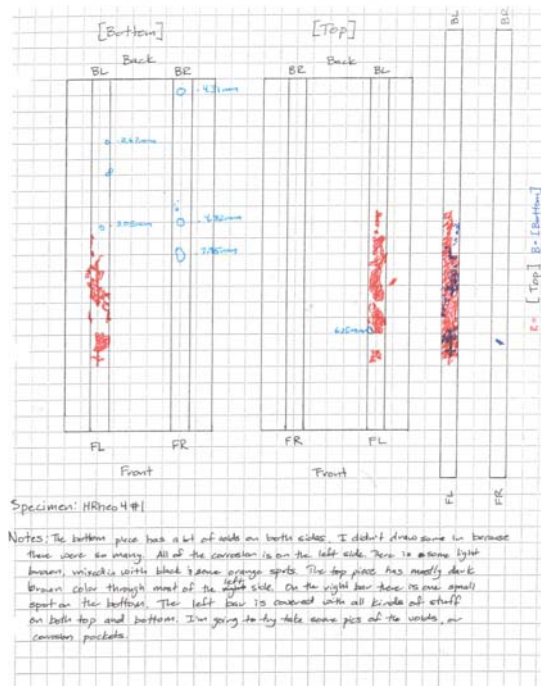


Figure 7.250 : HRrheo4 #1B

HRrheo4 #1 – The visual inspection showed a crack on the top surface on the left side. There were also cracks on the left side of the specimen. The majority of corrosion was located on the top of the left bar from the middle to the front. The bottom of the left bar has some corrosion but less than the top. There was a little bit of corrosion on the bottom of the right bar. The half cell potential number indicated that all the values fell into the 10% probability range. The voltage data showed that the specimen had failed. The inspection concluded the corrosion to be moderate to significant.



Figure 7.251 - Bars, bottom

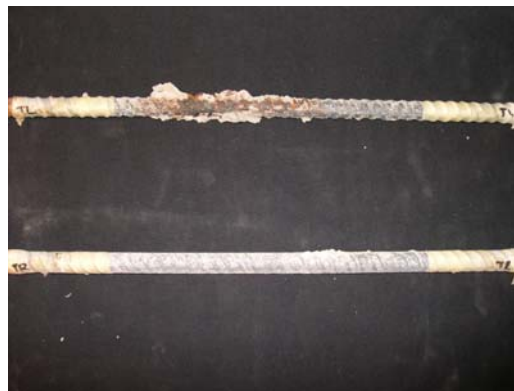


Figure 7.252 - Bars, top

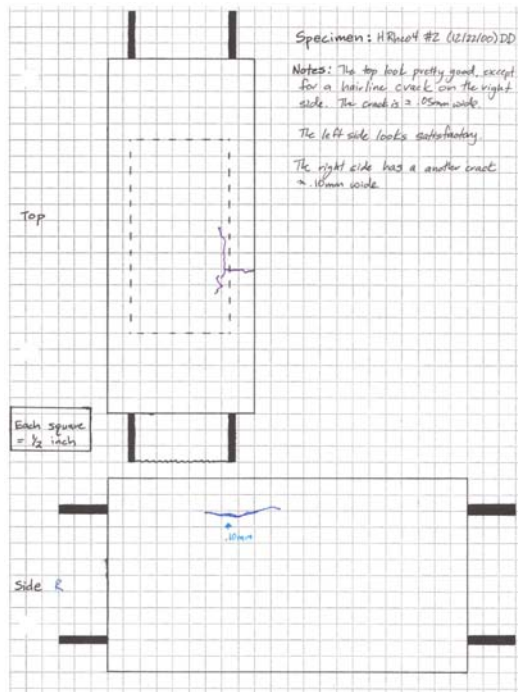


Figure 7.253 : HRheo4 #2A

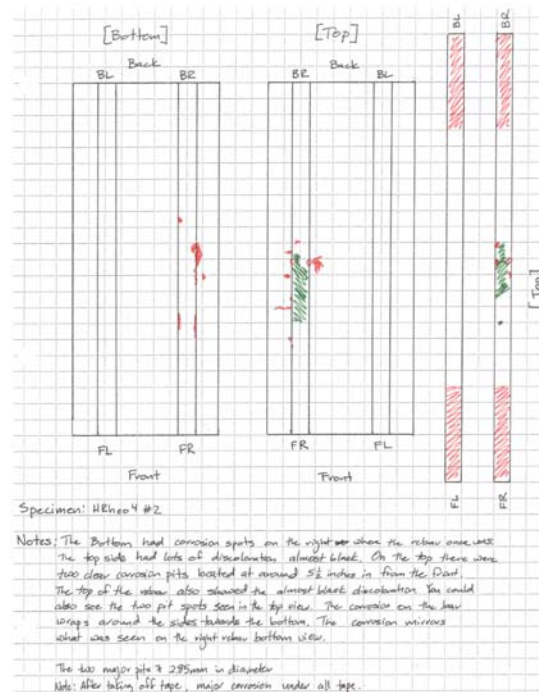


Figure 7.254 : HRheo4 #2B

HRheo4 #2 – There was a crack on the right side of the top surface. There was also a crack on the right side of the specimen. On the inside of the specimen there was an area of corrosion on the right bar on the top around 1.5 inches long. The half cell potential readings showed that all the values fell into the uncertain range. The voltage data indicated that the specimen had failed. The inspection concluded the corrosion to be moderate to significant.



Figure 7.255 - Bars, bottom



Figure 7.256 - Bars, top

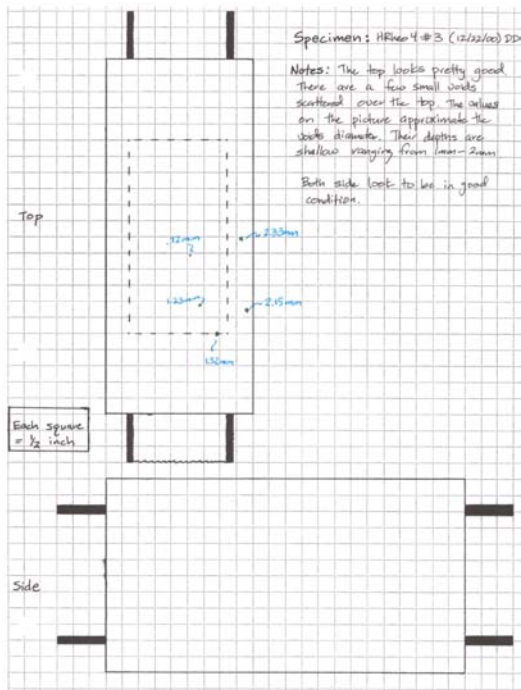


Figure 7.257 : HRheo4 #3 A

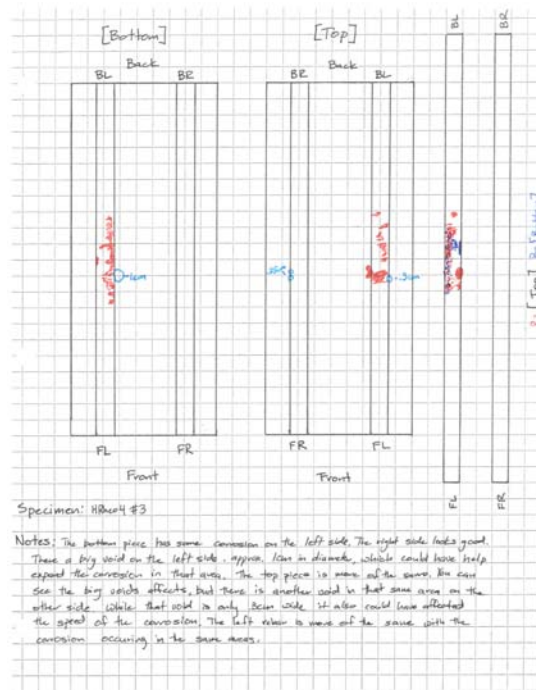


Figure 7.258 : HRheo4 #3 B

HRheo4 #3 – There were some small voids scattered over the top. The specimen showed no other signs of distress. The left bar had a small area of scattered corrosion on both the top and bottom. The half cell potential values all fell into the 10% probability range. The voltage results showed that the specimen was slowly moving toward failure. The inspection concluded the corrosion to be minor.



Figure 7.259 - Bars, bottom



Figure 7.260 - Bars, top

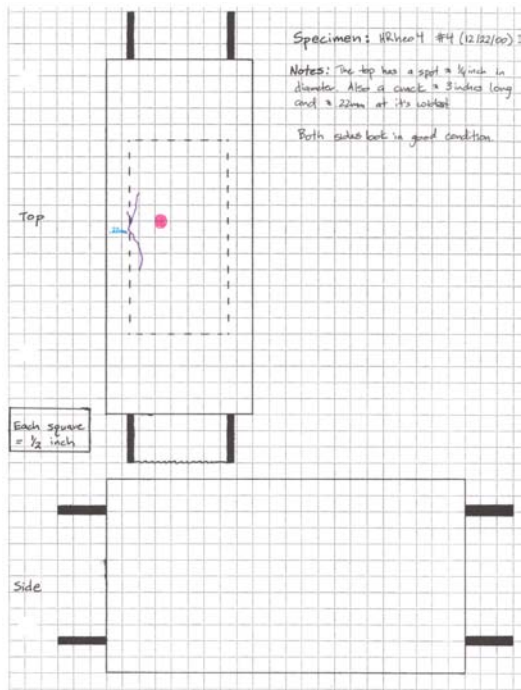


Figure 7.261 : HRheo4 #4A

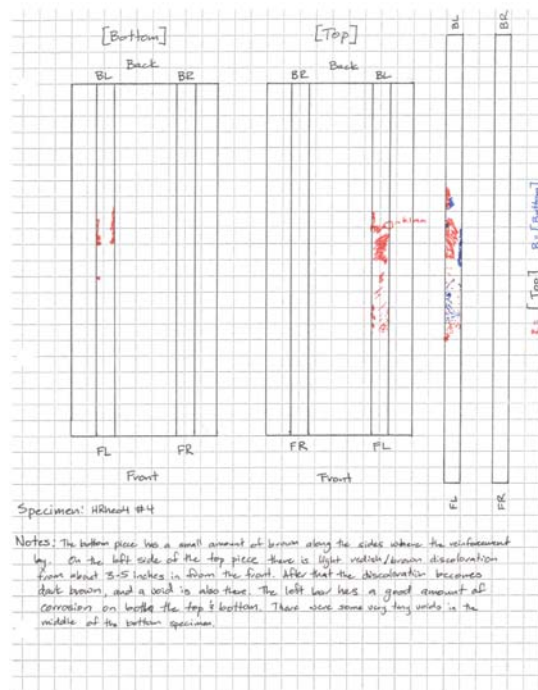


Figure 7.262 : HRheo4 #4B

HRheo4 #4 – The specimen has a crack on the top surface above the left bar. There is corrosion on the left bar on both the top and the bottom. The corrosion was spread out around certain small concentrated areas. The half cell potential values showed that one value on the left side fell into the 90% probability range. All the other values fell into the uncertain range. The voltage data showed that the specimen had failed. The inspection concluded the corrosion to be moderate to significant.



Figure 7.263 - Bars, bottom



Figure 7.264 - Bars, top

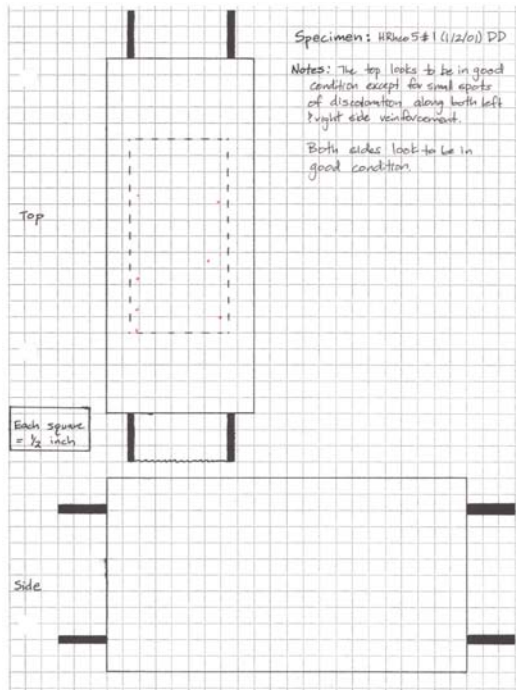


Figure 7.265 : HRheo5 #1A

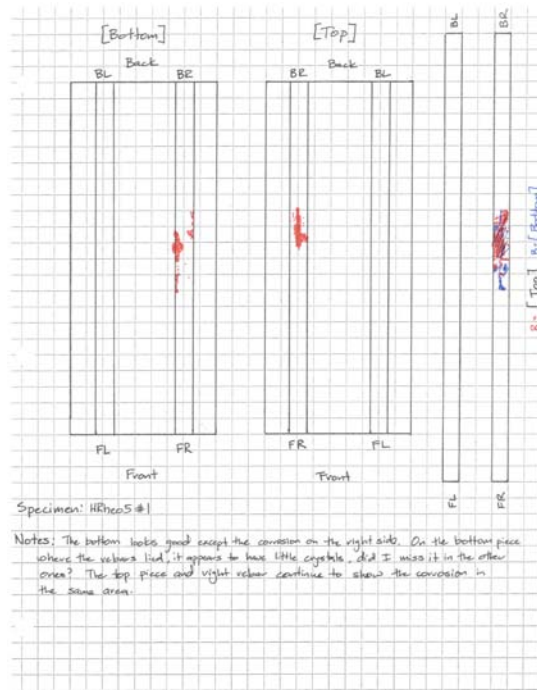


Figure 7.266 : HRheo5 #1B

HRheo5 #1 – From the outside the specimen looked in excellent condition. There was small corrosion area located on the right bar on both the top and bottom. The half cell potential readings show one value on the right side fell into the 90% probability range. All the other values fell into the uncertain range. The voltage readings showed the specimen was getting close to failure. The inspection concluded the corrosion to be moderate to significant.



Figure 7.267 - Bars, bottom



Figure 7.268 - Bars, top

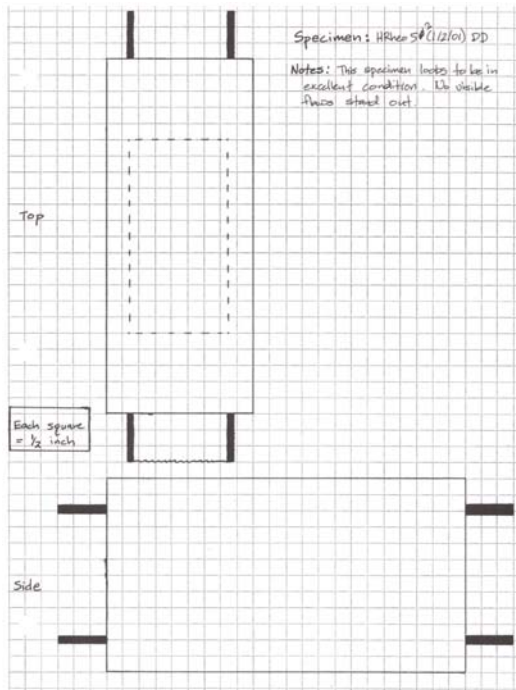


Figure 7.269 : HRheo5 #2A

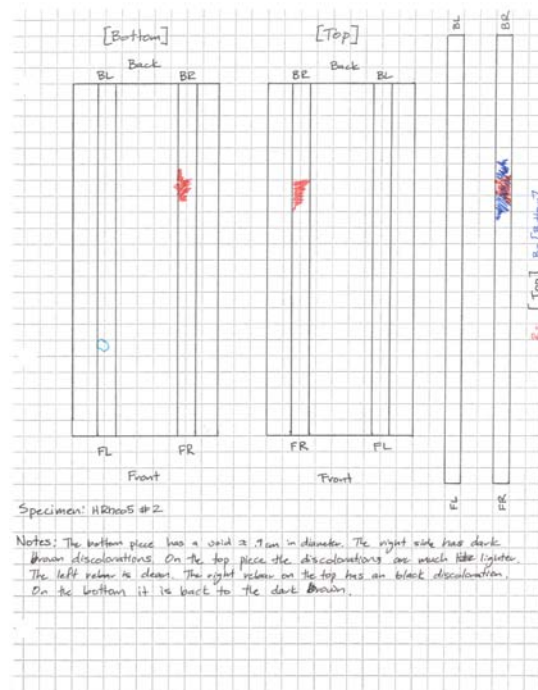


Figure 7.270 : HRheo5 #2B

HRheo5 #2 – The specimen has no major flaws on the outside. The right bar has a small area of corrosion on both the top and bottom toward the back of the bar. The half cell potential values all fall into the uncertain range. The voltage readings showed that the specimen was getting closer to failure, but not there yet. The inspection concluded the corrosion to be moderate to significant.



Figure 7.271 - Bars, bottom



Figure 7.272 - Bars, top

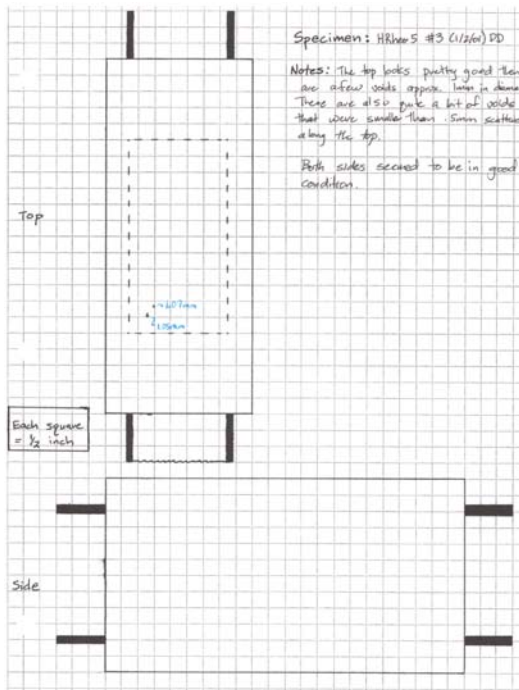


Figure 7.273 : HRheo5 #3 A

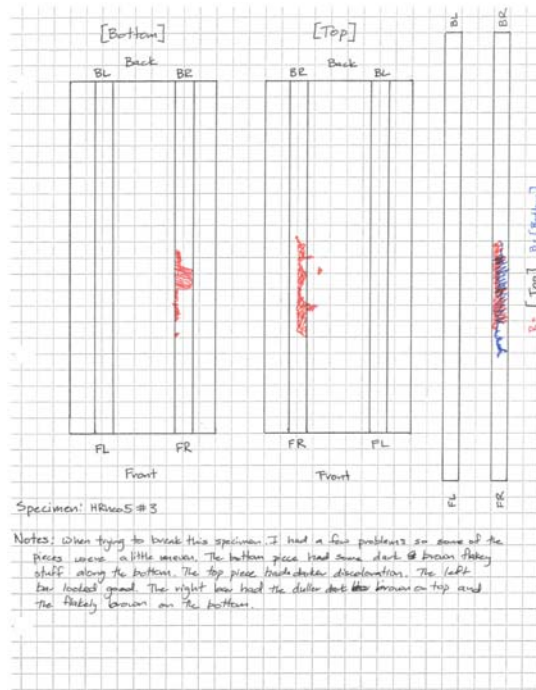


Figure 7.274 : HRheo5 #3 B

HRheo5 #3 – The top surface has two small voids on the left side. There were no other flaws. The right bar has an area of 3 inches of corrosion on the top and bottom of the bar. The half cell potential values showed one value on the right and left fell into the uncertain range. All the other values fell into the 90% probability range. The voltage data showed that the specimen had failed. The inspection concluded the corrosion to be moderate to significant.



Figure 7.275 - Bars, bottom



Figure 7.276 - Bars, top

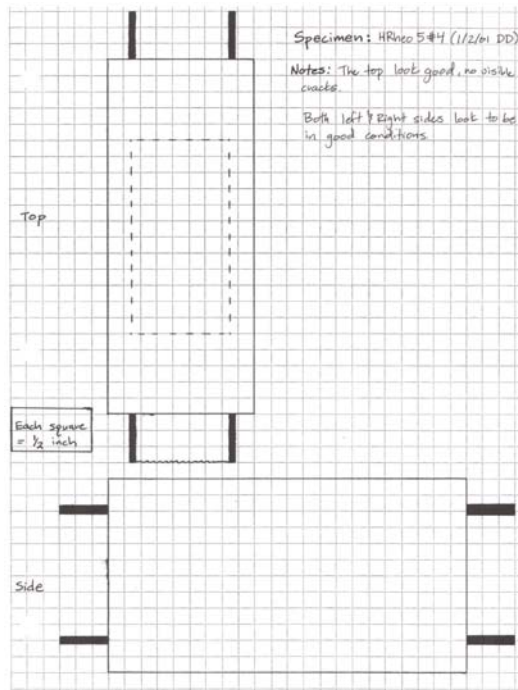


Figure 7.277 : HRheo5 #4A

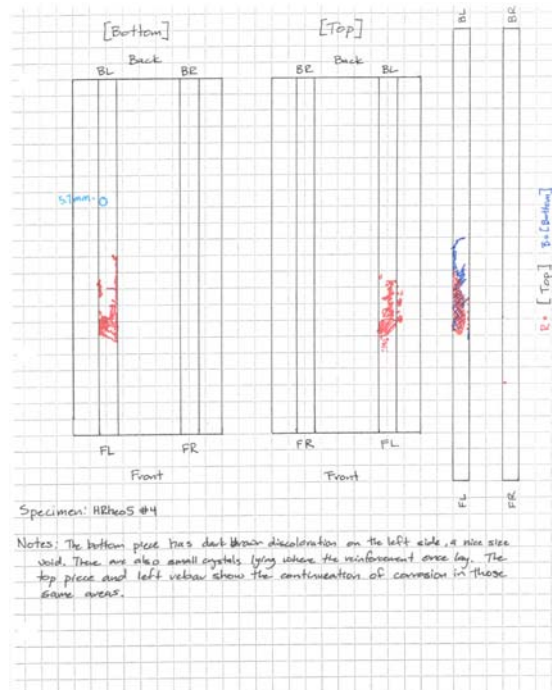


Figure 7.278 : HRheo5 #4B

HRheo5 #4 – The specimen showed no critical flaws on the outside. The left bar has an area of about 2 inches corrosion on both the top and the bottom. The half cell potential values showed one value on the left side fell into the 90% probability range. All the other values fell into the uncertain range. The voltage readings showed the specimen had failed. The inspection concluded the corrosion to be moderate to significant.



Figure 7.279 - Bars, bottom



Figure 7.280 - Bars, top

LATEX-MODIFIER

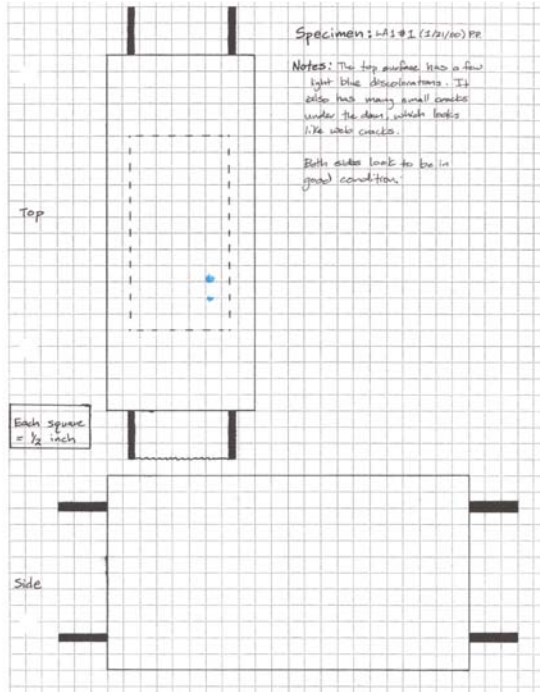


Figure 7.281 : LA1 #1A

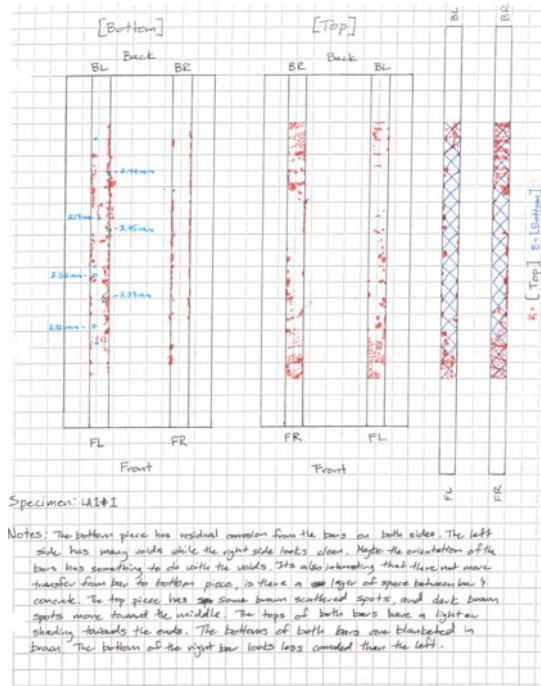


Figure 7.282 : LA1 #1B

LA1 #1 – The visual inspection showed no critical flaws on the outside of the specimen. The bottoms of both bars are completely covered in corrosion. The tops of both bars also have corrosion pits and spots all along the surface. The half cell potential numbers showed all the values fell into the uncertain range. The voltage readings indicated showed that the specimen was not close to failure. The inspection concluded the corrosion to be moderate to significant.



Figure 7.283 - Bars, bottom



Figure 7.284 - Bars, top

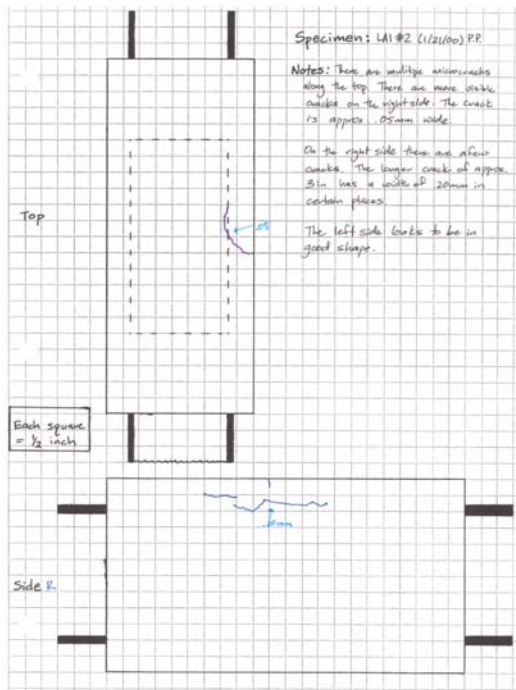


Figure 7.285 : LA1 #2 A

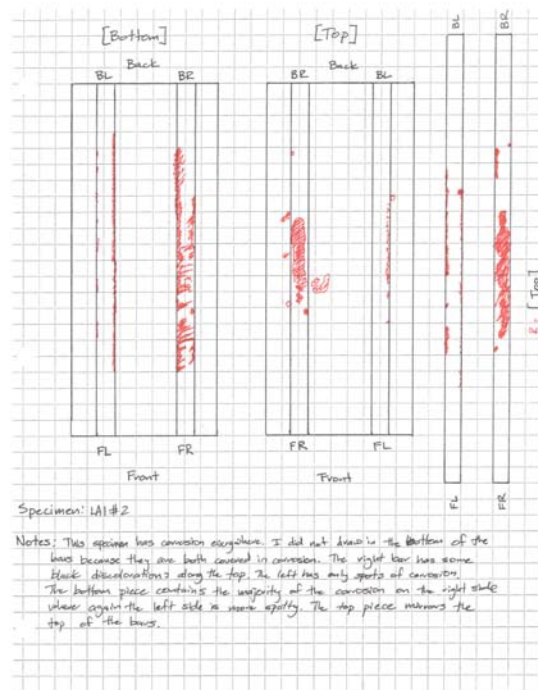


Figure 7.286 : LA1 #2 B

LA1 #2 – The visual inspection revealed a crack on the top surface around the right bar. There were also cracks on the right side of the specimen. Inside the specimen corrosion was found on the tops of both bars. The corrosion was more concentrated on the right bar, while the left bar corrosion was more along the edges. The half cell potential results indicated all the values fell into the uncertain range. The voltage readings showed the specimen had failed. The inspection concluded the corrosion to be moderate to significant.



Figure 7.287 - Bars, bottom



Figure 7.288 - Bars, top

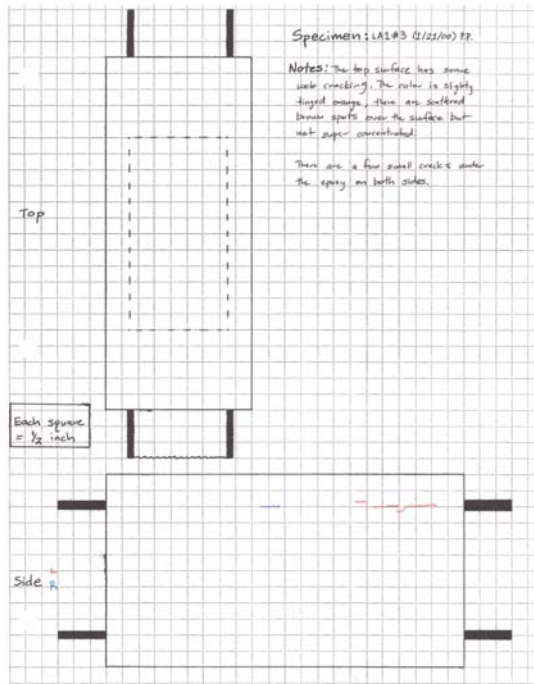


Figure 7.289 : LA1 #3 A

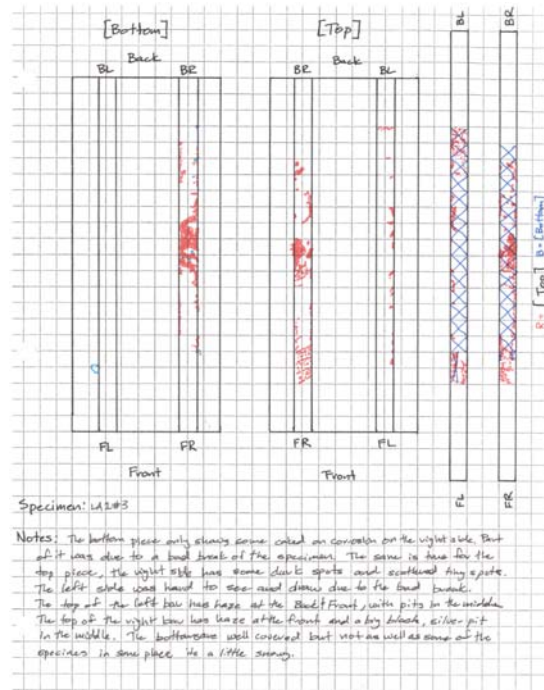


Figure 7.290 : LA1 #3 B

LA1 #3 – The top surface of the specimen looked in good condition. There were small cracks underneath the epoxy coating on both sides. Both bars were well covered in corrosion especially on the bottoms. The tops of the bars had many spots of corrosion along the length of the bars. The half cell potential readings showed that all of the numbers on the left side and one value on the right side fell into the 10% probability range. The other two values fell into the uncertain range. The voltage data indicated that the specimen had failed. The inspection concluded the corrosion to be moderate to significant.



Figure 7.291 - Bars, bottom



Figure 7.292 - Bars, top

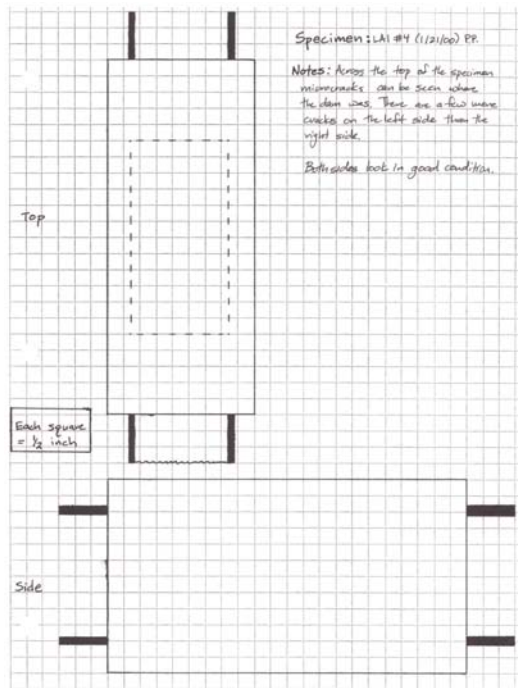


Figure 7.293 : LA1 #4 A

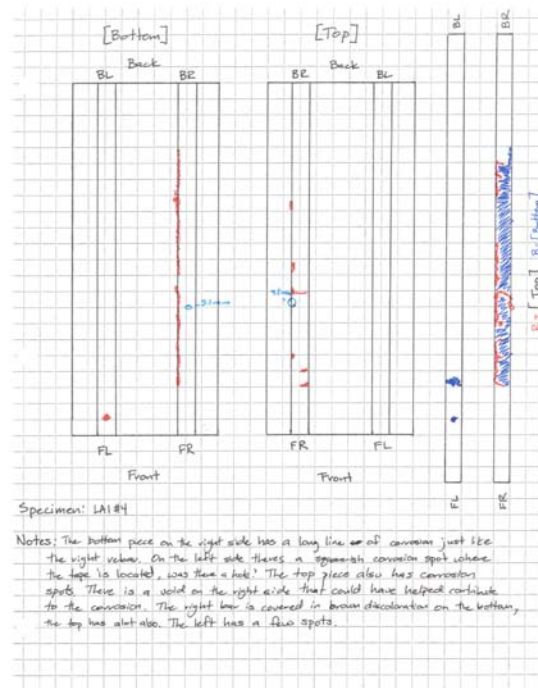


Figure 7.294 : LA1 #4 B

LA1 #4 – The top surface of the specimen contained web cracking. Everything else of the outside of the specimen looked in good condition. There were corrosion on both bars but the majority occurred on the bottom of the right bar. The top of the right bar had corrosion along the edges. The bottom of the left bar contained a small area of corrosion. The half cell potential numbers showed that all the values fell into the uncertain range. The voltage readings indicated that the specimen had not failed. The inspection concluded the corrosion to be moderate to significant.



Figure 7.295 - Bars, bottom



Figure 7.296 - Bars, top

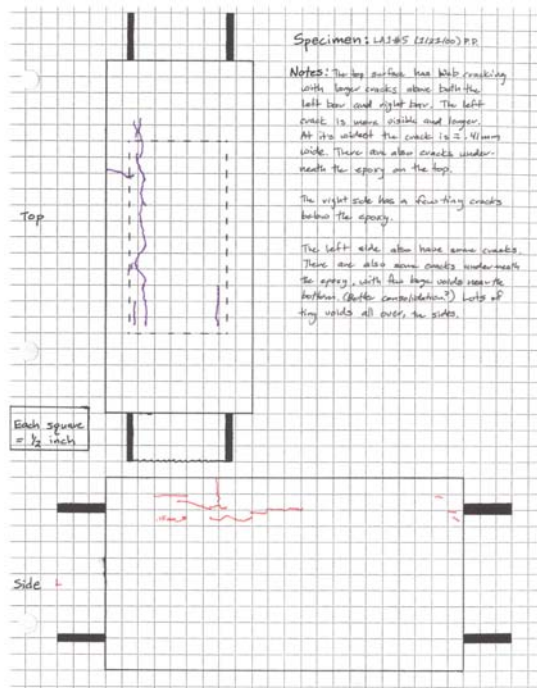


Figure 7.297 : LA1 #5 A

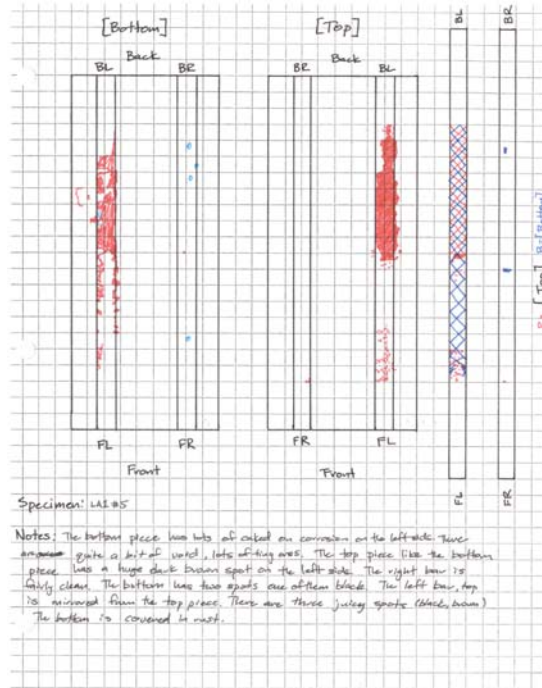


Figure 7.298 : LA1 #5 B

LA1 #5 – The visual inspection showed a long crack on the top surface above the left bar. There was also a smaller crack above the right bar. The left side of the specimen showed multiple cracks mostly toward the back. The left bar was covered in corrosion on both the top and bottom of the bar. The right bar had a few pits of corrosion on the bottom. The half cell potential readings all fell into the uncertain region. The voltage data showed that the specimen had failed. The inspection concluded the corrosion to be moderate to significant.



Figure 7.299 - Bars, bottom



Figure 7.300 - Bars, top

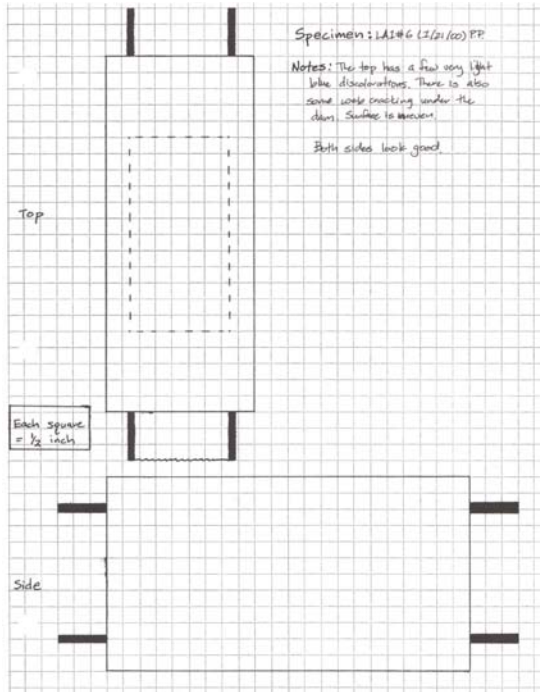


Figure 7.301 : LA1 #6 A

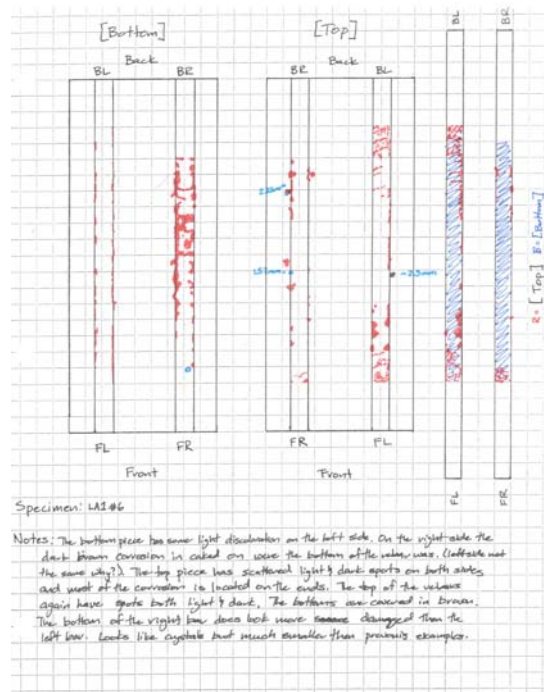


Figure 7.302 : LA1 #6 B

LA1 #6 – The specimen looked great from the outside. Both bars are completely covered in corrosion on the bottoms of the bars. The tops of the bars have spots or scattered areas of corrosion both toward the back and the front. The corrosion on the tops was more severe on the left side. The half cell potential readings all fell into the uncertain range. The voltage data showed the specimen had failed. The inspection concluded the corrosion to be moderate to significant.



Figure 7.303 - Bars, bottom



Figure 7.304 - Bars, top

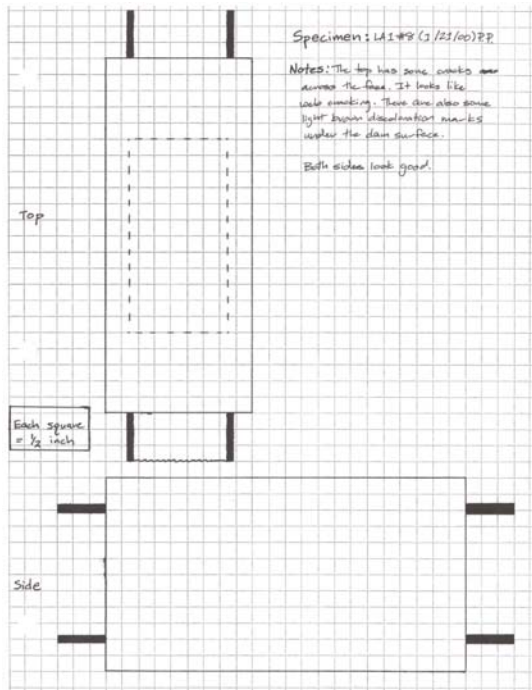


Figure 7.305 : LA1 #8 A

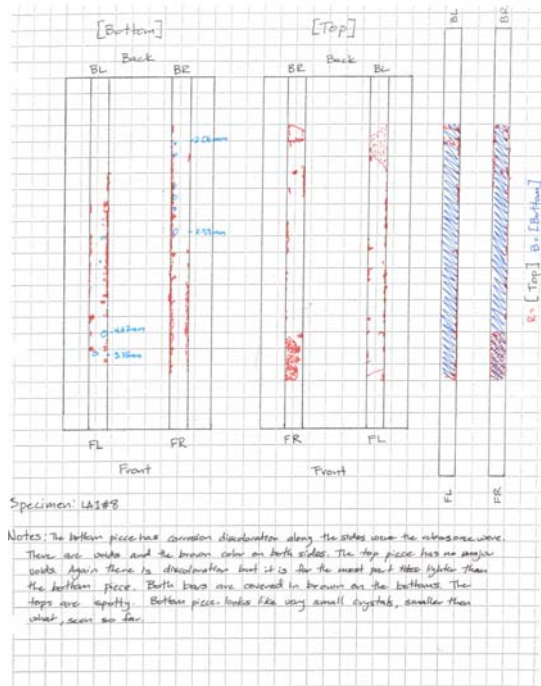


Figure 7.306 : LA1 #8 B

LA1 #8 – The top surface looked like there was some web cracking. Everything else looked fine. On the inside both bars were covered with corrosion on the bottoms. There was minimal corrosion on the top with small areas toward the front and back of both bars. The half cell potential readings showed that all the values on the left side fell into the 10% probability range. All the values on the right side fell into the uncertain range. The voltage data indicated the specimen had not failed but it was getting close. The inspection concluded the corrosion to be moderate to significant.



Figure 7.307 - Bars, bottom



Figure 7.308 - Bars, top

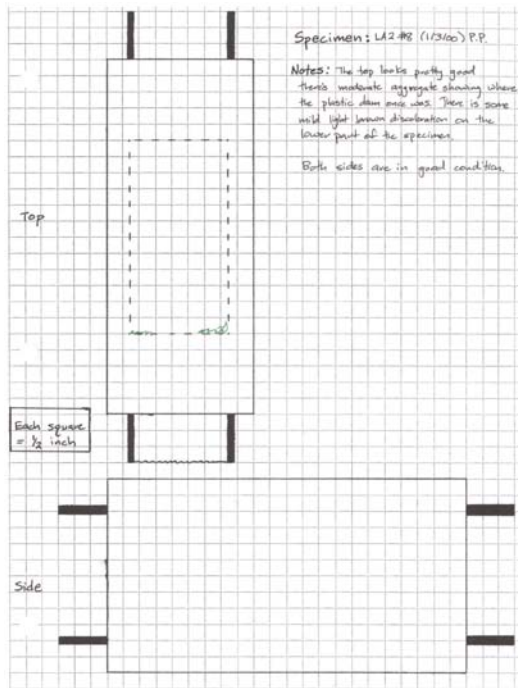


Figure 7.309 : LA2 #8A

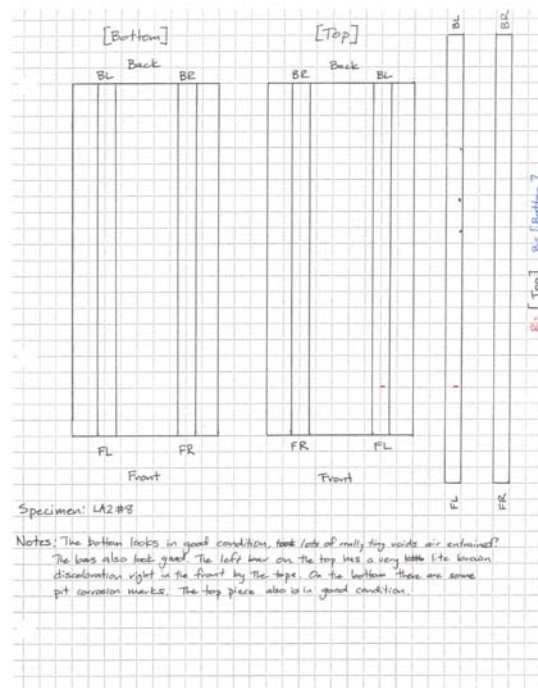


Figure 7.310 : LA2 #8B

LA2 #8 – The outside of the specimen has some light brown discoloration toward the bottom of the top surface. On the inside of the specimen there was virtually no corrosion. The half cell potential values all fell into the 10% probability range. The voltage readings showed the specimen had not failed. The inspection concluded the corrosion to be none.



Figure 7.311 - Bars, bottom



Figure 7.312 - Bars, top

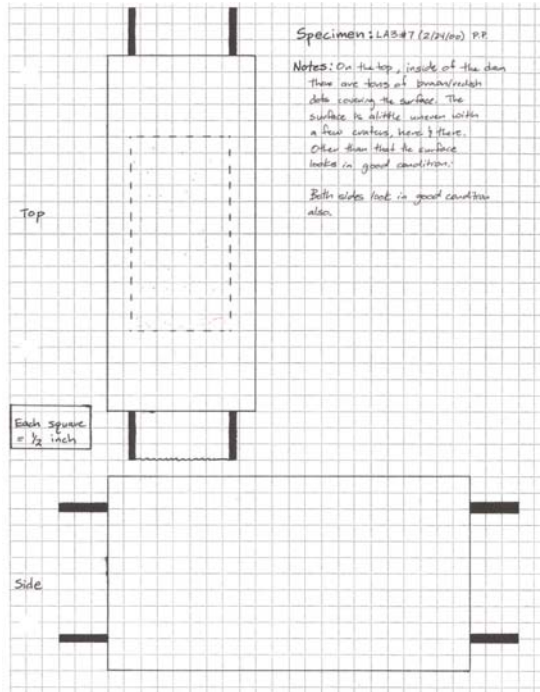


Figure 7.313 : LA3 #7 A

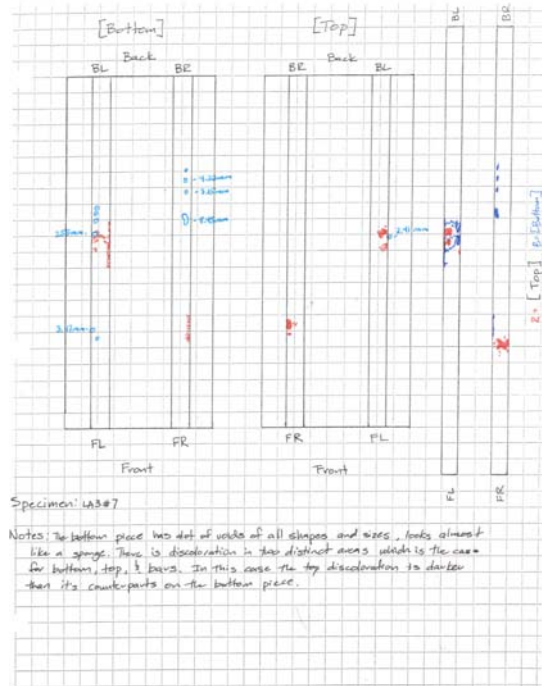


Figure 7.314 : LA3 #7 B

LA3 #7 – The outside surface contained no critical problems. Both bars have small areas of corrosion on both the top and bottom of the bars. The corrosion was not wide spread. The half cell potential values all fell into the uncertain range. The voltage readings showed the specimen was close to failure but had not reached it. The inspection concluded the corrosion to be minor.



Figure 7.315 - Bars, bottom

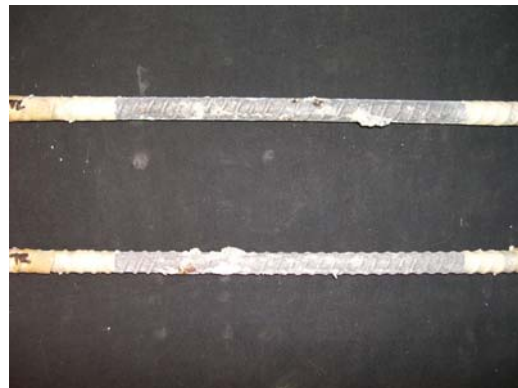


Figure 7.316 - Bars, top

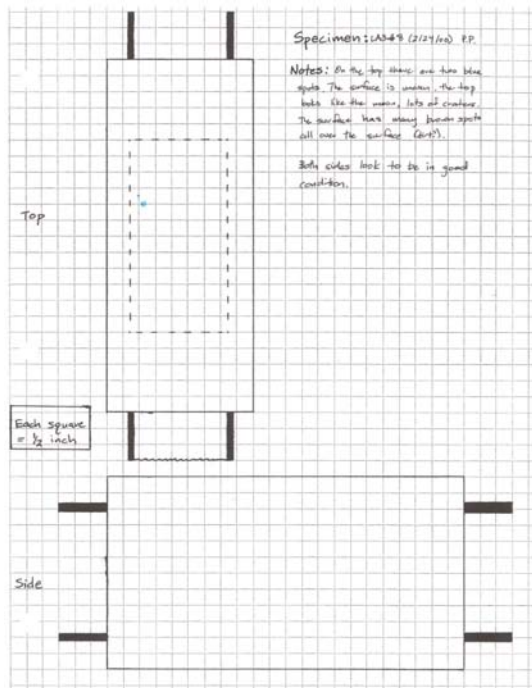


Figure 7.317 : LA3 #8 A

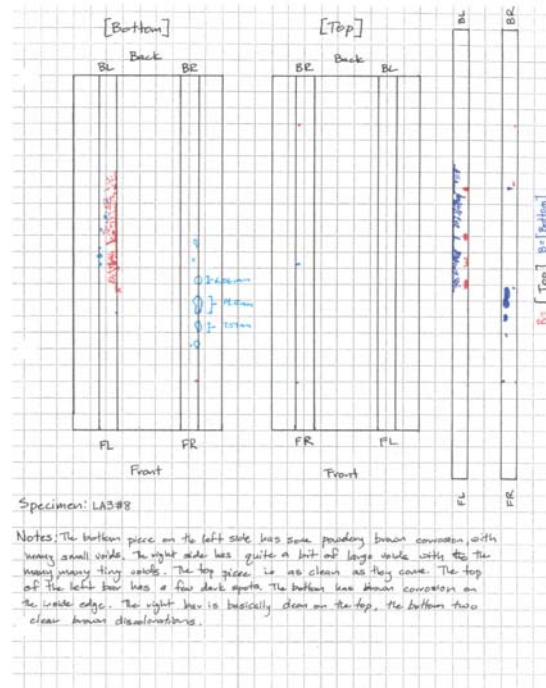


Figure 7.318 : LA3 #8 B

LA3 #8 – The visual inspection did not indicate any flaws on the outside. On the left bar there were pits on the top and strip of corrosion on the edge of the bottom of the bar. The right bar contains pits on both the top and the bottom. The half cell potential values all fell into the uncertain range. The voltage data indicated that the specimen had not failed. The inspection concluded the corrosion to be moderate to significant.



Figure 7.319 - Bars, bottom



Figure 7.320 - Bars, top

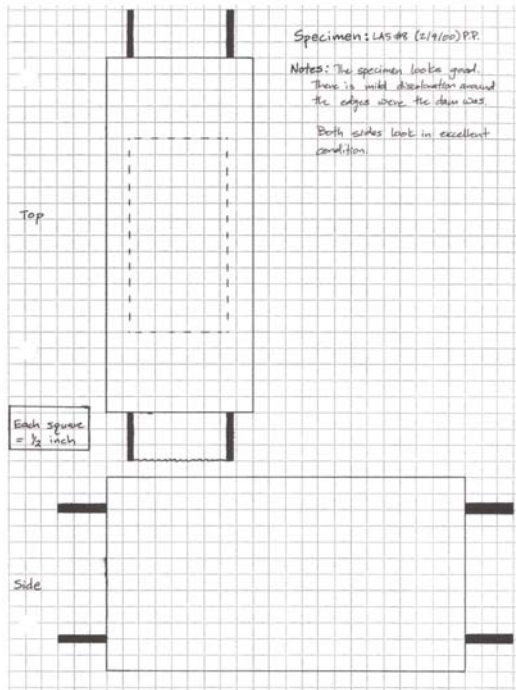


Figure 7.321 : LA5 #8 A

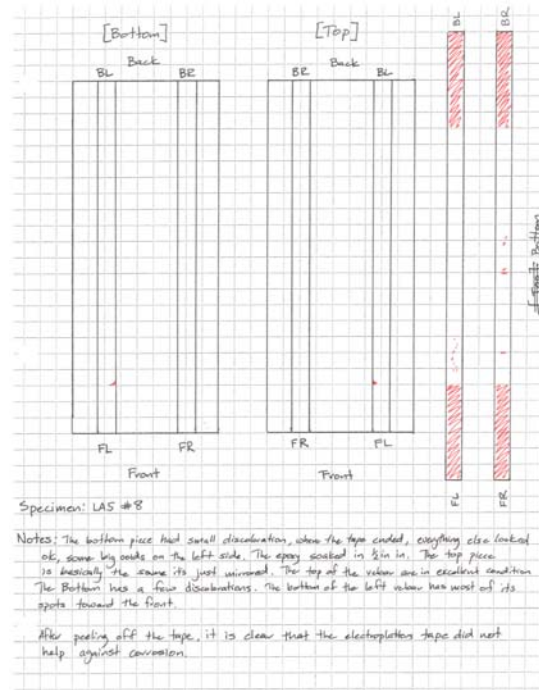


Figure 7.322 : LA5 #8 B

LA5 #8 – From the outside the specimen looks in excellent condition. There is minimal corrosion on the inside of the specimen. The half cell potential values all fell into the 10% probability range. The voltage readings showed that the specimen had not failed. The inspection concluded the corrosion to be none.



Figure 7.323 - Bars, bottom

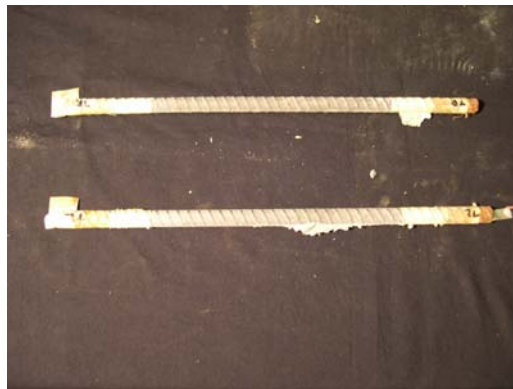


Figure 7.324 - Bars, top

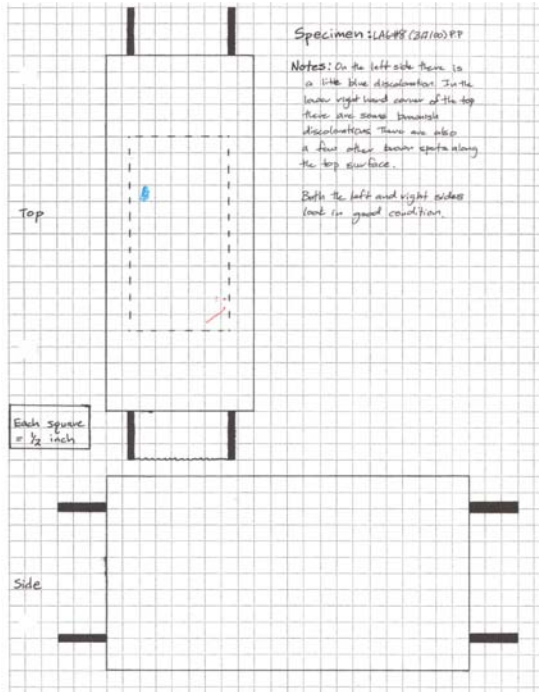


Figure 7.325 : LA6 #8 A

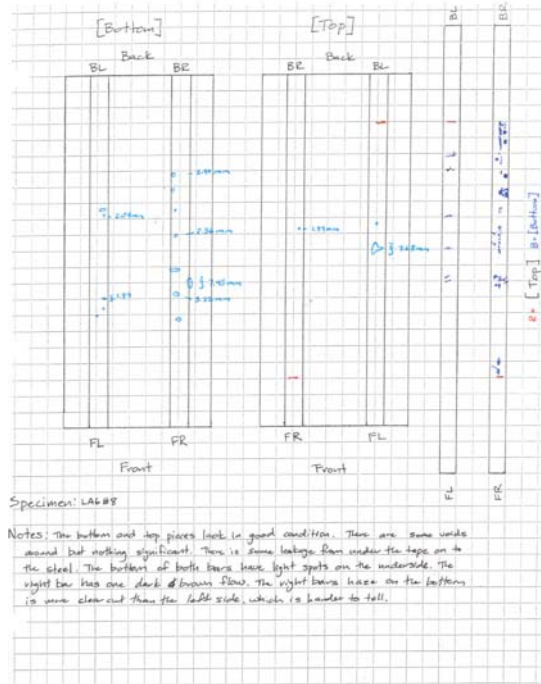


Figure 7.326 : LA6 #8 B

LA6 #8 – The top surface there was some brown discolorations in the lower right hand corner. Both bars have sparse corrosion along the length of the bottom. The half cell potential readings showed that the values all fell into the 10% probability range. The voltage data indicated the specimen had not failed. The inspection concluded the corrosion to be minor.

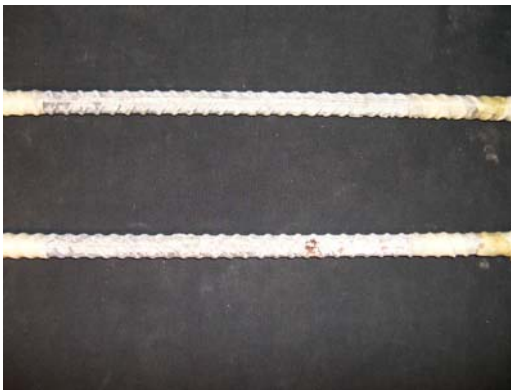


Figure 7.327 - Bars, bottom

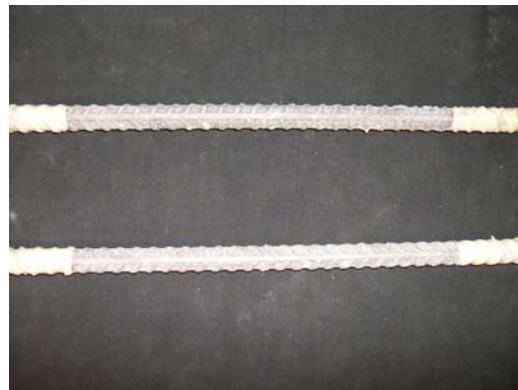


Figure 7.328 - Bars, top

RHEOCRETE 222+

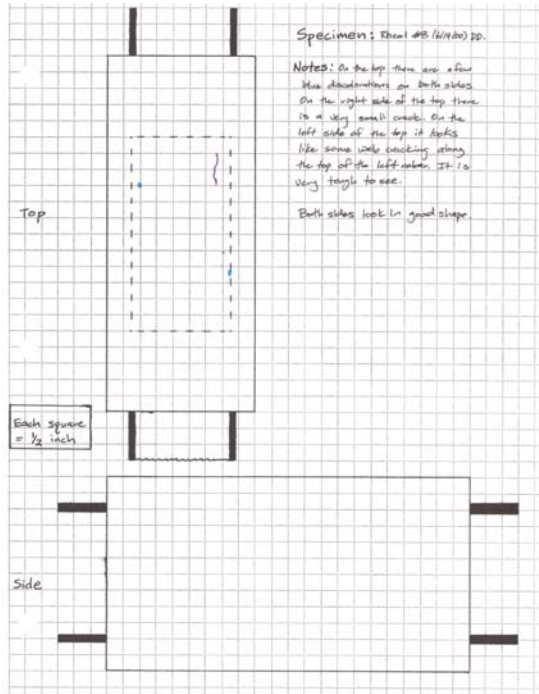


Figure 7.329 : Rheo1 #8A

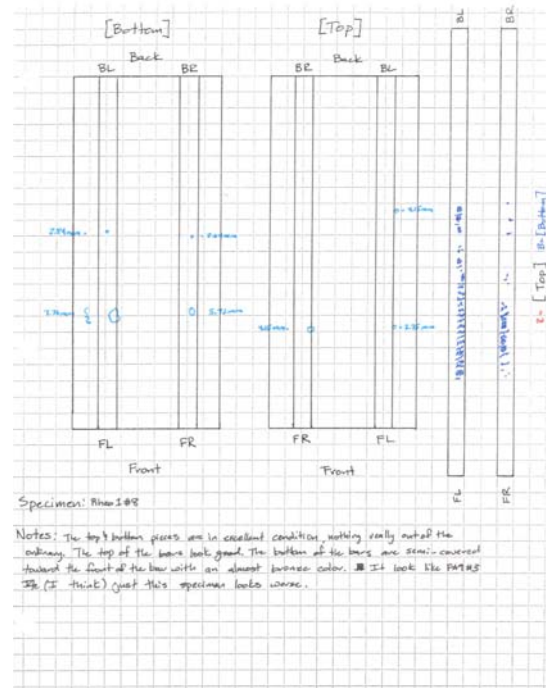


Figure 7.330 : Rheo1 #8B

Rheo1 #8 – The visual inspection revealed a small crack on the top surface that occurred to the left of the right bar. There was also some web cracking occurring. Both bars showed some consistent spaced corrosion on the bottoms. The half cell potential values all fell into the 10% probability range. The voltage readings indicated that the specimen had not failed. The inspection concluded the corrosion to be minor.



Figure 7.331 - Bars, bottom

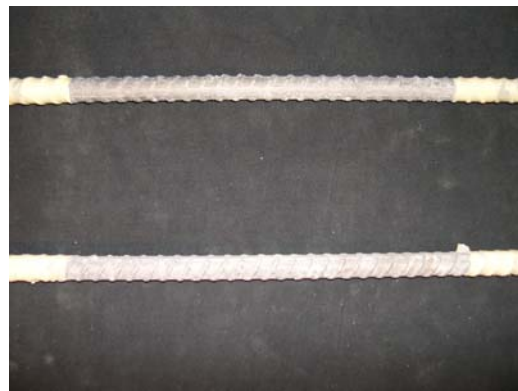


Figure 7.332 - Bars, top

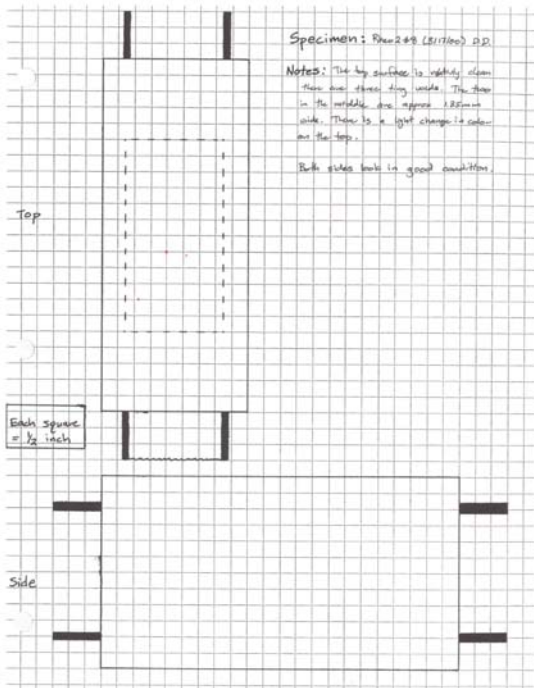


Figure 7.333 : Rheo2 #8A

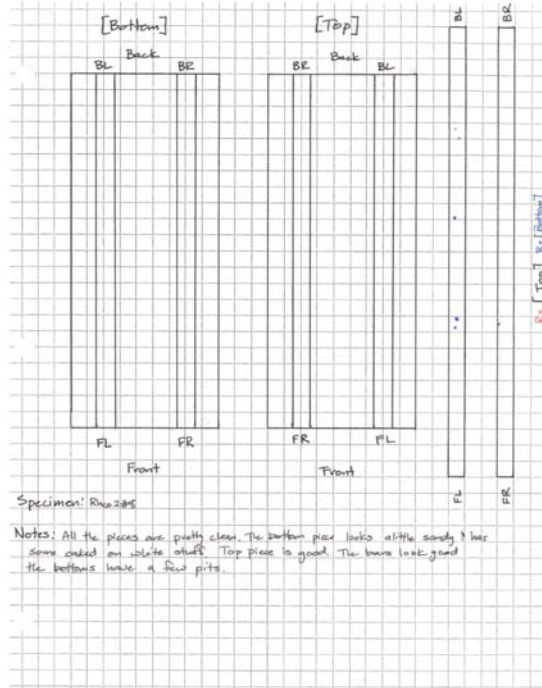


Figure 7.334 : Rheo2 #8B

Rheo2 #8 – There were a few void on the top surface. Otherwise the specimen looked to be in good condition. There were only a few pits of corrosion on bottom of both bars combined. The half cell potential values all fell into the 10% probability range. The voltage data showed that the specimen had not failed. The inspection concluded the corrosion to be none.



Figure 7.335 - Bars, bottom



Figure 7.336 - Bars, top

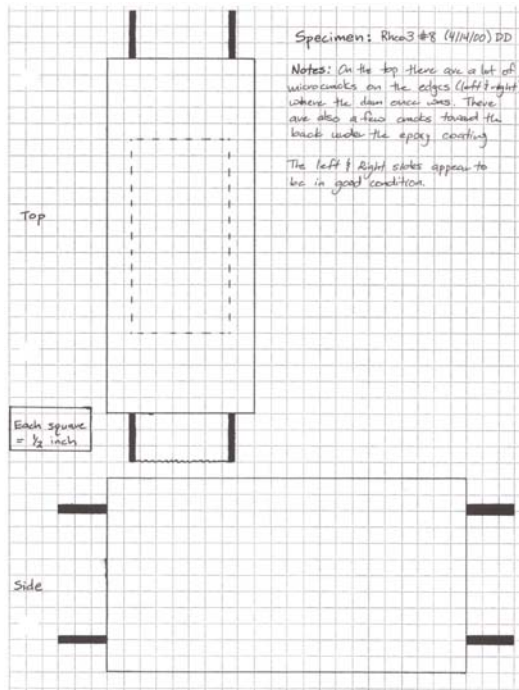


Figure 7.337 : Rheo3 #8A

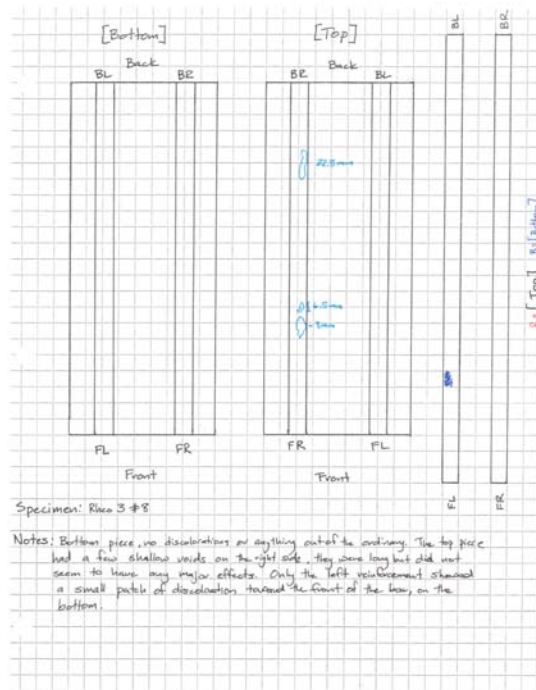


Figure 7.338 : Rheo3 #8B

Rheo3 #8 – The visual inspection revealed some wed cracking occurring on the top surface. On the inside there was one small area of corrosion on the bottom of the left bar. The half cell potential values all fell into the 10% probability range. The voltage readings indicated that the specimen had not failed. The inspection concluded the corrosion to be minor.

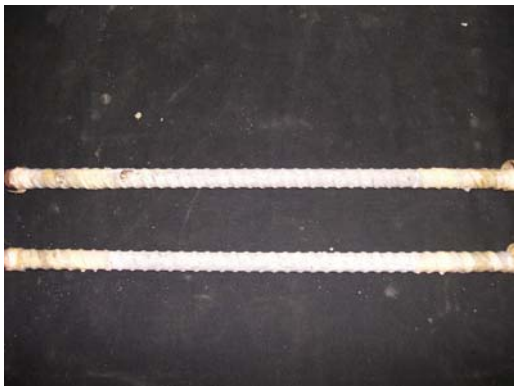


Figure 7.339 - Bars, bottom



Figure 7.340 - Bars, top

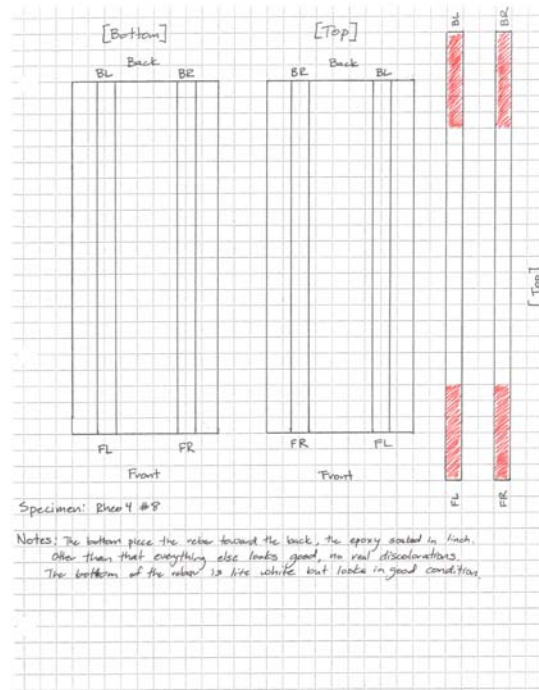
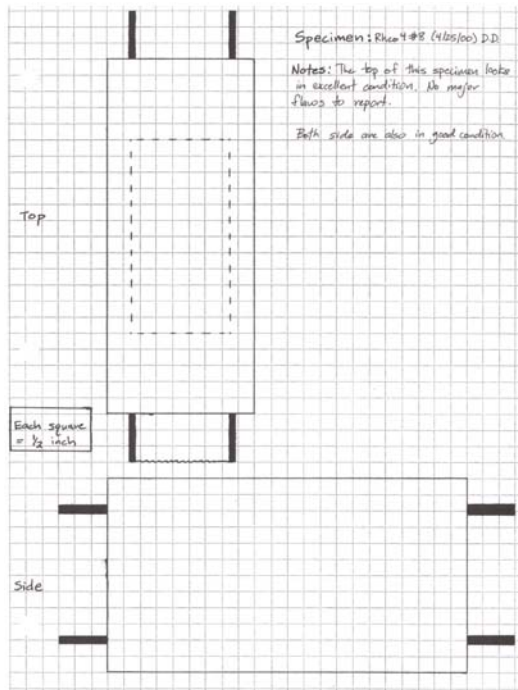


Figure 7.341 : Rheo4 #8A Figure 7.342 : Rheo4 #8B

Rheo4 #8 – On the outside the specimen appeared to be in excellent condition. Both bars were clean. The half cell potential readings showed the values in the 10% probability range. The voltage data pointed out that the specimen had not failed. The inspection concluded the corrosion to be none.



Figure 7.343 - Bars, bottom



Figure 7.344 - Bars, top

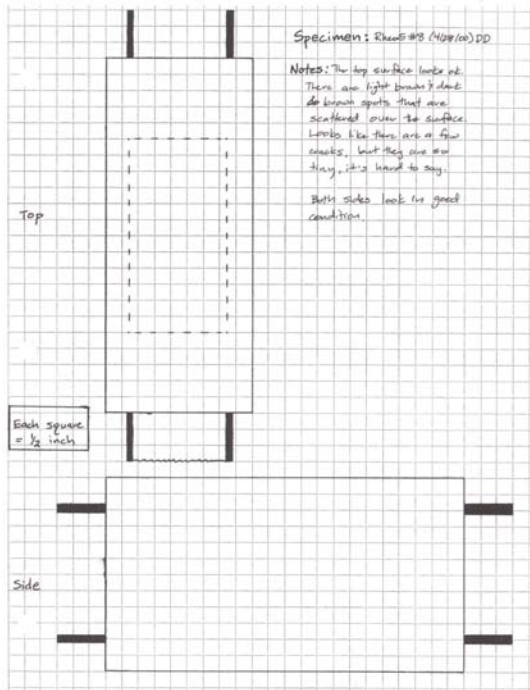


Figure 7.345 : Rheo5 #8 A

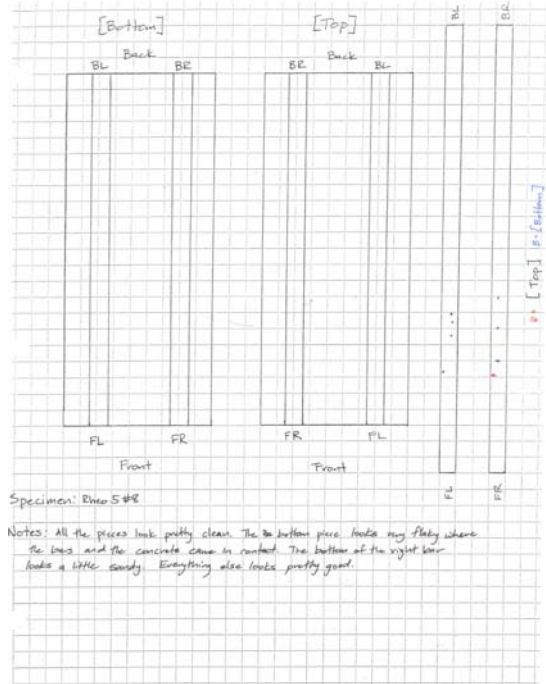


Figure 7.346 : Rheo5 #8 B

Rheo5 #8 – The outside of the specimen looked in fair condition. There are some discolorations and tiny cracks. The bars showed very little corrosion. There were a few spots on the bottom of both bars. The half cell potential values all fell into the 10% probability range. The voltage data indicated that the specimen had not failed. The inspection concluded the corrosion to be minor.



Figure 7.347 - Bars, bottom



Figure 7.348 - Bars, top

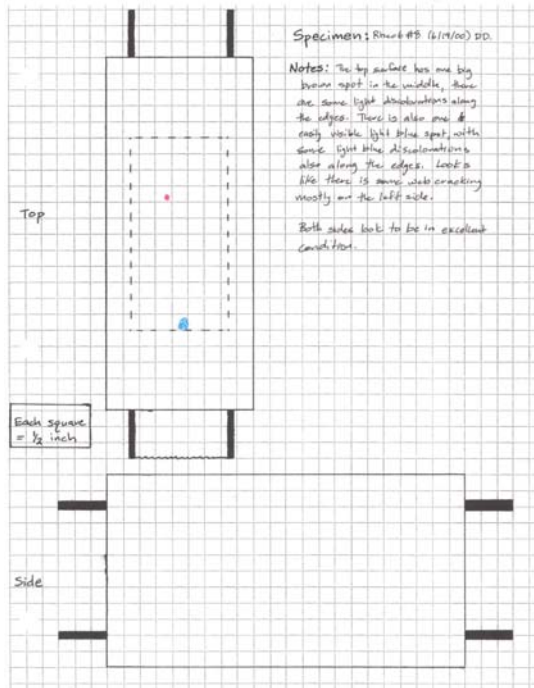


Figure 7.349 : Rheo6 #8A

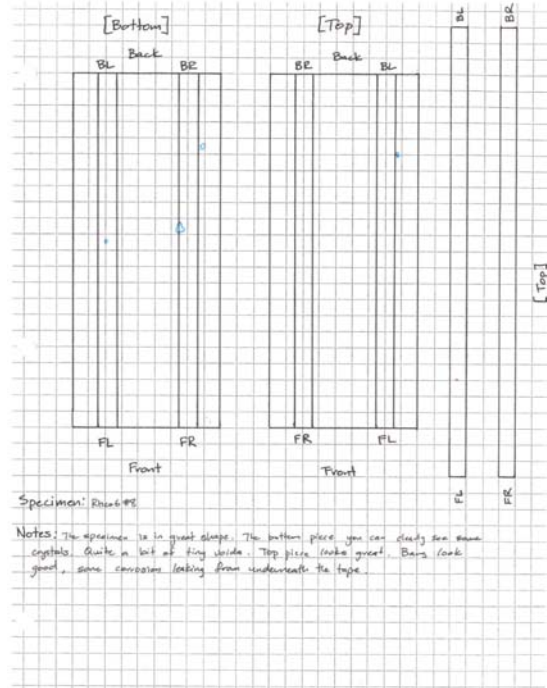


Figure 7.350 : Rheo6 #8B

Rheo6 #8 – The outside of the specimen looked in fair condition. There were some discolorations on the top surface. There was no corrosion located on the inside of the specimen. The half cell potential values showed all of them fell into the 10% probability region. The voltage readings showed that the specimen had not failed. The inspection concluded the corrosion to be none.

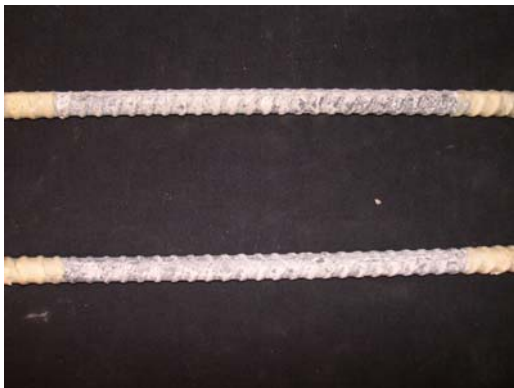


Figure 7.351 - Bars, bottom



Figure 7.352 - Bars, top

SILICA FUME

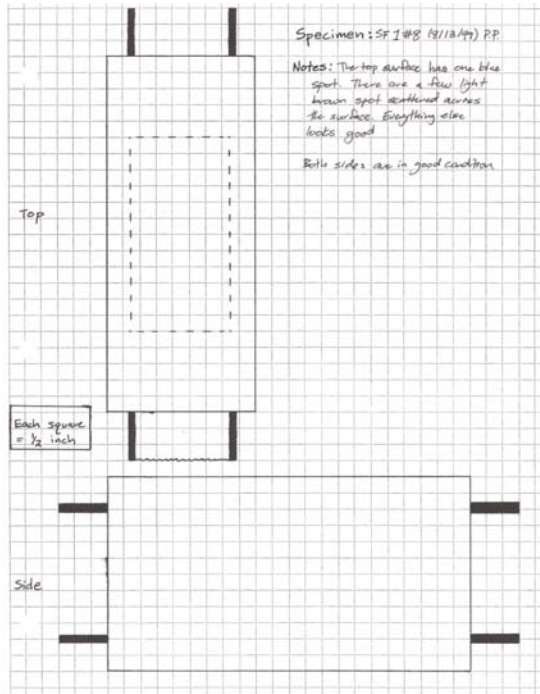


Figure 7.353 : SF1 #8 A

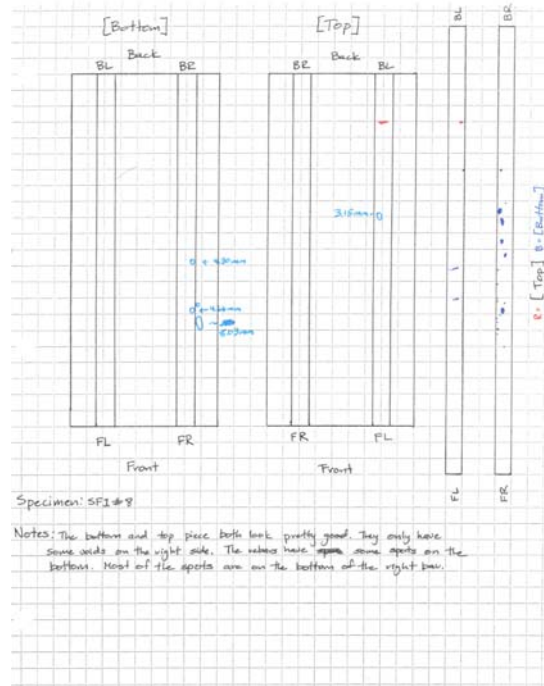


Figure 7.354 : SF1 #8 B

SF1 #8 – From the outside the specimen looked in excellent condition. Both bars have a nominal amount of corrosion in the form of pits along the bottoms of the bars. The half cell potential values all fell into the range of 10% probability. The voltage results concluded that the specimen had not reached failure. The inspection concluded the corrosion to be none.



Figure 7.355 - Bars, bottom



Figure 7.356 - Bars, top

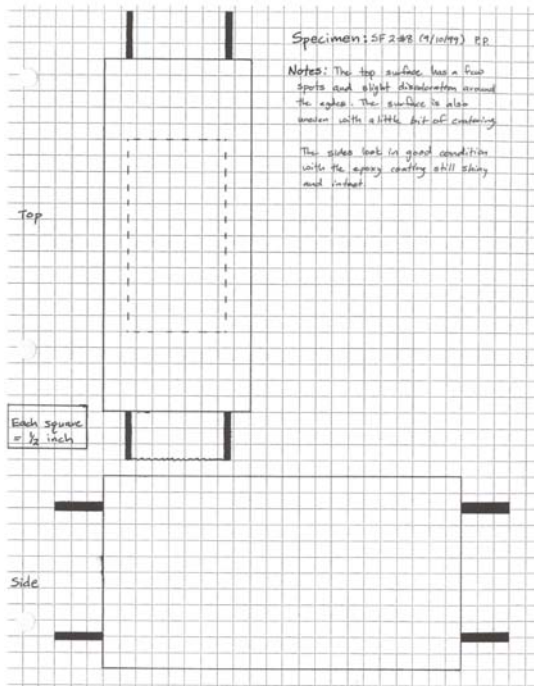


Figure 7.357 : SF2 #8 A

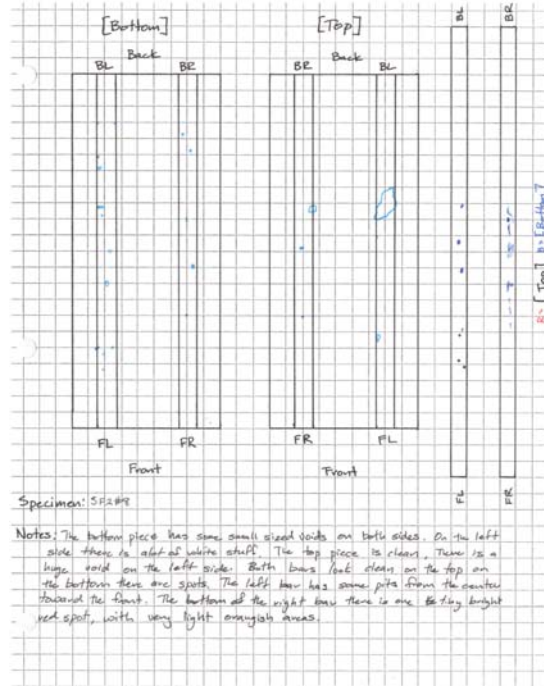


Figure 7.358 : SF2 #8 B

SF2 #8 – The outside of the specimen looked in good condition. There were scattered corrosion pits on the bottoms of both bars. The half cell potential values all fell into the 10% probability range. The voltage readings showed the specimen did not fail. The inspection concluded the corrosion to be none.



Figure 7.359 - Bars, bottom



Figure 7.360 - Bars, top

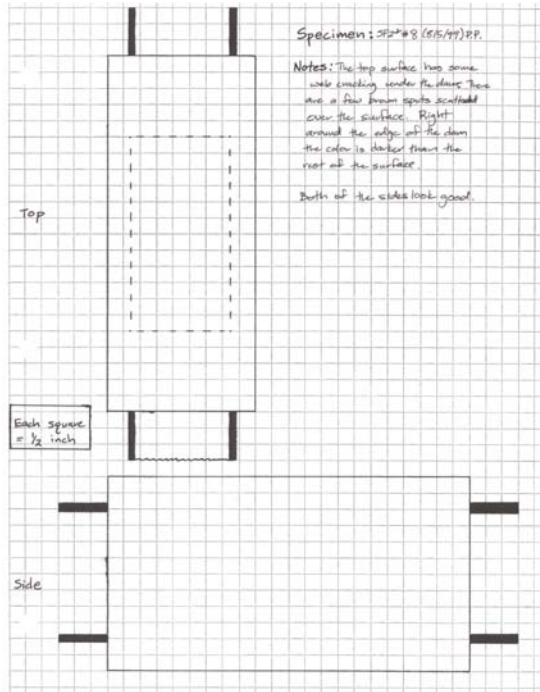


Figure 7.361 : SF2* #8 A

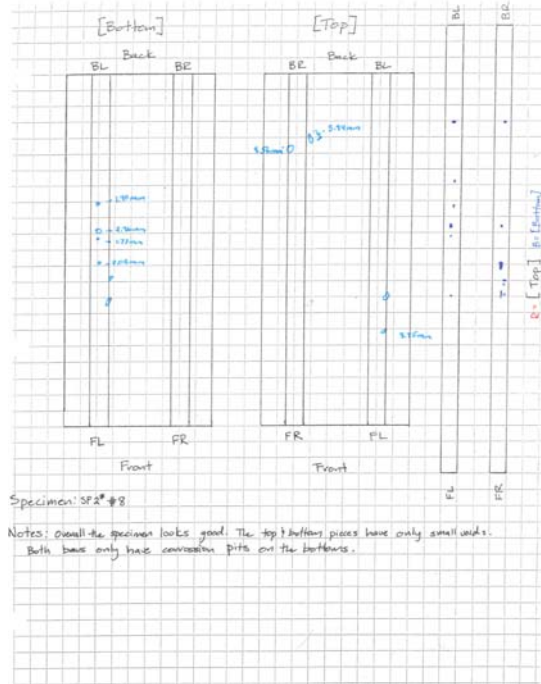


Figure 7.362 : SF2* #8 B

SF2* #8 – The outside of the surface looked in fair condition. Web cracking was occurring on the top surface and there were also some brown discolorations. Both bars only had a few pits of corrosion along the bottoms of the bars. The half cell potential readings all fell into the 10% probability range. The voltage data showed that the specimen had not failed. The inspection concluded the corrosion to be minor.

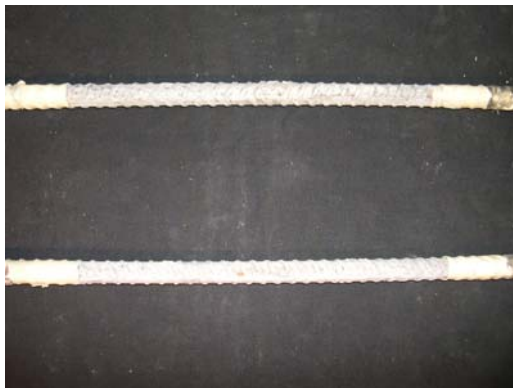


Figure 7.363 - Bars, bottom

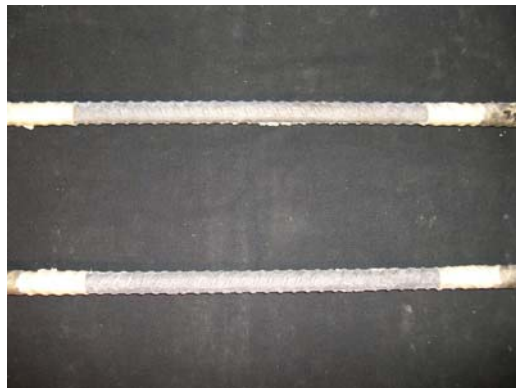


Figure 7.364 - Bars, top

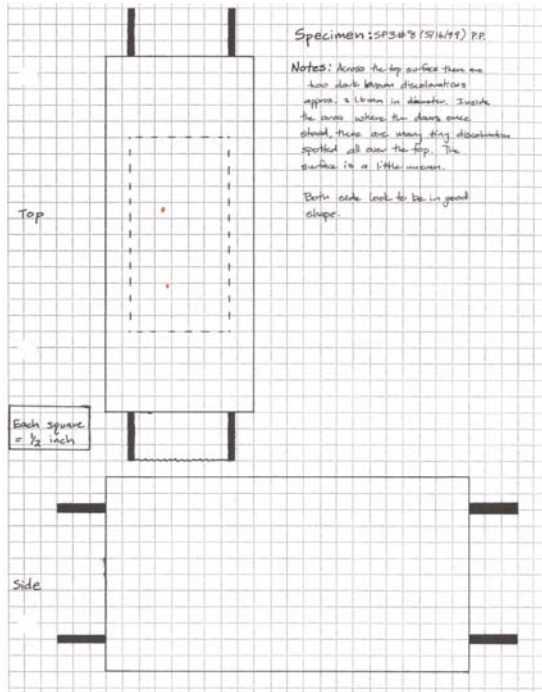


Figure 7.365 : SF3 #8 A

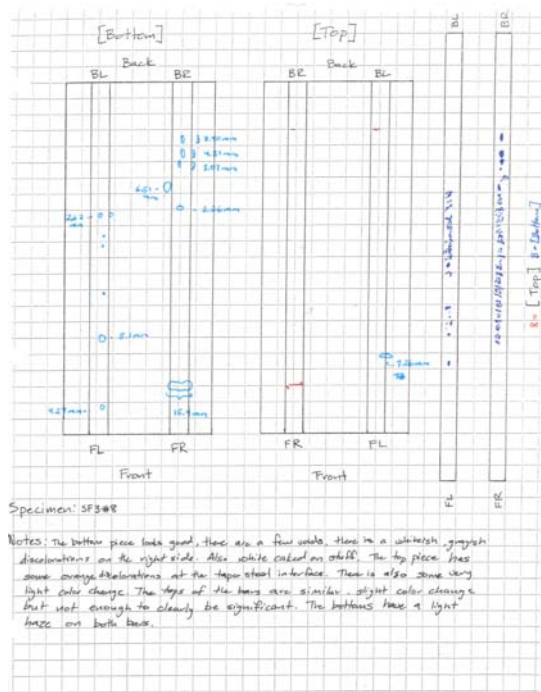


Figure 7.366 : SF3 #8 B

SF3 #8 – The top surface contained small discolorations. Both bars had a fair amount of scattered corrosion and pits along the bottoms. The half cell potential values all fell into the 10% probability range. The voltage results indicated the specimen had not failed. The inspection concluded the corrosion to be minor.



Figure 7.367 - Bars, bottom



Figure 7.368 - Bars, top

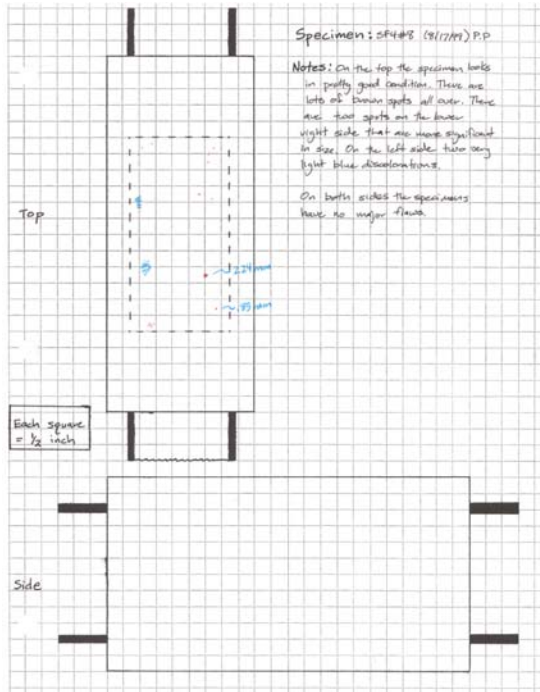


Figure 7.369 : SF4 #8 A

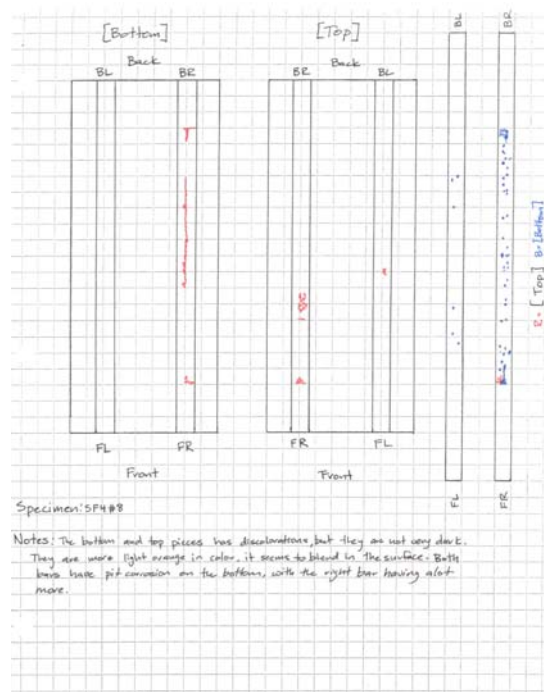


Figure 7.370 : SF4 #8 B

SF4 #8 – The outside of the specimen looked in good condition. There were a few discolorations on the top surface. The right bar contained a large amount of spots along the length of the bottom of the bar. The left bar contained a few spots along the bottom of the bar. The half cell potential numbers all fell into the uncertain range. The voltage data showed the specimen had not failed. The inspection concluded the corrosion to be minor.

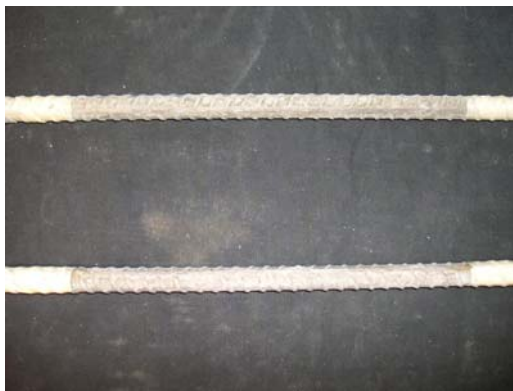


Figure 7.371 - Bars, bottom

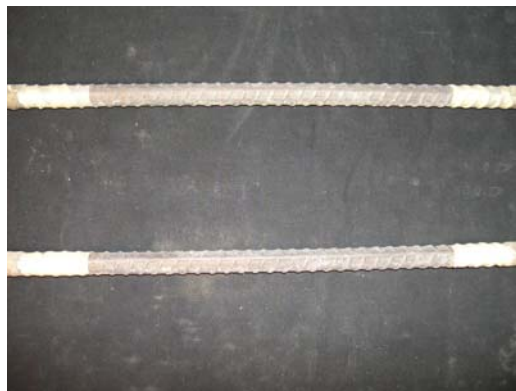


Figure 7.372 - Bars, top

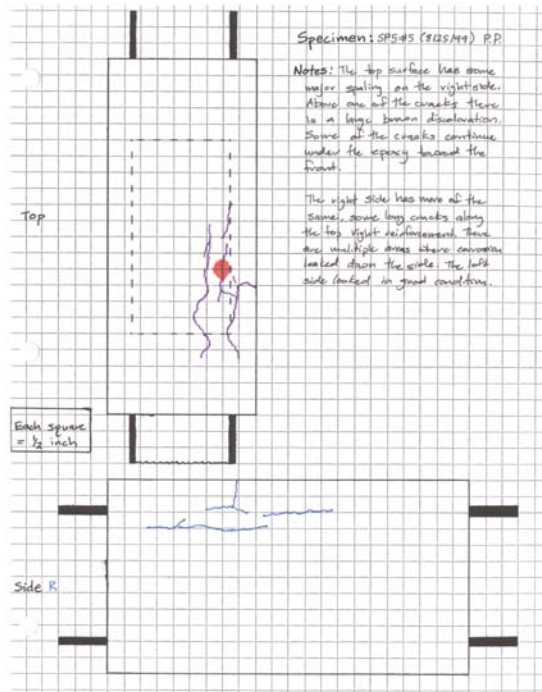


Figure 7.373 : SF5 #5A

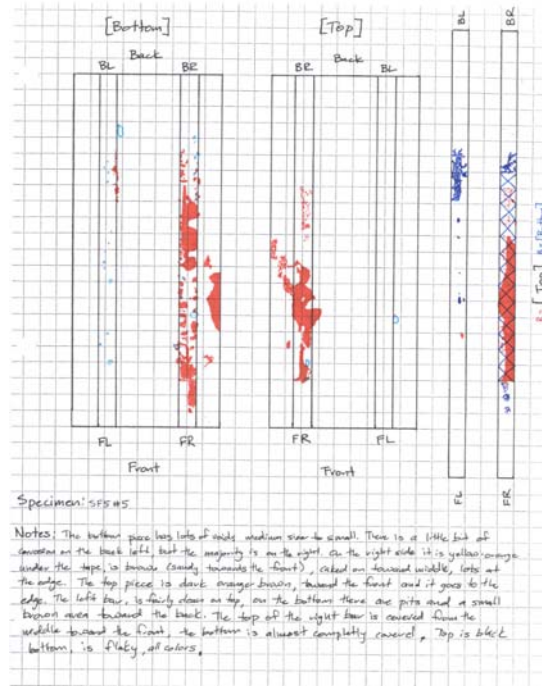


Figure 7.374 : SF5 #5B

SF5 #5 – The visual inspection revealed multiple cracks on the top surface above the right bar. In the vicinity of the cracks there was also an area of discoloration. Cracks were found on the right side of the specimen as well. The right bar was well covered in corrosion on the bottom. The top of the bar was also covered with a large area of corrosion. The left bar had a small area of corrosion on the bottom with a few other spots. The half cell potential values all fell into the uncertain range. The voltage readings had reached failure. The inspection concluded the corrosion to be moderate to significant.



Figure 7.375 - Bars, bottom



Figure 7.376 - Bars, top

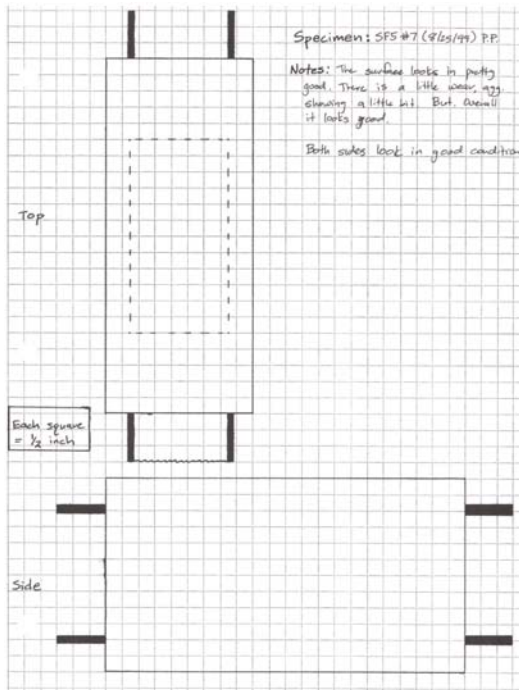


Figure 7.377 : SF5 #7 A

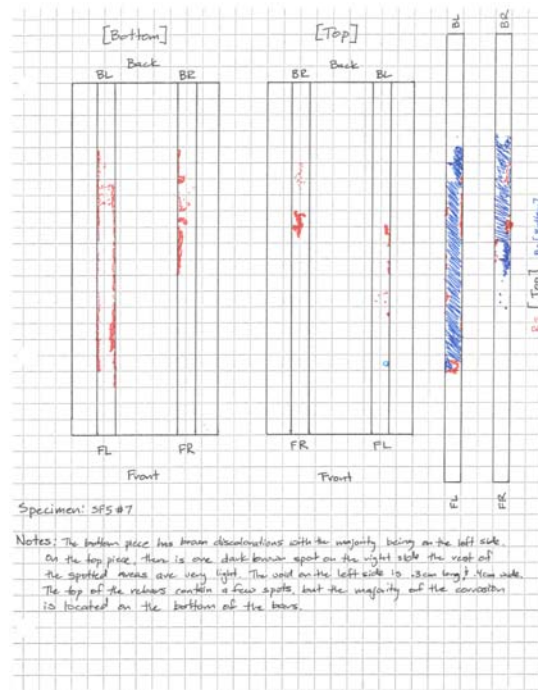


Figure 7.378 : SF5 #7 B

SF5 #7 – The outside of the specimen appeared to be in good condition. The bottom of the left bar was almost completely covered in corrosion. The top of the bar had some corrosion along the edges. The bottom of the right bar was about half way covered in corrosion. The top of the bar also had some corrosion pits. The half cell potential values all fell into the uncertain range. The voltage data showed that the specimen had failed. The inspection concluded the corrosion to be moderate to significant.



Figure 7.379 - Bars, bottom



Figure 7.380 - Bars, top

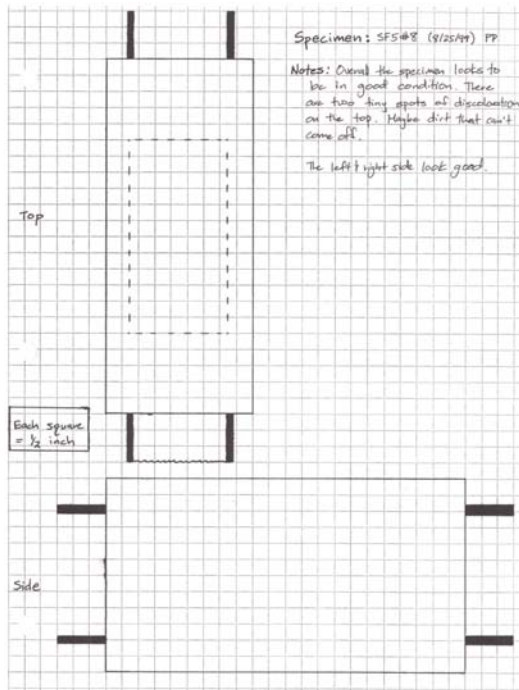


Figure 7.381 : SF5 #8 A

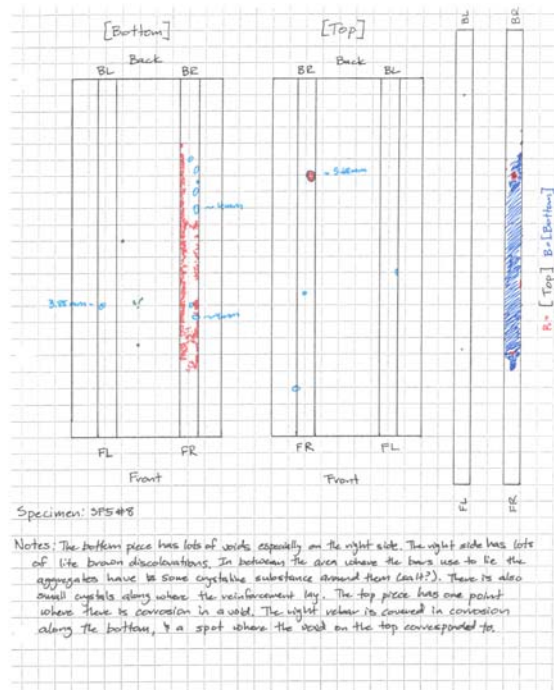


Figure 7.382 : SF5 #8 B

SF5 #8 – The outside of the specimen looked to be in good condition. The majority of the corrosion appeared on the bottom of the right bar. The rest of the spotted corrosion appeared on the top of the right bar and bottom of the left bar. The half cell potential values all fell into the 10% probability range. The voltage readings showed the specimen came close to failure but it did not reach it. The inspection concluded the corrosion to be moderate to significant.



Figure 7.383 - Bars, bottom



Figure 7.384 - Bars, top

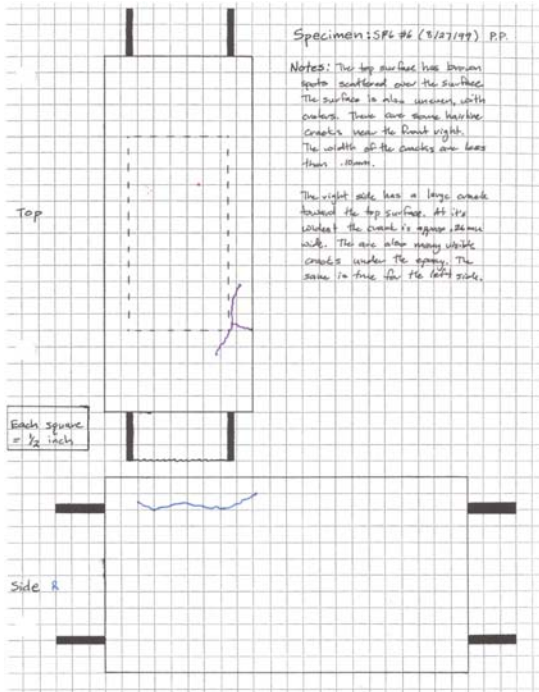


Figure 7.385 : SF6 #6 A

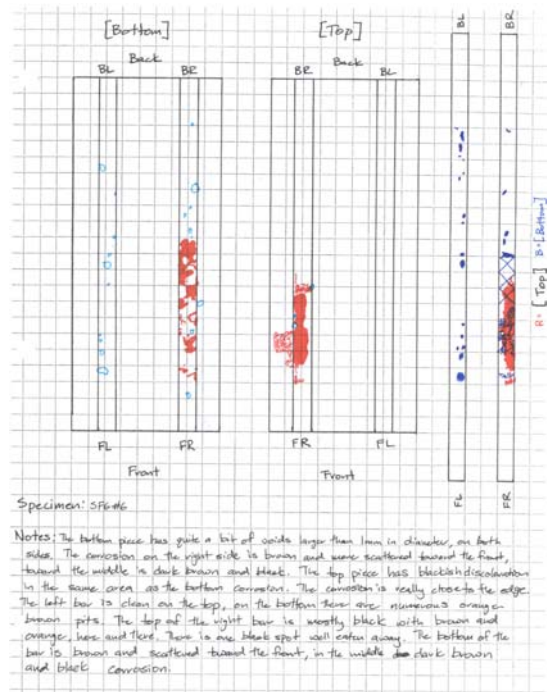


Figure 7.386 : SF6 #6 B

SF6 #6 – The visual inspection showed that there was a crack on the top surface toward the front of the right bar. There was also a crack on the right side surface. The corrosion mostly appeared were the crack occurred, on the right bar toward the front. The corrosion on the top of the bar was concentrated. The corrosion on the bottom of the bar was more spaced out in the same area. There was more corrosion mostly in the forms of pits along the rest of both bars. The half cell potential values showed one value on the right side fall into the 90% probability range. The rest of the numbers fell into the uncertain range. The voltage data indicated the specimen had failed. The inspection concluded the corrosion to be moderate to significant.



Figure 7.387 - Bars, bottom



Figure 7.388 - Bars, top

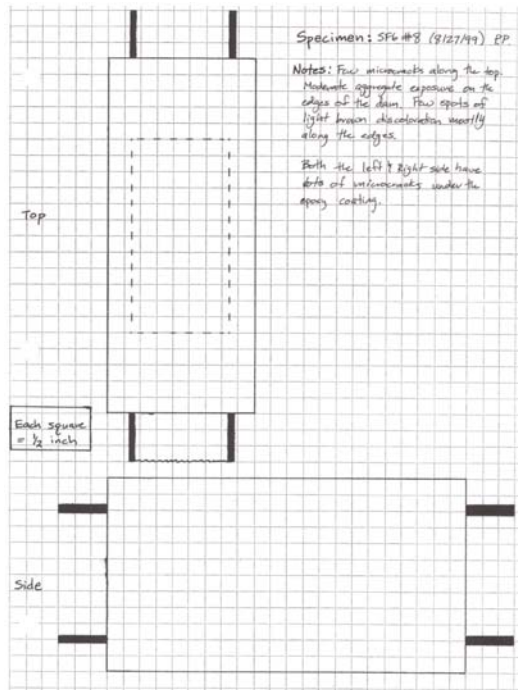


Figure 7.389 : SF6 #8 A

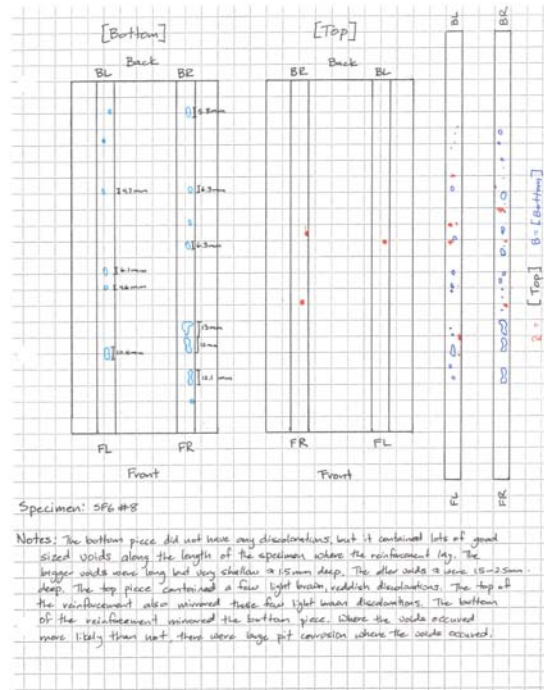


Figure 7.390 : SF6 #8 B

SF6 #8 – The specimen looked to be in good condition from the outside. There were lots of pits on the bottoms of both bars. The tops of the bars also contained a few spots. The large amount of pits was due to the large amount of voids between the concrete/reinforcement interfaces. The half cell potential values all fell into the 10% probability range. The voltage data showed that the specimen had not failed. The inspection concluded the corrosion to be minor.



Figure 7.391 - Bars, bottom



Figure 7.392 - Bars, top

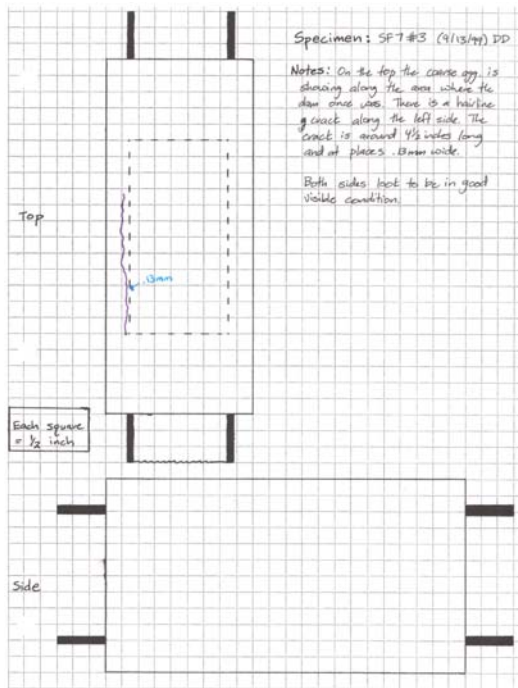


Figure 7.393 : SF7 #3 A

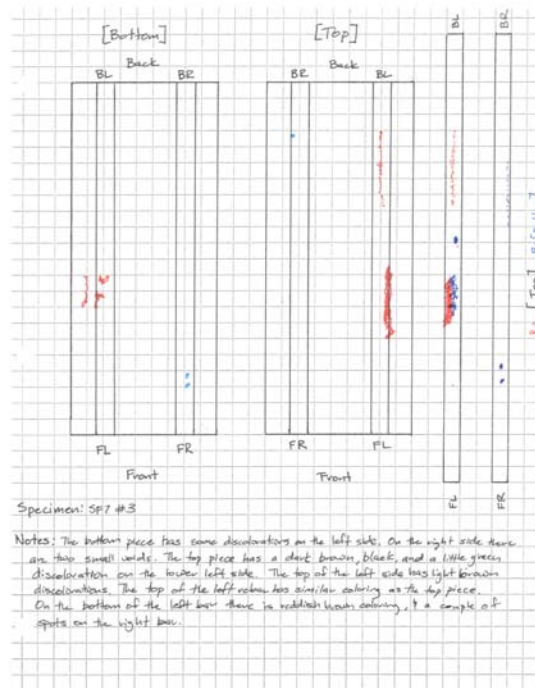


Figure 7.394 : SF7 #3 B

SF7 #3 – The visual inspection found a crack on the top surface above the left bar. The top of the left bar has a 1.5 inch area of corrosion in the middle and that corrosion continues to the bottom of the bar. There was also a line of light corrosion toward the back of the bar. The right bar has a few spots and pits on the bottom of the bar. The half cell potential values all fell into the 90% probability range. The voltage readings showed that the specimen had failed. The inspection concluded the corrosion to be moderate to significant.



Figure 7.395 - Bars, bottom



Figure 7.396 - Bars, top

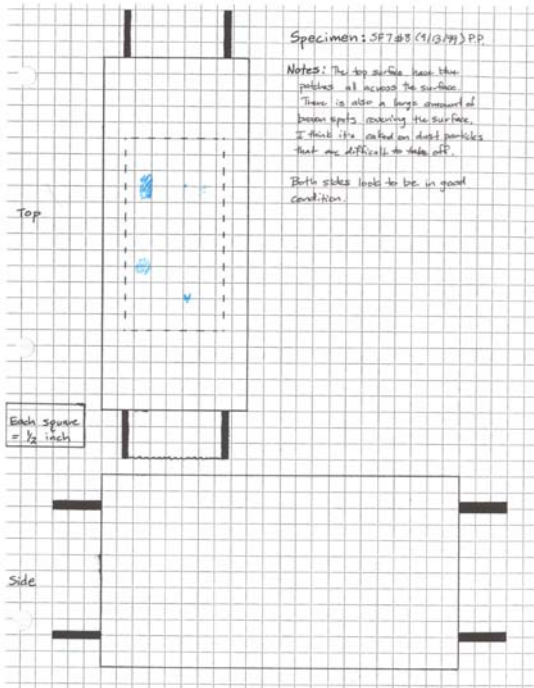


Figure 7.397 : SF7 #8 A

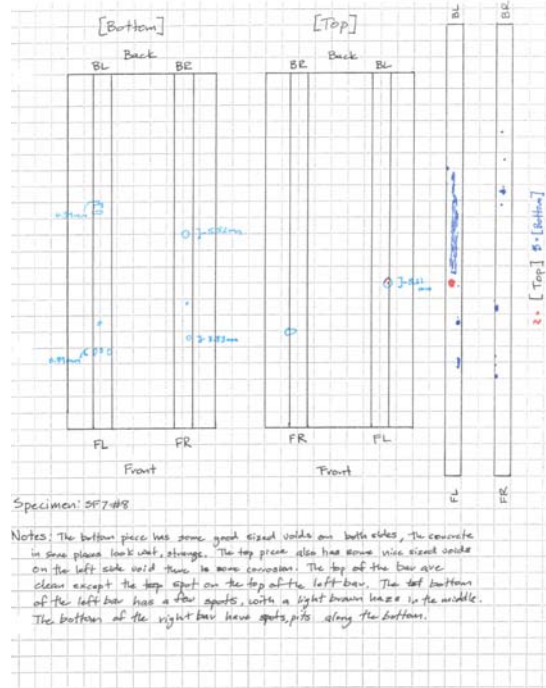


Figure 7.398 : SF7 #8 B

SF7 #8 – The top surface looked in fair condition. There were some brown particles that would not come off. Both bars have corrosion on the bottoms. The left bar has a line of corrosion with pits toward the front of the bar. The right bar has multiple pits along the bar. The half cell potential values all fell into the 10% probability range. The voltage results prove the specimen had not failed. The inspection concluded the corrosion to be minor.



Figure 7.399 - Bars, bottom



Figure 7.400 - Bars, top

XYPEX ADMIX C-2000

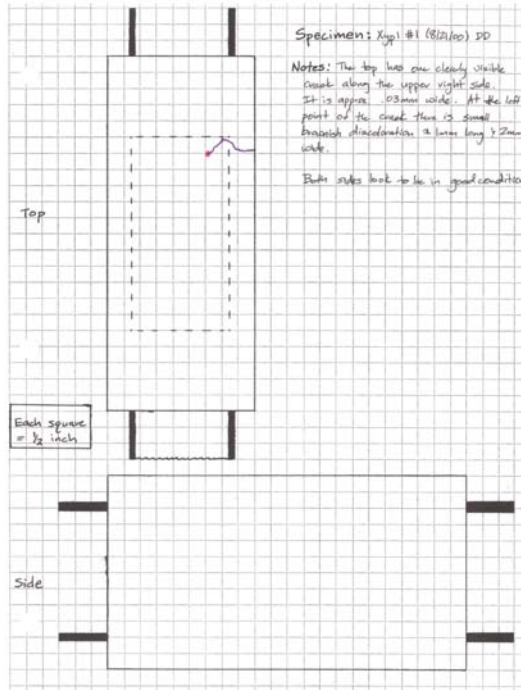


Figure 7.401 : Xyp1 #1 A

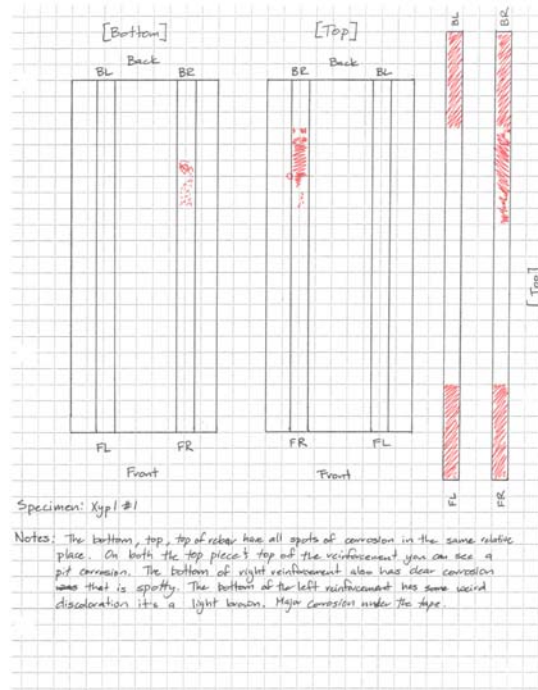


Figure 7.402 : Xyp1 #1 B

Xyp1 #1 – The visual inspection showed a crack on the top surface running perpendicular to the right bar. At the inmost point of the crack there was a brown discoloration. The inside of the specimen showed corrosion in the same area as the crack. The top corrosion was much more concentrated and darker than the corrosion on the bottom of the bar. All of the half cell potential values fell into the uncertain range. The voltage reading showed that the specimen was very close to failure. The inspection concluded the corrosion to be moderate to significant.



Figure 7.403 - Bars, bottom

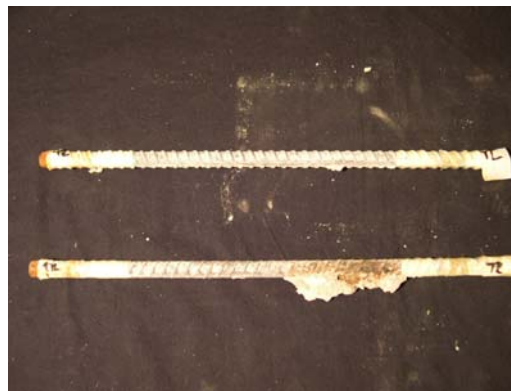


Figure 7.404- Bars, top

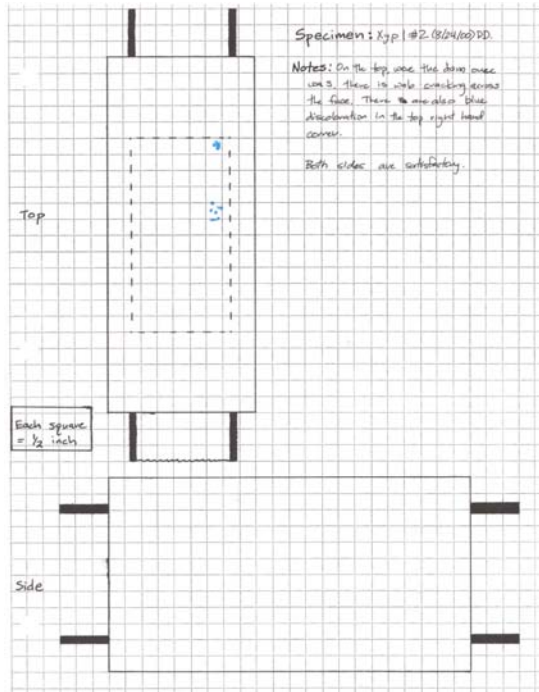


Figure 7.405 : Xyp1 #2 A

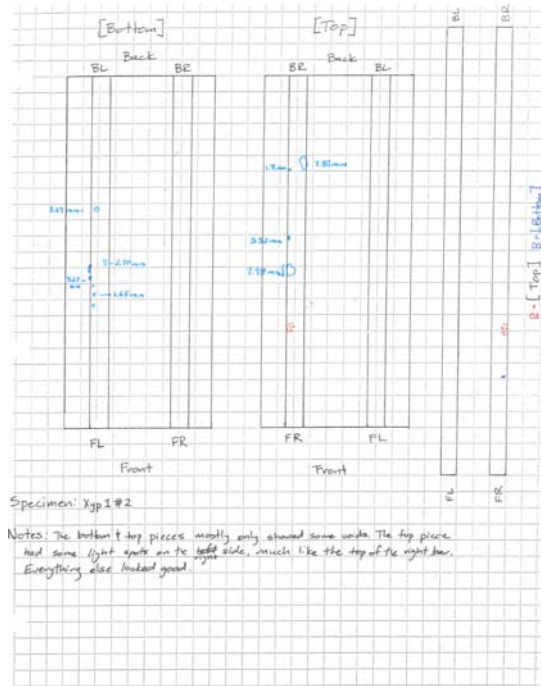


Figure 7.406 : Xyp1 #2 B

Xyp1 #2 – The visual inspection did not show any major flaws. There was some web cracking on the top surface. The inside of the specimen was very clean. There were only a few spots of corrosion on the top of the right bar. The half cell potential numbers all fell into the 10% probability of corrosion. The voltage readings showed that the specimen was not close to failure. The inspection concluded the corrosion to be none.



Figure 7.407 - Bars, bottom



Figure 7.408 - Bars, top

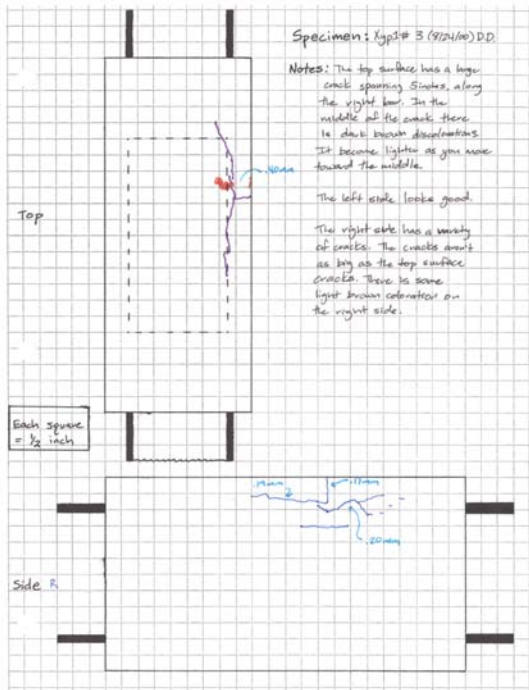


Figure 7.409 : Xyp1 #3 A

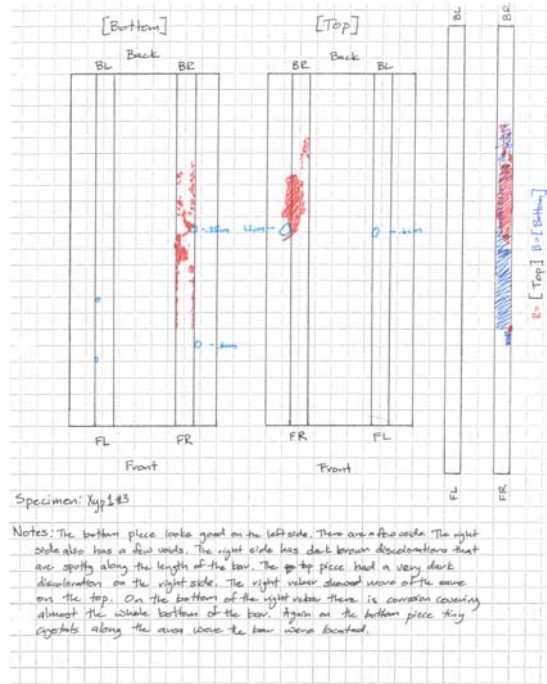


Figure 7.410 : Xyp1 #3 B

Xyp1 #3 – The visual inspection showed a large crack [on the surface running parallel to the right bar. There were also a few smaller cracks on the right side. The bar on the right side was well covered on the bottom. The top also had a well concentrated area of corrosion. All the half cell potential values fell into the uncertain range. The voltage readings showed that the specimen had failed. The inspection concluded the corrosion to be moderate to significant.



Figure 7.411 - Bars, bottom



Figure 7.412 - Bars, top

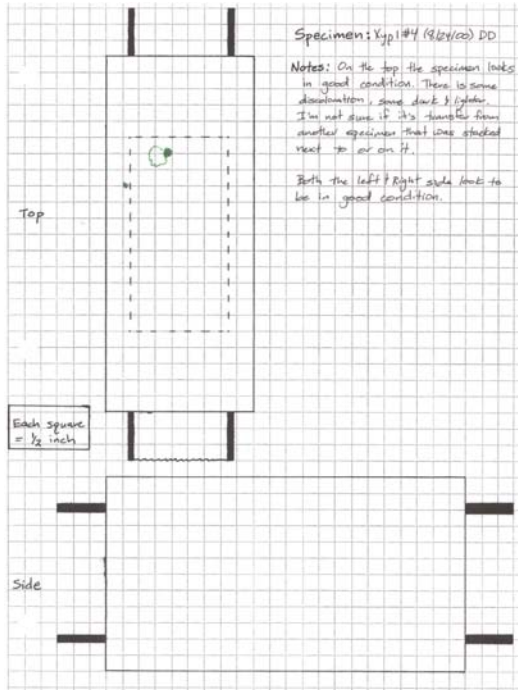


Figure 7.413 : Xyp1 #4 A

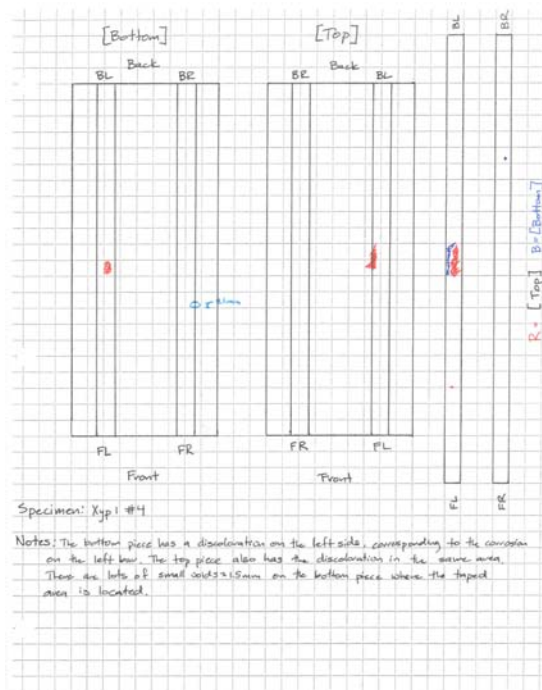


Figure 7.414 : Xyp1 #4 B

Xyp1 #4 – The visual inspection showed some brown discoloration on the top surface in the middle but toward the right side. On the inside of the specimen there were only a small area of corrosion located in the middle of the left bar. The half cell potential values all fell into the 10% probability range. The voltage numbers were very near to failure. The inspection concluded the corrosion to be minor.



Figure 7.415 - Bars, bottom

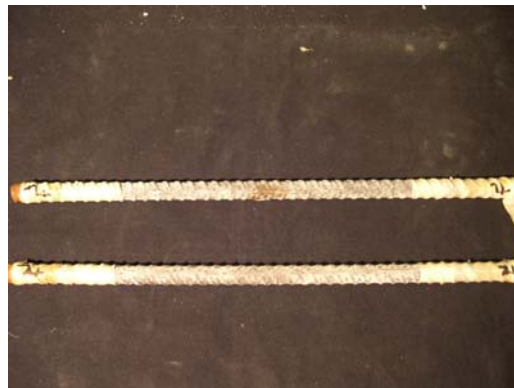


Figure 7.416 - Bars, top

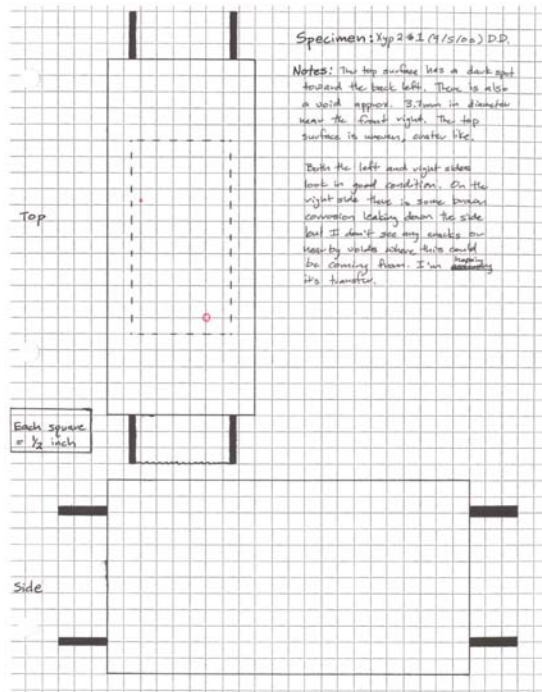


Figure 7.417 : Xyp2 #1A

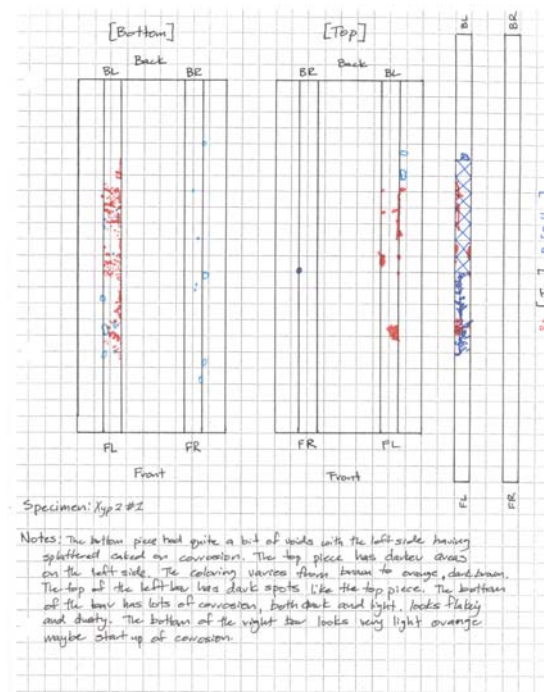


Figure 7.418 : Xyp2 #1B

Xyp2 #1 – The visual inspection did not show any cracks but there were a few voids. On the inside of the specimen the majority of corrosion fell on the bottom of the left bar. The top of the left bar had more pits and spots of corrosion while the bottom was well covered. The half cell potential values showed that two values on the left side fell into the 10% range while the other fell into the uncertain range. On the right side two values were uncertain and one was in the 10% range. The voltage readings had some fairly high numbers but never reached the failure threshold. The inspection concluded the corrosion to be moderate to significant.



Figure 7.419 - Bars, bottom



Figure 7.420 - Bars, top

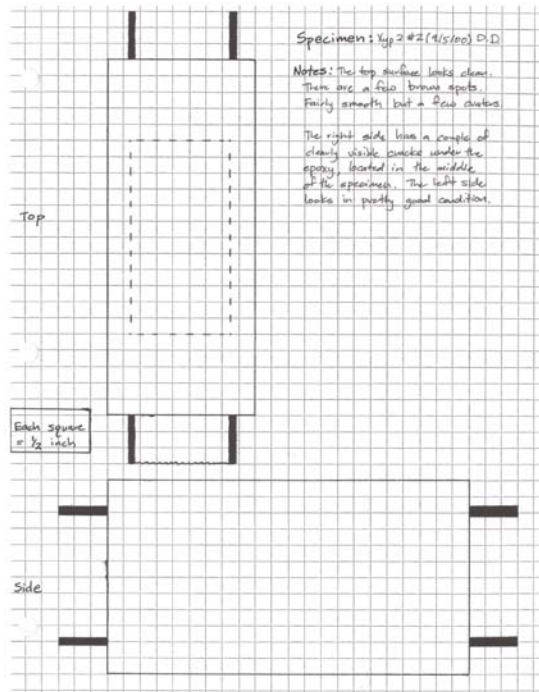


Figure 7.421 : Xyp2 #2 A

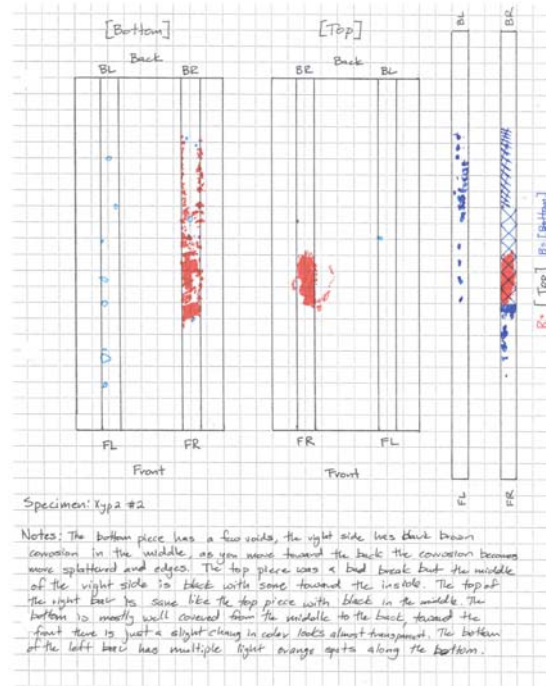


Figure 7.422 : Xyp2 #2 B

Xyp2 #2 – The outside of the specimen showed no major flaws. On the inside both bars had corrosion on them. The right bar contained most of the corrosion on the bottom with an area of corrosion on the top. The left bar had pits along the bottom of the bar. The half cell potential numbers showed that all the values fell into the uncertain region. The voltage readings indicated that the specimen had reached failure. The inspection concluded the corrosion to be moderate to significant.



Figure 7.423 - Bars, bottom



Figure 7.424 - Bars, top

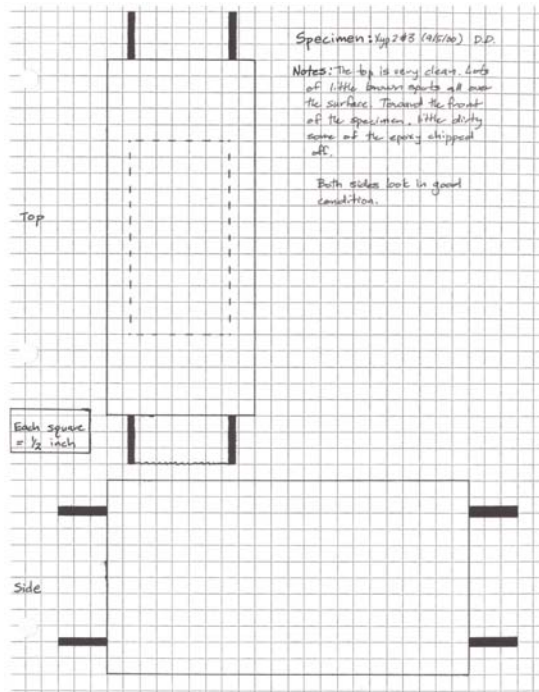


Figure 7.425 : Xyp2 #3 A

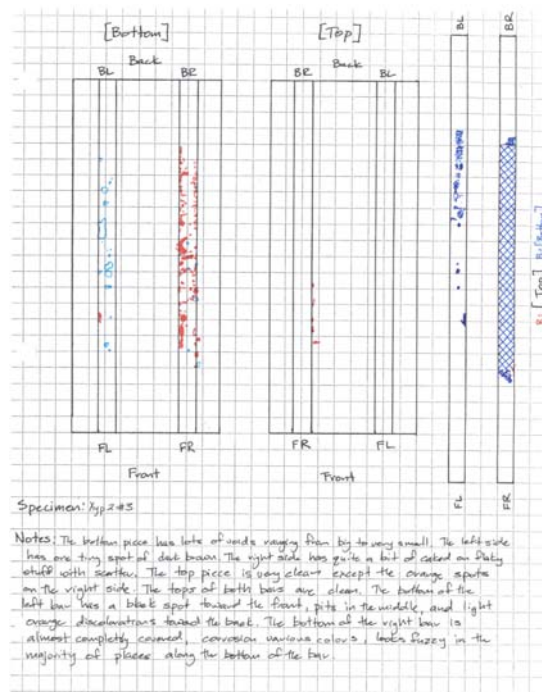


Figure 7.426 : Xyp2 #3 B

Xyp2 #3 – The visual inspection does not show any critical flaws. Both bars have corrosion on them but only on the bottom. The bottom of the right bar was completely covered. The bottom of the left bar has pits and spots mostly toward the back of the bar. The values from the half cell potential test indicated that the numbers fell into the 10% probability region. The voltage readings came close to failure but never reached the criteria of failure. The inspection concluded the corrosion to be moderate to significant.



Figure 7.427 - Bars, bottom



Figure 7.428 - Bars, top

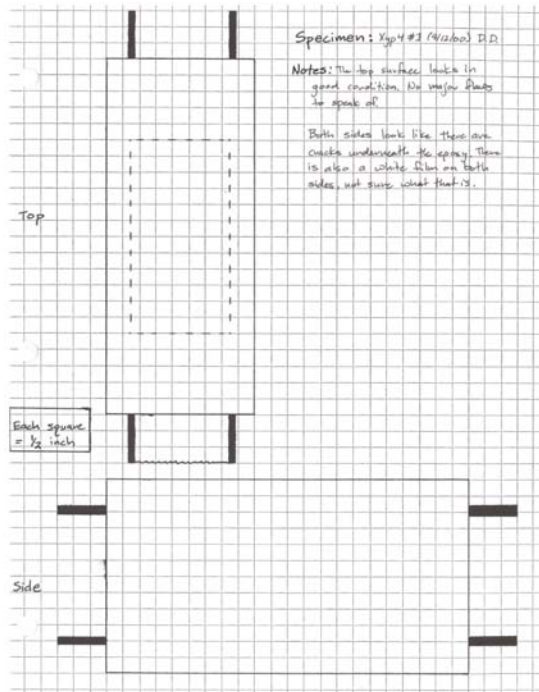


Figure 7.433 : Xyp4 #1A

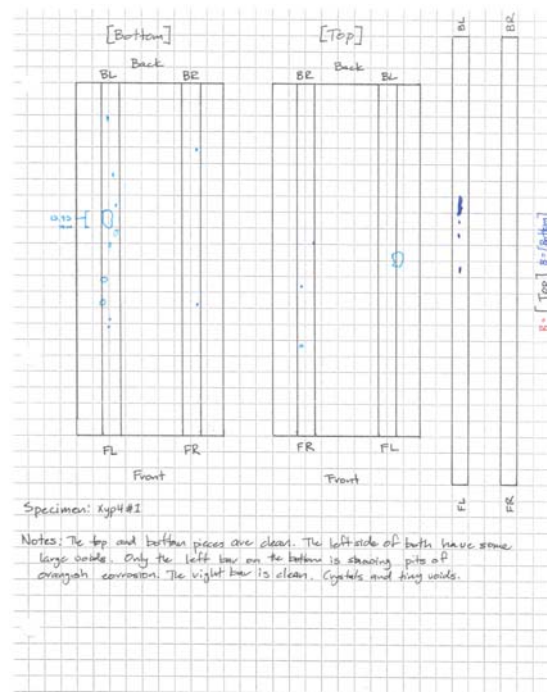


Figure 7.434 : Xyp4 #1B

Xyp4 #1 – The visual inspection showed some cracks underneath the epoxy coating on the sides. On the inside there was only a few pits on the bottom of the left bar. The half cell potential numbers all fell into the 10% probability range. The voltage numbers showed that the specimen was not close to failure. The inspection concluded the corrosion to be minor.

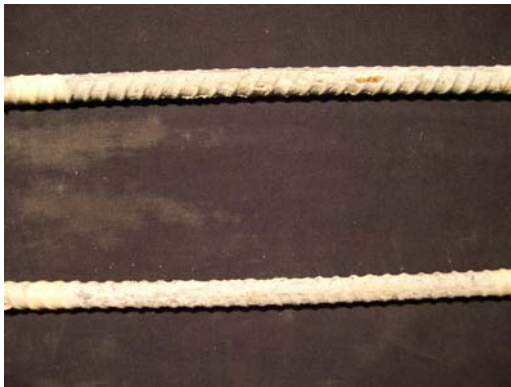


Figure 7.435 - Bars, bottom



Figure 7.436 - Bars, top

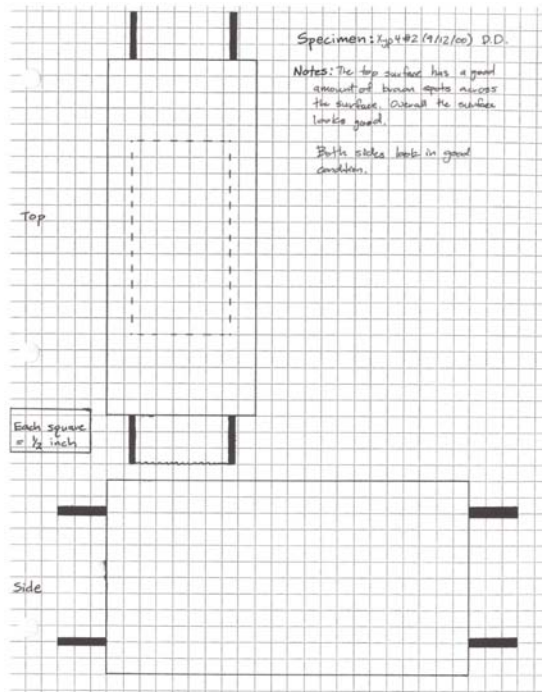


Figure 7.437 : Xyp4 #2 A

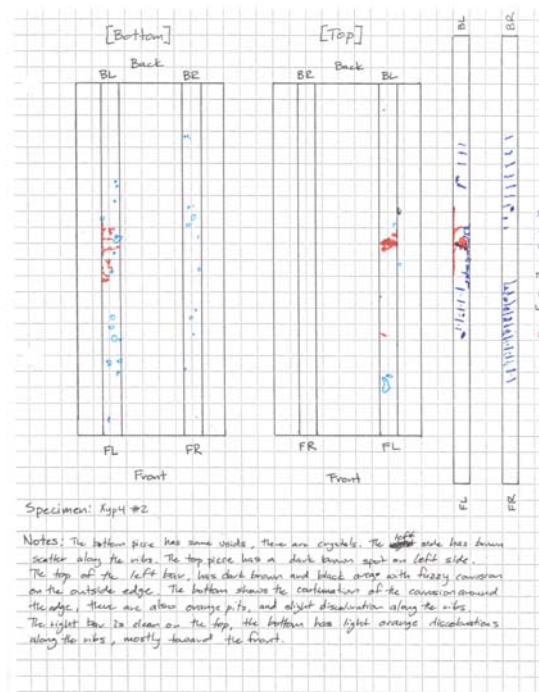


Figure 7.438 : Xyp4 #2 B

Xyp4 #2 – The outside of the specimen looked in excellent condition. Both bars showed some corrosion. The left bar had some corrosion on the top in the middle on the edges. The bottom of both bars had corrosion along the ribs of the steel. The half cell potential values all fell in the uncertain range. The voltage readings showed that the specimen was getting closer to failure but not yet there. The inspection concluded the corrosion to be minor.



Figure 7.439 - Bars, bottom



Figure 7.440 - Bars, top

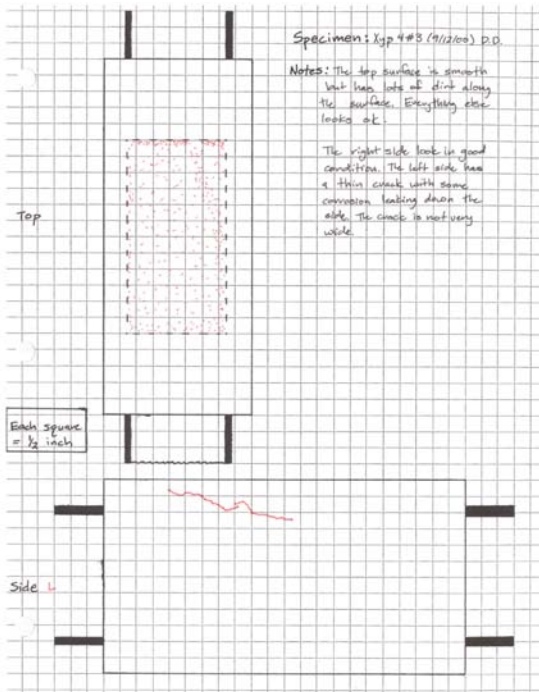


Figure 7.441 : Xyp 4 #3 A

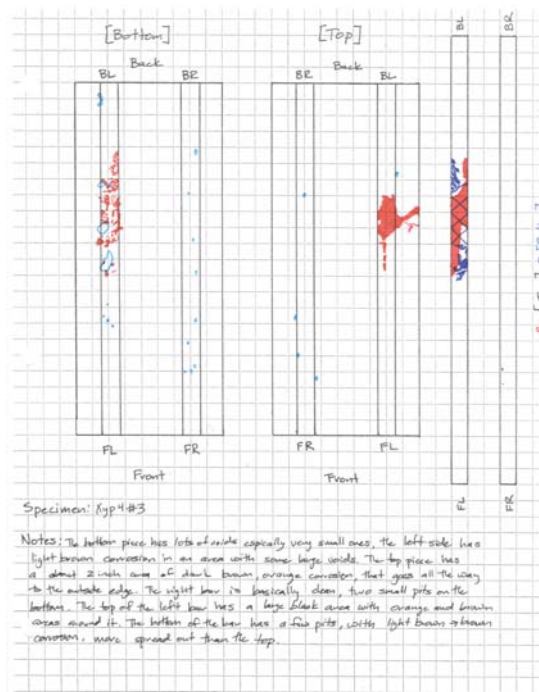


Figure 7.442 : Xyp 4 #3 B

Xyp4 #3 – The visual inspection showed a crack toward the back on the left side of the specimen. On the inside there was about a four inches area of corrosion on both the top and bottom of the left bar. The half cell potential readings showed that all the numbers fell into the uncertain range. The voltage values indicated that the specimen had failed. The inspection concluded the corrosion to be moderate to significant.



Figure 7.443 - Bars, bottom



Figure 7.444 - Bars, top

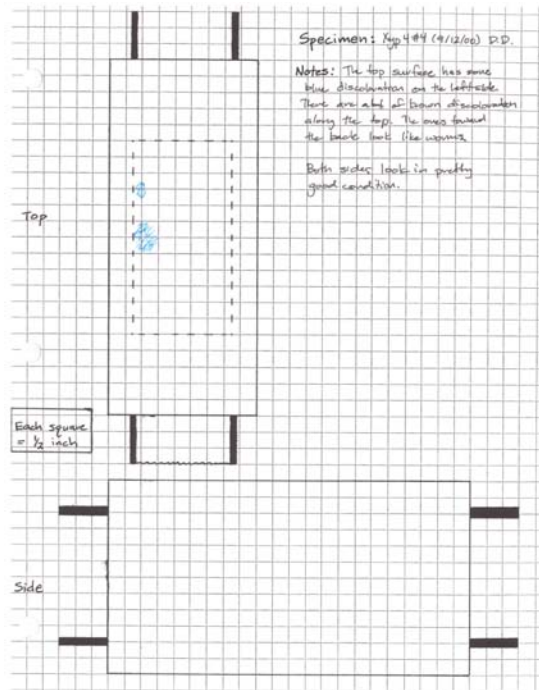


Figure 7.445 : Xyp4 #4 A

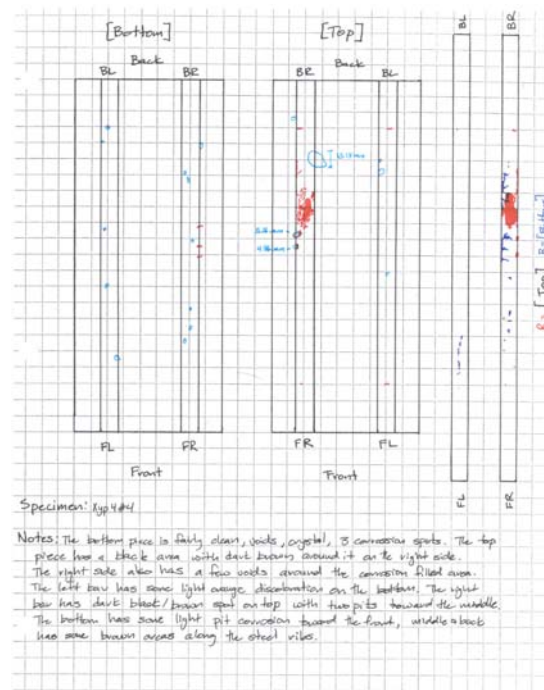


Figure 7.446 : Xyp4 #4 B

Xyp4 #4 – The outside of the specimen looked in good condition. The majority of corrosion was located on the right bar. The top of the right bar has a one inch long discoloration. The bottom of both bars had sparse corrosion. The two half cell potential values on the left side fell into the uncertain range and the other in the 10% probability range. The values on the right side all fell into the uncertain range. The voltage readings showed that the specimen had reached failure. The inspection concluded the corrosion to be moderate to significant.



Figure 7.447 - Bars, bottom



Figure 7.448 - Bars, top

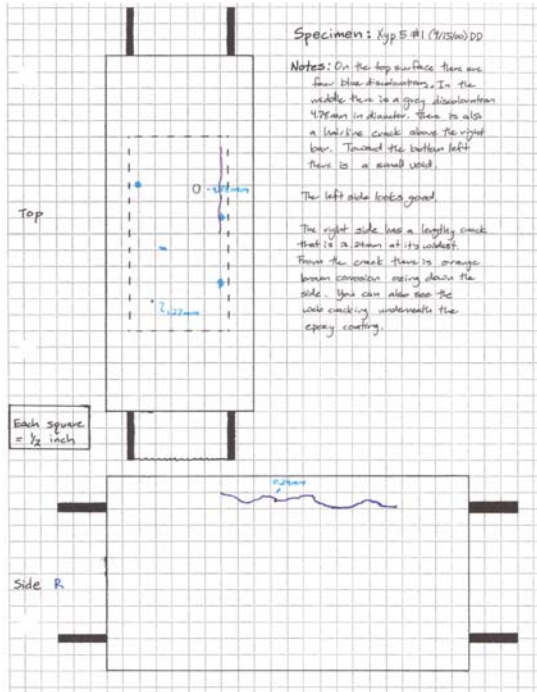


Figure 7.449 : Xyp 5 #1A

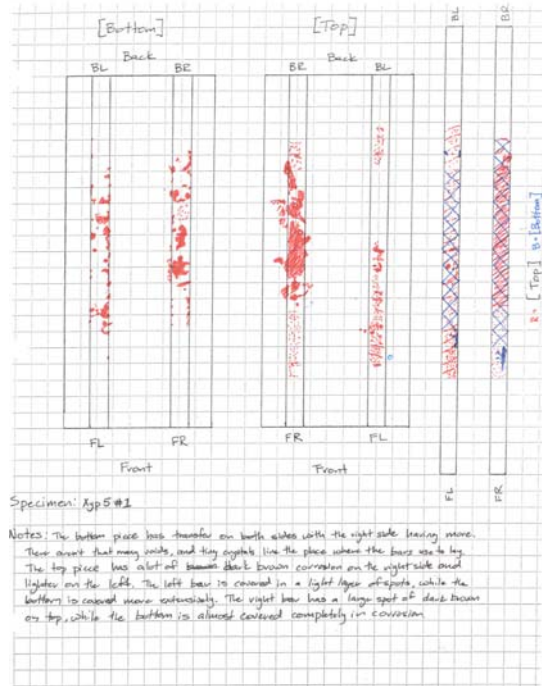


Figure 7.450 : Xyp 5 #1B

Xyp5 #1 – The visual inspection showed a crack on the top surface above the right bar. There was also a crack on the right side of the specimen. Both bars are well covered in corrosion especially on the bottom. The tops of the bars also had a fair amount of corrosion. The half cell numbers on the left side all fell into the 10% probability range. On the right side two values fell into the uncertain range and the other in the 10% probability range. The voltage readings indicated the specimen had failed. The inspection concluded the corrosion to be moderate to significant.



Figure 7.451 - Bars, bottom



Figure 7.452 - Bars, top

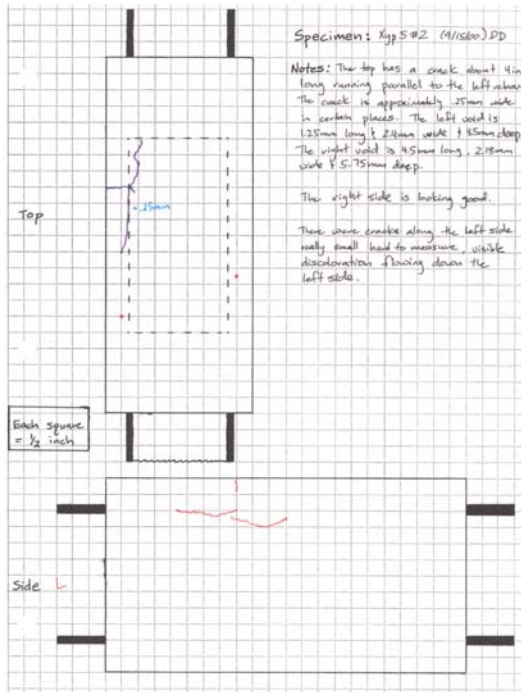


Figure 7.453 : Xyp5 #2 A

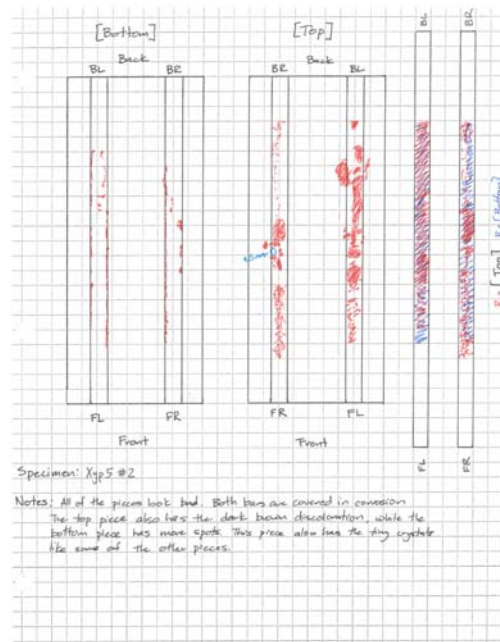


Figure 7.454 : Xyp5 #2 B

Xyp5 #2 – The visual inspection showed that there was a crack on the top surface above the left bars. There was also a crack on the left side. Both of the bars are completely covered in corrosion on the top and bottom. The half cell potential readings showed that all of the values except one on the left side fell into the uncertain range. The lone other value fell into the 10% probability range. The voltage numbers indicated the specimen had reached failure. The inspection concluded the corrosion to be moderate to significant.



Figure 7.455 - Bars, bottom



Figure 7.456 - Bars, top

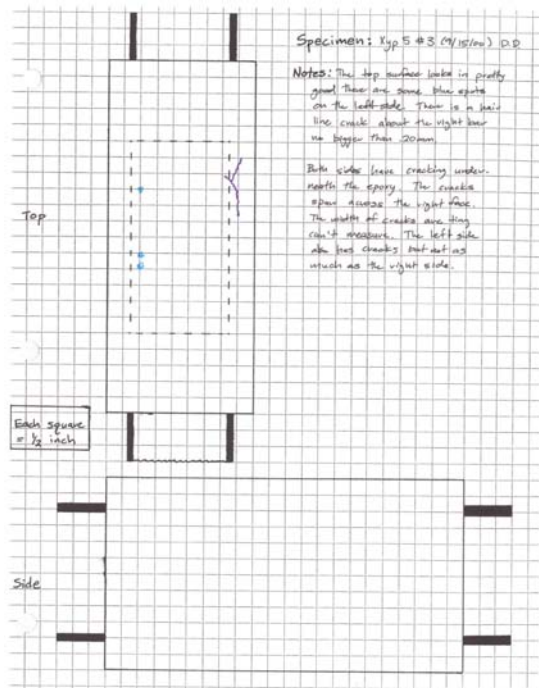


Figure 7.457 : Xyp 5 #3 A

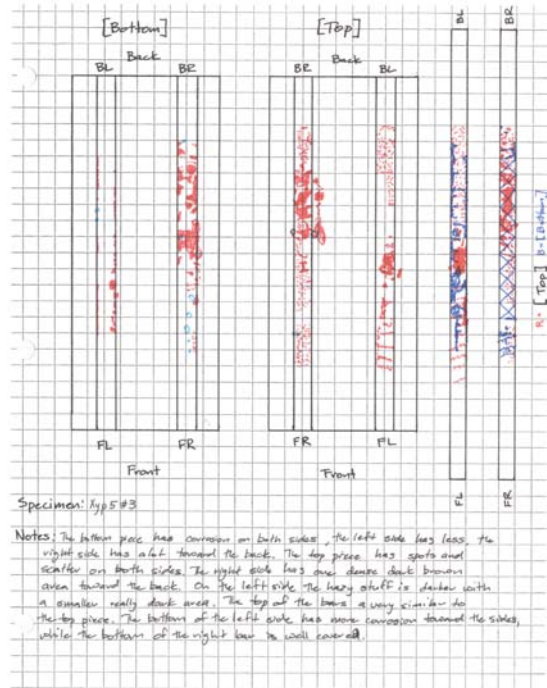


Figure 7.458 : Xyp 5 #3 B

Xyp5 #3 – The visual inspection showed a crack on the top surface above the right bar. Both bars were well covered on the bottoms. The tops of both bars also had corrosion areas with scattered spots all along the length of the bars. The half cell potential results reveal that all of the values fell into the 10% probability range. The voltage readings showed that the specimen had failed. The inspection concluded the corrosion to be moderate to significant.



Figure 7.459 - Bars, bottom



Figure 7.460 - Bars, top

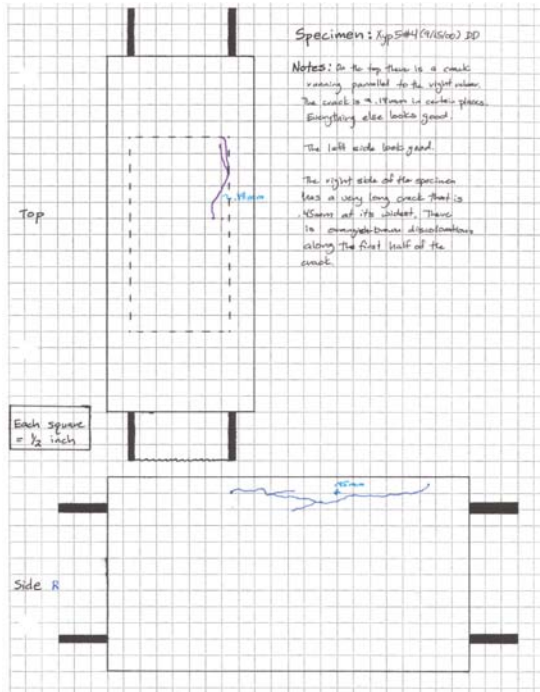


Figure 7.461 : Xyp5 #4 A

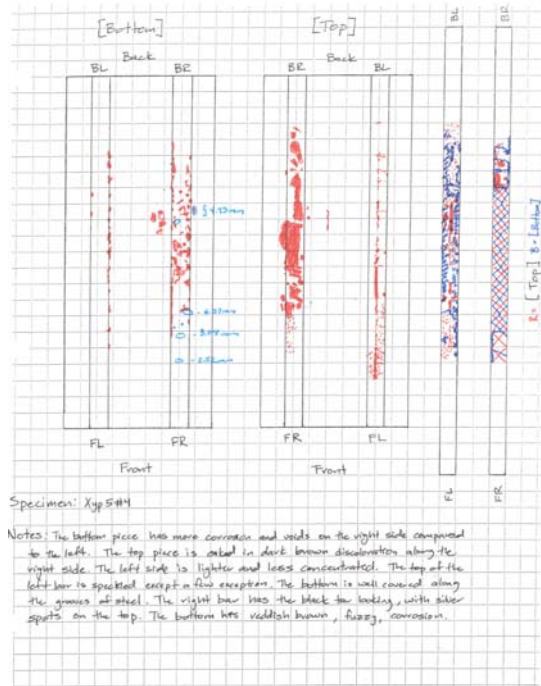


Figure 7.462 : Xyp5 #4 B

Xyp5 #4 – The visual inspection showed that there was a crack on the top surface above the right bar. There were also some cracks on the right side of the specimen. Both bars were well covered in corrosion on both the top and the bottom. The right bar corrosion seemed to be more severe than the left. The half cell potential values showed that the left side had one value in the 10% range and the other two in the uncertain range. The right side numbers were all in the uncertain range. The voltage readings indicated that the specimen had failed. The inspection concluded the corrosion to be moderate to significant.



Figure 7.463 - Bars, bottom



Figure 7.464 - Bars, top

REFERENCES

- ASTM, (1997), *1997 Annual Book of ASTM Standards*, Easton, Maryland.
- Berke, N.S., Scali, M. J., Regan, J. C., and Shen, D. F. (1991), “Long-Term Corrosion Resistance of Steel in Silica Fume and/or Fly Ash Containing Concretes,” *Durability of Concrete* (Second International Conference, Montreal, Canada), Volume 1, ACI SP-126, pp.393-415.
- Berke, Neal S., Shen, Ding Feng., and Sundberg, Kathleen M. (1990), “Comparison of the Polarization Resistance Technique to the Macrocell Corrosion Technique,” *Corrosion Rates of Steel in Concrete*, STP 1065, pp. 38-51.
- Bola, M., and Newton, C.M., (2000), *Field Evaluation of Corrosion in Reinforced Concrete Structures in Marine Environment*, Research Report UHM/CE/00-01, Department of Civil and Environmental Engineering, University of Hawaii at Manoa.
- Briggs, Andrew (1985), *An introduction to scanning acoustic microscopy*. New York : Oxford University Press, Royal Microscopical Society.
- Civjan, Scott A., LaFave, James M., Lovett, Daniel , Sund, Daneil J., Trybulski, Joanna, (2003), *Performance Evaluation and Economic Analysis of Combinations of Durability Enhancing Admixtures (Mineral and Chemical) in Structural Concrete for the Northeast U.S.A.*, Research Report prepared for The New England Transportation Consortium, NETCR36 Project No. 97-2.
- Corrosion Doctors, (2004), <http://www.corrosion-doctors.org/References/Potential.htm>
- Dhir, R.K., Hewlett, P.C., and Chan, Y.N., (1989), “Near Surface Characteristics of Concrete: Intrinsic Permeability,” *Magazine of Concrete Research*, Vol. 41, No. 147, pp.87-97.
- Dhir, R..K., Hewlett, P.C., Byars, E.A., and Shaaban, I.G., (1995), “A New Technique for Measuring the Air Permeability of Near-surface Concrete,” *Magazine of Concrete Research*, Vol. 47, No.171, pp. 167-176.
- Dhir, R.K., Jones, R.J., and McCarthy, M.J., (1993), “Quantifying Chloride-Induced Corrosion From Half-Cell Potential.” *Cement and Concrete Research*, Vol. 23, pp.1443-1454.

- EPA, (2002), *Test Methods for Evaluating Solid Wastes, Physical/Chemical Methods*. SW-846, Environmental Protection Agency.
- Figg, J.W., (1973), "Methods of Measuring the Air and Water Permeability of Concrete," *Magazine of Concrete Research*, Vol. 25, No. 85, pp.213-219.
- Gray, Peter (1973), *Encyclopedia of Microscopy and Microtechnique*. Litton Educational Publishing Inc.
- Hussain, S.E., and Rasheeduzzafar (1994), "Corrosion Resistance Performance of Fly Ash Blended Cement Concrete." *ACI Materials Journal*, Vol. 91, No. 4, May-June, pp.264-272.
- James Instruments Inc. www.ndtjames.com
- Keck, Roy H. (2001), "Improving Concrete Durability with Cementitious Materials," *Concrete International*, Vol.23, No.9, pp.47-51.
- Kouloumbi, N., and Batis, G. (1992), "Chloride Corrosion of Steel Rebars in Mortars with Fly Ash Admixtures." *Cement and Concrete Composites*, Vol. 14, No. 3, pp. 199-207.
- Kosmatka, Steven H. and Panarese, William C., (1994), *Design and Control of Concrete Mixtures*, Portland Cement Association. pp. 63-76
- Gjorv, O.E. (1975), "Control of Steel Corrosion in Concrete Sea Structures," *Corrosion of Metals in Concrete*, SP-49, American Concrete Institute, pp. 1-9.
- Griffin, D.F. (1975), "Corrosion Inhibitors for Reinforced Concrete," *Corrosion of Metals in Concrete*, SP-49, American Concrete Institute, Detroit, pp.95-102.
- Holland, Terence D., (1992), "Corrosion Protection for Reinforced Concrete: A Summary of Corrosion Prevention Strategies," *Concrete Construction*, Vol.37, No.3, pp. 230-236.
- Lee, C., and Lee, M. G. (1997), "Effect of Fly Ash and Corrosion Inhibitor on Reinforced Concrete in Marine Environments." *Durability of Concrete* (Proceedings Fourth CANMET/ACI International Conference), ACI SP-170, Vol. 1, pp. 141-156.
- Malisch, Ward R. and Terence C. Holland, (2000), "Combating Rebar Corrosion," *Concrete Construction*, November.
- Nmai, Charles K., Farrington, Stephen A., and Bobrowski, Gregory S., (1992), "Organic-Based Corrosion-Inhibiting Admixtures for Reinforced Concrete." *Concrete International: Design and Construction*, Vol.14, No.4, pp.45-51.

- Ohama, Y., (1987), "Principle of Latex Modification and Some Typical Properties of Latex-Modified Mortars and Concretes," *ACI Materials Journal*, Vol. 84, No. 6, pp. 511-518.
- Okunaga, Grant, Robertson, Ian., and Newton Craig, (2004), *Electrochemical Properties of Concrete Produced with Admixtures Intended to Inhibit Corrosion*, Research Report (Draft).
- Pham, Phong A. and Newton, Craig M, (2001), *Properties of Concrete Produced with Admixtures Intended to Inhibit Corrosion*, Research Report UHM/CE/01-01, Department of Civil Engineering, University of Hawaii at Manoa.
- Sharp, J.V., Figg, J.W., and Leeming, M.B., (1988), "The Assessment of Corrosion of The Reinforcement in Marine Concrete by Electrochemical and Other Methods." *Proceedings, Second International Conference on Concrete in Marine Environment*. SP-109-5, pp. 105-125.
- Sika Australia Pty Limited (2003), www.sika.com.au .
- Srinivasan, S., Rengaswamy, N.S., and Pranesh, M.R., (1994), "Corrosion Monitoring of Marine Concrete Structures – An Appraisal." *The Indian Concrete Journal*, Vol. 68, No. 1, pp. 13-19.
- Wolsiefer, Jr., J.T. (1993), "Silica Fume Concrete: A Solution to Steel Reinforcement Corrosion in Concrete." *Utilization of Industrial By-Products for Construction Materials* (Proceedings of the Session Sponsored by the Materials Engineering Division in Conjunction with the ASCE National Convention in Dallas, Texas), pp.15-29.
- Xypex Chemical Corporation (1999), http://www.xypex.com/products/admix2_desc.html.
- P. Zinin, M.H. Manghnani, Y.C. Wang, and R.A. Livingston (2000), *Detection of cracks in concrete composites using acoustic microscopy*. *NDT&E International*, **33**(5): p.283 – 287.
- P. Zinin, M.H. Manghnani, C. Newton, and R.A. Livingston (2004), "Acoustic Microscopy of Steel Reinforcing Bar in Concrete". *Journal of Nondestructive Evaluation*, Vol. 21, No.4, pp.105.